An analysis of *wnt* signalling molecules in *Xenopus* pronephros development.

Stéphanie Tételin

A thesis submitted to the University of Warwick
for the degree of Doctor of Philosophy.

Genes and Development,
Department of Biological Sciences,
University of Warwick,
Coventry,
CV4 7AL.

September 2008.

Contents

List of figures

List of tables

Acknowledgements

I would like to thank my supervisor Professor Elizabeth Oliver-Jones for her advice, encouragement and support to complete this work and for giving me the unique opportunity to carry on my studies here at the University of Warwick.

I would also like to thank the members of Liz's lab, Dr Karine Massé, Dr Junichi Kyuno, Richard Naylor and Surinder Bhamra for the cooperative team work, and in particular Karine for teaching me Bioinformatics and Molecular Biology.

But I would not have been part of this adventure without the unconditional support of my very good friends, Dr Laura Howard, Craig Tucker, Nader Amin, Jean-Christophe and Mella Bommé and Didier Borget.

A la mémoire de Papi, sans qui nous pourrions parfois oublier que le travail c'est la santé.

Declaration

The results presented in this thesis are the work of the author unless specified.

Microinjections and dissections were carried out together with Professor Elizabeth Oliver-Jones.

Hormone injections to *X. laevis* females were given by Mr Robert Taylor and Mr Paul Jarrett.

Sources of information have been acknowledges by reference.

None of this work has been previously used to apply for a degree.

Summary

The aim of the project was to characterise known *wnt* signalling molecules during the early pronephros patterning using novel and effective bioassays in *Xenopus* embryos. Anterior somites have been shown previously to have unique biological activity to induce pronephros formation in *Xenopus* embryos (Seufert et al., 1999).

A molecular approach consisted of analysing the expression of canonical *wnts* (*wnt6, wnt7b, wnt8, wnt9a* and *wnt9b*) and the non-canonical *wnts* (*wnt4, wnt5a, wnt11* and *wnt11b*) genes in isolated pronephric anlagen and pronephros from stage 12.5 to stage 35 and in anterior and posterior somites. This allowed the identification of potential candidate *wnt* genes which could act as pronephric inducers. Their potential to induce pronephros was tested *in vitro* using the Holtfreter sandwich culture pronephrogenesis assay, which consists of unspecified intermediate mesoderm cultured inside two animal caps over-expressing the *wnt* molecule of interest. Results suggest that the canonical *wnt* molecules (*wnt6* and *wnt8*) are capable of modifying the intermediate mesoderm leading to formation of somite and neural tissue that in turn, can secondarily induce pronephric tubule formation. By contrast, signals of the non-canonical *wnt11* and *wnt11b* are sufficient to directly specify the intermediate mesoderm to become kidney.

In vivo, the role of the canonical *wnt6*, non-canonical *wnt11b* and the closely related *wnt11* gene was investigated by gain and loss-of-function experiments. Results suggest that mis-expression of these genes disturb the normal formation of the pronephric tubules and suggest that both canonical and non-canonical *wnt* molecules are required for formation of functional pronephros.

This thesis also reports the identification of the novel *Xlwnt9a* and *Xlwnt9b* genes, their temporal and spatial expression in both *X. laevis* and *X. tropicalis* embryos and dissected adult organs and analyses the effects of *Xtwnt9b* mis-expression on *X. laevis* pronephros development.

Abbreviations

AP	alkaline phosphatase
ATP	adensonsine triphosphate
bFGF	basic fibroblast growth factor
bp	base pairs
BSA	bovine serum albumin
cDNA	complementary deoxyribonucleic acid
C-terminal	carboxyl-terminal
dATP	deoxyadenosine triphosphate
dCTP	deoxycytidine triphosphate
dGTP	deoxyguanosine triphosphate
dH_2O	distilled water
DIG	digoxygenin
DNA	deoxyribonucleic acid
DNase	deoxyribonuclease
dNTPs	deoxyribonucleoside triphosphates
dpc	days postcoitum
dTTP	deoxythymidine triphosphate
E	embryonic day
E.coli	*Escherichia coli*
EDTA	ethylene diamine tetra acid
EST	expressed sequence tag
FGF	fibroblast growth factor
g	gram
GFP	green fluorescent protein
HCl	hydrochloric acid
H_2O	water
H_2O_2	hydrogen peroxide
l	litre
LBroth	Luria Broth
kb	kilobases

kD	kilo Dalton
M	molar
MBT	mid-blastula transition
mg	milligram
ml	millilitre
mM	millimolar
MMLV	moloney murine leukaemia virus
MOPS	3-[N-morpholino] propane sulphonic acid
MO	morpholino oligonucleotide
mRNA	messenger ribonucleic acid
NaCl	sodium chloride
ng	nanogram
nl	nanolitre
nM	nanomolar
nt	nucleotides
N-terminal	amino-terminal
PAGE	polyacrylamide gel electrophoresis
PBS	phosphate buffered saline
PBT	phosphate buffered tris
PBST	phosphate buffered tris
PCR	polymerase chain reaction
pM	picomolar
pmol	picomoles
RA	retinoic acid
RNA	ribonucleic acid
RNase	ribonuclease
rpm	revolutions per minute
RT-PCR	reverse transcription PCR
SDS	sodium dodecylsulphate
TBE	tris buffered EDTA
TBS	tris buffered saline
TdT	Terminal deoxynucleotidyl transferase
TGFβ	transforming growth factor β
Tris	tris (hydroxymethyl) aminomethane

Tris-Cl	tris (hydroxymethyl) aminomethane, pH adjusted with HCl
UTR	untranslated region
V	volts
v/v	volume/volume
w/v	weight/volume
U	units
μg	microgram
μl	microlitre
μM	micromolar

Chapter 1 Introduction

1.1 Overview, aims of the project.

The aim of the project was to characterise known *wnt* signalling molecules during the early pronephros patterning using novel and effective bioassays in *Xenopus* embryos. Anterior somites have been shown previously to have unique biological activity to signal to unspecified intermediate mesoderm to induce pronephros formation in *Xenopus* embryos (Seufert et al., 1999). A molecular approach consisting of analysing the canonical and non-canonical *wnt* genes expression in isolated pronephric anlagen and pronephros from stage 12.5 to stage 35 and in anterior and posterior somites will allow the identification of potential candidate *wnt* genes and will be directly tested in pronephrogenesis assay. Gain and loss-of-function experiments of the newly identified pronephric inductive *wnt* genes will investigate the full role of these genes in pronephric induction and patterning.

1.2 Why use *X. laevis* embryos in developmental studies?

X. laevis embryos are an extremely attractive model vertebrate system to study organogenesis. The African clawed frog can be easily housed in the laboratory as the female adult frog does not exceed 6 inches long and the male adult is even smaller. In *X. tropicalis,* the newly established genetic amphibian model, the adult female frog is even smaller than *X. laevis* and is only about 2 inches long with the adult male smaller still (Fig 1.1 , panel A). Figure 1.1, panel B summarises the advantages of using *X. laevis* embryos in developmental studies. Husbandry of the adult animal requires minimum infrastructure, consisting of a tank with soft to medium soft water with neutral to acidic pH maintained at room temperature. Adult frogs necessitate low maintenance. Animals need to be fed only 2 or 3 days weekly, althought froglets and growing animals need to be fed more frequently. However, embryos do not need to be fed until an advanced stage of development, late swimming tadpole (stage 46, about 4.5 days of development at 23˚C). A *X. laevis* female adult frog can lay thousands of eggs under the stimulation of the human chorionic gonadotropin

Panel A

Picture from the Genome News Network, 2002.

Panel B

- **Animals housed in the laboratory.**
- **1000 plus eggs collected with HCG injection.**
- **Embryogenesis occurs outside the mother.**
- **Defined stages of embryonic development obtained by *in vitro* fertilization.**
- **Embryos are large allowing micromanipulations.**
- **Organogenesis easily monitored.**
- **Transgenic techniques.**
- **No feeding required up to the swimming tadpole.**

Figure 1.1 Why use *Xenopus* embryos in developmental studies? Panel A shows the adult African clawed frog *X. laevis,* on the left and its close relative, the smaller *X. tropicalis,* on the right. Panel B summarises the advantages of using *X. laevis* embryos in developmental studies.

hormone (hCG) and *X. tropicalis* female adults can lay many hundreds of eggs. Then, eggs can be collected in a Petri dish and are subsequently fertilised *in vitro* by simply brushing over the male frog testis, thus releasing sperm and providing a synchronously fertilised group of embryos. As embryogenesis occurs outside the mother, development and subsequent organogenesis can be easily monitored. Defined stages of embryonic development can be easily obtained and correctly identified following the Normal Table of Nieuwkoop and Faber, 1994.

Embryos are large, approximately 2mm diameter, and relatively sturdy allowing micromanipulation. These micromanipulations are one of the greatest advantages of using *X. laevis* embryos in developmental studies as injection of DNA, RNA or protein molecules allow the introduction of defined gene products. Injection of mRNA results in the over-expression of protein and injection of morpholino antisense oligonucleotide results in inhibition of translation of a defined gene product. Morpholino oligos are short chains of 25 morpholino subunits. Each subunit is comprised of a nucleic acid base, a morpholine ring and a non-ionic phosphorodiamidate intersubunit linkage. Morpholinos act via an RNase H-independent steric blocking mechanism. With their high mRNA binding affinity and specificity, they result in knocking down gene expression by blocking translation initiation in the cytosol (by targeting the 5'UTR through the first 25 bases of coding sequence) (Heasman et al., 2000). Both techniques, over-expression or inhibition of specific gene product, allow the alteration of the gene function and therefore give indication about their role during development. Injection can be performed into the fertilized egg or into one blastomere of the early cleaving stage, allowing targeting to specific regions of the embryo (Dale and Slack, 1987 and Moody, 1987). In addition, injection can be restricted to one side of the embryo, allowing the uninjected side to be used as a contralateral control within the same embryo. Additional micromanipulations such as fine dissections, grafting experiments and embryo explant culture can also be carried out in simple saline solution.

During the last decade, *Xenopus* has also been developed as a genetic system. A number of reports have identified successful strategies for generating both transgenic *X. laevis* and *X. tropicalis*. Some techniques have used restriction endonuclease mediated integration (REMI) (Ogino et al., 2006). This results in the insertion of

extrachromosomal transgenic DNA into genomic DNA. The use of inducible constructs allow the investigation to control the time of the expression of the transgene (Wheeler et al., 2000, Waldner et al., 2006). Moreover, the recently opened European Resource Centre for *Xenopus* provides a means of obtaining a supply of genetically altered animals along with wild type. To augment these genetic studies, in August 2005, the whole genome of the diploid *X. tropicalis* was sequenced and assembled by the Joint Genome Institute (JGI). This genomic resource constitutes a great tool for genomic and genetic research in amphibia.

The advantages stated above make *Xenopus* an excellent model organism to study both early development and organogenesis. In this study, we have exploited this model system to study the formation of the embryonic kidney, the pronephros.

1.3 The kidney as a model organ to study organogenesis.

1.3.1 The three kidney forms, function, organisation and similarities.

The function of the kidney is to filter blood thus retaining useful molecules inside the organism and disposing of metabolic waste outside the organism.

During vertebrate life, the kidney, which derives from the intermediate mesoderm, undergoes spatial and size rearrangement but its basic organisation and function remain identical. The first embryonic kidney to form is the pronephros which is functional in lower vertebrates such as amphibian and fish. Later in development the pronephros is replaced by the mesonephros that constitutes the adult kidney form of the amphibians and fish but acts as the functional embryonic kidney form for the higher vertebrates. In mammals, the adult kidney form is the metanephros.

The basic structural and functional unit of the vertebrate kidney is the nephron. Figure 1.2 shows the organisation of nephrons into the three different forms of kidneys. The nephron is organised into segments, composed of distinct specialized renal epithelial cell types with unique function and properties. All the segments are fully integrated to insure normal excretory function. The glomus filters the blood, the tubules reabsorb the useful molecules from the filtrate and the wastes are collected

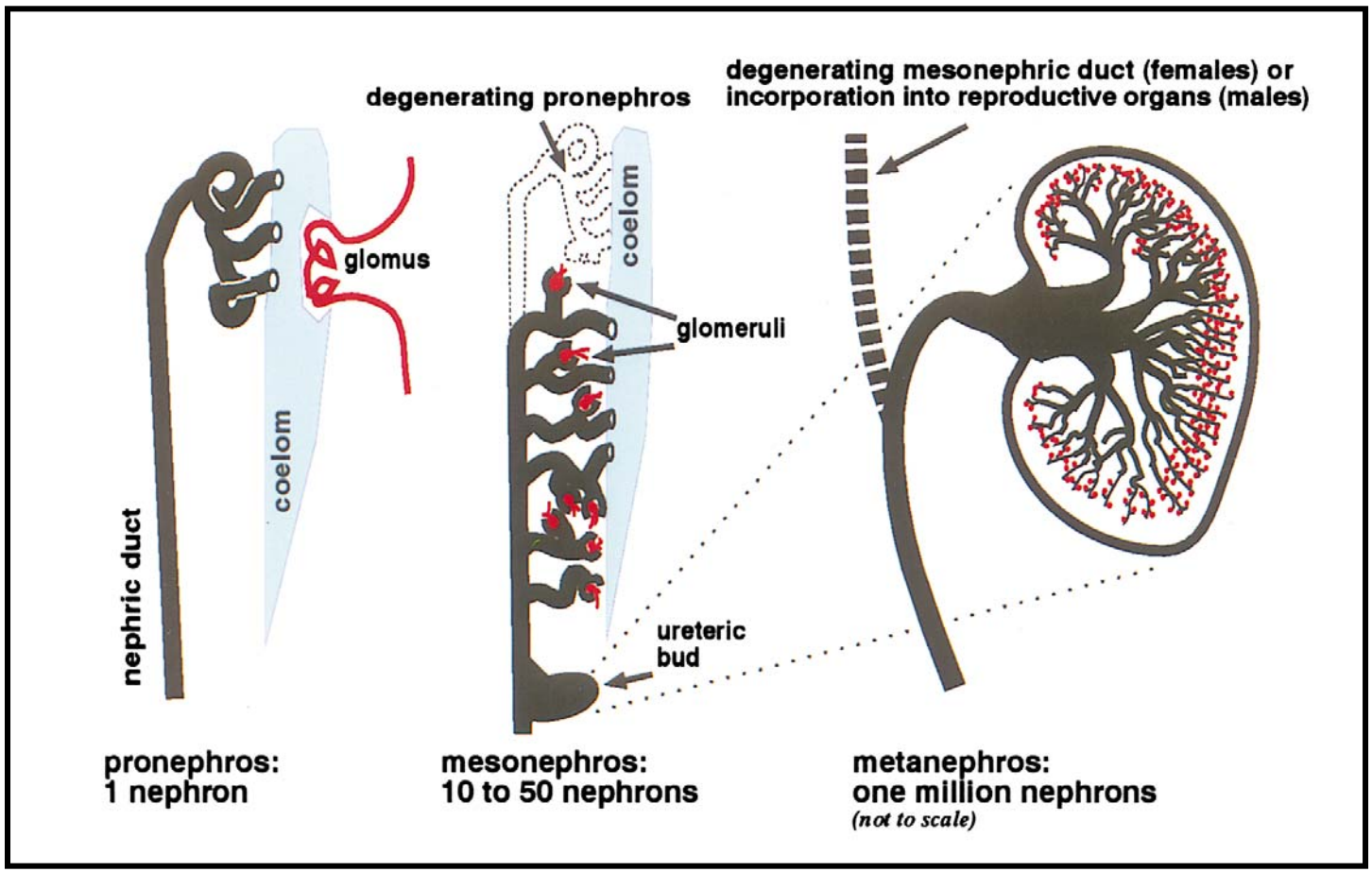

Figure 1.2 Organisation of nephrons into kidneys. The pronephros has one nephron, the mesonephros is constituted of 10-50 nephrons and the most complex form of kidney, the metanephros has one million nephrons. Figure from Vize et al., 1997.

into the collecting tubule system. The pronephros is one single nephron, while the mesonephros is composed of 10 to 50 nephrons and the most complicated form of the kidney, the metanephros is formed of about a million nephrons.

1.3.1.1 The mesonephros in mammals.

All three kidney forms of the developing urinary system derive from the intermediate mesoderm. In vertebrates, the second embryonic kidney to form, the mesonephros, follows the primitive kidney, the pronephros and precedes the development of the permanent kidney, the metanephros. Thus, it is also called the intermediate kidney. In adult lower vertebrates, amphibians and teleost fish, the mesonephros serves as the adult excretory organ. The mesonephros undergoes epithelial differentiation, cell migration, developmental changes, apoptosis and is a source of stem cell differentiation and hormonal determination of gene activity.

In mammalian mesonephrogenesis, the caudally descending nephric duct, the pronephric duct, also called the Wolffian or mesonephric duct at later stages, forms in the anterior region from the pronephros (Smith and MacKay, 1991). The duct is permanent, but the pronephric tubules regress and are eventually replaced by a new type of embryonic kidney, the mesonephros. The nephric duct is essential as both the common urinary drain and the terminal inducer of mesonephric tubules. No mesonephric nephrons differentiate if the inductive interaction between the duct and the blastema is disrupted (Waddington, 1938).

The mesonephric mesenchyme first aggregates and forms a renal vesicle (Burns, 1955). That vesicle that makes connection to the Wolffian duct seems to grow finger-like protrusions towards the basement membrane of the duct (Lawrence, 1992). The renal vesicle then differentiates in epithelial S-shaped structures that elongate and eventually form proximal tubules. In murine species, small glomerular-like structures develop in the medial part of the tubules (Sainio et al., 1997a), with primitive endothelial tufts (Smith and MacKay, 1991). The cranial mesonephric tubules form branches. The mesonephros functions physiologically to produce urine (Tiedemann and Egerer, 1984).

The mesonephric kidney regresses prenatally in mammals. Degradation is completed in mouse by day E-15 (Saxén, 1987). Murine regression seems to start from the caudal mesonephric tubules and spread cranially (Sainio et al., 1997a). In females, degradation is complete, but in males, the remaining mesonephric tubules form part of the gonadal ducts (Moore, 1977). The molecular mechanism regulating the mesonephric degradation is not known, but apoptosis has been described by morphological criteria. Mesonephric tubule differentiation and regression are controlled by tissue surrounding the mesonephric tubules.

Some key regulatory molecules in the mesonephros are the same as those in the primitive and permanent kidney forms. For example, *hox* genes are essential for normal specification and differentiation of the urogenital tissue (Patterson et al., 2001); *pax2* is necessary for the development of the excretory system and is associated with the initial steps in the differentiation of the intermediate mesoderm (Torres et al., 1995); *bmp4* is a candidate molecule to regulate early steps in the differentiation of the Wolffian duct and budding of the ureter (Miyazaki et al., 2000); *gdnf* is a second factor crucial for ureteric budding (Sainio et al., 1997b). *wt1* regulates mesonephric tubule differentiation (Kreidberg et al., 1993) and the homeobox gene *emx2* regulates at least the Wolffian duct maintenance (Yoshida et al., 1997).

The mesonephros contributes to the development of other organ systems and is a source of several cell lineages. The mesonephros is important for the somatic cell differentiation of both the testis and the ovary (McLaren, 2000), is a source of hematopoietic cells (Medvinsky et al., 1996) and a source of adrenal cortex cells (Worbel and Süß, 2000).

The mesonephric kidney is an embryonic organ that disappears in all mammalian species when the permanent kidney, the metanephros, is functional.

1.3.1.2 The metanephros in mammals.

The mammalian metanephros kidney constitutes the third and final member of the kidney form developing from the intermediate mesoderm. The metanephros is stable throughout adult life.

Figure 1.3 shows the first steps of metanephros formation. Renal development starts when an epithelial ureter bud forms from the nephric duct and invades the metanephric mesenchyme. Continuous interaction between the epithelium of this ureter bud and the metanephric mesenchyme is required for the development of the metanephric kidney. This interaction is referred to as a reciprocal epithelium-mesenchymal interaction. In response to signals from the mesenchyme, the ureter grows, branches and eventually forms the collecting duct system of the mature kidney. In turn, in response to signals from the developing ureter, the mesenchymal cells, condense, aggregate and undergo epithelialisation. Once the ureteric bud has invaded the blastema and adjacent metanephric mesenchyme cells have condensed around the tip, the bud grows and bifurcates. As each tip extends, it remains surrounded by a cap of dense cells, but leaves behind a small condensation of cells, the future nephrons. Once the tip reaches the periphery of the kidney, the condensed cells spread out and form a population of blastema cells that, is the source of all future nephrons. These blastema cells have a rapid growth rate ensuring that most kidney enlargement is at the periphery (Saxén, 1987).

Apoptosis is also prominently present during metanephros formation and was shown to modulate the growth of the kidney (Koseki et al., 1992). First, the metanephric mesenchyme dies if it fails to be induced by the ureteric bud (Kreidberg et al., 1993). Secondly, the periphery of the early blastema is delimited by an envelope of apoptosis that gives integrity to the early kidney. Third, there is cell death in the induced metanephric mesenchyme, particularly around the developing nephrons (Koseki et al., 1992) and apoptosis here may help sculpt these complex epithelial tubules. Finally, there is apoptosis in the stroma cells toward the end of development (Koseki et al., 1992).

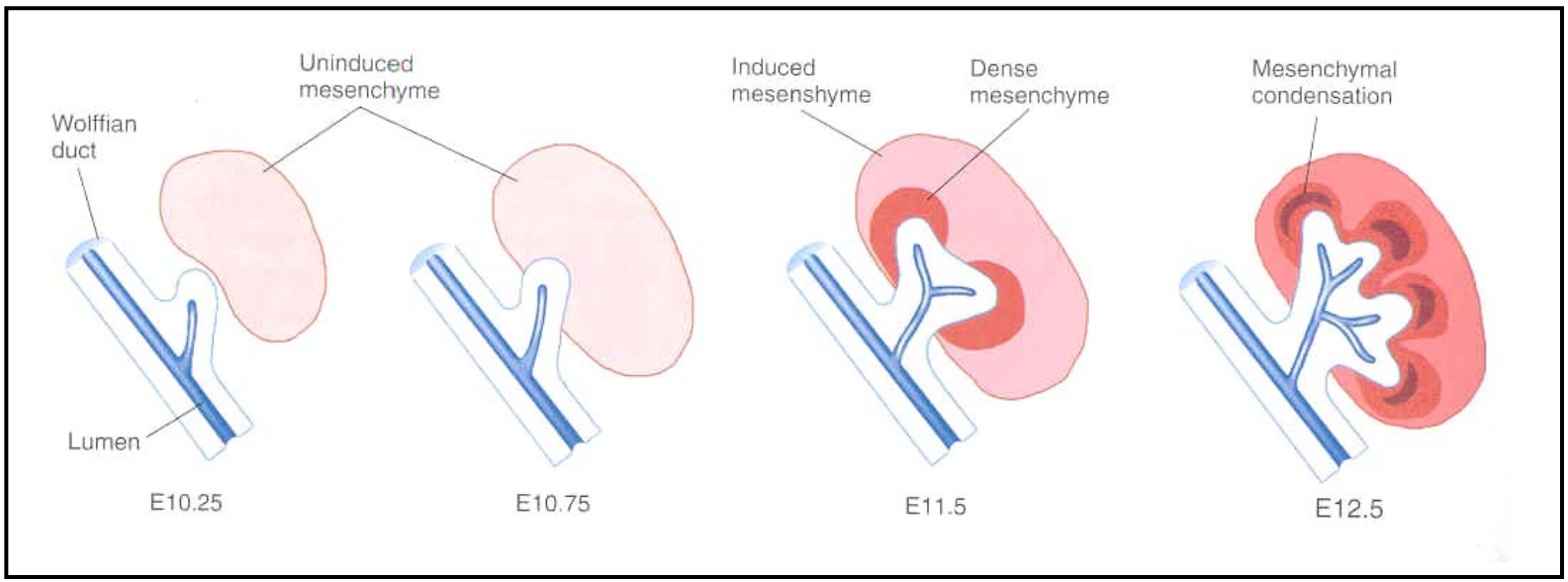

Figure 1.3 The first steps of the metanephros development. At stage E10.25-10.75, an epithelial ureter bud forms from the nephric duct and invades the metanephric mesenchyme. At stage E11.5 the epithelium of this ureter bud and the metanephric mesenchyme reciprocally interact to form the metanephric kidney. In response to signals from the mesenchyme, the ureter grows, branches and eventually forms the collecting duct system of the mature kidney. In turn, in response to signals from the developing ureter, the mesenchymal cells, condense, aggregate and undergo epithelialisation (E12.5), until they finally form a functional nephron. Figure adapted from Davies and Bard, 1998.

Similar genes that are involved in mesonephros formation, are also found to regulate the metanephros formation. A number of specific genes, such as *wt1*, *pax2* and *gdnf* are already expressed prior to induction and mark the metanephric anlagen (Brophy et al., 2001). *pax2* and *wt1* are required to enable the mesenchyme to respond to inductive signals, they may also be necessary for the proliferation and differentiation of tubular epithelium after induction occurs. Many of the properties associated with the inductive signals emanating from the uteric bud to induce the metanephric mesenchyme are common to the *wnt* molecules (Stark et al., 1994).

All the three kidney forms have essential developmental and functional similarities. First of all, the three kidney forms undergo the central event of conversion from mesenchymal to epithelial tissue. Secondly, almost all of the cell types found in the metanephros are also found in the pronephros. Finally, many of the genes responsible for the induction and patterning of the pronephros have been shown to be expressed in the mesonephric and metanephric kidneys in higher vertebrates. Additionally, the development of the mesonephros and the metanephros is dependent on the previous kidney form from which they are derived. However, the metanephros remains a complex system to study with many distinct developmental events required to produce a working organ. Therefore using the *Xenopus* pronephros as a simple model for understanding the function, the organisation, the cell patterning and identification of the genes involved in the early development of the kidney will have predictive value for the study of nephrogenesis in more complex kidney forms such as the metanephros in higher vertebrates.

1.3.2 The pronephros in frog.

1.3.2.1 Pronephros formation.

The pronephros is a paired organ that consists of a single non-integrated nephron found in a lateral position on each side of the embryo. The pronephros is derived from the intermediate mesoderm that lies between the paraxial mesoderm (presumptive somites) and the lateral plate. If the intermediate mesoderm from the presumptive pronephric region is removed at the early gastrula stage, the embryo will not form pronephric components. The early gastrula stage unspecified intermediate

mesoderm requires inductive signals during early neurulation to specify the pronephric anlagen and then undergo morphogenesis to give rise to a functional renal unit, the nephron. Specification of all three components of the pronephros occurs between stages 12.5 and 14 (Brennan et al., 1998, 1999).

The induction of the pronephric anlagen, in which cells of the intermediate mesoderm are instructed to change their future development by another cell type, starts with a signal coming from the anterior somites (Seufert et al., 1999, Mauch et al., 2000, Mitchell and al., 2007). It has been shown that the anterior somites can induce pronephric tubules when cultured in combination with unspecified intermediate mesoderm. The molecular mechanism responsible for giving such inductive signals has not been yet identified. This constitutes the main research interest of this thesis. However, some genes have been shown to be crucially involved in the patterning of the pronephric mesoderm. Such genes are *pax8* (Carroll and Vize, 1999), *lhx1* (previously called *lim1,* Taira et al., 1994) and *wt1* (Carroll and Vize 1996). Together *pax8, lhx1* and *wt1* give the switch to the specified intermediate mesoderm for mediolateral patterning. Figure 1.4 shows the patterning events that subdivide the *Xenopus* pronephric anlagen. *wt1* is only expressed in the medial portion of the developing pronephric mesoderm at stage 18. Shortly after *wt1* activation, genes that were initially expressed throughout the pronephric mesoderm, such as *pax8* and *lhx1,* become restricted to the lateral pronephros. From this point, the original pronephric mesoderm is subdivided into the medial region that will form the glomus, the dorsolateral region that will give rise to the proximal tubules and the ventrolateral region that will establish the intermediate/distal tubules. The glomus and the tubules are specified at the same time, stage 12.5 but the glomus can develop after removal of the pronephric tubules primordial, confirming that these structures come from independent origins (Carroll and Vize 1996). Complementary to *wt1*, epidermal *bmp4* constitutes a source for mediolateral patterning (Majumdar et al., 2000).

Following mediolateral patterning, pronephric mesoderm becomes patterned dorsoventrally. As the pronephros forms between the somites and the lateral plate, it is most likely that the source of dorsoventral patterning signal is given by the adjacent paraxial mesoderm, the presumptive somites, or by more distant axial

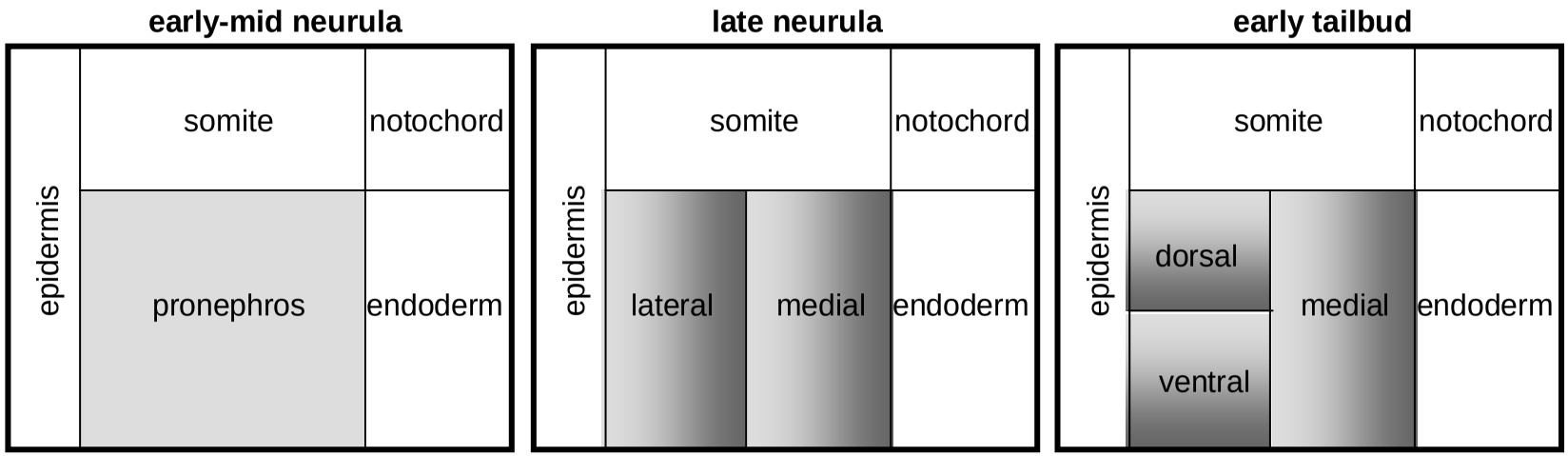

Figure 1.4 Patterning events that subdivide the *Xenopus* pronephric anlagen. By late neurula (stage 20), the pronephric anlagen get subdivided into the lateral and medial domains. By late neurula (stage 26), the lateral domain is once more divided into dorsal and ventral domains. Figure adapted from Vize et al., 2003.

mesoderm, the presumptive notochord. Some markers of early dorsoventral patterning include the signalling molecule *wnt4* and members of the *notch* family. At stage 18, *wnt4* is the first gene to be activated, followed by *delta1* at stage 19, *notch1* at stage 20 and *serrate1* at stage 22. It has been shown that over-expression of the *notch* pathway blocks the intermediate/distal tubules formation, whereas blocking *notch* signalling enhances it (McLaughlin et al., 2000). These results suggested that this system plays a role in defining pronephric compartment boundaries.

Once the pronephric mesoderm has been specified, it undergoes morphogenesis, ultimately resulting in a functional organ. The pronephric nephron forms by a process of rearrangement or segregation. The first sign of pronephric morphogenesis is a change in cell shape in the somatic intermediate mesoderm at early tailbud stage. Pronephric cells reorganize to form a compact structure just ventral to the somites. The cell mass that forms is then called the pronephric primordium or anlagen. At stage 25, once the pronephric anlage has formed, the intermediate/distal/ connective tubule that derives from a rudiment, begins its caudal migration which is completed at stage 37 when it fuses with the rostrally migrating rectal diverticulum (Nieuwkoop and Faber, 1994). Following segregation, the pronephric primordium begins to be shaped both dorsally and ventroposteriorly. On the dorsal side, the anlagen change from a round shape into a 'τ' shape. On the ventroposterior margin, the future distal tubule is pushed anteriorly so that it lies below the most anterior of the forming dorsal branches. Finally, the proximal and distal tubule grows and extends and the pronephric sinus becomed vascularised.

Around stage 55-57, the function of the pronephros is no longer sufficient as the animal has grown and needs a more complex excretory system. As the animal is ready to undergo metamorphosis, the pronephros will degenerate by apoptosis and will be replaced by the mesonephros, the adult functioning organ.

1.3.2.2 Pronephros anatomy.

The best stage to describe *X. laevis* pronephros anatomy is at stage 38, when the pronephric components have fully differentiated and are functional. The blood is filtered by the pronephric glomus or glomerulus, which is vascularised by capillaries branching from the dorsal aorta and which projects into the coelom (Fig 1.5, figure adapted from Reggiani et al., 2007). Fluids are then driven from the coelom into the pronephric tubules by the nephrostomes that are thin epithelial ciliated funnels. Nephrostomes have no resorptive or excretory activity (Fig 1.5, arrows pointing three nephrostomes). The nephrostomes are linked to the proximal tubules by short branches. The surface of the proximal tubules is covered with microvilli, called brush borders, which function to reabsorb molecules by enhancing surface area (Fig 1.5 PT1 and PT2). Fluids moving through the proximal tubules drain into a single common tubule that has a greater diameter (Fig 1.5 PT3). Useful molecules that have been reabsorbed by the proximal tubules from the glomerular filtrate, return to the blood circulation through a network of veins that surrounds the proximal tubules known as the pronephric sinus. The sinus receives blood from the glomus, the anterior/posterior cardinal veins, the branchial veins and the external jugular veins (Fig 1.5 red arrow). Urine and molecules that were not reabsorbed by the proximal tubules are moved through the intermediate/distal tubules, which forms an "S" shape (Fig 1.5 IT1, IT2, DT1 and DT2). The intermediate/distal tubules are constituted of two types of cells. Cells that stain with the 4A6 antibody which probably correspond to principal cells and those which do not stain with 4A6 which probably correspond to intercalating cells observed histologically. These latter cells are characterised by large number of mitochondria. Finally, urine is eliminated from the organism by the connecting tubule that connects with the cloaca (Fig 1.5 CT).

1.3.2.3 The pronephros function.

We understand that vertebrates that live in water have to constantly excrete large volumes of dilute urine to cope with the constant influx of water through the skin and gut (Vize et al., 2003). However, ions are in low concentration in such environments. Vertebrates consume energy using active transport processes to take up ions from the surrounding medium. Thus, the need of producing large volumes of urine and the

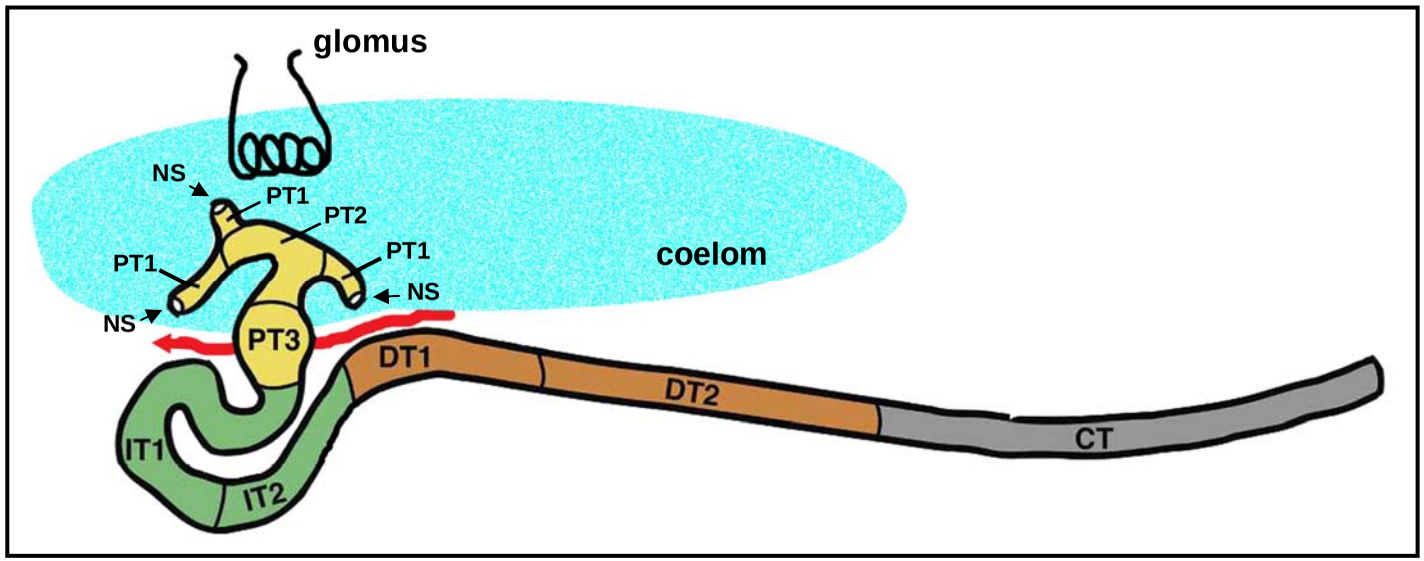

The anatomy of the *Xenopus* pronephros. Figure adapted from Vize et al., 1997, Reggiani et al., 2007 and Raciti et al., 2008. Key: Nephrostomes, NS. Proximal tubule, PT1, PT2, PT3. Intermediate tubule, IT1, IT2. Distal tubule DT1, DT2. Connecting tubule, CT.

Figure 1.5 The anatomy of the *Xenopus* pronephros at stage 38. Blood is filtered by the glomus, then, useful molecules are reabsorbed by the pronephric proximal tubules and finally, the wastes are driven outside the organism by the connecting tubule.

need of minimizing ion loss implicate the pronephros in effective resorptive processes. Molecules that must be effectively recovered from the kidney filtrate are organic and inorganic ions, amino acids, bicarbonates, carbohydrates, lipids and water itself (Dantzler et al., 1988). A key player in active transport of small molecules and ions across the kidney epithelial membranes is the sodium potassium ATPase. This transporter uses the energy from hydrolysis of one molecule of ATP to extrude three cytoplasmic Na^+ into the body fluids for two extracellular K^+. These, in turn, power cotransporters that utilize the resulting electrochemical gradient to reabsorb the useful molecules from the kidney filtrate (Drummond et al., 1998).

The single pronephric nephron, organised into discrete functional segments, is composed of distinct renal epithelial cell types. Each cell type carries out specific functions to regulate fluid balance, osmolarity and metabolic waste excretion. The segments do not operate independently but rely on the correct spatial organisation along the nephron to insure normal excretory functions. The segmental organisation of the pronephric nephron also demonstrates regionalised expression of transporters and ion channel genes along the proximodistal axis (Eid, et al., 2002). For example, *scl5a11, slc5a2* and *slc7a13* mark the proximal tubule whereas, *clcnk*, *slc12a1* and *slc12a3* mark the intermediate/distal and connecting tubules (Reggiani et al., 2007 and Raciti et al., 2008).

More generally, the role of the pronephros is to filtrate blood, reabsorb useful molecules and excrete wastes. In addition to these three major functions, the regulation of water balance is controlled by the glomus. The proximal tubules can reabsorb large particles such as blood cholesterol (Gérard and Cordier, 1934). The distal tubules control the water reabsorption and recovery of solutes from the glomeral filtrate, insuring a physiological osmoregularity (Ultsch et al., 1999). The pronephros functions to excrete toxic nitrogenous waste such as ammonia (Munro, 1953). There is some evidence suggesting that the pronephros contributes to the regulation of blood pH (Vize et al., 2003). Amphibian pronephroi also function as hematopoietic organs and are a major site of myeloid cell differentiation (Carpenter and Turpen, 1979). The hematopoietic tissue is distinct from the vascular sinus surrounding the tubules, being separated from it by an endothelial barrier.

1.4 Molecular markers of early kidney development, used in this thesis.

Figure 1.6 shows the three pronephric compartments and the key times of expression of some known molecular markers that have been used in this work. Figure 1.6 does not show the full expression pattern of these genes, it only represents the expression of pronephric genes during the key events of pronephric specification, morphogenesis or maturation. *lhx1, pax8* and *wt1* will be used to perform *in situ* hybridization in whole *Xenopus* embryos as markers of specification. The antibodies 3G8 and 4A6, recognising specifically the pronephric proximal and intermediate/distal tubules respectively will be used to perform antibody staining in whole mount *Xenopus* embryos or in embryonic explants to identify these differentiated components. Finally, the remaining pronephric markers will be used in RT-PCR analysis to confirm the presence of pronephric tissue in embryonic explants and whole embryos. Where these molecules have been used in gene function studies in another organism, mouse, they are shown in table 1.1.

1.4.1 Markers of pronephros specification.

1.4.1.1 *lhx1*, the first marker of pronephros specification.

lhx1 encodes a DNA binding homeodomain and constitutes the earliest marker of nephrogenesis (Taira et al., 1994). *lhx1* is activated in the pre-pronephric region immediately following gastrulation. It expression extends from the ventral border of the somites to the ventral mesoderm in a vertical strap-like shape. By stage 22, *lhx1* is expressed in a broad teardrop-shaped pattern in both the proximal and the intermediate/distal tubules anlagen. During early tadpole stages, when the proximal tubule begins to lumenize, *lhx1* expression becomes restricted to the proximal tubule and more specifically to the very dorsal tips of the tubule. Close analysis of the *lhx1 in situ* pattern in early tadpoles revealed that the *lhx1* expression domain demarcates a zone of tubule growth, where new cells are being added to the tip of each proximal tubule branch (Carroll et al., 1999). Similarly, in the developing intermediate/distal tubule extending posteriorly from the pronephric anlagen toward the cloaca, *lhx1* is reduced in the anterior portion of the intermediate/distal tubule but is maintained in

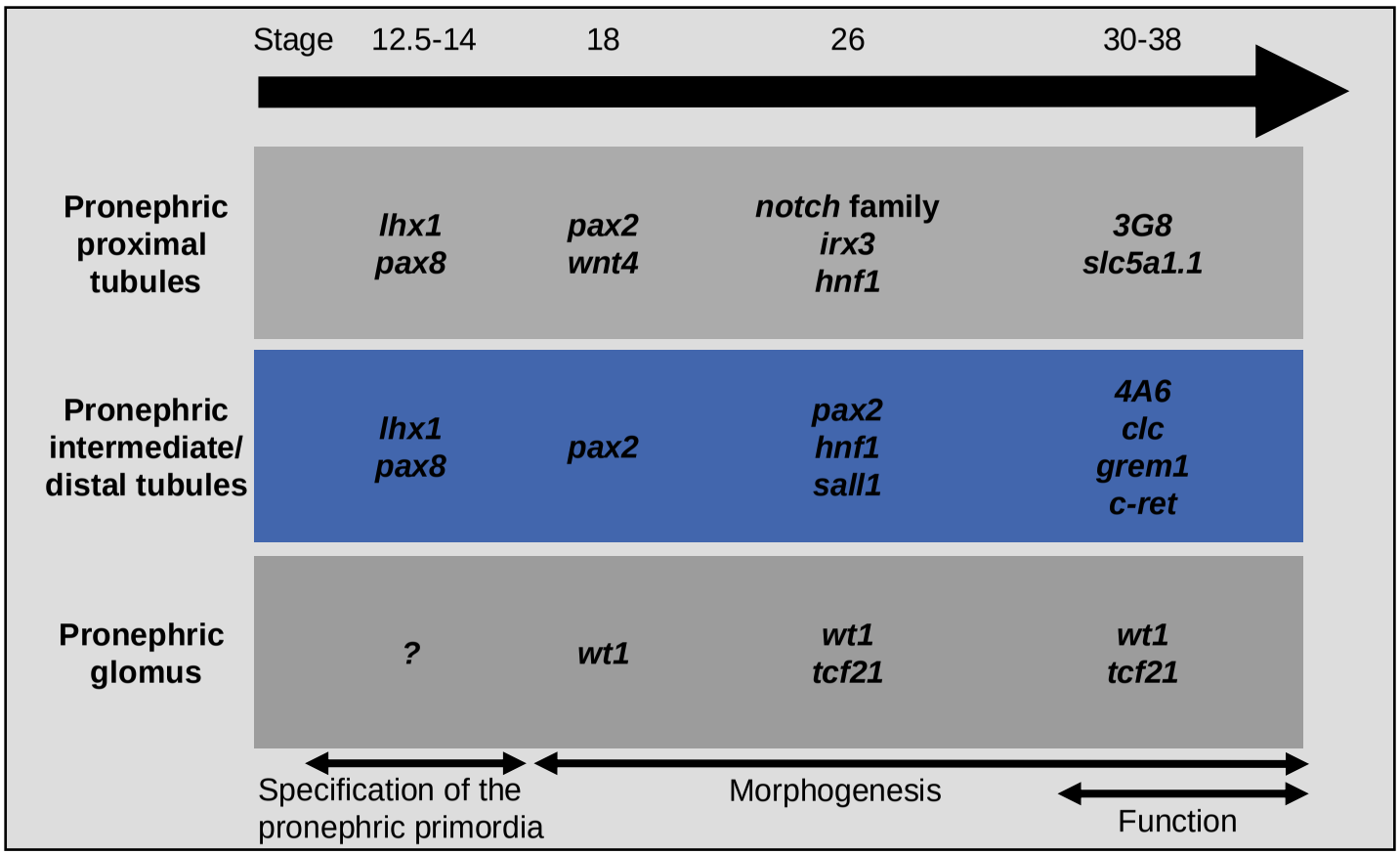

Figure adapted from Ryffel (2003)

Figure 1.6 Pronephric compartments and key expression time of some molecular markers. During the pronephros specification, morphogenesis and function, various set of genes are turned on specifically marking one of the three pronephric compartments, proximal tubules, intermediate/distal tubules and the glomus.

	Expression					
Marker	**Pronephros**	**Nephric duct**	**Mesonephros**	**Metanephros**	**Mutant phenotype**	**References**
bmp7	+	+	+	+	No metanephros	Hawley et al., 1995. Dudley et al., 1995.
lhx1	+	+	+	+	No metanephros	Taira et al., 1994a. Shawlot and Behringer, 1995.
pax8	+	?	+	+	Normal kidney	Mansouri et al., 1998
wt1	+	-	+	+	No metanephros	Carroll and Vize, 1996. Kreidberg et al., 1993.
wnt4	+	-	+	+	No metanephros	Stark et al., 1994.
pax2	+	+	+	+	No metanephros	Torres et al., 1995.
notch1	+	?	+	+	Glomerular defects	Leimeister et al., 2003. McCright et al., 2001.
hnf1α	+	-	+	+	Renal dysfunction	Weber et al., 1996. Pontoglio et al., 1996.

Table 1.1 Some kidney markers and their expression within the three kidneys forms and their phenotypic consequences of targeted mutagenesis in developing mice. Table adapted from Vize et al., 1997.

the posterior portion. This again supports the idea that *lhx1* is defining the growth zone of the forming intermediate/distal tubule (Carroll et al., 1999).

1.4.1.2 *pax8*, a second marker of pronephros specification.

pax8, belongs to the *pax* gene family of transcription factors playing fundamental roles during organogenesis. This family is characterised by the presence of a 128 amino acid paired domain encoding a unique DNA-binding motif. *pax8* is expressed in the prospective otic placode and in the intermediate mesoderm, indicating that *pax8* plays a central role in auditory and excretory system development (Heller and Brändli, 1999).
At the time at which the pronephric anlagen is specified, stage 12.5, *pax8* is actively expressed in a patch directly behind the head and ventral to the anterior somites (Carroll and Vize, 1999). It is believed that *pax8* plays a role in the specification of the pronephric mesoderm and constitutes a direct response to the anterior somite-derived inductive signal. After neurulation, *pax8* expression can be seen in both the pronephric proximal and intermediate/distal tubules. During pronephric kidney morphogenesis, *pax8* is found in the proximal tubule and in the elongating distal tubule. By stage 31, expression in the distal tubule progressively ceases, while transcription in the differentiating proximal tubule remains at high levels until stage 36-37, when the pronephric kidney becomes functional (Heller and Brändli, 1999). To summarise, *pax8* is one of the initial responses to specification of the pronephric primordia between stage 12.5 and 14. its expression responding to the somitic inducing signal.

1.4.1.3 *wt1*, a marker of medial patterning during pronephros specification.

The zinc-finger transcription factor encoded by the Wilm's tumor suppresser gene *wt1* is required primarily for the development of the vascular component of the pronephros, the glomus (Carroll and Vize, 1996). Expression of *wt1* is initiated at stage 18 and is expressed only in the medial portion of the developing pronephric mesoderm. It is the first obvious indicator of medio-lateral patterning. *wt1* acts in pronephros formation by restricting cell fate and reserving a pool of cells in the pronephric anlagen for the later formation of the glomus (Carroll et al., 1999). From

stage 20 onwards, *wt1* is a marker of the pronephric glomus, but not after stage 35, where its expression is also found in the heart.

1.4.1.4 *wnt4*, a source of dorsoventral patterning.

At stage 18, just prior to the first morphological signs of pronephric differentiation, *wnt4* is weakly expressed throughout the pronephric mesoderm. As the embryo develops, *wnt4* expression increases in the pronephric proximal tubules and proximal intermediate/distal tubule anlagen. During the tailbud stage, *wnt4* expression is quite strong in the developing proximal tubule but starts declining in the developing intermediate/distal tubule. By the early tadpole stage, *wnt4* ceases to be expressed in the pronephric intermediate/distal tubule and is restricted to the anterodorsal portion of the proximal tubule anlagen corresponding to the dorsal tips of the growing tubule (Carroll et al., 1999). The role of *wnt4* in pronephros formation has been shown to be essential for tubulogenesis (Saulnier et al., 2002). This will be discussed in section 1.4.2.1.

1.4.1.5 *pax2* is associated with the onset of the pronephros morphogenesis.

pax2, another member of the the *pax* gene family of transcription factors, is expressed at very low level in the pronephric mesoderm at stage 22. However, its expression strengthens progressively throughout the tailbud stage. By late tailbud stage, *pax2* is strongly expressed in both the proximal and intermediate/distal tubule anlagen, suggesting a role in the maintenance of the pronephric fate (Heller and Brändli, 1997). As the tubules develop further, *pax2* is relatively stronger in the nephrostomes of the proximal tubule and in cell migrating caudally from the rectal diverticulum to joint the distal tubule.

1.4.1.6 Functional synergism between *lhx1*, *pax8* and *pax2*.

In *Xenopus* embryos, targeted over-expression of *pax8* mRNA results in the development of large and ectopic pronephroi. Moreover, coinjection of *pax8* and *lhx1,* enhanced this effect and resulted, at a high frequency, in the formation of greatly enlarged and ectopic kidney structures (Taira et al., 1994). This effect was

shown to be synergistic rather than additive (Carroll and Vize, 1999). *pax8* and *lhx1* are initially expressed in overlapping domains in late gastrula embryo and cells expressing both genes lead to pronephros formation. This observed synergism between *pax8* and its cofactor *lhx1* is very likely to be responsible for the establishment of the pronephric primordia during normal development.

The closely related gene *pax2*, is also capable to synergise with *lhx1* in a similar manner, suggesting that *pax2* and *pax8* are functionally redundant in pronephros development. However, *pax2* expression normally starts in tailbud embryos (Brennan et al., 1998) when the *pax8* and *lhx1* domains are already established. Therefore, *pax2* is more likely to play a role in *Xenopus* pronephric morphogenesis than in pronephros patterning.

By late gastrula, at stage 12.5, expression of both *pax8* and *lhx1* can be detected in the pronephric primordia. At stage 14, *pax8* expression appears in a large round area ventral to the presumptive anterior somites. In contrast to *lhx1*, the *pax8* expression domain does not extend into the ventral lateral plate mesoderm. Although, these two genes seem to be activated within/in the intermediate mesoderm at the same time, *pax8* is only expressed in a dorsal subset of cells that express *lhx1*, implying that the transcription of the two genes is controlled independently. Then, over a similar time period, the *pax8* and *lhx1* expression pattern refines to a teardrop shape that corresponds to the future pronephric primordium. By stage 23, the pronephric expression of both genes is indistinguishable (Carroll and Vize, 1999).

Following the onset of *pax2* expression, around stage 22, the expression pattern of *pax8* and *lhx1* diverges. *pax2* and *lhx1* expression becomes refined to the nephrostomal tips of the proximal tubule, while *pax8* expression remains throughout the proximal tubule. *lhx1* and *pax2* are also expressed in the intermediate/distal tubule at this stage, while *pax8* is not. This suggests that the *lhx1* expression domain initially refines to become coincident with *pax8* and later possibly undergoes a second refinement to become coincident with *pax2*. *pax2* may substitute for *pax8* as the cofactor of *lhx1* during the later stages of kidney development (Carroll and Vize, 1999).

1.4.2 Markers of pronephros morphogenesis.

1.4.2.1 The notch signalling pathway is involved in pronephric tubule differentiation.

During development, the transmembrane notch protein (notch1) recognizes its membrane-bound ligands delta (dll1) and serrate (jag1) and controls cell fates through local cell-cell interactions in a number of different tissues. *dll1* and *notch1* can first be detected in the region of the developing pronephric anlage at stages 21-22, which correspond to the time that the pronephros can be distinguished morphologically as a thickening layer below somites 3-5. *jag1* starts to be expressed within the pronephric anlagen around stage 23-24. At stages 30-31, *dll1* expression pattern is restricted to the dorsoanterior portion of the tubule anlage, whereas *jag1* is expressed throughout the developing proximal tubule. The expression of *notch1* is maintained in a pattern overlapping both ligands. *dll1* is no longer detectable in the pronephros from stage 33 onwards.

Studies of McLaughlin et al., 2000 have suggested that the *notch* signalling pathway functions to inhibit the intermediate/distal tubule differentiation in the dorsoanterior region of the pronephric anlage where cells are normally fated to form proximal tubules. However, recently in our lab, the role of *notch* signalling during pronephros formation has been reinvestigated. In early tailbud, around stage 30, *notch* has been shown to be expressed in the dorsoanterior pronephric mesoderm. We have shown that over-expression of *notch* promotes formation of the glomus and the nephrostomes at the expense of more distal tubule structure. This suggests that *notch* signalling is involved in the medio-lateral separation of the glomus and nephrostomes rather than proximal tubules versus distal tubule as suggested by McLaughlin. There is evidence suggesting that this might be achieved by setting up a boundary rather than by lateral inhibition (Naylor, personal communication).

1.4.2.2 *irx3* directs nephron segment identity.

The *Iroquois* (*irx*) gene family encodes homeodomain containing transcription factors and studies in *Xenopus* and mouse have shown that *irx1*, *irx2* and *irx3* are expressed in the developing nephron but that *irx4*, *irx5* and *irx6* are not (Bellefroid et

al., 1998, Houweling et al., 2001). Within the *Xenopus* pronephros, *irx3* expression is initiated at stage 25 and ceases at stage 35. During this time, *irx3* is confined to the common proximal tubule that links the three other smaller proximal tubules together, and in the intermediate tubule IT1 and IT2. *irx3* expression is followed, at stage 30, by the expression of *irx1* and *irx2*, that persists within the pronephros after stage 35. *irx1* and *irx2* expression is confined to the intermediate tubule segment IT1 (Reggiani et al., 2007).

Loss-of function studies, using 5ng of morpholino injected into single V2 blastomere of 8-cell stage, indicate that *irx1* and *irx2* morpholinos injected alone or together do not affect kidney formation. In contrast, *irx3* morpholino led to highly specific defects in pronephric kidney development, affecting the formation of PT3 and intermediate tubules. This result suggests that *irx3* is required for the early specification of the large common proximal tubule and the entire intermediate tubule. Gain-of-function studies, over-expressing 0.15 to 0.25ng of *irx3* mRNA into one blastomere of 2-cell stage or into single V2 blastomere of 8-cell stage embryos, resulted in the formation of ectopic development of intermediate tubules in the *Xenopus* mesoderm. These results show that irx3 is necessary and sufficient to specify nephron segment fate *in vivo* (Reggiani et al., 2007).

1.4.2.3 *hnf1*, marker of pronephros morphogenesis.

In human, the tissue-specific transcription factors *hepatocyte nuclear factor hnf1α, hnf1β* and *hnf4* are responsible for maturity onset diabetes of the young (MODY). In addition, the mutated *hnf1β* gene causes defective development of the kidney and genital malformation. Wild et al., 2000, showed that introduction of two *hnf1β* mutants responsible for the onset of MODY and severe primary renal defects, into *Xenopus* embryos, leads to defective development and agenesis of the pronephros. This result suggests that *hnf1β* is not only an early marker of kidney development but is also functionally involved in the pronephros morphogenetic events.
Moreover, as *hnf1β* together with *pax8* and *lhx1* constitute the earliest regulators in the pronephric anlage, it is possible that they cooperate during early nephrogenesis (Wu et al., 2004). In this study, these authors have shown that *hnf1β* over-expression can overcome the enlargement and the induction of an ectopic pronephros caused by

over-expression of *pax8* and *lhx1*. They observed that *hnf1β* acts antagonistically to *pax8* and *lhx1* during nephrogenesis, confirming previous studies of Wild et al., 2000, that *hnf1β* have distinct morphognetic properties during nephrogenesis (Wu et al., 2004).

1.4.2.4 *sall1*, marker of anterior tubule epithelium.

The spatial and temporal expression pattern, in *Xenopus* embryos, of the zinc-finger transcription factor *sall1* was characterised by Hollemann et al., 1996. They reported that *sall1* is mainly expressed within the central nervous system, in the midbrain, the hindbrain and the spinal chord. *sall1* was also found weakly expressed in the pronephric intermediate/distal tubule around stage 30. *sall1* mRNA transcripts were also detected in the kidney of adult frogs among others organs. However, in 1999, Brändli redefined *sall1* expression pattern and showed that at stage 38 *sall1* is strongly expressed in the common tubule and in the anterior segment of the pronephric intermediate/distal tubule. This result strongly suggests that *sall1* has a role in the patterning of the anterior part of the tubule epithelia and therefore constitutes an excellent pronephric tubule marker.

1.4.2.5 *tcf21*, marker of the pronephric glomus.

Transcription factor 21 (*tcf21*), also known as *pod1*, belongs to the class B basic helix-loop-helix transcription factor family that are involved in cell lineage commitment and organogenesis. In mammalian metanephrogenesis, *tcf21* has been shown to be required for the terminal differentiation and branching morphogenesis of the glomeruli (Cui et al., 2003). Simrick et al., 2005 carried out RT-PCR analysis in dissected pronephric anlagen of *X. laevis* embryos from stage 12.5 until stage 35 and in the three isolated pronephric components, proximal tubules, intermediate/distal tubules and glomus in embryos at stage 42. Their results showed that *tcf1* starts to be expressed within the pronephric anlagen around stage 15, increases gradually as the pronephros develops, to reach its maximal expression in the functional glomus in stage 42 embryos. This result suggests that *tcf1* is involved in the pronephric glomus formation but by yet an unknown mechanism. Preliminary functional analysis by both over-expression and morpholino analysis also supports this.

1.4.3 Markers of pronephros maturation.

1.4.3.1 Antibodies 3G8 and 4A6, markers of the proximal tubules and intermediate/distal tubules, respectively.

Kidney extracts from adult and larval *X. laevis* were used to immunize 6-week-old Balb/c females and spleen cells were isolated and fused to raise monoclonal antibodies against kidney specific antigens. Two monoclonal antibodies were selected as pronephros specific, 3G8 and 4A6, both of which are of the IgG subclass. The molecular nature of the antigen recognized by 3G8 is unknown, but antibody 4A6 recognizes a 50 x 10^3 M_r protein present on Western blots containing extracts of isolated stage 47 pronephroi. Antibody 3G8 stains only the apical surface of tubule epithelia, whereas, antibody 4A6 stains the entire cell surface (Vize et al., 1995). Antibody 3G8 recognizes the pronephric proximal tubules and the nephrostomes from stage 31 onwards, and also stains the border of the otic vesicule but does not react with the intermediate/distal tubule. The initiation of the 3G8 staining pattern corresponds to the time at which the lumen of the pronephros forms and expands. By stage 34, the entire tubular structure is strongly stained (Vize et al., 1995).

Antibody 4A6 is first detected in the anterior-most portion of the intermediate/distal tubules around stage 38. At this stage, antibody 4A6 binds to most, but not all, the cell in the intermediate/distal tubule, with a smaller proportion of cells staining positively at their posterior end. Positive staining is seen over the entire surface of those cells that bind 4A6. By stage 41, the duct has retracted as the endoderm and cloaca have migrated anteriorly. As a consequence, 4A6 staining is now more dense in posterior regions of the intermediate/distal tubule (Vize et al., 1995).

Therefore, antibodies 3G8 and 4A6 are excellent markers of the pronephros terminal differentiation as they stain respectively the proximal tubules and the intermediate/distal tubules without cross reacting.

1.4.3.2 *slc5a1.1*, an highly specific molecular marker for pronephric proximal tubule epithelia undergoing maturation and terminal differentiation.

Tadpoles cannot afford to excrete glucose and the sodium-dependent glucose co-transporter (*SGLT, slc5a1.1*), member of the solute carrier family 5 (*slc5*), plays a key role in resorption of this critical solute (Zhou and Vize, 2004). 91 solute carrier genes have been identified in the *Xenopus* pronephros, with highly regionalized patterns. For example, *slc5a2*, *slc5a1.1*, *slc7a1.3* are strictly restricted to the proximal tubules, whereas, *slc12a1* is expressed in intermediate/distal tubule, and *slc12a3* in distal/connective tubule (Reggiani et al., 2007).

In *Xenopus* embryos, no *slc5a1.1* expression could be observed at gastrula and neurula stages. *slc5a1.1* expression occurs in late tailbud stages (stage 29/30), and was restricted to the developing pronephric kidney. *slc5a1.1* transcripts are exclusively detected in the epithelia of the proximal tubules, including the three connecting tubules and the common tubule but absent in the intermediate/distal tubule. Up to stage 40, all other organs are devoid of *slc5a1.1* expression. It was observed that *slc5a1.1* expression, detectable at stage 29/30, follows the expression of Na^+, K-ATPase at stage 26. This suggesting that the sodium gradients generated by the activity of Na^+,K-ATPase provide the driving force for the onset of *slc5a1.1* expression (Eid et al., 2002). In *Xenopus* adults, *slc5a1.1*is abundantly expressed in the small intestine and the kidney (Eid et al., 2002).

In mouse embryos, *slc5a1.1* transcripts and protein are detected as early as day E16 in tubular segments of the renal cortex and outer medulla (Yang et al., 2000). It was suggested, that *slc5* genes are associated with late phases of metanephric kidney development, when tubules begin to mature and acquire reabsorptive transport properties (Horster, 2000).

In conclusion, expression of the sodium-dependent solute cotransporter genes in segments of the excretory system appears to be conserved between the pronephric and the metanephric kidneys (Eid et al., 2002). Also, in *Xenopus* embryos, *slc5a1.1* constitutes an excellent marker for both *in situ* and RT-PCR analysis of the late maturing pronephric proximal tubule epithelia (Zhou and Vize, 2004).

1.4.3.3 *clc-k*, specific marker for the *Xenopus* pronephric intermediate/distal and connective tubule.

Chloride channel kidney-(specific) (*clc-k*) is expressed in the vertebrate kidney and is involved in the chloride resorption. Renal expression of *clc-k* is confined to the maturing epithelia of the pronephric intermediate/distal tubule (Maulet et al., 1999). In adult frog, *clc-k* expression is restricted to the kidney and is not expressed in any other tissues examined, including, liver, lung, muscle, heart and brain (Maulet et al., 1999). In *Xenopus* embryos, *clc-k* expression is first observed at stage 31 in the intermediate/distal segment of the pronephric nephron and at lower levels in the connective tubule (Vize, 2003). Its expression in these pronephric segments is robust by stage 32 and continued to the latest stage examined, stage 43. The intermediate/distal segment is a major site of filtrate resorption that is essential for larva survival (Vize et al., 2002). The tissue specificity of *clc-k* along with its exclusion from the proximal tubule makes this gene a very useful marker for analysing the development of the embryonic kidney. In addition, *clc-k* localization corresponds to the beginning of the physiological characterisation of the pronephros, as early as stage 31 (Vize 2003).

1.4.3.4 *grem1*, a marker of differentiated intermediate/distal tubule.

grem1 belongs to the DAN family of cystein knot proteins involved in regulation of BMP activity. *grem1* is particularly known to act as an antagonist of the BMP signalling that is expressed in the neural crest (Hsu et al., 1998). In fact, in the developing *Xenopus* embryo, *in situ* analyses have revealed that *grem1* expression begins at the tailbud stage in the neural crest lineage. At stage 27, *grem1* appears in the pronephric intermediate/distal tubule and as the embryo extends, *grem1* expression seems to be extending anteriorly and caudally within the intermediate/distal tubule. *grem1* expression has been weakly observed in the intermediate/distal tubule of stage 42 embryos (Osafune et al., 2002). This result suggests a requirement for *grem1* activity during pronephros differentiation and final maturation.

1.5 The *wnt* gene family.

1.5.1 Introducing the *wnt* molecules.

Historically, two developmentally important genes have identified the founder members of the *wnt* gene family. The fly wingless (*wg*) was identified as a segment polarity gene in *Drosophila melanogaster,* functions during embryogenesis and during metamorphosis. The *int* genes were identified as homologuous vertebrate genes near several integration sites of the mouse mammary tumor virus (MMTV) (Uusitalo et al., 1999). Mutations of the *wingless* gene in the fruit fly were found in wingless flies, while tumors caused by MMTV were found to have copies of the virus integrated into the genome forcing overproduction of one of several *wnt* genes. The name *wnt* is the result of the acronym between **w**ingless and i**nt**. During development, *wnt* molecules have been shown to govern cell fate, proliferation, migration, polarity and death. In adults, inappropriate activation of the *wnt* pathway is implicated in a variety of cancers, in particular, mutation of the components of the *wnt/ß-catenin* pathway (Polakis, 2000).

wnt genes encode a large family of secreted proteins. In humans, 19 *wnt* proteins have been identified that share 27% to 83% amino-acid sequence identity and a conserved pattern of 23 to 24 cysteine residues. The *X. tropicalis* genome contains 24 *wnt* genes, with an additional copy of *wnt11*, *wnt11b,* and also *wnt7c, wnt9b, wnt10a* and *wnt16* (Garriock et al., 2007). The majority of *wnt* genes contain 4 coding exons, with exon1 containing the initiation methionine. *wnt* proteins are approximately 40kDa.

Analysis of the signalling activities has shown that the carboxy-terminal region of the wnt proteins play a role in determining the specificity of responses to different wnt. Abolition of the carboxy-terminal third of a wnt protein result in a dominant-negative protein, suggesting that the amino-terminal region mediate interaction with frizzled receptors but requires the carboxyl-terminus to activate these receptors (Du et al., 1995, Hoppler et al., 1996).

1.5.2 The *wnt* signalling transduction pathways.

Once secreted, *wnt* proteins associate with glycosaminoglycans in the extracellular matrix and bind tightly to the cell surface (Bradly et al., 1990, Reichsman et al., 1996). Reception and transduction of wnt signals involves binding of wnt proteins to members of two distinct families of cell-surface receptors, members of the frizzled gene family and members of the LDL-receptor-related protein (LRP) family (Bejsovec, 2000, Pandur and Kühl, 2001, Cadigan and Liu, 2006). The frizzled-receptor has an amino-terminal cystein-rich domain (CRD) that bind *wnt* ligands, a seven transmembrane domain and a short cytoplasmic tail containing a consensus PDZ domain binding motif (S/T-X-V) at the carboxyl terminus. Frizzled-receptors can signal through G-proteins to stimulate an increase in intracellular Ca^{2+} and activate a PKC (Sheldahl et al., 1999, Liu et al., 1999, Kühl et al., 2000).

wnt signalling is transduced through at least three distinct intracellular signalling pathways, the canonical *wnt/ß-catenin*, the non-canonical *wnt/*Ca^{2+} and the non-canonical *wnt/JNK* (also called the planar cell polarity (PCP) pathway). These pathways all lead to unique cellular responses. The *wnt/ß-catenin* pathway regulates cell fate determination during development, *wnt/JNK* pathway regulates cytoskeletal organisation and the biological function of the *wnt/*Ca^{2+} pathway is unclear.
Distinct classes of *wnts* molecules signal through either the canonical pathway (the *wnt1*-class, *wnt1, wnt3* and *wnt8*) or through the *wnt/*Ca^{2+} pathway (*wnt5a*-class, *wnt4, wnt5a* and *wnt11*). It seems that the *frizzled*-receptor proteins are also subdivided into similar functional groups. However, the activity of the *wnt* molecules *in vivo* might be determined by the nature of the frizzled-receptor present at the cell surface.

Figure 1.7 shows a simplified schematic representation of the *wnt* signalling transduction pathways. Intracellularly, canonical *wnt* signalling leads to stabilisation of cytosolic ß-catenin. *wnt* molecules bind to the seven-transmembrane frizzled receptor and *LRP5/6,* essential co-receptors of the *wnt* ligands, and this binding causes the frizzled protein to activate the Dishevelled protein (Dsh). Activated Dsh, in turn, inhibits the activation of the glycogen synthase kinase-3 (GSK3) enzyme. If GSK3 was activated, it would prevent the dissociation of the ß-catenin protein from

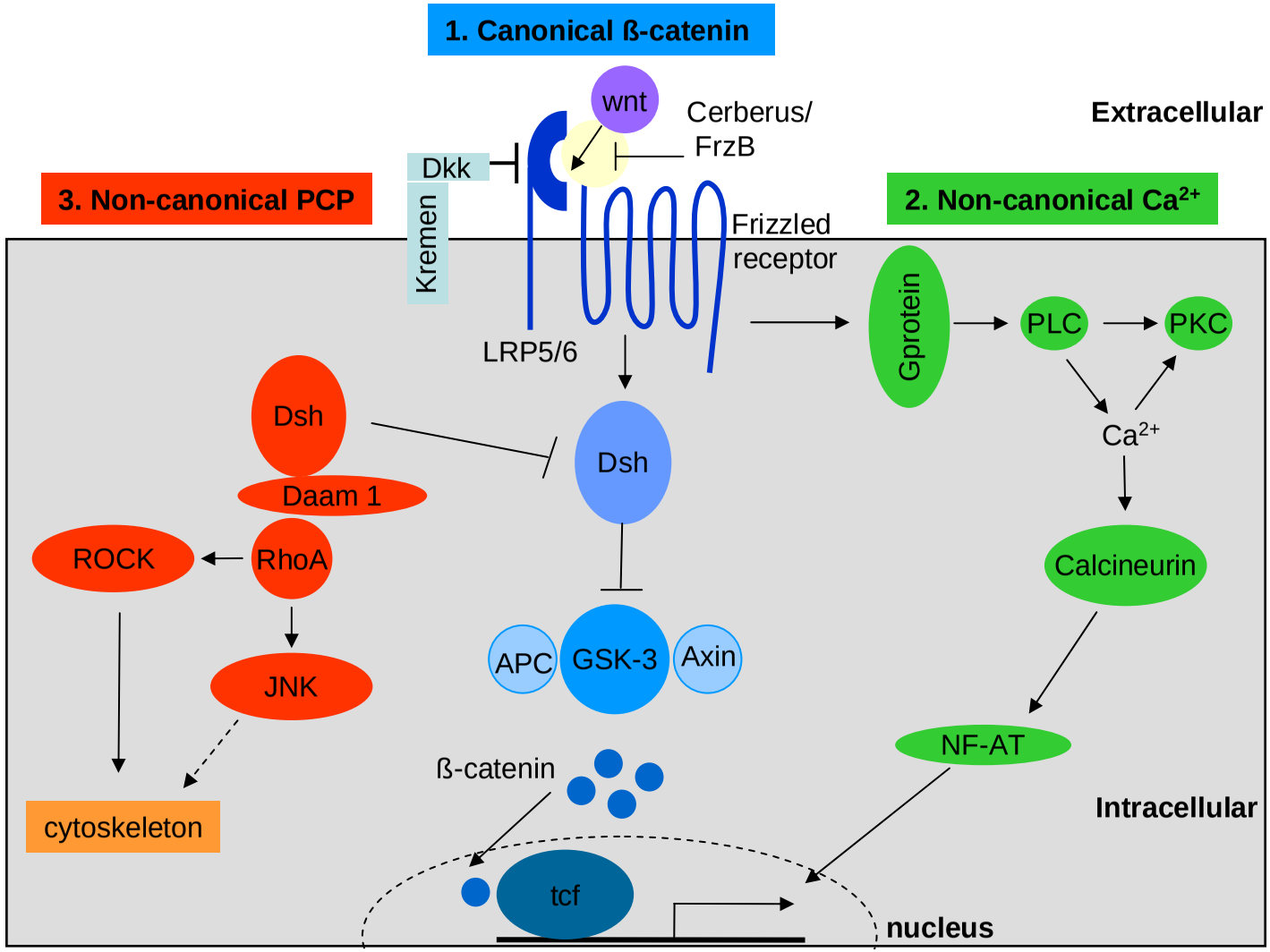

Figure adapted from Huelsken and Behrens, 2002.

Figure 1.7 Simplified schematic representation of the *wnt* signalling pathways. *wnt* molecules bind to the seven transmembrane Frizzled receptor and LRP5/6 co-receptors. Intracellularly, this binding leads to the activation of dsh protein that results in the inactivation of the GSK-3/APC/Axin complex, ensuring the stabilisation of the ß-catenin in the nucleus and activation of targeted genes via the transcription factor *tcf*. Non-canonical Ca^{2+}/*wnt* signalling acts through a G-Protein and results in the accumulation of Ca^{2+} in the cytoplasm. Non-canonical PCP pathway activates JNK and small protein RhoA and directs convergent extension movement during embryonic development.

the APC protein, which targets ß-catenin for degradation. However, when the *wnt* signal is given, and GSK3 is inhibited, ß-catenin can dissociate from the APC protein and enter the nucleus, where it binds to the transcription factor *tcf* and activates downstream target genes (Huesken and Berens, 2002). One way to inhibit the canonical *wnt/ß-catenin* pathway is to over-express a *dominant-negative tcf* (*dntcf*). The N-terminal deletion of the dntcf abrogates the interaction with ß-catenin, as well as the consequent transcription activation of specific *tcf* target genes, such as genes involved in axis formation (Molenaar et al., 1996). ß-catenin was also shown to function as a component of the cadherin complex, which controls cell-cell adhesion and influences cell migration (Nelson and Nusse, 2004). In the planar cell polarity pathway, *frizzled* activates JNK and directs asymmetric cytoskeletal organisation and coordinates polarization of cells. *dsh* is connected via *daam1* to downstream effectors such as the small *GTase rho* (Huesken and Berens, 2002). The *wnt/*Ca^{2+} pathway leads to release of intracellular calcium via activation of a G-protein. This pathway involves activation of phospholipase C (PLC) and protein kinase C (PKC). Elevated Ca^{2+} can activate the phosphatase calcineurin which leads to dephosphorylation of the transcription factor *NF-AT* and results in its accumulation in the nucleus. In *Xenopus* embryos, *NF-AT* activity suppresses canonical *wnt* signalling during axis formation (Huesken and Berens, 2002). Recently, the non-canonical *wnt* signalling pathway has been sub-divided into three pathways. One pathway involves activation of calcium/calmodulin-dependent kinase II (CamKII) and PKC. Another includes recruitment of GPT-binding proteins to activate PLC and phosphodiesterase (PDE). The last one concerns the PCP pathway that activates JNK. Calcium has been identified as an important second messenger in all of these pathways (Kohn and Moon, 2005).

wnt signals are modulated extracellularly by diverse secreted proteins, including members of the frizzled-related protein family (frp or frzB) (Moon et al., 1997), wnt-inhibitory factor-1 (wif1), (Hsieh et al., 1999), Cerberus (Piccolo et al., 1999), and dickkopf (dkk) (Nusse et al., 2001). frps, wif1 and Cerberus can bind wnt proteins directly and are thought to antagonize wnt function by preventing their interaction with frizzled-receptor. Frps can also interact with the frizzled-receptor and form a non-functional complex. dkk does not bind wnt but instead interacts with

the extracellular domain of LRP5/6, thereby blocking activation of *wnt* signalling (Bafico et al., 2001, Semënov et al., 2001).

1.6 *wnts* molecules used in this study.

Wnt signalling molecules are required at several stages of kidney development. For example, in the mammalian metanephros, the ureteric bud synthesizes *Wnt9b*, which is essential for induction of the mesenchyme to form nephrons, in response *Wnt4* is secreted by the induced metanephric mechenchyme and finally *Wnt11* is secreted by the ureteric bud tips, participating in a positive feedback loop promoting nephrogenesis. Also, there is evidence showing that *Wnt4* and *Wnt11*, at least in some cases, signal through the non-canonical *Wnt* signalling pathway, whereas *Wnt9b* activates the canonical *Wnt* signalling pathway in the kidney (Carroll et al., 2005).
As the *wnt* molecules are involved in a large spectrum of biological processes, in this section, I will focus only on the *wnt* molecules that have been utilised for the completion of this work, and summarise the literature concerning these *wnt* molecules in *Xenopus* development and in vertebrate kidney formation. *wnt* genes will be presented in numerical order but also grouped according to subclass.

1.6.1 The canonical *wnt* molecules used in this study.

1.6.1.1 *wnt6*, a somite epithelialisation factor from the ectoderm of chick embryos, plays a role in mouse kidney formation, and is expressed in various organs as they form during *Xenopus* embryogenesis.

In *Xenopus* embryos, the first *wnt6* temporal and spatial expression pattern was published by Wolda and Moon, in 1992. Unfortunately, they encountered difficulties in getting convincing and reliable data using the conventional RNA *in situ* method. They suggested that this might be due to a low mRNA abundance and secondary structure within the *wnt6* mRNA molecule itself. However, in adult *Xenopus* tissues, *wnt6* was clearly detected in the kidney, brain, muscle, lung and the heart (Wolda and Moon, 1992). In 2008, Lavery et al. published extensive data showing the expression of *wnt6* mRNA and protein during *Xenopus* development. They used a

novel digoxigenin (DIG)-labeled LNA modified oligonucleotide that has an increased affinity for RNA molecules compared with conventional RNA probes. *wnt6* mRNA is first detected at stage 18-19 and seems to be up-regulated in the dorsal tissue of the neural folds. By stage 23, *wnt6* is expressed in the surface ectoderm and in the developing organs such as the eye, the head region, the pronephric anlagen and the somites. By stage 28, *wnt6* is additionally expressed in the branchial arches, the fin, and in the ectoderm overlying the heart. At stage 40-43, the latest stages tested, *wnt6* is also observed in the pronephric tubules, the cloaca and the migrating hypaxial muscle. Immunochemistry using a specific *wnt6* antibody detected *wnt6* protein in the same spatial and temporal expression pattern as the *wnt6* mRNA. They noticed that *wnt6* mRNA and protein are expressed in epithelial tissues undergoing architectural rearrangement via epithelial-mesenchymal transition (EMT) and mesenchymal-epithelial transition (MET), essential steps in organogenesis.

In mouse embryos, *Wnt6* was shown to be expressed in the ureteric bud and to induce kidney tubule development *in vitro* (Itäranta et al., 2002). *Wnt6* is expressed throughout the ureteric bud during the growth of the epithelium into the nephric mesenchyme and in the branching ureter tips during subsequent metanephric development. Cell lines over-expressing *Wnt6* induce tubulogenesis and express early kidney induction markers such as *Pax2*, *Pax8* and *E-cadherin*. This result showed that *Wnt6*-expressing cells are sufficient to trigger the complete program of mesenchyme to epithelium transition. *Wnt6* is believed to give the signal that controls the differentiation of the mesenchyme during early mammalian metanephros formation (Itäranta et al., 2002).

The developmental role of *wnt6* has also been studied in chick embryos. *wnt6* was shown to be required for the epithelialisation leading to somite formation and subsequent compartmentalisation into the sclerotome and the dermomyotomes (Schmidt et al., 2004, Geetha-Loganathan et al., 2006, Schubert et al., 2002, Rodríguez-Niedenführ et al., 2003). Somites arise from the paraxial mesoderm that undergoes a mesenchymal to epithelial transition. The newly formed somites consist of an epithelial ball enclosing the somitocoel. Subsequent interactions between the somitocoel, the ventral and the dorsal part of the somites results in the formation of muscle among with other structures such as the vertebral column, the ribs and dermis

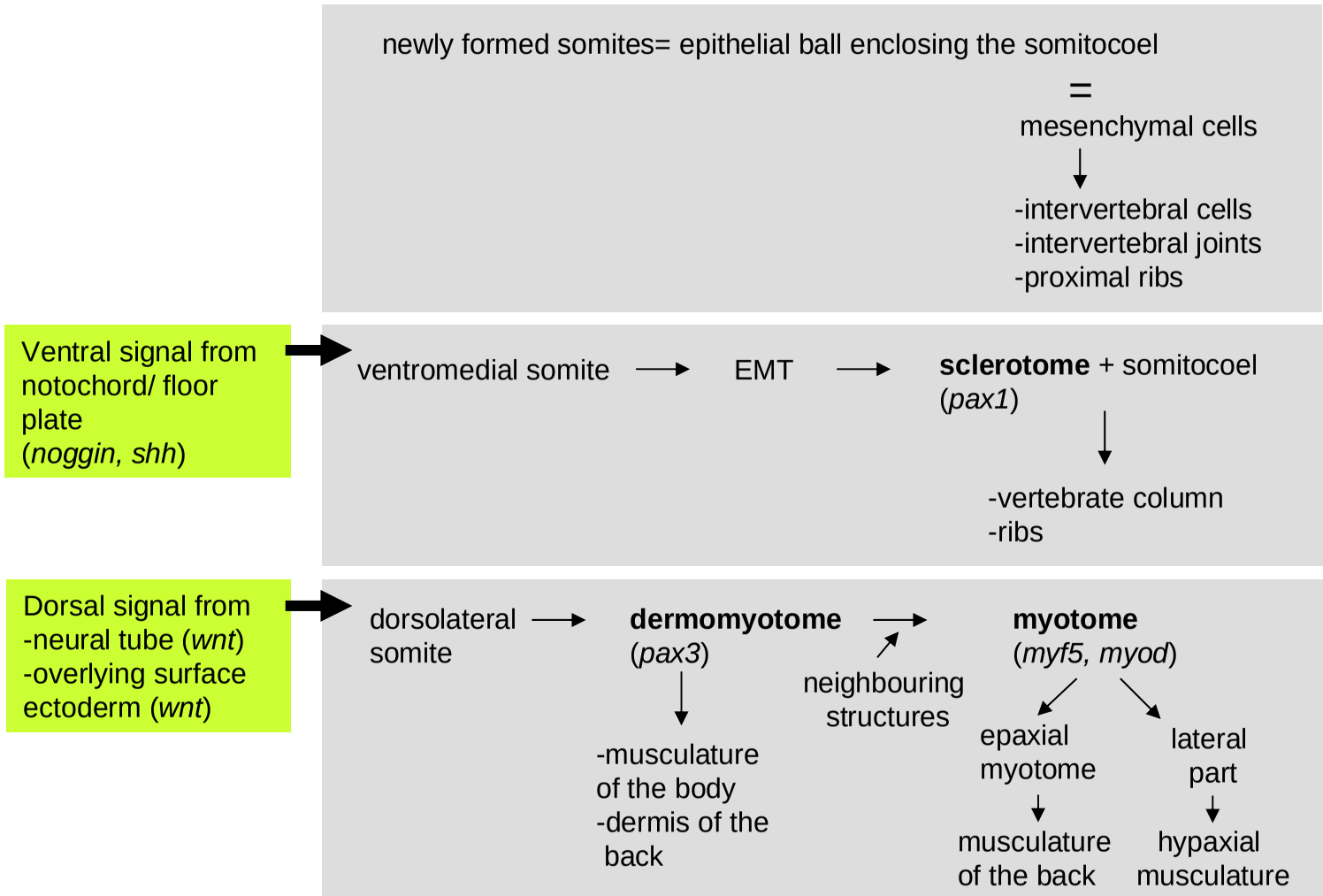

Figure 1.8 Signals inducing the different parts of the somites to differentiate into the sclerotome, the dermomyotome, the myotomes and their subsequent derivatives. Figure created from Schmidt et al., 2004.

(Schmidt et al., 2004). Figure 1.8 summarises the signals inducing the different parts of the somites to differentiate into sclerotome and dermomyotome and their subsequent derivatives, in chick embryos.

Signals from ectoderm overlying the somites or from midline structures are required for the transformation of the mesenchymally organised segmental plate into epithelial somites. *wnt6* expressed in the ectoderm overlying the somites is a candidate for this somite epithelialisation factor from the ectoderm. *wnt6* producing cells are capable of rescuing somite formation after ectoderm ablation. Over-expression of *wnt6* maintains the somites in an epithelial state showing that *wnt6* has a profound effect on the differentiation of somite derivatives (Schmidt et al., 2004).

E-cadherins are transmembrane adhesion molecules found on epithelial cells and are linked to the cytoskeleton by ß-catenin and form adherens junctions, a key feature of epithelial tissue. Translocation of free ß-catenin to the plasma membrane, where it complexes with E-cadherin confers epithelial characteristics to the cell, without protein translation or gene transcription (Wiggan and Hamel, 2002). The mechanism by which *wnt6* could hypothetically operate during the epithelialisation of the segmental plate during somite formation, suggests that *wnt6* acts to stabilise adherens junctions possibly by translocating ß-catenin to the plasma membrane and not to the nucleus.

The medial-ventral portion of the somites escapes the epithelialising properties of *wnt6* through the action of an antagonist, *sfrp2* (secreted frizzled-related proteins 2). Together, expression and regulation of the *wnts* and their antagonists could explain the formation of somites (Schmidt et al., 2004).

In chick limb myogenesis, the precursors of limb muscle are provided by the lateral portion of somites, where the limb muscle precursor cells migrate from the dermomyotome as single cells into the limb bud. However, in the absence of ectoderm, the precursor cells never form muscle cells, but differentiate into endothelial cells. Both dorsal and ventral limb ectoderm is able to influence myogenesis. In early embryos, *wnt6* is expressed in a subset of ectodermal cells. Later, *wnt6* is strongly expressed in both, the dorsal and the ventral limb ectoderm. *wnt6* is secreted from the ectoderm and influences the precursors cells to form muscle even in the absence of ectoderm. All together, these results suggest that *wnt6* provides the ectodermal signal that induces somite-derived progenitor cells to form

muscle cells in the limb, possibly by inducing the *myf5*-dependent myogenic pathway (Geetha-Loganathan et al., 2006).
Additionally, *wnt6* is expressed in the epidermis at site of cranial muscle formation, including regions around the eye and also in the inner ear, during cardiac cushion formation and signals during the development of the neural folds. The precise pattern of *wnt6* expression during chick embryo development shows that *wnt6* marks sites of epithelial transformations were crucial changes in tissue architecture are taking place (Schubert et al., 2002).

Finally, *wnt6* has been shown to function as a neural crest inducer (García-Castro et al., 2002) and to be involved in the feather formation in chick embryos.

1.6.1.2 *wnt7b* induces neural crest markers in *Xenopus* embryos and tubulogenesis in cell lines.

In *Xenopus, wnt7b* was shown to be maternally expressed. During embryonic development, *wnt7b* is evenly distributed over the animal half and marginal zone of the embryo at gastrula stage. Expression of *wnt7b* gradually localises to the dorsal neural tube as well as in the epidermis after neural tube closure. *wnt7b* is detected in the roof plate of the neural tube, in a segmented pattern of expression along the dorsal half of the somites immediately underneath the skin and in the epidermal tissue (Chang and Hemmati-Brivanlou, 1998). In *Xenopus* embryos, *wnt7b* was shown to induce neural crest markers *slug* and *twist* in ectodermal explants co-injected with neural inducer *noggin* and in ectodermal cells neuralized by dissociation and to alter the expression pattern of several neural genes, the pan-neural marker, *ncam*, the anterior brain marker, *otxa*, the hindbrain marker, *krox20* (Chang and Hemmati-Brivanlou, 1998).

In mouse embryos, *wnt7b* is expressed in the collecting duct epithelium which derives from the ureteric duct, from E13.5 onwards (Kispert et al., 1996, Carroll and al., 2005). *In vitro*, NIH3T3 cells expressing *wnt7b* co-cultured with metanephric mesenchyme formed complex epithelial tubules with differentiated glomeruli, suggesting that *wnt7b* is sufficient to trigger tubulogenesis (Kispert et al., 1998). However, expression of *wnt7b* in the collecting ducts makes it unlikely that it is

involved in inductive events between the ureter and the mesenchyme (Kispert et al., 1996). It is more likely that *wnt7b* expressed in the spinal chord, gives the signal for tubulogenesis, as spinal chord constitutes a robust inducing activity for renal tubule formation (Parr et al., 1993). This thesis will directly test the ability of *wnt7b* in inducing tubule formation in *Xenopus* Holtfreter sandwich cultures.

1.6.1.3 *wnt8*, a *wnt1*-related gene, is responsive to mesoderm-inducing growth factors and plays a role in dorsoventral patterning of *Xenopus* embryos.

In *Xenopus* embryos, *wnt8* transcripts are first detected during the blastula stage and the level of expression increases rapidly, reaching a maximum by early gastrula (stage 10). At stage 10, transcripts are localised within the ventral vegetal quadrant of gastrulae, specifically within ventral mesodermal cells. At stage 18, *wnt8* increases gradually towards the posterior end of the embryo. At stage 22, the *wnt8* gene is expressed predominantly in the ventral region. Transcripts decline during the neurula and tailbud stages, becoming undetectable by the tadpole stage (Christian et al., 1992, Li et al., 2006). Assays in *Xenopus* embryos showed that mesoderm induced by growth factors like *bfgf* or *activin A* lead to *wnt8* expression, however, the converse does not appear to be true. *wnt8* might normally function in specifying a ventral fate to newly induced mesoderm (Christian et al., 1992). Furthermore, *wnt8* might ventralize the response of lateral mesodermal cells to dorsalizing signals from the organizer, and thus contributing to dorsoventral patterning of the embryonic mesoderm, contributing to body pattern (Moon and Christian, 1992).
In the literature *wnt8* has never been described as having a role to play during kidney formation. In this work, the expression of the different *wnt* molecules within the developing pronephros was investigated and *wnt8* was detected in the early isolated pronephric anlagen but not after stage 20 (Chapter4). Also, *wnt8* was detected more strongly in the posterior somites than in the anterior somites. All together, these data suggest that *wnt8* is unlikely to control the early events of pronephros formation. For this reason, in this thesis, *wnt8* was chosen and expected to act as a non-pronephric inducer with the aim of validating the specific pronephric inductive activity that some of the other *wnt* molecules might display. However, Chapter 5 will show very unexpected results with regards to this.

1.6.1.4 *wnt9* genes have a role to play during *Xenopus* and mouse kidney development.

1.6.1.4.1 Mouse *Wnt9b* is required for mammalian urogenital system formation.

Expression of *Wnt9b* in mouse embryos was found throughout gestation from E9.5 to E17.5 with a peak of expression at E10.5 to E12.5. *In situ* hybridization analysis of E16.5 mouse embryos showed that *Wnt9b* is detected in organs or tissues that normally undergo epithelial-mesenchymal transition during development. Examples of such tissues are the lung, the nephrons of the kidney, the enamel epithelium of the developing tooth and the epithelium of the submandibular gland (Qian et al., 2003). Within the forming kidney, *Wnt9b* is expressed throughout the Wolffian duct epithelium and its derivatives in both sexes from E9.5 to E14.5, in the ureteric bud as it invades the metanephric anlage at E10.5-E11.0, and continues to be expressed in the developing collecting duct system throughout nephrogenesis. By E15.5, expression is confined to the kidney (Carroll et al., 2005). *Wnt9b* is also detected in the brain, the spinal chord, cranial ganglion, olfactory epithelium, intestinal epithelium, epidermis and muscle. There is little or no expression of *Wnt9b* in the heart, liver or cartilage. *Wnt9b* is strongly expressed in the newborn mouse kidney. In the mouse adult organs, transcripts of *Wnt9b* are most abundant in kidney, low but detectable in male preputial gland, the female mammary gland, liver and brain (Qian et al., 2003).

The role of *Wnt9b* in kidney formation is as a common organizing signal. *Wnt9b* is essential for metanephric kidney development as embryos homozygous for null *Wnt9b* develop to term but die within 24 hours of birth. Pups possess only vestigial kidneys and lack reproductive ducts at birth. *Wnt9b* is required for multiple aspects of the urogenital system development, for both mesonephric and metanephric tubule induction, for posterior extension of the Müllerian duct and the generation of a functional female reproductive tract. *Wnt1* can rescue all aspects of *Wnt9b* deficiency, implicating a canonical *Wnt* pathway downstream of receptor activation in mouse urogenital development (Carroll et al., 2005).

Some *Wnt* molecules have transforming activity. *Wnt1*, can morphologically transform the epithelial cell line (C57MG) from an epithelial to a fibroblastic morphology. There is evidence showing that this transforming activity is dependent on the stabilization of β-catenin by *Wnts* (Shimizu et al., 1997). Over-expression of *Wnt9b* in C57MG mammary epithelial cells caused small transformed foci in cell monolayers and a moderate morphological transformation in pooled colonies compared to *Wnt1*. This result suggests that *Wnt9b* can transform C57MG cells but is not as potent as *Wnt1*, the transforming *Wnt* molecule used as a positive control in this assay. Similarly, the majority of G418 resistant cells infected by *Wnt9b* expressing retroviral vectors changed to a spindle-shaped elongated morphology, but retained more of their contact inhibition and adhesion characteristics than did *Wnt1* transformed cells. Because *Wnt9b* has a transforming activity, but this activity is not as strong as that of *Wnt1*, *Wnt9b* is termed a moderately transforming *Wnt* molecule (Qian et al., 2003).

1.6.1.4.2 The *Xenopus* paralogues *wnt9a* and *wnt9b* have a different expression pattern during early *Xenopus* development.

Analyses of gene synteny combined with comparisons of primary peptide sequence alignments and BLAST searches have allowed the identification of previously uncharacterised *wnt* genes in bird, frog and fish genomes (Garriock et al., 2007). Conservation of synteny is defined as the presence of two or more pairs of orthologous genes at equivalent positions in the genome of two species, regardless of orientation or order (Nadeau and Sankoff, 1998). Genes sharing synteny in different organisms will be orthologues. Results of their searches identified the *X. tropicalis* *wnt9a* and *wnt9b* genes.

The *X. tropicalis wnt9a* (formerly *wnt14*) sequence encodes a protein that is 90% and 82% identical to chicken and human *wnt9a*, respectively. *wnt9a* is first detected at the early tail bud stage, stage 32, throughout the length of the developing pronephric intermediate/distal tubule. At stage 37, *wnt9a* expression persists in the pronephros and is also detected in endoderm tissue corresponding to the lung primordium. *wnt9a* expression remains prominent in the pronephric intermediate/distal tubule and in the lung buds until stage 40, the latest stage tested (Garriock et al., 2007).

In the frog genome, the *wnt9b* (formerly *wnt15*) gene is duplicated. The two sequences, *wnt9b* and *wnt9b.2,* are 98% identical. The *X. tropicalis wnt9b* gene encodes a protein that is 64% and 65% identical to chicken and human *wnt9b*, respectively. *wnt9b* transcripts are first observed at stage 22 in the epidermal ectoderm overlying the branchial arch region and expression persists until stage 26. Transverse sections revealed that *wnt9b* expression was limited to the inner ectodermal layer of the branchial arches. At stage 35, *wnt9b* is weakly expressed in the eye. By stage 39, *wnt9b* is visible in the ectoderm adjacent to the cement gland and persists weakly in the eye (Garriock et al., 2007). This expression pattern contrasts with that observed in mouse, where *wnt9b* is expressed in the Wolffian duct epithelium and in the ureteric bud (Carroll et al., 2005). These observations suggest that the embryonic expression pattern of *wnt9b* is not conserved among species. Chapter 3 of this thesis will further address this point by examining the embryonic expression pattern of *wnt9b* during *X. laevis* and *X. tropicalis* early development.

1.6.2 The non-canonical *wnt* molecules used in this study.

1.6.2.1 *wnt4* is critically required for pronephros and metanephros tubulogenesis.

In mouse embryos, *Wnt4* is expressed in kidney mesenchyme and its derivatives. *Wnt4* starts to be detected in condensed mesenchyme cells on both sides of the stalk of the ureter from day E11.5, and its expression correlates with the site where the first pretubular cell aggregates form. During subsequent development, this expression pattern is repeated in newly forming aggregates, as well as in the epithelial tubular derivatives. At later stages, *Wnt4* expression becomes restricted to the periphery of the kidney where new tubules are forming. During mesonephric formation, *Wnt4* is expressed throughout the mesonephric tubules from the aggregating mesenchyme until fusion of the epithelial tubule with the Wolfian duct. Thus, it is likely that the role of *Wnt4* is conserved during the mesonephros and metanephros formation (Stark et al., 1994).

To explore *Wnt4* function, *Wnt4* null allele mice were generated. Adult mice heterozygous for the disrupted allele showed no obvious phenotype. However, homozygous *Wnt4*$^{-}$ pups died within 24hours of birth. Embryos showed small agenic kidneys, consisting of undifferentiated mesenchyme. Thus, death of homozygous

pups is almost certainly due to the lack of kidney function. Analyses of kidney development in mutant embryos, revealed that induction of kidney mesenchyme by the ureter was unaffected. However, mutant embryos had undergone excessive branching of the ureter epithelium into a mesenchyme that remained morphologically undifferentiated, thus, resulting in no mesenchyme aggregation and hence no nephrons (Stark et al., 1994). At the molecular level, expression of *wt1* was unchanged. *n-myc*, an early marker of tubule induction, and *pax2* were absent in the tubule of the mutant embryos, suggesting that the mesenchyme cells fated to form tubule were induced but failed to convert into an epithelial structure (Stark et al., 1994). Regulation of cell adhesion is critical for mesenchyme to epithelial transition and *Wnt4* may regulate mesenchyme aggregation and tubule formation through modulation of cell adhesion factors. In conclusion, *Wnt4* acts as an autoinducer of the mesenchyme to epithelial transition that underlies nephron development (Stark et al., 1994).

Further analyses in mouse embryos, *Wnt4* was shown to be required for tubule formation, and sufficient to trigger tubulogenesis in isolated metanephric mesenchyme, whereas *Wnt11* which is expressed in the tip of the growing ureter is not (see later). These results lend additional support to the notion that *Wnt4* is a key autoregulator of the MET during nephrogenesis (Kispert et al., 1998).

It has been shown that *wnt4* is highly expressed in the kidney epithelial MDCK cells (Madin-Darby Canine Kidney cells), that are competent to form tubules *in vitro* (Lyons et al., 2004). These authors confirmed that the canonical *wnt/ß-catenin* pathway mediated by *wnt4* is active in MDCK cells. MDCK cells express the *Frizzled-6* (*frz6*) receptor which forms a molecule complex with *wnt4*. However, *frz6* does not appear to transduce *wnt4* canonical signalling. Thus, presumably, there exists another unknown *frizzled* receptor that mediates *wnt4* activation during kidney tubulogenesis. To conclude, one can speculate that *wnt4* binds both canonical and non-canonical frizzled receptors, activating *wnt* signalling pathways that may each contribute to kidney tubule formation (Lyons et al., 2004).

In *Xenopus*, *wnt4* expression starts to be detected ventrally to the anterior somites at stage 19 embryos. By stage 24, *wnt4* is expressed in the anterior region of the

pronephric anlage contributing to the proximal tubule. By stage 32, *wnt4* is expressed in the nephrostomal segments of the pronephric tubule. Transverse sections showed that *wnt4* is expressed in tubule epithelia. From stage 35, *wnt4* expression begins to decline, concomitant with the maturation of pronephric tubule. Throughout pronephros development, *wnt4* is absent from intermediate/distal tubule. These observations suggest that transformation of the intermediate mesoderm to tubule epithelia is associated with the onset and sustained expression of *wnt4* (Saulnier et al., 2002).

Injection of 0.25ng of *wnt4* mRNA into a single V2 blastomere at the 8-cell stage did not lead to ectopic pronephric tissue formation. *In situ* hybridization with the pronephric markers *lhx1* and *pou2* showed normal expression in the intermediate/distal tubule. However, *lhx1* expression in the nephrostomes was not longer visible as the three characteristic distinct entities. The nephrostomes appeared to be fused into a single structure (Saulnier et al., 2002). Injection of 5ng of *wnt4* morpholino into a single V2 blastomere at the 8-cell stage resulted in strong down-regulation of tubule specific markers. *pax2* was absent in proximal tubule but its expression in the intermediate/distal tubule was unaffected. *clc-k*, a marker of terminal differentiation, expressed normally in maturing epithelia of the intermediate/distal tubule, was also unaffected. *slc5a1*, a marker of late maturing pronephric tubule epithelia, was not detected in such embryos. Together, these data suggest that inhibition of *wnt4* functions result in inhibiting specifically the expression of early and late markers of the pronephric proximal tubule (Saulnier et al., 2002). Presumably, ectopic expression of *wnt4* may prematurely drive cells of the pronephric anlagen into differentiation and thus prevent the attribution of sufficient progenitor cells to form three proximal tubules. Alternatively, *wnt4* inhibits morphogenetic movements in pronephric tubule anlagen, which may normally ensure the establishment of three distinct proximal tubules. The role of *wnt4* in tubulogenesis appears to be conserved between pronephric and metanephric kidneys (Saulnier et al., 2002). Controversially, in our lab, it was recently shown that injection of 1ng of *wnt4* mRNA into a single V2 blastomere at the 8-cell stage resulted in ectopic formation of nephrostomal and glomeral tissues and in drastic reduction of proximal/intermediate and distal tubular tissues, when embryos were analysed at tadpole stage by *in situ* hybridization with the glomus marker, *nephrin*,

the nephrostome marker, *odf3*, and the proximal/intermediate/distal tubule antibodies 3G8 and 4A6 (Naylor and Jones, personal communication). Also, in such embryos, the expression of the *notch* ligand *serrate* was increased whereas *delta1* was decreased. These results suggest that *wnt4* is likely to be required for nephrostome and glomus formation rather than pronephric tubules formation. Presumably *wnt4* would promote glomus and nephrostomal cell fate in the dorsal proximal region of the pronephros by interfering with the *notch* signalling pathway.
In this thesis, the capability of *wnt4* in inducing pronephros formation will be directly tested using the Holtfreter sandwich cultures assay (Chapter 5).

1.6.2.2 Non-canonical *wnt5a* is involved in morphogenetic movements during early embryonic development.

WNT5A has been shown to be expressed in multiple organs in early human embryos from 28 to 42 days of gestation. *WNT5A* was found in the mesenchyme surrounding the Müllerian duct, the Wolfian duct and the nephric tubule of the developing kidney, in the gonads, in the heart, the frontonasal mesenchyme, the midbrain, the hypophysis and the branchial arches. *WNT5A* was observed in the mesonephros of a 38-day embryo but not at 42-days (Danielson et al., 1995). A highly similar expression pattern was found in mouse embryos from day E6.5 to E14.5 with the exception of the renal expression (Gavin et al., 1990).

In mouse embryos, *Wnt5a* has been shown to regulate cell proliferation and differentiation processes in several structures that require extension. *Wnt5a* mutant mouse embryos showed an inability to extend the anterior-posterior axis due to a progressive reduction in the size of caudal structures. In limb development, inhibition of *Wnt5a* function results in reduced proliferation of putative progenitors cells within the progress zone. *Wnt5a* mutant embryos also showed outgrowth defects in the developing face, ears and genitals. Thus, *Wnt5a* is required for the regulation of the development of many structures that require extension from the primary body axis, by regulating the proliferation of progenitors cells (Yamaguchi et al., 1999).

In *Xenopus* embryos, *wnt5a* transcripts are detected in oocytes and throughout development. At late gastrula stage (approximately stage 11), *wnt5a* transcripts are

detectable in a diffuse pattern, enriched in the ectoderm. By late neurula stage (stage 20), *wnt5a* transcripts are enriched in the anterior and posterior of the embryo, relative to the middle of the embryo. At tadpole stage (stage 34), *wnt5a* is expressed in both neural and non-neural ectoderm and in the somitic mesoderm (Moon et al., 1993). Injection of 20 to 75pg of *wnt5a* mRNA resulted in embryos developing with abnormal phenotypes. Embryos showed complex head abnormalities, when mRNA was injected into dorsal blastomeres at the 4-cell stage, and supernumerary tails or other tail defects, when mRNA was injected into ventral blastomeres at the 4-cell stage (Moon et al., 1993). However, injection of *wnt5a* mRNA has no effect until the movements of gastrulation commence. Furthermore, injection of *wnt5a* mRNA blocks the elongation of animal caps in response to activin, without blocking the differentiation of either dorsal or ventral mesoderm within these explants. These results suggest that *wnt5a* acts as a modulator of morphogenetic movements (Moon et al., 1993).

When over-expressed in *Xenopus* embryos, the *wnt1* class (*wnt1, wnt3a, wnt8* and *wnt8b*) promotes duplication of the embryonic axis, whereas *wnt5a* class (*wnt5a*, *wnt4* and *wnt11*) alters morphogenetic movements (Du et al., 1995). Members of the *wnt5a* class antagonize the ability of ectopic *wnt1* class to induce a secondary axis, possibly by decreasing cell adhesion, since ectopic expression of *wnt5a* leads to decreased Ca^{2+}-dependent cell adhesion. Thus, *wnt5a* class can interact with *wnt1* class in an antagonistic manner (Torres et al., 1996). However, inhibition of convergent extension movements by *wnt5a* over-expression in the dorsal mesoderm of *Xenopus* embryos is independent of the canonical *wnt* signalling (Wallingford et al., 2001). In other words, *wnt5a* does not inhibit morphogenesis by down-regulating the canonical *wnt* pathway but by activating a different pathway (Wallingford et al., 2001). In zebrafish embryos, it was shown that ectopic expression of *wnt5a* enhances the concentration of intracellular Ca^{2+}, whereas *wnt8* does not. Thus, intracellular signalling by non-canonical *wnt5a* involves modulation of an intracellular Ca^{2+} signalling pathway (Slusarski et al., 1996), which may involve G-protein activity.

1.6.2.3 *wnt11* (formerly *Xenopus wnt11-related*), is involved in various organ formation.

Xenopus, zebrafish and chicken have two distinct *wnt11* genes, whereas mammalian genomes contain a single *wnt11* sequence (Garriock et al., 2007). The first *Xenopus wnt11* identified was characterised by Ku and Melton in 1993 and the second *Xenopus wnt11-related* gene was identified and characterised by Garriock et al. in 2005. The two *Xenopus wnt11* genes share 65% of DNA sequence identity. Sequence alignments and analysis of gene synteny within *X. tropicalis*, chicken, zebrafish and human genomes have revealed that the previously described *Xenopus wnt11-related* gene is actually the *wnt11* mammalian ortholog and therefore should be referred to as *Xenopus wnt11* (*wnt11*), whereas the first identified *Xenopus wnt11,* having no mammalian gene ortholog, should be referred as *wnt11b*, according to the *wnt* molecule nomenclature (Garriock et al., 2007). In this thesis we will adopt this nomenclature throughout.

In *Xenopus* embryos, *wnt11* does not start to be expressed before the late gastrulation stage. At stage 13, *wnt11* is expressed in two symmetrical lines very close to the position of the neural folds. At early organogenesis, stage 22, *wnt11* transcripts are detected along the dorsal axis in the brain, the dorsal neural tube and the extreme dorsal region of the somites. At mid-organogenesis, stage 26, *wnt11* is expressed in the dorsal mesenchyme extending from the otic vesicle to the tail, in the branchial arch region and in the nervous system. At late organogenesis, stage 28, when the first cardiac differentiation markers are expressed, and immediately prior to fusion of the heart tube, *wnt11* expression is visible in the heart primordia. In the tailbud embryos, stage 35, *wnt11* is also detected in the mesenchymal cells of the dorsal fin and within the heart, its expression is restricted to the anterior myocardium including the outflow and the ventricle. By the tadpole stage, stage 45, *wnt11* is expressed throughout the myocardium but more strongly in the ventricular tissue (Garriock et al., 2005).
wnt11 does not induce a secondary axis when mis-expressed in *Xenopus* embryos. However, over-expression of *wnt11* causes severe disruption of normal gastrulation movements with embryos showing incomplete closure of the blastopore and neural tube (Garriock et al., 2005). *wnt11* was shown to act through the non-canonical JNK

pathway. Inhibition of function of *wnt11,* using an oligo morpholino approach, showed that it had no detectable effect on expression of *mhcα*, which is an early and very strong marker of myocardial differentiation. Injected embryos showed that the heart primordial did not fuse properly and 10% of the embryos exhibited a pronounced cardia bifida phenotype. *wnt11* morpholino-injected embryos also showed a thicker myocardial layer on the injected side. Histological analyses revealed that the extracellular space between neighboring cells was increased possibly due to decreased adhesion between cells. All together these results suggest that *wnt11,* not expressed in cardiac tissues until about the time of myocardial differentiation, is very unlikely to have a role in cardiac lineage induction. However, *wnt11* might function to control cell behaviour during morphological movements, possibly via the JNK pathway (Garriock et al., 2005).

In *Xenopus* embryos, *wnt11* is expressed in both the neural crest cells and somites that migrate to contribute to the fin mesenchyme. *wnt11* is expressed prior to migration and persists in the mesenchyme cells after they have migrate throughout the fin. Loss-of-function experiments demonstrate that *wnt11* activity is required for an epithelial-to-mesenchymal transformation (EMT). Inhibition of *wnt11* function results in embryos lacking the fin core cells and lead to defective dorsal fin development and collapse of the fin structure. Experiments using molecules inhibitors of the non-canonical *wnt* pathway indicates that *wnt11* activity, in the dorsal migration of fin core cells, is dependent on calcium signalling through calcium/calmodulin-dependent kinase II (CaMKII) (Garriock and Krieg, 2007).

In mouse embryos, after the outgrowth of the ureteric bud, the reciprocal interaction between the ureteric bud and the metanephric mesenchyme induces branching of the ureteric bud and rescues the metanephric mesenchyme from apoptosis (Saxén, 1987). *wnt11* has an unique expression pattern with the developing metanephros and is expressed in the branching ureteric tips epithelium throughout renal development suggesting a possible function in regulating ureteric branching morphogenesis (Kispert et al., 1996). The *wnt11* mouse mutant embryos, develop reduced branching and smaller kidneys and *gdnf* expression level is reduced whereas *pax2* expression remains unaffected (Yu et al., 2004). *wnt11* functions, in part, by maintaining normal expression levels of *gdnf*, a mesenchymally produced ligand for the *ret tyrosine*

kinase receptor that is crucial for normal branching. Conversely, *wnt11* expression is reduced in the absence of *ret/gdnf* signalling. These observations suggest that *wnt11* and *ret/gdnf* cooperate in a positive autoregulatory feedback loop to coordinate ureteric branching by maintaining an appropriate balance of *wnt11* expression in the ureteric epithelium and *gdnf* in the mesenchyme to ensure continued metanephric development (Majumbar et al., 2003, Chi et al., 2004). However, although *wnt11* is expressed in the tips of the growing ureter where tubules induce activity, *wnt11* was shown not to be able to induce tubule formation in cell lines assay (Kispert et al., 1998).

1.6.2.4 Maternal *wnt11b* (formerly *Xenopus wnt11*) is required for dorso-ventral axis formation, for convergent extension movements during gastrulation, in heart formation and in neural crest cells migration.

During *Xenopus* development, *wnt11b* is expressed in oocytes and throughout development. The vegetal localization of *wnt11b* mRNA in oocytes is consistent with the idea that *wnt11b* could contribute to a signal, which emanates from vegetal cells to induce and/or pattern mesoderm in the marginal zone and which also signal from the dorsal marginal zone which can dorsalize more lateral and ventral mesoderm (Spemann, 1938, Yamada, 1950, Dale and Slack, 1987), suggesting that *wnt11b* might be involved in dorsal-ventral axis formation (Ku and Melton, 1993, White and Heasman, 2008). At the 8-cell stage, *wnt11b* mRNA is localised to the vegetal hemisphere. From late blastula (stage 9), *wnt11b* mRNA is visible as a crescent in the marginal zone on one side of the embryo, with higher levels on the dorsal side above the blastopore lip. Staining is present initially in both the superficial and deep layer of marginal zone cells. As gastrulation proceeds (stage 12.5), *wnt11b* is expressed in a ring around the closing blastopore. At late neurula, *wnt11b* is expressed both dorsal to and ventral to the closed blastopore. By early tailbud (stage 22-23), *wnt11b* is detected in the somites and in the first branchial arch (Ku and Melton, 1993). Additionaly, it was shown that wnt11b protein is asymmetrically distributed along the dorsal-ventral axis. This asymmetry occurs by the 64-cell stage, before the beginning of zygotic transcription. These observations suggest that wnt11b distribution is dependent on the cytoplasmic rotation in the first cell cycle that establishes the vertebrate dorsal-ventral axis (Schroeder et al., 1999). It has also

been shown that maternal *wnt11b* is both necessary and sufficient for the activation of axis formation, possibly by acting through the activation of the canonical pathway (Tao et al., 2005, Jessen et al., 2005). This idea was further supported as it was shown that establishment of the dorsal axis requires maternal *lrp6*, a component of the canonical *wnt* pathway, that degrades axin protein resulting in stabilization of *ß-catenin* that is enriched on the dorsal side of the embryo (Kofron et al., 2007).

Injection of *wnt11b* mRNA into UV-ventralised embryos can significantly rescue the formation of dorsal axial structures. Embryos developed a well-formed trunk, with somitic muscle and a neural tube but failed to develop notochord and head structures (Ku and Melton, 1993). However, *wnt11b* is not capable of inducing mesoderm in animal cap assays. Together, these results suggest that *wnt11b* is not a mesoderm inducer but is capable of dorsalizing pre-existing mesoderm (Ku and Melton, 1993).

Transcription factor *τ* (*brachyury*) is essential for gastrulation movements in *Xenopus* and mouse embryos (Conlon et al., 1996, Kispert et al., 1995a). *wnt11b* is a downstream target of *τ* and is required for normal gastrulation movements in *Xenopus* (Smith et al., 2000, Tada and Smith., 2000). A C-terminally truncated form of wnt11b protein was constructed and was shown to act in a dominant-negative fashion (dnwnt11b). *dnwnt11b* inhibits the function of the class of *wnt* which includes *wnt5a* and *wnt11b* but does not inhibit the function of the *wnt1* class. This same dnwnt11b construct will be used in Chapter 6 of this thesis. dnwnt11b blocks gastrulation movements and embryos showed a lack of posterior structures, although differentiation of muscle and notochord in anterior regions occurres normally (Smith et al., 2000). These results were supported by the fact that dnwnt11b prevents elongation of activin-induced animal caps. This suggests that *dnwnt11b* prevents normal convergent extension movements but does not affect mesodermal specification (Smith et al., 2000). During gastrulation movements, *wnt11b* has been shown not to signal through the canonical *wnt* pathway involving *gsk3* and *ß-catenin* but through another pathway that is similarly required in planar cell polarity (PCP) in *Drosophila*. This pathway involves small GTPases such as rho and rac, followed by the activation of JNK kinase protein (Axelrod et al., 1998, Boutros et al., 1998, Zhu et al., 2006). This pathway has been implicated in migration and cell shape changes which occur during gastrulation and dorsal closure in *Drosophila* (Barett et al., 1997,

Noselli and Agnes, 1999). In summary, *wnt11b* might be controlling convergent extension movements and cell polarity during gastrulation (Smith et al., 2000, Tada and Smith., 2000). This role for *wnt11b* is further supported by studies on the homeobox gene *otx2,* expressed during gastrulation in the anterior domain of the embryo, and involved in neural and head induction during *Xenopus* early development. *otx2* prevents convergent extension movements in trunk and posterior mesoderm by repressing the expression of *τ* and *wnt11b* and blocking the Jun N-Terminal Kinase pathway (Carron et al., 2005). The *heparin sulphate proteoglycan 4* (*gly4*) has been shown to be expressed in the dorsal mesoderm and ectoderm during gastrulation. Downregulation of *gly4* inhibits cell-membrane accumulation of *dsh* and disturbs cell movements during gastrulation. *gly4* protein physically binds *wnt* ligand and functions in the non-canonical PCP pathway (Ohkawara et al., 2003). Another component of the JNK pathway, *prickle* (*pk*), a *Xenopus* homolog of a *Drosophila* PCP gene, has been shown to severely perturb gastrulation movements when mis-expressed in *Xenopus* embryos (Takeuchi et al., 2003). Also, during Zebrafish gastrulation, *rok2* a downstream effector of the non-canonical *wnt* pathway, acts downstream of *wnt11b* and mediates mediolateral cell elongation required for dorsal cell movement (Marlow et al., 2002). Controversially, it was shown that *lrp6,* which plays a role in the *ß-catenin wnt* signalling, regulates convergent extension movements during *Xenopus* gastrulation by opposing the *wnt11b* activity and inhibiting the PCP pathway (Tahinci et al., 2007).

wnt11b was also shown to promote ventral cell fates in *Xenopus* embryos by modulating the non-canonical Ca^{2+}/calmodulin dependent pathway that activates a PKC and results in release of calcium intracellularly (Kühl et al., 2000).

In *Xenopus* heart formation, cardiac specification occurs during gastrulation and requires signals from the dorsal lip and underlying endoderm (Nascone et al., 1995). *wnt11b* shows a spatio-temporal pattern of expression that correlates with cardiac specification, indicating that *wnt11b* may be involved in heart development. Loss-of-function experiments using the *dnwnt11b*, injected into the presumptive cardiac region, strongly decreased subsequent expression of the cardiac markers *nhx2.5, cardiac troponin I (tnIc)*. This effect was rescued by injection of wild-type *wnt11b*. Inhibition of *wnt11b* function using a *wnt11b* morpholino gave identical results than

the one observed with *dnwnt11b*. These results indicate that *wnt11b* is required for normal heart development (Pandur et al., 2002). Over-expression of *wnt11b* alone in animal caps was sufficient to induce the early cardiac genes *gata4, gata6, nkx2.5, mhcα* and *tnIc*, which are specific for terminally differentiated cardiomyocytes. *wnt11b* and *activin* also cooperate in the activation of cardiac genes. *wnt11b* mediates this effect by activation of non-canonical signalling, that might involve the activation of the JNK pathway (Pandur et al., 2002). Together, these results suggest that *wnt11b* induces both early cardiac genes and expression of myocardial structural proteins, showing that *wnt11b* is both required and sufficient for cardiac specification.

Finally, more recently, in *Xenopus* embryos, *wnt11b* was shown to be required for neural crest cells migration. *wnt11b* is expressed in tissue adjacent to neural crest cells expressing the *wnt* receptor *frizzled7*. Loss and gain-of-function studies showed that *wnt11b* might be involved in neural cell crest migration by acting through the non-canonical PCP pathway (De Calisto et al., 2005).

In this thesis, a new insight of the *wnt11b* function during *Xenopus* development will be explored and I will investigate the role of *wnt11b* during pronephros formation.

Chapter 2 Materials and Methods

2.1 Materials.

Restriction enzymes were supplied by Invitrogen Life Technologies (Gibco BRL) and MBI Fermentas. Proteinase K, DNase I and calf intestinal alkaline phosphatase were supplied by Roche. T4 DNA Ligase, dNTP's and RNase inhibitor were supplied by MBI Fermentas. RNase A, Gentamycin and antibodies used for immunohistochemistry (goat-anti-mouse-AP) were supplied by Sigma. Chemicals were supplied by Becton Dickinson and Co., Helena Biosciences, Fisher Scientific, Merck, and Sigma. ^{35}S-methionine was supplied by New England Nuclear (NEN) Dupont. Activin for growth factor treatments was supplied by Invitrogen Life Technologies (Gibco BRL). DNA ladder was from Eurogentec (Belgium) and protein ladder was from New England Biolabs. mMESSAGE mMACHINE™ kits were supplied by Ambion®. Gel extraction kits were supplied by Qiagen, whilst miniprep plasmid DNA isolation kits were supplied by Sigma. X-ray film was supplied by Fuji.

2.2 Media and stock solutions.

All general media and stock solutions were prepared according to Sambrook *et al.,* 1989.

2.3 *Escherichia coli* bacterial strains.

DH5α: F$^-$ *supE*44 Δ*lacU*169 (∅80*lacZ*Δ*M*15) *hsdR*17 *recA*1 *gyrA*96 *thi*-1 *relA*1.

2.4 Plasmid template DNA.

2.4.1 Plasmid template DNA used to clone PCR product.

pGEM-T® Easy vector from Promega was used in any primary cloning of PCR products.

2.4.2 Plasmid DNA used as template *in situ* hybridization.

Table 2.1 shows the name of the DNA construct, which enzyme is used to linearise the plasmid, which RNA polymerase is used for *in vitro* transcription and finally how the DNA constructs were obtained.

Name	Linearize with	Transcribe with	Information
lhx1::pBS^{KS}	Antisense: XhoI. Sense: SacI.	T7 T3	Taira et al., 1993.
pax8::pCS^{2+}	Antisense: NotI. Sense: XhoI.	T7 T3	Carroll and Vize, 1999.
wt1::pGEMT7	Antisense: SacI	T3	Carroll and Vize, 1996.
wnt11b::pGEMT 3' UTR region	Antisense, MP3:SacI. Sense, MP1: SacI.	T7 T7	This work.
wnt11::pGEMT 5' UTR region	Antisense: PstI. Sense: NcoI.	T7 SP6	This work.
wnt6::pCS2+	Antisense: EcoRI. Sense: NotI.	T7 SP6	Lavery et al., 2008.
Xlwnt9a::pBSKS	Antisense: ClaI. Sense: PstI.	T7 T3	This work.
Xlwnt9b::pBSKS	Antisense: HindIII. Sense: BamHI.	T7 T3	This work.
Xtwnt9a::pBSKS	Antisense: ClaI. Sense: PstI.	T7 T3	This work.
Xtwnt9b::pBSKS	Antisense: BamHI. Sense: XhoI.	T3 T7	This work.

2.4.3 Plasmid template DNA used for capped mRNA synthesis for microinjection.

Table 2.2 shows the name of the DNA construct, which enzyme is used to linearise the plasmid, which RNA polymerase is used for *in vitro* transcription and finally how the DNA constructs were obtained.

Name	Linearize with	Transcribe with	Information
JCGF2	XhoI.	SP6	Gift of Woodland.
β-GAL	XhoI	SP6	Gift of Philpott, Vernon et al., 2003.
dntcf::pT7TS	XBaI.	T7	Gift of Clevers, Koriek et al., 1997.
wnt4::pSP64T	SalI.	SP6	McGrew et al., 1992.
wnt5a::pSP64T	XbaI.	SP6	Moon et al., 1993.
wnt6::pCS2+	NotI.	SP6	Lavery et al., 2008.
wnt7b::pBSK	HindIII.	T3	Chang and Hemmati-Brivanlou, 1998.

wnt8::pSP64T	BamH1.	SP6	Christian et al., 1991.
Xtwnt9b::pGEMt	NotI.	SP6	Garriock et al., 2007. Subcloned in pCS2+ for mRNA synthesis.
wnt11b::pT7TS	XBaI.	T7	Ku and Melton, 1993.
wnt11::pT7TS	XBaI.	T7	Garriock et al., 2005.
dnwnt11b::pSP64T	BamHI.	SP6	Hoppler et al., 1996. Tada and Smith, 2000.

2.5 Antisense oligo morpholinos.

The 5'UTR sequence and 1- 25 base of the coding region of *Xlwnt9a* and *Xlwnt9b* were submitted to GeneTools who designed antisense oligo morpholinos for translational blocking (Heasman et al., 2000). *wnt11* and *wnt11b* oligo morpholino sequences were accessed from published data before being ordered from GeneTools.

Table 2.3 shows the name of the genes and the oligo morpholino sequences used in this thesis.

Name of the gene	Sequence	Reference
Xlwnt9a	5'-aaggtgtccatccagcattttgctg- 3'	This work.
Xlwnt9b	5'-gttgtgctgagcttctcctcatctc-3'	This work.
wnt11b	5'-ccagtgacgggtcggagccattggt-3'	Pandur et al., 2005.
wnt11	5'-cttcatcttcaaaacccaataacaa-3'	Garriock et al., 2005.

2.6 DNA techniques.

2.6.1 Agarose gel electrophoresis.

Agarose gels of 1–1.5 % were prepared using 1x TBE with ethidium bromide to give a final concentration of 0.5μg/ml. DNA/RNA was separated using electrophoresis in 1x TBE at 50–150V and then photographed under ultra-violet light. When appropriate, DNA was extracted from the gel using a Qiagen gel extraction kit according to the manufacturer's instructions.

2.6.2 Restriction enzyme digestion.

Restriction digests were carried out according to the manufacturer's instructions. Following digestion of plasmids for ligation, treatment with phosphatase prevented plasmid re-ligation. 1µl of calf intestinal alkaline phosphatase was added per 10µl of reaction, and the reaction was incubated at 37°C for a further 20 minutes. When necessary, DNA was purified using the Qiagen gel extraction kit according to the manufacturer's instructions, except the gel extraction step was omitted and 3 reaction volumes of QG buffer were added to start purification.

2.6.3 DNA minipreps.

DNA was extracted from overnight cultures set up in 5ml of liquid broth containing 100µg/ml ampicillin using the Qiagen miniprep kit procedure.

2.6.4 Ligation of DNA into plasmid vectors.

50ng of vector was mixed with insert digested with appropriate restriction enzymes (molar ratio 1:3) to make a final volume of 20µl with T4 DNA ligase (MBI Fermentas) and ligation buffer. PCR products were sub-cloned into pGEM-T Easy® using the t-tailed overhangs. The ligation mix was incubated overnight at room temperature to maximize the number of ligations.

2.6.5 Transformation of plasmid DNA into competent *Escherichia coli*.

E. coli strain DH5α competent cells were prepared for heat shock transformation according to Sambrook et al., 1989. 50ng of the chilled ligation mix or 50ng of plasmid was added to 150µl of *E. coli* DH5α and incubated on ice for 20 minutes. Cells were then heat shocked at 42°C for 1 minute, incubated on ice for 3 minutes and plated onto L-broth plates containing ampicillin at 100µg/ml. Plates were incubated overnight at 37°C.

2.6.6 Primer design.

All primers were designed using Primer Designer (Scientific and Educational Software version 3.0).

2.6.7 Automated DNA sequencing.

Automated DNA sequencing was set up as follows. 250-500ng of plasmid DNA or 2-33ng of PCR product (depending on the length of the PCR product amplified) was added to 5.5pmol of primer and made up to a total volume of 10µl. Samples were then submitted to the departmental Molecular Biology Service for sequencing.

2.7 RNA techniques.

2.7.1 RNA extraction from embryos and animal caps.

The volumes given below are for 10 animal caps or 2 whole embryos. Where different numbers of animal caps or whole embryos were used, the volumes were adjusted accordingly. Two whole embryos were homogenized in 300µl XT extraction buffer (300mM NaCl, 20mM Tris pH 7.5, 1mM EDTA pH 8, 1% SDS) with 6µl of proteinase K (15mg/ml) and incubated for 15 minutes at 37°C. Samples were then extracted with an equal volume of phenol. The upper phase was removed to a fresh tube and 5µg of glycogen was added to the upper phase. RNA was precipitated with two volumes of ethanol at –20°C for at least 30 minutes and centrifuged for 20 minutes at 13, 000 rpm at 4˚C. The pellet was resuspended in 60µl of DNase I buffer (20mM Tris pH 8.3, 30mM NaCl, 2.5mM $MgCl_2$) containing 80U of DNase I and 80U of RNase inhibitor, and incubated for 20 minutes at 37°C.The samples were treated with 240µl of XT extraction buffer and 6µl of proteinase K and returned to 37˚C for another 20 minutes. The samples were then extracted with an equal volume of phenol followed by phenol / chloroform, with the aqueous layer being precipitated by adding 2 volumes of ethanol at room temperature for no longer than 30 minutes. This was centrifuged at 13, 000 rpm for 20 minutes at 4˚C, the

pellet washed with 70% ethanol before being dried and resuspended in 20µl H_2O. 1µl of RNA was analysed on a 1% agarose gel to check the integrity and yield.

2.7.2 New *Xenopus* gene names and symbols.

Recently, the *Xenopus* gene names and symbols have been reviewed to match identically the human gene names and symbols whenever possible. However, gene names are not necessarily the same as symbols. Among the nomenclature rules, gene names should not begin with an "X" unless the "X" is a part of a standard word. In *Xenopus*, duplicated genes should be denoted with an "a" or a "b" tag. In the same way, the gene symbols should be the same as the human gene symbols. Symbols are short-form representation (or abbreviation) of the descriptive gene name. Symbols should only contain Latin letters and Arabic numerals and all be in lower case. Symbols should not contain punctuation. The list of the rules cited above is not exhaustive and the full guidance can be found on the web page, www.xenbase.org.
The table below shows the name of the genes used in this work, one of the previous synonym for the gene symbols and the new nomenclature for the gene symbol.

Table 2.4 shows the name of the gene, a synonym of the previous gene symbol and the new gene symbol.

Name of the gene.	Previous gene symbol.	New gene symbol.
actin, alpha, cardiac muscle 1	*cardiac actin*	*actc1*
activin A receptor, type 1	*activin*	*acvr1*
bone morphogenetic protein 4	*BMP4*	*bmp4*
bone morphogenetic protein 7	*BMP7*	*bmp7*
cytokeratin	*cytokeratin*	*unnamed*
delta-like-1	*Xdelta1*	*dll1*
eukaryotic translation elongation factor 1 alpha 1	*EF1-α*	*eef1a1*
EPH receptor A7	*Pagliaccio*	*epha7*
follistatin	*follistatin*	*fst*
gremlin1	*Gremlin*	*grem1*

hepatocyte growth factor	*HGF*	*hgf (unnamed)*
hepatocyte nuclear factor 4	*HNF4*	*hnf4*
iroquois homeobox	*Xiro-3*	*irx3*
jagged1 (Alagille syndrome)	*XSerrate-1*	*jag1*
lim homeobox 1	*XLim1*	*lhx1*
myogenic differentiation 1 (provisional)	*MyoD*	*myod1*
myogenic factor 5	*Myf5*	*myf5*
neural cell adhesion molecule 1	*NCAM*	*ncam*
NK2 transcription factor related, locus 5	*XNkx2-5*	*nkx2-5*
nodal related 3 (provisional)	*Xnr3*	*nodal3*
notch homolog 1	*Xotch*	*notch*
orithine decarboxylase	*ODC*	*odc*
paired box 2	*XPax2*	*pax2*
paired box 8	*XPax8*	*pax8*
sal-like 1	*XSal1*	*sall1*
solute carrier family 5 (sodium/glucose cotransporter), member 1, gene 1	*SGLT-1*	*slc5a1.1*
sonic hedgehog homolog	*XShh*	*shh*
SRY (sex determination region Y)-box 3	*XSox3*	*sox3*
transcription factor 21	*XPod1*	*tcf21*
wingless-type MMTV integration site family, member 4	*XWnt4*	*wnt4*
wingless-type MMTV integration site family, member 5a	*XWnt5a*	*wnt5a*
wingless-type MMTV integration site family, member 6	*XWnt6*	*wnt6*
wingless-type MMTV integration site family, member 7b	*XWnt7b*	*wnt7b*
wingless-type MMTV integration site	*XWnt8*	*wnt8*

family, member 8		
wingless-type MMTV integration site family, member 9a	*XWnt9a*	*wnt9a*
wingless-type MMTV integration site family, member 9b	*XWnt9b*	*wnt9b*
wingless-type MMTV integration site family, member 11	*XWnt11-R*	*wnt11*
wingless-type MMTV integration site family, member 11b	*XWnt11*	*wnt11b*
Wilms tumor 1	*WT-1*	*wt1*

2.7.3 Reverse transcription PCR.

RT-PCR was performed according to Barnett et al., 1998. 0.5µg of RNA extracted from animal caps or whole embryos was made up to a total volume of 21.1µl with H_2O, heated at 75°C for 5 minutes before placing on ice. 7.9µl of reaction mix (3.3µM random hexamers, 1x PCR buffer, 3mM $MgCl_2$, 500µM dNTPs, 1U/µl RNase inhibitor) was added to each tube and incubated at 37°C for 5 minutes before addition of 2µl MMLV reverse transcriptase (200U/µl) and further incubation at 37°C for 1 hour. Reactions were denatured at 95°C for 5 minutes and stored at -20°C. Samples lacking RNA and RT were added as negative controls.

The prepared cDNA was subjected to PCR analysis. 1µl of cDNA + 1µl H_2O was made up to a final volume of 25µl with reaction mix containing 1x PCR buffer, 1.5mM $MgCl_2$, 200µM dNTPs, 1µM of each primer, and 1U Taq polymerase. A sample lacking cDNA was checked for contamination in any of the components used and a linearity series (0.2µl, 0.4µl, 0.8µl, 1.6µl) of control cDNA was added to verify that the PCR was in the linear range and semi-quantitative. *eef1a1* and *odc* were used as loading controls, with the amount of cDNA being added equalized with respect to these markers. Samples were run with standard PCR conditions; a denaturation cycle at 94°C for 3 minutes, a cycle at the appropriate annealing temperature for 1 minute followed by an elongation cycle at 72°C for 1 minute. Then using the appropriate number of cycles for denaturation at 94°C for 30 seconds, the appropriate annealing temperature for 30 seconds, followed by elongation at 72°C for 30 seconds. The final

elongation step was performed at 72°C for 5 minutes. 15µl of sample was analysed on a 1.5% agarose gel. Primer sequences, number of cycles and the annealing temperatures are shown in table 2.1.

Table 2.5. Primer sequences and PCR condition used in RT-PCR analysis. U, primer Upstream and D, primer Downstream.

Markers (bp)	Primer sequence (5'–3')	Annealing temp. (°C)	No. cycles	Reference / Details
actc1 (252)	U-tccctgtacgcttctggtcgta D-tctcaaagtccaaagccacata	62	25	Mohun, 1986
bmp7 (209)	U-ctacgtcagcttcaaagac D-gcaggatttgatgctggtg	55	28	Wang et al., 1997
bmp4 (480)	U-acaggcttcagtcagcgg D-ggtgaatgacctcaatgg	55	28	Metz, 1998
clc-k (229)	U-ggcagccgctgacaagtatt D-acacggctcatgatgagtcg	59	26	Maulet et al., 1999
c-ret (390)	U-ctcaaccggagtcttgacag D-gtgcgtaaggctcacttcag	60	28	Good, 2000
dll1 (265)	U-gcacagcagcgaccgaacag D-gccttgccaacccactctacattt	55	28	Chitnis et al., 1995
epha7 (361)	U-atggtgtctccaagcagaac D-gatggcactgtattcgtggt	58	28	Winning and Sargent,1994
fst (229)	U-cagtgcagcgctggaaag D- tgcgttgcggtaattcac	55	25	Hemmati-Brivalou, 1994
gdnf (205)	U-ttccaactggttggctggta D-tgcttgttggacgaccttct	60	30	Kyuno, 2006
grem1 (236)	U-aagcactagcggctgaagaa D-gcagaaggagcaggattgaa	55	28	Hsu et al., 1998
hgf (369)	U-gtccagaggttcgacatgat D-tgctgacacttccacgatac	58	28	Nakamura et al., 1995
hnf4 (403)	U-atggatatggcggattatac D-aactcgacctcctcgtac	55 45	18 13	Holewa et al., 1997
irx3 (258)	U-gacctggtccactcagatca D-tcagttccgctcctggttac	63	30	Bellefroid et al., 1998
jag1 (258)	U-cttgcccgcctggtcgtagtggt D-agcccggtgcaaggaggaacaaag	55	30	NCBI # BC084953
lhx1 (444)	U-gaaggatgagaccactggtgg D-cactgccgtttcgttcatttc	55	25	Witta et al., 1997
myf5 (407)	U-aggtccaactgctccgacggcatgaa D-aggagagaatccagttgatggaaaca	55	30	Hopwood and Gurdon, 1991
myod (305)	U-actgctccgatggcatga D-atgtgagtgcaggtattg	50	28	Woodland, unpublished

notch (495)	U-gacggcattgctaccttcac D-gctccatcctgcttcacagt	58	28	Coffman et al., 1990
pax8 (276)	U-ccaacagcagcatcagatc D-caatgacacctggccggata	53	25	Carroll and Vize, 1999
rgn (262)	U-ttagactggtctctggatcac D-cgataggtaactttacagtcttg	53	30	Sato et al., 1999
sall1 (294)	U-gacgaggtcgtcggctatca D-ggctactgccagtgcgtgtt	53	30	Hollemann et al., 1996
slc5a1.1 (255)	U-tgtcgtcgaggacatctcag D-gcgctcatgcagaggataac	55	30	Nagata et al., 1999
tcf21 (384)	U-tctcagtgatgtggaggactt D-tgacgcaggtgagctatgtaa	57	22	Simrick et al., 2005
wnt4	U-gagtggaatgcaagtgtc D-tacactgccgaccagttg	57	30	Seville et al., 2002
wnt5a	U-actccaagcacagaccttag D-catgacctcctggataactc	55	28	NCBI # L19716
wnt6	U-cacgacctgctggaagaaga D-acgtccagagcagtgctgtt	61	28	NCBI # EU332158
wnt7b	U-ccgcacttctccatacactg D-actgtcaccggagtgcctta	61	30	NCBI # AF026894
wnt8 (268)	U-agatgacggcattccaga D-ttcggaacggaagcatgt	58	30	Christian and Moon, 1991
wnt9a (361)	U-ggcgaataagtccagcaagg D-ccggagagtacttgctcatc	61	30	This work
wnt9b (274)	U-agaatggagcgatgtacc D-ggcgagagttgcttccaaca	61	30	This work
wnt11b (325)	U-gaagtcaagcaagtctgctgg D-gcagtagtcaggggaactaaccag	55	30	Ku and Melton, 1993
wnt11 (250)	U-agctcatgcacctgcacaac D-tcctgcaccggccttatatc	53	30	Garriock and Krieg , 2004
wt1 (436)	U-cacacgcacggggtct D-tgcatgttgtgatgacg	55	27	Carroll and Vize, 1996
odc (131)	U-ggagctgcaagttggaga D-tcagttgccagtgtgtggtc	55	19	Bassez et al., 1990
eef1a1 (270)	U-cagattggtgctggatatgc D-cactgccttgatgactccta	55	19	Mohun et al., 1989

2.7.4 RACE PCR.

Rapid Amplification of cDNA Ends of 5’ *Xlwnt9a* and *Xlwnt9b* was carried out according to the manufacturer instruction (Invitrogen, version 2.0). The gene specific primers (GSP) were designed from *Xlwnt9a* and *Xlwnt9b* sequences previously identified from generating *in situ* hybridization probes (chapter 3, section 3.3.1). According to the manufacturer’s instructions, GSP1 primers were designed to anneal at least 300bp from the mRNA 5’-end and GSP2 and 3 are located 5’ to GSP1. 5’

RACE PCR was carried out using an adult *X. laevis* pancreas RNA sample. An annealing temperature of 55ºC was used for the 35 cycles in each nested PCR.

2.7.5 Preparation of *in vitro* transcription of mRNA.

Plasmid template DNA was linearised with the appropriate restriction enzyme and purified using a gel extraction kit. Capped mRNA was prepared using the mMESSAGE mMACHINE® kit, T3, T7 and Sp6, according to the manufacturer's instructions (Ambion®).

2.7.6 Wholemount *in situ* hybridisation.

Plasmid templates were linearised with the appropriate restriction enzyme and purified using a gel extraction kit. Sense / antisense RNA probes were prepared using digoxygenin (DIG) labelling kit (Boehringer-Mannheim), and single labelled wholemount *in situ* hybridisation was carried out using a standard protocol adapted from Hemmati-Brivanlou *et al.,* 1990 and Harland, 1991. Where pigmented embryos were used, they were bleached (1% H_2O_2, 5% formamide, 0.5 x SSC in H_2O) on a light box following hybridisation for approximately 1–5 hours.

2.8 Protein techniques.

2.8.1 Protein expression in oocytes.

Oocytes were injected with 50nl of mRNA at a concentration of 0.5mg/ml and incubated at 18°C for 2 hours. Radio-labelling of proteins was carried out by selecting the best 7 oocytes and incubating them overnight at 18°C in 100µl Barth X containing 10µCi ^{35}S-methionine.

2.8.2 Protein extraction from oocytes.

Oocytes were washed twice in Barth X before being homogenised in cell lysis buffer (150mM NaCl, 1% NP40, 50 mM Tris-Cl pH 8) and 1mM PMSF. Samples were recovered by centrifugation at 13 000 rpm for 5 minutes to remove cell debris and

recover the middle layer containing solubilised protein. Care was taken not to remove the liquid layer. 5µl of this layer was mixed with 5µl of protein loading buffer and heated for 3 minutes at 95°C before being loaded onto an SDS-PAGE gel. Samples were run on a 4% acrylamide stacking gel at 100V, followed by separation through a 10% acrylamide resolving gel in a tris-glycine running buffer using the BioRad Mini Protean II system. The gel was dried for 20 minutes at 80°C for autoradiography.

2.9 Wholemount immunohistochemistry.

Embryos, caps or Holtfreter sandwich cultures were fixed overnight in MEMFA (0.5M MOPS pH 7.4, 100mM EGTA, 1mM $MgSO_4$, 4% formaldehyde), and transferred to H_2O for 1 hour at room temperature before being dehydrated through serial dilutions of methanol/H_2O. Embryos were left in methanol for 30 minutes at room temperature and then rehydrated in serial dilutions of methanol/PBS. Pigmented embryos were bleached (0.9% H_2O_2, 5% formamide, 0.5x SSC) on a light box. They were then washed 3x with PBT (2mg/ml BSA, 0.1% Triton X-100 in PBS) to remove the bleaching solution and blocked in PBT for 2 hours at 4°C on a nutator. Primary antibody was added as follows with dilutions in parenthesis; pronephric proximal tubule specific monoclonal antibody 3G8 (1:40) and pronephric intermediate/distal tubules specific monoclonal antibody 4A6 (1:1) (Vize et al., 1995) and incubated rocking at 4°C overnight. Embryos were then washed with PBT 5x 1 hour at 4°C on a nutator, and then secondary antibody, alkaline phosphatase conjugated goat anti-mouse (1:500) (Sigma F-2012), was added overnight at 4°C. Embryos were then washed 4 times for 1 hour with PBT at 4°C and were left to equilibrate for 1 hour in colour buffer (0.1M Tris-Cl pH 9, 25mM $MgCl_2$, 100mM NaCl, 0.1% Tween-20) at room temperature on a nutator. Embryos were transferred to a 24-well tissue culture plate with 350µl of AP colour substrate (colour buffer with 1% v/v NBT/BCIP, Roche). Staining was carried out in the dark, with the reaction stopped with a PBS wash. The staining was fixed in MEMFA for 1 hour at room temperature. Where double staining was required, embryos were washed 3x 5 minutes with PBT to remove the MEMFA and blocked for 2 hours at 4°C on a nutator before undiluted 4A6 was added and incubated overnight at 4°C. Subsequent washes were repeated as for 3G8 except that the second colour reaction used Fast

Red TR/Napthol AS/MX (Sigma) according to the manufacturer's instructions. When fluorescent staining was required, antibodies 3G8 and 4A6 were used neat and somite monoclonal antibody 12/101 was diluted 1:500 (Brockes and Kintner, 1984). Secondary FITC goat anti-mouse (1:25) (Invitrogen) was used to detect the primary 3G8 antibody, TRITC goat anti-mouse (1:50) (Invitrogen) was used to detect the primary 4A6 antibody and Alexa fluor 405 goat anti-mouse (1:200) (Invitrogen) was used to detect the primary 12/101 antibody. Embryos were then washed 4 times for 1 hour with PBT at 4°C and fixed in MEMFA, dehydrated in methanol and cleared in Murrays (1:2 benzyl alcohol, benzyl benzoate) before being read under UV light.

2.10 Embryo manipulations.

2.10.1 *In vitro* fertilisation of *Xenopus* eggs.

In vitro fertilisation was carried out on *Xenopus* eggs according to standard procedures. Embryos were dejellied in 2% (w/v) cysteine-HCl pH 8, and washed twice with 1/10th Barth X solution. Embryos were cultured to the desired stage in 1/10th Barth X solution with 10μg/ml gentamycin at 12–24°C. Staging was performed according to Nieuwkoop and Faber (1994).

2.10.2 Microinjection of embryos and oocytes.

For standard microinjection of embryos, 18-27nl of mRNA was injected into a one-cell embryo. Targeted injections involved injecting 18-27nl of mRNA into one ventral cell of a four cell embryo (left versus right comparison) or into the V2 blastomere at the 8-cell stage, which gives rise to the pronephric lineage (Moody, 1987). *GFP* or *β-GAL* mRNA was injected as a lineage tracer to determine targeting to the pronephric region. Injections were performed in 5% Ficoll in full strength Barth X. Oocytes were injected with 50nl of mRNA and incubated overnight at 18°C until required.

2.10.3 Growth factor treatments.

Animal caps dissected from stage 9 were incubated at 12°C in 5ng/ml activin A growth factor, supplemented with 0.001% BSA in 24-well tissue culture plates and incubate to the desired stage where they were scored for elongation or subjected to RT-PCR analysis.

2.10.4 Dissections of animal caps and embryonic material.

All dissections were performed using fine forceps and an eyebrow hair mounted in a needle, in 5 cm^2 Petri dish, in full strength Barth X. When necessary, embryos were dissected on a 1% agar in Barth X support base. Embryos were incubated between 12 to 18˚C until the desired stage. Animal caps were dissected from embryos at stage 9 and grown to required stages according to undissected control embryos. Lateral plate mesoderm was removed in a wedge of 60˚ to 80˚ from the vertical midline of stage 10.5-11 donor embryos. Presumptive anterior somitic tissue was dissected from embryos at stage 17. To investigate specific gene expression patterns, fine dissections were performed on various staged embryos from the presumptive pronephros area and the somitic mesoderm in embryos at stage 17.

2.10.5 Holtfreter sandwich cultures.

Lateral plate mesoderm from stage 11.5 embryos and presumptive anterior somites from stage 17 embryos were cultured together and separately within ectodermal wraps in full strength Barth X for approximately 4 hours. Sandwich cultures were then switched into ½ Barth X with 10µg/ml gentamycin and cultured at room temperature until stage 40 equivalent, according to the stage of control embryos used for lateral plate dissection. Holtfreter sandwich cultures were finally fixed in MEMFA before being subjected to immunohistochemistry for the presence of pronephric proximal, intermediate/distal tubules with antibodies 3G8 and 4A6 respectively.

Chapter 3 Identification of *Xenopus wnt9a* and *wnt9b* genes potentially involved in pronephros formation.

3.1 Introduction.

There is evidence in the literature for the *wnt* family member, *wnt9b*, to have a critical role to play in vertebrate kidney formation. Qian et al., in 2003 have reported an analysis of mouse *Wnt9b* and deduced the full-length amino acid sequence of its close relative *Wnt9a*. Amino acid sequence comparison showed that *Wnt9b* and *Wnt9a* are close paralogs of each other and are orthologs of *Wnt9* genes from shark and hagfish. In mouse embryos, *Wnt9b* is expressed from 9.5 to 17.5 days of gestation, the latest stage tested, with a peak of expression at day 10.5. In the adult mouse *Wnt9b* is mainly restricted to the kidney. Moreover, Carroll et al, (2005) have shown that *Wnt9b* is required for multiple aspects of mouse urogenital development, including induction of the metanephric mesenchyme and the generation of a functional female reproductive tract. In *Xenopus*, Garriock et al., 2007 analysed *wnt* gene synteny and identified the previously uncharacterised *X. tropicalis wnt9a* (*Xtwnt9a)* and *wnt9b* (*Xtwnt9b)* and showed that *Xtwnt9a* is expressed in the developing pronephric intermediate/distal tubules and the lung primordia, while *Xtwnt9b* is in the branchial arches, the eye and in the ectoderm adjacent to the cement gland. However, the *X. laevis wnt9a* (*Xlwnt9a*) and *wnt9b* (*Xlwnt9b*) have not been previously identified. This chapter describes a bioinformatic and molecular search that leads to the identification of the *Xlwnt9a* and *Xlwnt9b*, reports the temporal and spatial expression of *wnt9a* and *wnt9b* in *X. laevis* and *X. tropicalis* embryos and dissected adult organs and analyses the effects of *Xtwnt9b* mis-expression on *X. laevis* pronephros development.

3.2 Identification of *Xlwnt9b*.

3.2.1 Sequence analysis of the genomic database identifies *X. tropicalis wnt9b* in scaffold 43.

In August 2005, the whole genome of the frog *X. tropicalis*, was sequenced and assembled by the Joint Genome Institute (JGI). *Wnt9b* was shown by Carroll et al. (2005) to be essential for metanephric mouse kidney development. However, neither of *X. laevis* or *X. tropicalis wnt9b* genes were yet identified. The tBLASTn tool of the JGI website allowed us to search for the *X. tropicalis wnt9b* sequences in unannotated genomic DNA sequence. The full protein sequence of mouse *Wnt9b* was used to interrogate the entire *X. tropicalis* genome by BLAST. Queries returned alignments of *Wnt9b* with two *X. tropicalis* scaffolds. The first scaffold identified was scaffold 43. The total length of scaffold 43 is 3,852,807 base pairs and the *wnt9b* gene sequence identified was 1794 base pairs. BLAST showed three alignments corresponding to partial exon 1, exons 2 and 3, each of them showing scores above 250, indicating a strong alignment. The C-terminal end of the protein was not predicted with certainty with scores below 200 for exon 4. The second scaffold identified was scaffold 14668. The total length of scaffold 14668 is only 7087 base pairs and the *wnt9b* gene sequence identified was 1706 base pairs. BLAST analysis showed a similar alignment as scaffold 43, suggesting that scaffold 43 and scaffold 14668 might possibly over-lap. We chose to work with scaffold 43 as the available gene sequence is longer than scaffold 14668. Having identified the correct scaffold, the newly identified *X. tropicalis* coding sequence was conceptually translated and the 231 amino acid sequence was aligned with protein sequences of human WNT9B (also called WNT14) and mouse Wnt9b (Wnt9b). Figure 3.1 shows that the wnt9b protein is highly conserved between *Human*, *Mouse* and *X. tropicalis*. Dashes indicate gaps in the alignment. Black boxes indicate identical amino acid for the 3 analysed proteins at one position, grey boxes indicate identical amino acid for 2 protein sequences only at one position and no similarity is indicated by a white box. WNT9B and Wnt9b are 94% identical at the amino acid level. Both WNT9B and Wnt9b are 60% identical to the protein translated from scaffold 43. Only 231 amino acids were identified from scaffold 43, therefore only the first 257 of 357 amino acids of WNT9B and the first 260 of 359 amino acids of Wnt9b were analysed. In

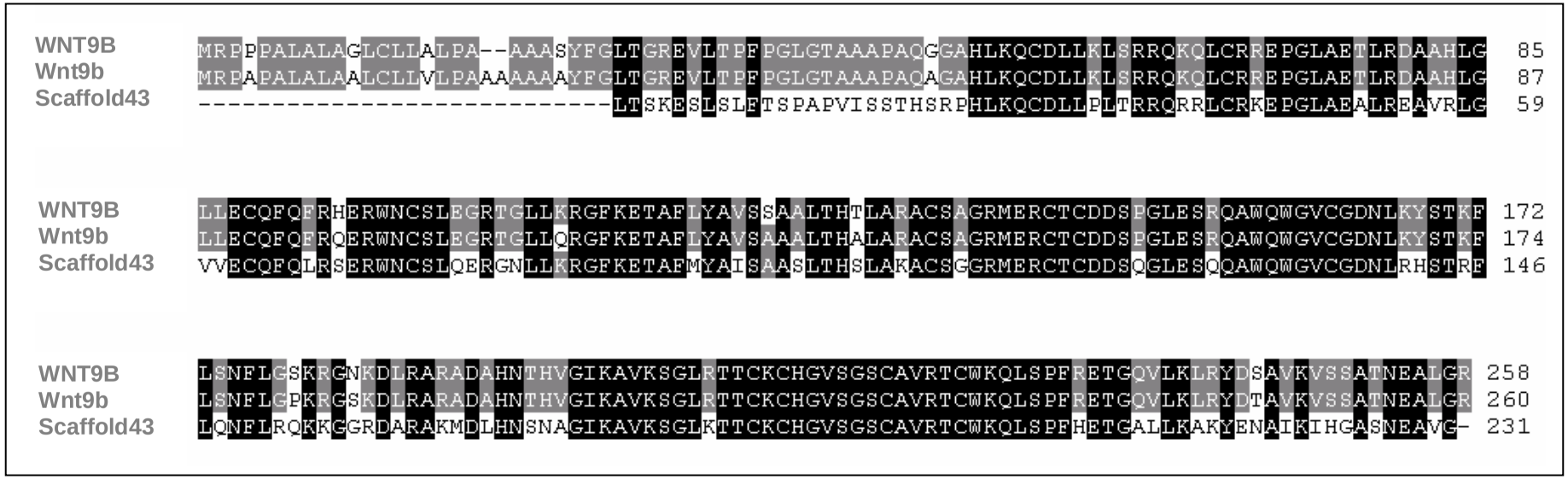

Key: Dashes indicate gaps in the alignment. Black box indicates identical amino acid between the 3 sequences. Grey box indicates identical amino acid between 2 sequences. White box indicates dissimilar amino acid between the 3 sequences.

Figure 3.1 Amino acid sequence alignment shows that protein wnt9b is highly conserved between human, mouse and *X. tropicalis*. Protein sequences of human wnt9b (WNT9B), mouse wnt9b (Wnt9b) and the newly found translated sequence from *X. tropicalis* genomic DNA scaffold 43 were aligned. Dashes indicate gaps in the alignment. Black boxes indicate identical amino acid for the 3 analysed proteins at one position. Grey boxes indicate identical amino acid for 2 protein sequences only at one position and no similarity was indicated by a white box. WNT9B and Wnt9b are 94% identical in amino acids level. Both WNT9B and Wnt9b are 60% identical to the protein translated from scaffold 43. Only 231 amino acids were identified from scaffold 43, therefore only the first 258 of 357 amino acids of WNT9B and the first 260 of 359 amino acids of Wnt9b were analysed. Accession numbers are BAB70499 and NP_035849 for WNT9B and Wnt9b respectively.

conclusion, the newly identified partial *X. tropicalis* wnt9b protein shows 60% of identity in its amino acid sequence with *mouse* and *human* wnt9b proteins. As a result, it is highly likely that the newly identified *X. tropicalis wnt9b* sequence constitutes the *mouse* and *human wnt9b* ortholog.

3.2.2 Strategy for amplification of *Xlwnt9b.*

The coding nucleotide sequence of the partial identified *Xtwnt9b* gene was assembled. To amplify *Xlwnt9b*, primers were designed that would amplify *wnt9b* without amplifying the other *Xenopus wnt* genes. To design these primers, we focused on the conserved sequences of *wnt9b* genes cross species and on the dissimilarity with the other *wnt* genes in *X. laevis*. Figures 3.2 and 3.3 show two alignments performed to design specific *wnt9b* primers. All possible primer pair combinations were tested. However, only primers 3 and 6 were capable of amplifying a 274bp *Xlwnt9b* fragment. Forward primer 3 and reverse primer 6 were chosen in a highly conserved region of *wnt9b* nucleotide sequence, identified when *wnt9b* sequences were analysed cross species (figure 3.2). These two primers were designed to not cross-react with the other *X. laevis wnt* genes (figure 3.3). Figure 3.4 shows partial nucleotide sequence alignments of *X. laevis wnt* genes with scaffold 43 around the position of primers 3 and 6. *X. laevis* wnt molecules differ in their nucleotide sequences at this position. Forward primer 3 and reverse primer 6 designed as shown should preferentially amplify *wnt9b* sequence and not other *wnt* genes. The sequence of forward primer 3 is 5'-AGAATGGAGCGATGTACC-3' and the sequence of reverse primer 6 is 5'-GGCGAGAGTTGCTTCCAACA-3'. The primer pair should amplify a 274 base pair long fragment from *X. laevis.*

3.2.3 Verification of *Xlwnt9b* sequence amplified by RT-PCR.

Primers 3 and 6 designed from *X. tropicalis wnt9b* DNA sequence were used to specifically amplify *Xlwnt9b* from *X. laevis* whole embryo stage 28 cDNA by RT-PCR. The 274 base pair fragment obtained was sequenced using primers 3 and 6 and the sequence subsequently analysed. A BLAST search using the NCBI website indicated that the *X. laevis* PCR product corresponded to the *Xtwnt9b*. BLAST results also showed that the PCR fragment is highly similar to the *wnt9b* gene in

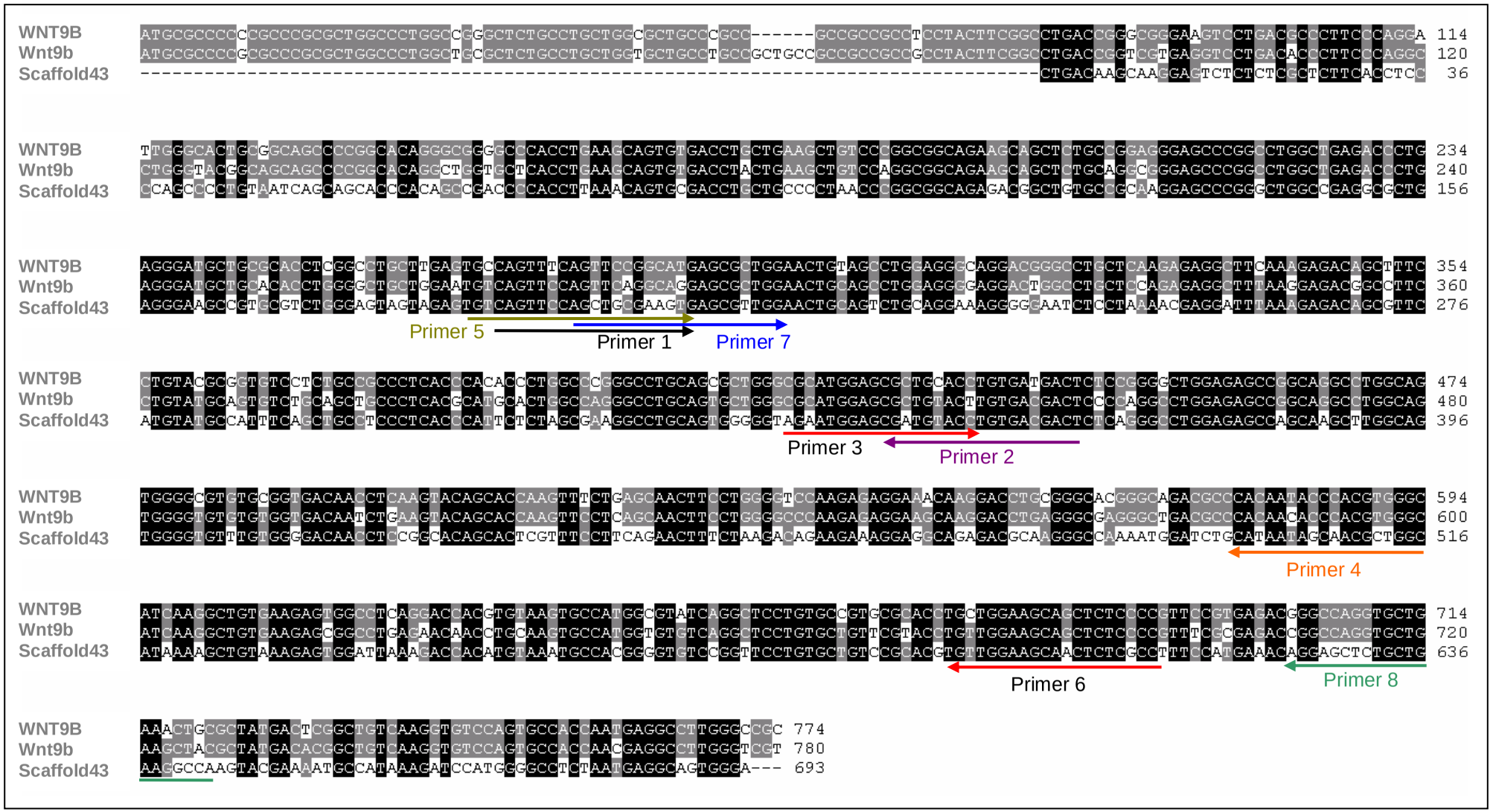
WNT9B
Wnt9b
Scaffold43
Primer 5
Primer 1
Primer 7
Primer 3
Primer 2
Primer 4
Primer 6
Primer 8

Key: Dashes indicate gaps in the alignment. Black box indicates identical amino acid between the 3 sequences. Grey box indicates identical amino acid between 2 sequences. White box indicates dissimilar amino acid between the 3 sequences.

Figure 3.2 Design of specific *Xenopus wnt9b* primers based on the complete nucleotide sequences alignment of human and mouse *wnt9b* with scaffold 43. Eight forward and reverse primers were designed in conserved region of *wnt9b* gene in order to specifically amplify the *X. laevis wnt9b* using RT-PCR based on *X. tropicalis* sequence. The result showed that only the pair of primers 3+ 6 was capable of amplifying a 274bp fragment of *X. laevis wnt9b*.

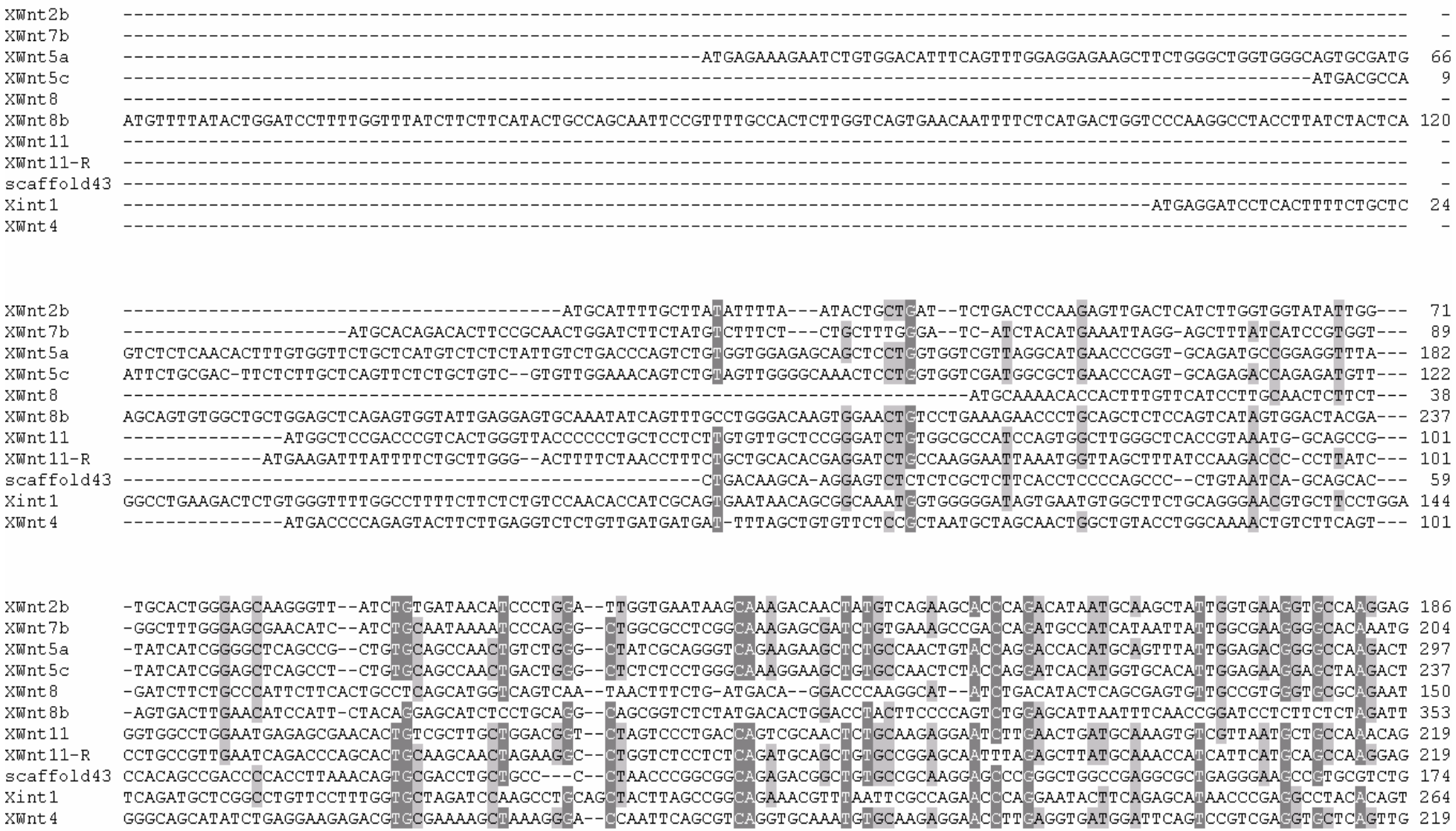
XWnt2b
XWnt7b
XWnt5a
XWnt5c
XWnt8
XWnt8b
XWnt11
XWnt11-R
scaffold43
Xint1
XWnt4

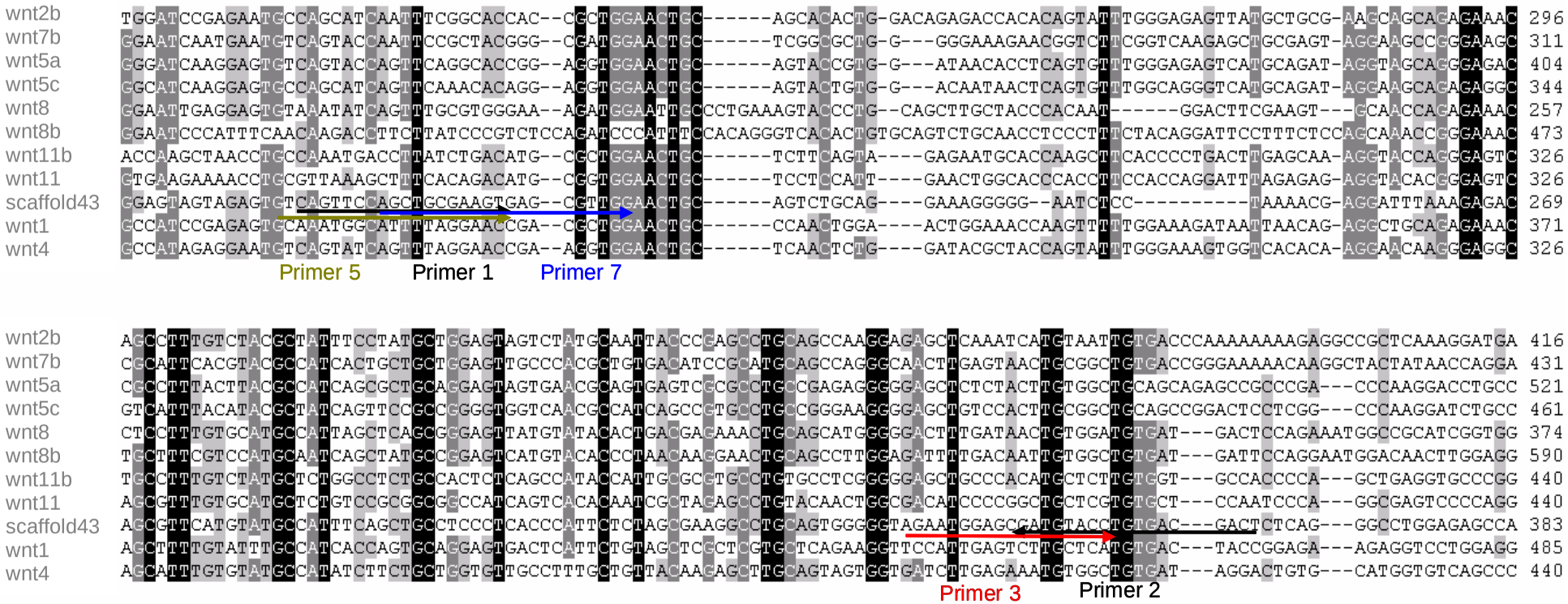
wnt2b
wnt7b
wnt5a
wnt5c
wnt8
wnt8b
wnt11b
wnt11
scaffold43
wnt1
wnt4
Primer 5
Primer 1
Primer 7
Primer 3
Primer 2

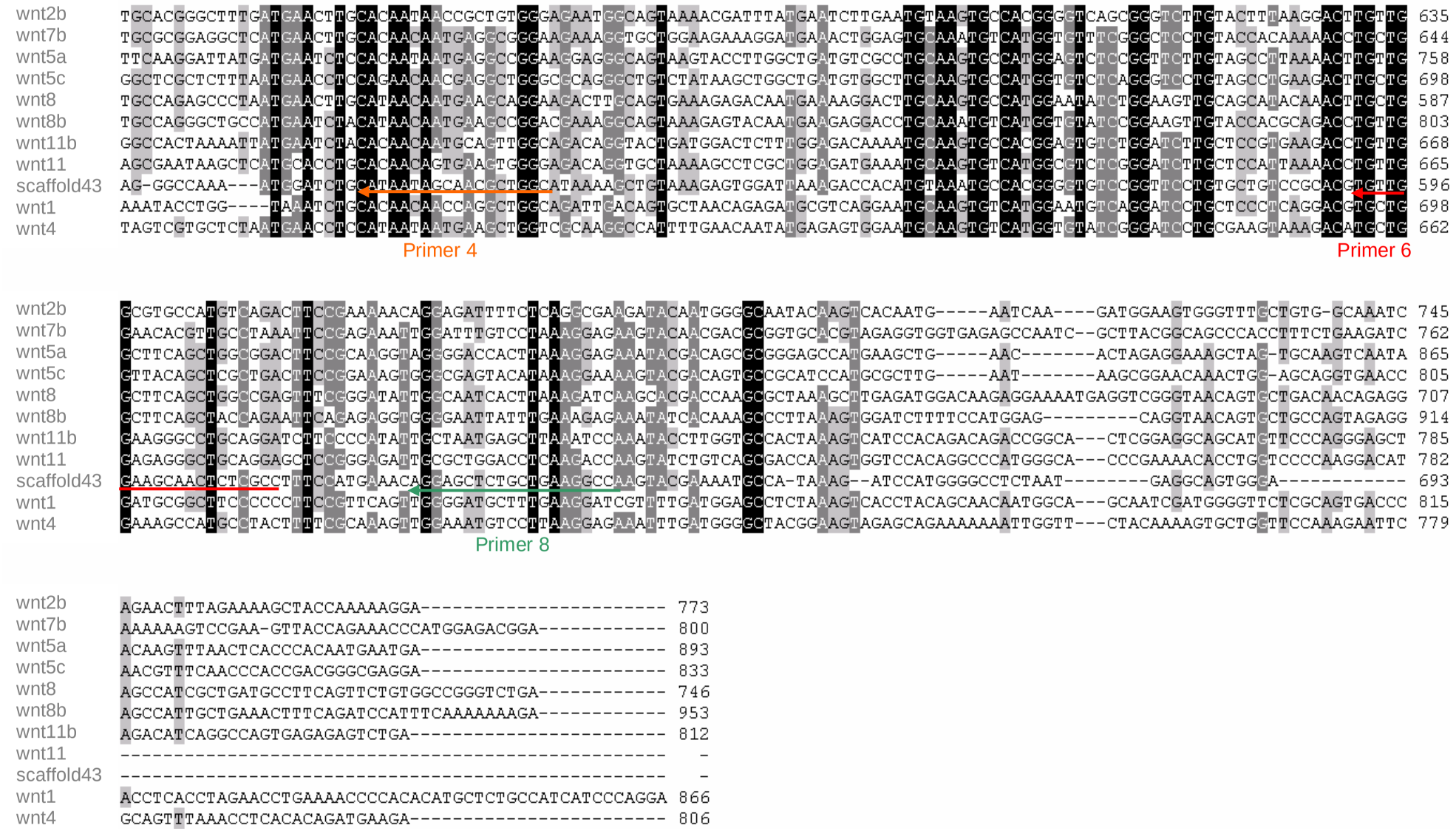
wnt2b
wnt7b
wnt5a
wnt5c
wnt8
wnt8b
wnt11b
wnt11
scaffold43
wnt1
wnt4
Primer 4
Primer 6
Primer 8

Key: Dashes indicate gaps in the alignment. Black box indicates identical amino acid between the 3 sequences. Grey box indicates identical amino acid between 2 sequences. White box indicates dissimilar amino acid between the 3 sequences.

Figure 3.3 Design of specific *Xenopus wnt9b* primers based on the complete nucleotide sequences alignment of *X. laevis wnt* genes with scaffold 43. Eight forward and reverse primers were designed in semi-conserved region of *Xenopus wnt* gene in order to specifically amplify the *X. laevis wnt9b*. Results show that only primers 3+6 were capable of amplifying a 274bp *X. laevis wnt9b* fragment. Accession number of the wnt molecules used in this analysis are *wnt1a*: X13138, *wnt2b*: U66288, *wnt4*: U13183, *wnt5a*: L19716, *wnt5c*: X73510, *wnt7b*: AF026894, *wnt8*: X57234, *wnt8b*: U22173, *wnt11b*: L23542, *wnt11*, AY695415.

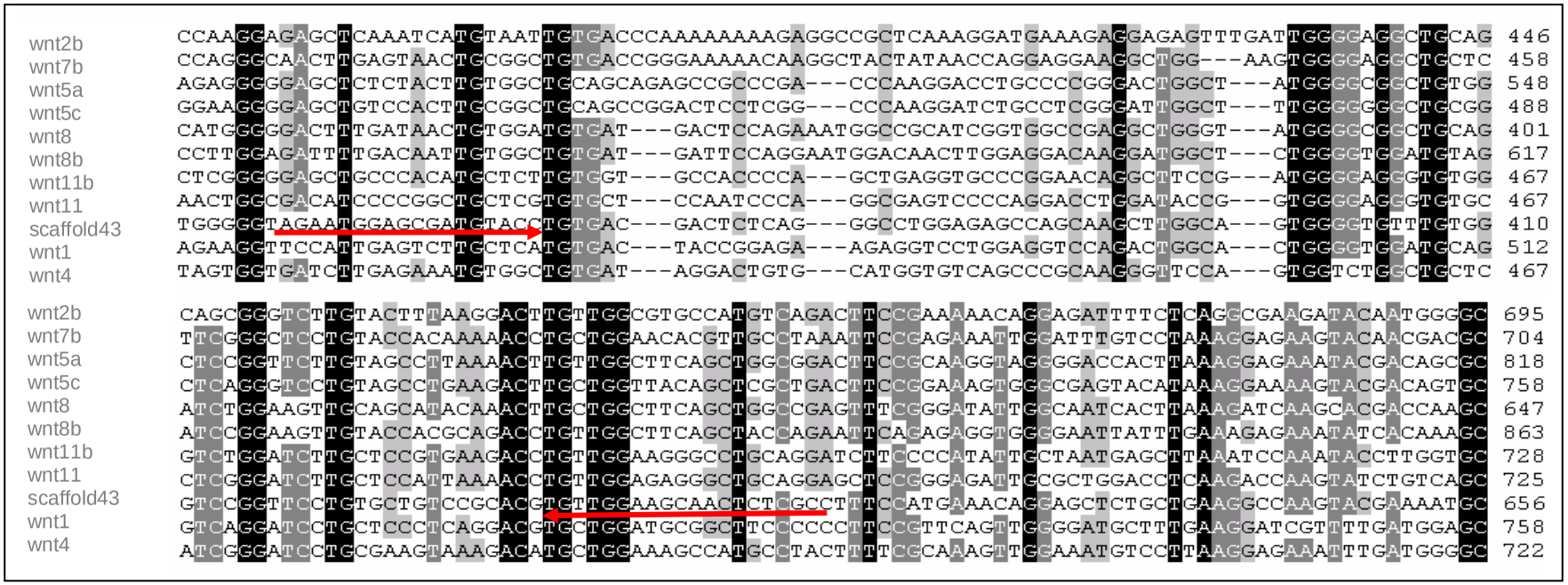

Key: Dashes indicate gaps in the alignment. Black box indicates identical amino acid between the 3 sequences. Grey box indicates identical amino acid between 2 sequences. White box indicates dissimilar amino acid between the 3 sequences.

Figure 3.4 Partial nucleotide sequence alignments of *X. laevis wnt* genes with scaffold 43 around the position of primers 3 and 6. *X. laevis wnt* genes differ in their nucleotide sequences and therefore the designed primers forward 3 and reverse 6 should preferentially amplify *wnt9b* without cross-reacting with the other *Xenopus wnt* genes. Accession number of the wnt molecules used in this analysis are w*nt1a*: X13138, *wnt2b*: U66288, *wnt4*: U13183, *wnt5a*: L19716, *wnt5c*: X73510, *wnt7b*: AF026894, *wnt8*: X57234, *wnt8b*: U22173, *wnt11b*: L23542, *wnt11*, AY695415.

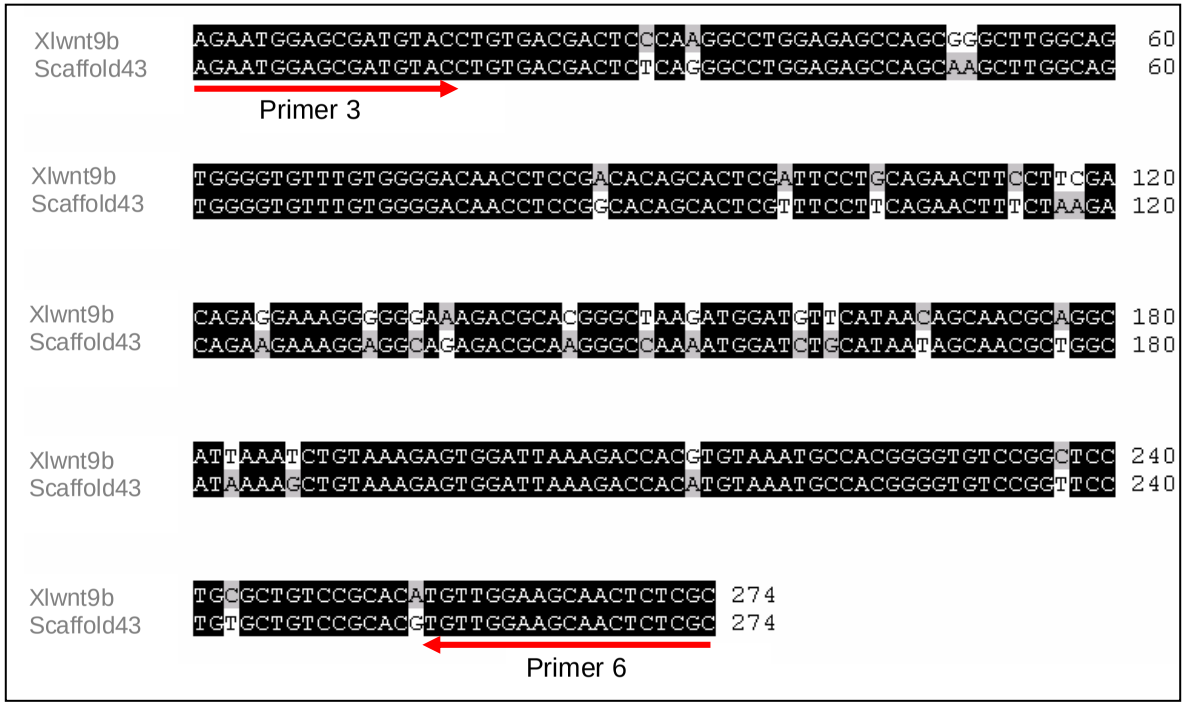

Figure 3.5 Nucleotide sequence alignment of PCR product amplified from *Xlwnt9b* with *X. tropicalis* scaffold 43 coding sequence. The PCR product *Xlwnt9b* is 274 base pairs long and was obtained by RT-PCR using primers forward 3 and reverse 6 and *X. laevis* stage 28 whole embryo cDNA. The two sequences are 90% identical at the nucleotide level, confirming that amplification of *Xlwnt9b* was successful. Forward and reverse primers can now be used to study *Xlwnt9b* expression pattern in embryonic stages and adult tissues.

others species such as *Bos taurus, Macaca mulatta, Canis familiaris, Mus musculus, Homo sapiens* and *Gallus gallus* (data not shown). Sequence alignment was performed and figure 3.5 shows the nucleotide sequence alignment of the PCR product from *Xlwnt9b* with *X. tropicalis* scaffold 43 coding sequence. The two sequences are 90% identical at the nucleotide level, confirming that amplification of *Xlwnt9b* was successful. Forward primer 3 and reverse primer 6 can now be used to study *Xlwnt9b* expression pattern in embryonic stages and adult tissues using RT-PCR.

3.3 Temporal and spatial expression *of wnt9a* and *wnt9b* in *X. laevis* and *X. tropicalis* embryos.

3.3.1 Generation of *X. tropicalis* and *X. laevis wnt9a* and *wnt9b in situ* probes.

In April 2007, the new version of Xenbase became available on the web (www.xenbase.org/gene/gene.do). This new website offers the possibility of searching for genes in annotated genome sequence. The same month, Garriock et al. (2007) published an analysis of wnt genes synteny of the orthologues of all 19 human wnt genes in chicken (*Gallus gallus*), frog (*X. tropicalis*) and fish (*Danio rerio* and *Tetraodon nigroviridis*). Of the 19 wnts observed in human, the *X. tropicalis* genome contains the frog orthologues of the previously uncharacterized *wnt2, wnt3, wnt9a, wnt9b, wnt10a* and *wnt16*. Garriock presented data showing expression of *wnt9a* and *wnt9b* during early *X. tropicalis* development. *Xtwnt9a* was detected throughout the length of the developing pronephric intermediate/distal tubules from stage 32 and also in the lung primordial. *Xtwnt9b* was detected in the branchial arches, the eye and in the ectoderm adjacent to the cement gland from stage 35. To complement the study of Garriock et al., 2007, we carried out *in situ* hybridization using species specific *wnt9a* and *wnt9b in situ* probes in both *X. tropicalis* and *X. laevis* embryos. *Xtwnt9a* and *Xtwnt9b* sequences from Xenbase show 100% identity on nucleotide level with published *Xtwnt9a* and *Xtwnt9b* sequences (Garriock et al., 2007). Therefore, in this chapter, I will refer solely to these published *Xtwnt9a* and *Xtwnt9b* sequences.

3.3.1.1 Design of *wnt9a* and *wnt9b* primers to amplify gene for species specific probes.

Primers for *wnt9a* and *wnt9b* RT-PCR amplification were designed according to published *Xtwnt9a* and *Xtwnt9b* sequences (Garriock et al., 2007). *Xtwnt9a* and *Xtwnt9b* nucleotide sequences were aligned and primers were chosen in a region that would preferentially amplify either the *X. laevis* and *X. tropicalis wnt9a* or *wnt9b*. Forward primer 5'-TAAGCTTGAGCGGAAGCAAC-3' and reverse primer 5'-CTGGCATGGCCTTGTAACTA-3' were used to amplify an 822 base pair fragment of *wnt9a*. Forward primer 5'-AGAATGGAGCGATGTACC-3'and reverse primer 5'-CTTGGCCTGTAGAAGTTGGG-3' were used to amplify a 432 base pair fragment of *wnt9b*. PCR products were analysed by sequencing.

3.3.1.2 Verification of sequences amplified by PCR and generation of an *in situ* probe clone.

Both the *Xtwnt9a* and *Xtwnt9b* sequences amplified by PCR are 99% identical to the original published sequence (Garriock et al., 2007). Table 3.1 shows a comparison between the four nucleotide sequences of the genes *Xlwnt9a, Xlwnt9b, Xtwnt9a* and *Xtwnt9b.* GenBank accession number of published gene sequences of *Xtwnt9a and Xtwnt9b* are DQ658159 and DQ658160 respectively and were used in this analysis (Garriock et al., 2007). Gene sequences of *Xlwnt9a and Xlwnt9b* are generated from this work. For each comparison two types of alignments were done. The first one used the NCBI BLAST align function and shows a ratio of the number of nucleotides aligning identically between two sequences and the total number of nucleotides aligning for this region. The result is also expressed in percentage. A second alignment using the ClustalW multi-alignment function was carried out which considers the full length of sequences given even if no alignment was found. These results are expressed as a score value. The result of this sequencing showed that *Xlwnt9a* and *Xtwnt9a* are 95% identical. *Xlwnt9b* and *Xtwnt9b* are 90% identical. *Xtwnt9b* and *Xtwnt9a* are 82% identical and *Xlwnt9b* and *Xlwnt9a* are 78% identical. *Xtwnt9b* is 78% and 74% identical to *Xlwnt9a* (gap in the alignment). *Xtwnt9a* is 78% identical to *Xlwnt9b*. RT-PCR products confirmed by sequence analysis were

	XtWnt9a (DQ658159) 942bp	***XlWnt9a*** 729bp	***XtWnt9b*** (DQ658160) 1074bp
XlWnt9a 729bp	693/729 (95%) Score 95		
XtWnt9b (DQ658160) 1074bp	73/89 (82%) Score 61	70/89 (78%) 83/112 (74%) Score 60	
XlWnt9b 380bp	70/89 (78%) Score 49	70/89 (78%) Score 49	342/380 (90%) Score 90

Table 3.1 Comparison between the four nucleotide sequences of *XlWnt9a, XlWnt9b, XtWnt9a* and *XtWnt9b* generated by PCR amplification. Genes sequences of *XtWnt9a and XtWnt9b* are from GenBank (Garriock et al., 2007). Genes sequences of *XlWnt9a and XlWnt9b* are generated by PCR amplification. For each comparison two types of alignments were done. The first one used the NCBI BLAST align function and shows a ratio of the number of nucleotides aligning between two sequences and the total number of nucleotides aligning for this region. The result is also expressed in percentage. A second alignment using the ClustalW multi-alignment function was carried out and considers the full length of sequences given even if no alignment was found. The results are expressed as a score value.

cloned into the pGEMT-easy vector before being subcloned to pBSKS, that contains the T3 and T7 polymerase promoter initiation sites.
To conclude, the result of sequencing and nucleotide sequence alignments show that *Xlwnt9a* and *Xlwnt9b* are highly similar to their *Xtwnt9a* and *Xtwnt9b* orthologues respectively. However, within a given species, both *wnt9a* and *wnt9b* genes are related but distinct in their nucleotide sequence since they show between 74% to 82% of nucleotide identity. This last result suggests that the *X. laevis* and *X. tropicalis wnt9a* and *wnt9b in situ* hybridization probes generated, should hybridize specifically to their corresponding mRNA within embryos.

3.3.2 Temporal and spatial expression of *wnt9a* and *wnt9b* in *X. laevis* and *X. tropicalis* embryos.

In order to confirm and extend the study of Garriock et al., 2007, we repeated the *in situ* analysis of *wnt9a* and *wnt9b* using a wider range of stages and on both *Xenopus* species. *Xlwnt9a* and *Xlwnt9b in situ* probes were used to hybridize to *X. laevis* embryos and *Xtwnt9a* and *Xtwnt9b in situ* probes were used to hybridize to *X. tropicalis* embryos to establish that transcript distributions were identified correctly in each species (Massé et al., 2007). *X. laevis* and *X. tropicalis wnt9a* and *wnt9b* sense *in situ* probes were also generated and used to verify non-specific hybridization within *X. laevis* and *X. tropicalis* embryos (see chapter 2 for details of probe generation).

3.3.2.1 Temporal and spatial embryonic expression of *Xtwnt9a* and *Xlwnt9a.*

Figure 3.6 shows spatial and temporal embryonic expression of *Xtwnt9a* and *Xlwnt9a*. *wnt9a* cannot be detected in embryos of either species at stage 20 (Fig 3.6 a and e). Expression is detectable in the pronephros around stage 30 in both *X. tropicalis* and *X. laevis* (Fig 3.6 b and f, arrows highlighting pronephros position). At stage 35, *wnt9a* is visible throughout the length of the pronephric proximal and distal tubules, in the heart and in the lung bud (Fig 3.6 c and g). At stage 40, *wnt9a* expression remains strong in the pronephric proximal and distal tubules, in the heart and in *X. tropicalis* lung bud (Fig 3.6 d and h). Non-specific background shown by *X. laevis* and *X. tropicalis* embryos hybridized with sense *wnt9a in situ* probes

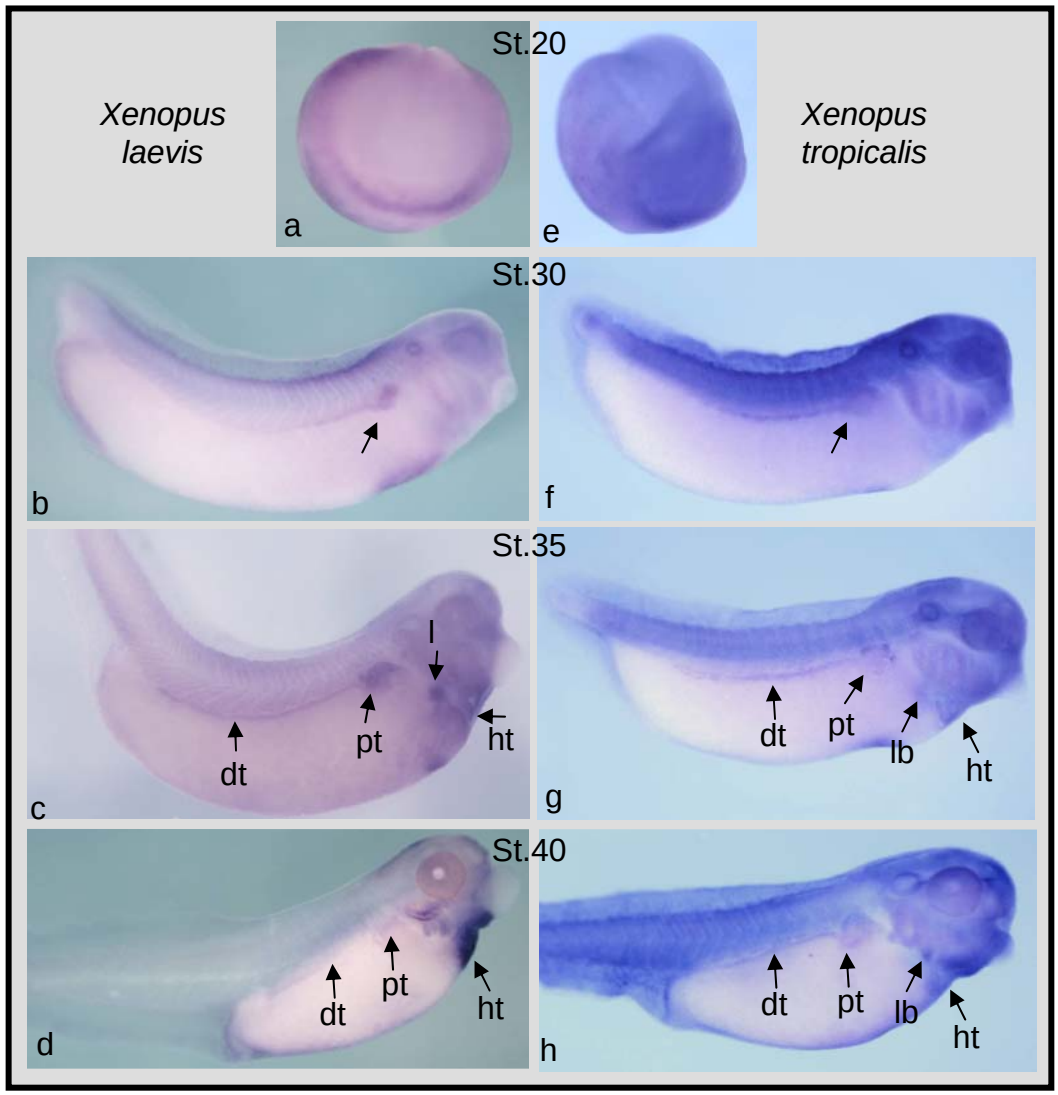

Figure 3.6 Spatial and temporal embryonic expression of *XlWnt9a* and *XtWnt9a*. *In situ* hybridization analysis in whole-mount *Xenopus* embryos using DIG-labelled antisense probes shows that *wnt9a* cannot be detected in embryos at stage 20 (a and e). Expression is detectable in the pronephros around stage 30 in both species (b and f, arrows highlighting pronephros position). At stage 35, *wnt9a* is visible throughout the length of the pronephric proximal tubule (pt) and distal tubules (pd), in the heart (ht) and in the lung bud (lb) (c and g). At stage 40, *wnt9a* expression remains strong in the pronephric proximal and distal tubules (pt, dt), in the heart (ht) and in *X. tropicalis* lung bud (lb) (d and h).

show expression in the somites, the otic vesicule, the eye and the branchial arches (data not shown).
To conclude, *wnt9a* expression is most visible in *X. laevis* and *X. tropicalis* embryos around stage 35 to 40, where it is expressed in the pronephric tubules, the heart and the lung primordia.

3.3.2.2 Temporal and spatial embryonic expression of *Xtwnt9b* and *Xlwnt9b.*

Figure 3.7 shows spatial and temporal expression pattern of *wnt9b* in *X. laevis* and *X. tropicalis* embryos. *In situ* hybridization analysis in whole-mount *Xenopus* embryos using DIG-labelled antisense probes shows that *wnt9b* cannot be detected in embryos at stage 20 (Fig 3.7 a and e). *wnt9b* starts to be expressed around stage 24-25 in the branchial arches region (Fig 3.7 b and f, arrows pointing to the region). By stage 35, in both *X. tropicalis* and *X. laevis, wnt9b is* observed in the pronephros, the branchial arches, the otic vesicle, the eye and the heart and in the neural tube and the brain in *X. laevis* embryos (Fig 3.7 c and g). Control sense probes from *Xtwnt9b* and *Xlwnt9b* show some background expression in the somites only (data not shown). By stage 40, *wnt9b* expression persists in the *X. laevis* and *X. tropicalis* embryos in the branchial arches, the proximal and distal pronephric tubules and the heart (Fig 3.7 d and h, arrows highlighting position of organs). *wnt9b* is no longer expressed in the eye, the neural tube and the brain in *Xenopus* embryos at stage 40.
To summarise, *wnt9b* shows a similar expression pattern in *X. laevis* and *X. tropicalis* embryos and is most prominent in stage 35 embryos in the pronephros, branchial arches, eye, heart, otic vesicule. Only expression in the pronephros, the branchial arches and the heart remain at stage 40.

To conclude, the embryonic expression pattern of *Xtwnt9a* and *Xtwnt9b* published by Garriock et al. (2007) have now been confirmed. Moreover, we present new data to demonstrate that *Xlwnt9a* and *Xlwnt9b* show identical expression patterns to their orthologous genes in *X. tropicalis* embryos. However, in contrast to Garriock et al., 2007, our *in situ* studies provide evidence that *wnt9b* is expressed in the pronephros of *X. laevis* and *X. tropicalis* embryos from stage 35 onwards and that *wnt9a* expression is clearly obvious in both proximal/intermediate and more distal tubule components.

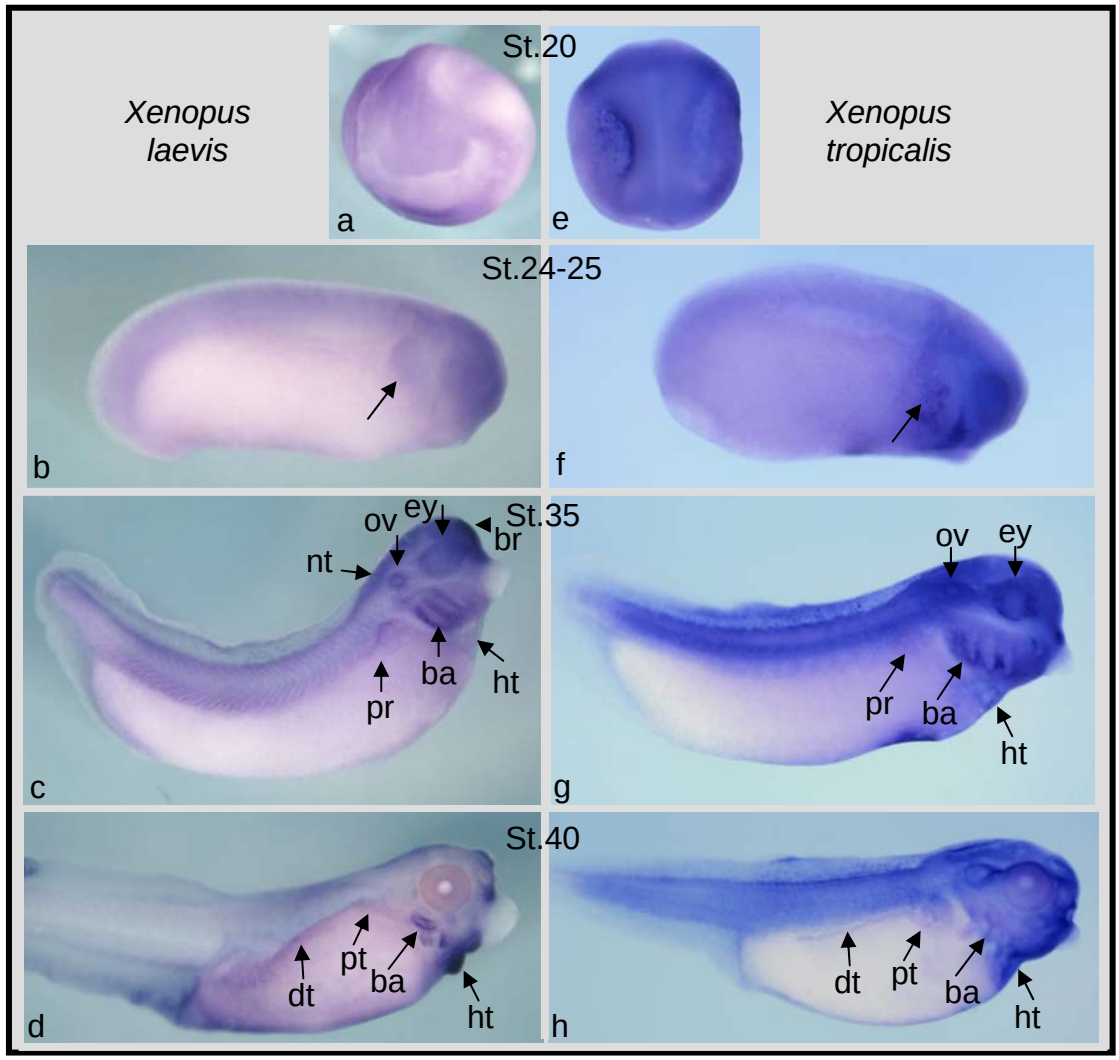

Figure 3.7 Spatial and temporal embryonic expression of *XlWnt9b* and *XtWnt9b*. *In situ* hybridization analysis in whole-mount *Xenopus* embryos using DIG-labelled antisense probes shows that *wnt9b* cannot be detected in embryos at stage 20 (a and e). *wnt9b* starts to be expressed around stage 24-25 in the branchial arches region (b and f, arrows pointing the region). By stage 35, *wnt9b is* observed in the pronephros (pr), the branchial arches (ba), the heart (ht), the otic vesicle (ov), the eye (ey) in both species and in the neural tube (nt) and the brain (br) in *X. laevis* embryos (c and g, arrows highlighting position of organs). By stage 40, *wnt9b* is still expressed in the branchial arches (ba), the proximal and distal pronephric tubules (pt, dt), and the heart (ht) (d and h, arrows highlighting position of organs).

3.3.3 Expression profile of *Xlwnt9a* and *Xlwnt9b* in early embryonic development.

In situ hybridization analyses have shown that in *Xenopus* embryos, *wnt9a* was first detected at the early tail bud stage, stage 30, in the developing pronephros and that *wnt9b* was first observed at approximately stage 22, in the branchial arch region. RT-PCR analysis, using RNA purified from *X. laevis* embryos from oocytes until late tadpole stage, stage 45, reveals the temporal expression pattern of *Xlwnt9a* and *Xlwnt9b*, figure 3.8. Maternal *Xlwnt9b* expression is weakly detected in the oocyte and the unfertilised eggs and in the embryos until stage 8. Zygotic *Xlwnt9b* expression initiates at stage 13 and is strongly up-regulated at stage 19. High levels of expression are maintained until stage 45.
Expression of *Xlwnt9a* is undetectable in the oocyte and in unfertilised eggs. Zygotic *Xlwnt9a* expression is not detected until stage 13 and its level of expression remains strong and constant until stage 45, the last stage tested, where there is a notable strong expression. In conclusion, the highly sensitive RT-PCR technique detects maternal expression for *Xlwnt9b*, and both genes are expressed from the end of gastrulation onwards in *X. laevis* embryos.

3.3.4 Expression of *wnt9a* and *wnt9b* in adult *X. laevis* and *X. tropicalis* organs.

In situ hybridization studies in *X. laevis* and *X. tropicalis* early embryos have shown that *wnt9a* is expressed mostly in the pronephros and in the lung primordial. In contrast, *wnt9b* is expressed mainly in the branchial arches, in the heart, in the eye and in the pronephros. Does *wnt9a* and *wnt9b* expression persist in the same tissues in the adult frogs? Figure 3.9 shows expression of *wnt9a* and *wnt9b* in *X. tropicalis* and *X. laevis* dissected adult organs. Figure 3.9, panel A shows that *Xtwnt9a* is expressed in almost all tissues, in brain, gall bladder, heart, liver, muscle, ovary, stomach and testis, with exception of skin. *Xtwnt9a* is relatively more expressed in eye and kidney. However, *Xtwnt9b* is tissue restricted to the eye, the kidney, the stomach and the reproductive organs. *Xtwnt9b* is also weakly expressed in the brain. Figure 3.9, panel B shows the distribution in *X. laevis* organs. *Xlwnt9a* is ubiquitously expressed, in brain, heart, kidney, liver, lung, muscle, ovary, testis, spinal chord, rectum and bladder with particularly strong expression in stomach, pancreas and bladder. *Xlwnt9a* is not expressed in blood, spleen and digestive tract

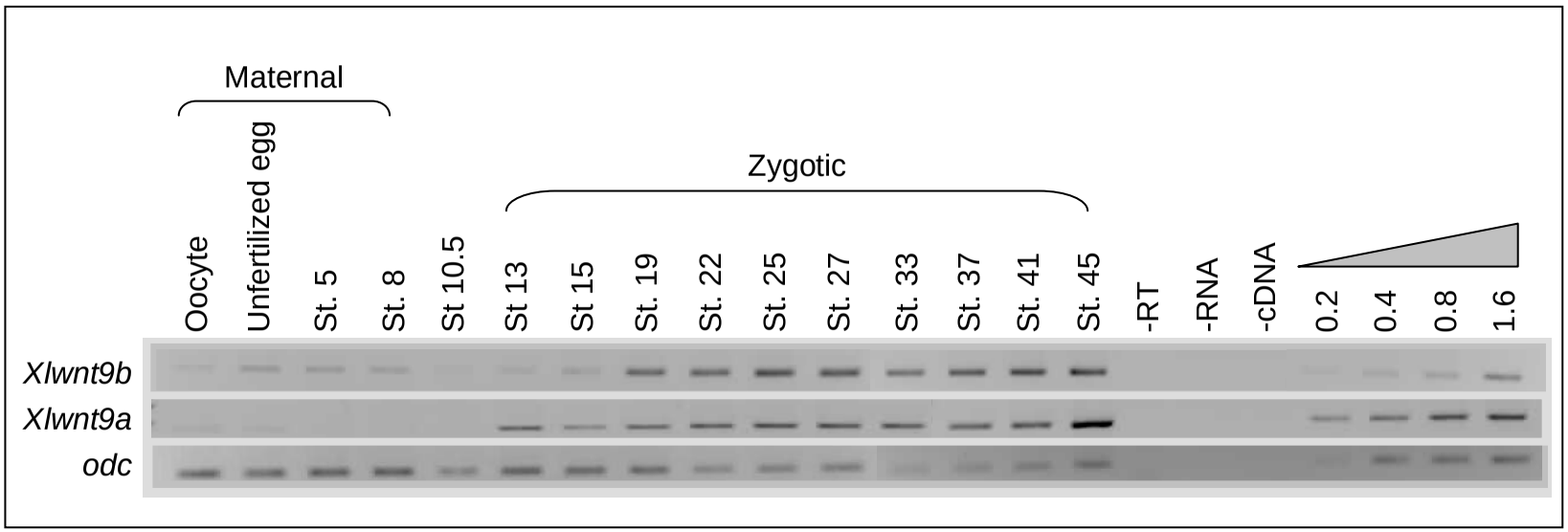

Figure 3.8 Temporal expression of *Xlwnt9b* and *Xlwnt9a* during *X. laevis* early development. Total RNA was extracted from various maternal and zygotic stages of *X. laevis* before being subjected to RT-PCR analysis. *odc* was used for equalizing cDNA samples. The grey triangle illustrates sequentially increasing cDNA inputs of whole embryo stage 37 cDNA. Maternal *Xlwnt9b* expression is weakly detected. Zygotic *Xlwnt9b* expression initiates at stage 13 and is strongly up-regulated at stage 19. High levels of expression are maintained until stage 45. Expression of *Xlwnt9a* is undetectable at maternal stages. Zygotic *Xlwnt9a* starts to be expressed from stage 13 and remains strong until stage 45, the last stage tested.

but weakly expressed in the eye. *Xlwnt9b* is highly expressed in eye, kidney, reproductive organs, pancreas and bladder. *Xlwnt9b* is more weakly expressed in brain, heart, skin, stomach, spinal chord, duodenum, ileum and rectum. *Xlwnt9b* is not expressed in liver, lung, muscle, blood and spleen.

Taken together, analysis of expression of *wnt9a* and *wnt9b* in frog adult tissues shows that the two genes are expressed differently in adult organs but expression is conserved between *X. laevis* and *X. tropicalis* species. *wnt9a* is broadly expressed in the frog adult organs, while *wnt9b* is predominantly expressed in eye, kidney and reproductive organs. *wnt9a* embryonic expression in pronephric intermediate/distal tubules and lung primordial emphasized by Garriock et al. (2007) persists in the corresponding adult organ. However, in the adult frog *wnt9a* becomes more generally distributed. Expression of *wnt9b* in the embryonic eye also persists in the adult eye besides being expressed in kidney and reproductive organs.

To conclude, analyses of expression of the *X. laevis* and *X. tropicalis wnt9a* and *wnt9b* using *in situ* hybridization and RT-PCR has revealed an expression for both genes in the embryonic and the adult kidney. In order to investigate the role of *wnt9b* in pronephros formation, functional studies were carried out in *X. laevis* embryos.

3.4 Over-expression of *Xtwnt9b* leads to abnormal kidney formation.

Fate mapping of blastomeres at the 8-cell and 32-cell stages allows us to identify the blastomere V2 of an 8-cell stage embryo to be the cell fated to contribute to pronephric structures (Dale and Slack, 1987 and Moody, 1987). We therefore, decided to look at the effects of *wnt9b* mRNA over-expression, when injected into one V2 ventral blastomere at 8-cell stage embryo. Only *X. tropicalis wnt9b* full length coding region mRNA clone is available to date and was a gift from Garriock and al. We will therefore in this chapter, study the effects of *wnt9b* over-expression using *Xtwnt9b* mRNA to inject into *X. laevis* embryos. In order to assay embryos that have received mRNA over-expression localised to the correct region only, *green fluorescent protein (GFP)* or *ß-GAL* mRNA was co-injected with the test mRNA, as

Panel A: Adult *X. tropicalis* organs.

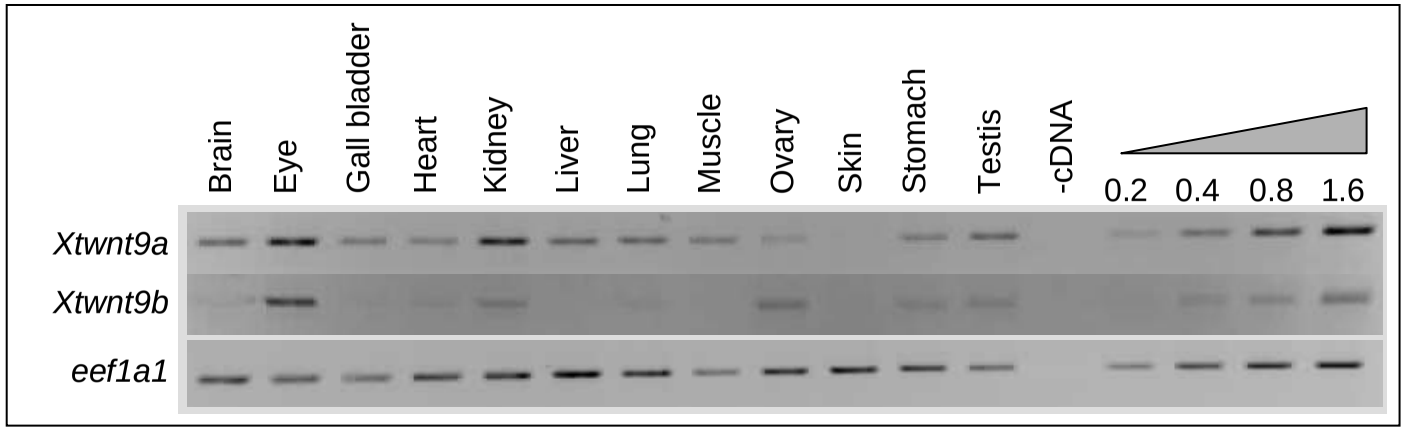

Panel B: Adult *X. laevis* organs.

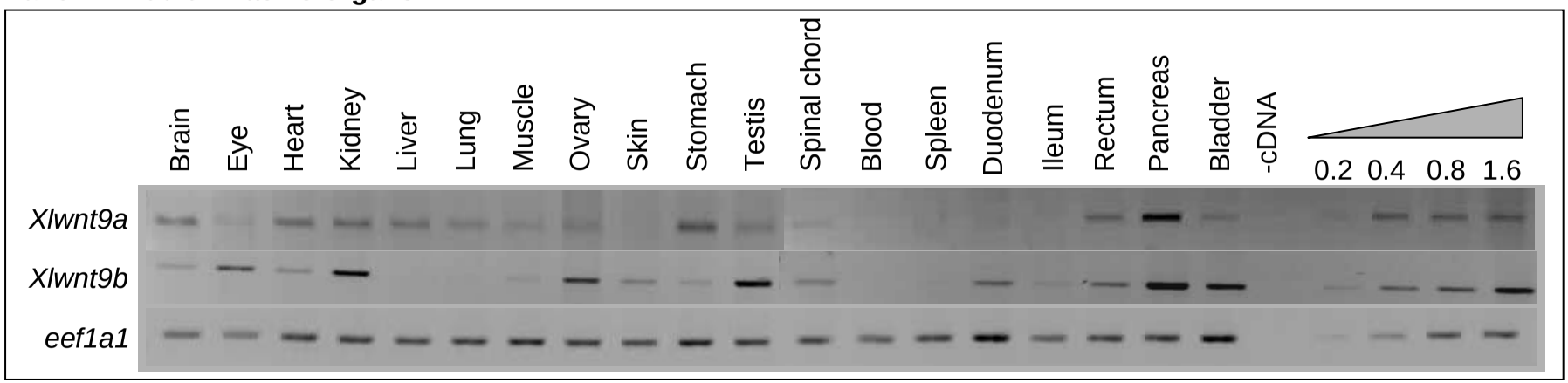

Figure 3.9 Expression of *wnt9a* and *wnt9b* in *X. tropicalis* and *X. laevis* adult organs. Adult *X. laevis* and *X. tropicalis* organs were dissected and total RNA was extracted from each sample before being subjected to RT-PCR analysis. *eef1a1* was used to equalize cDNA samples. The triangle illustrates sequentially increasing cDNA inputs of kidney cDNA. Panel A shows the expression of *wnt9a* and *wnt9b* in adult *X. tropicalis* organs. *Xtwnt9a* is expressed in most tissues (with exception of skin) and is relatively more expressed in the eye and the kidney. *Xtwnt9b* is tissue restricted to the eye, the kidney, the stomach and the reproductive organs. In panel B, *Xlwnt9a* is also expressed in most tissues in adult *X.* laevis organs, except blood, the spleen and the digestive tract and is weakly expressed in the eye. *Xlwnt9b* is highly expressed in the eye, the kidney, the reproductive organs, the duodenum, the rectum, the pancreas and the bladder. *Xlwnt9b* is also weakly expressed in the brain, the heart, the skin, the stomach, the spinal chord and the ileum.

a lineage tracer. *GFP* fluorescence or blue *ß-GAL* staining identify the correctly targeted embryos. Figure 3.10 shows the results of injecting *GFP* mRNA targeted into the 8-cell stage embryo, followed through development to stage 28 (Nieuwkoop and Faber, 1994). Figure 3.10, panel A shows a schematic dorso-lateral view of an embryo at the 8-cell stage, the black arrow represents the injection point in the equatorial region of one of the four ventral blastomeres, and specifically into one of the two V2 blastomeres. The spatial localisation of cells expressing *GFP* can be followed as the embryo develops. Figure 3.10, panel B shows a stage 28 embryo, recorded under white light and then UV light. Exposure to UV light reveals that *GFP* fluorescence is concentrated in the lateral mesoderm including the pronephric tissue. This experiment demonstrates that ventral blastomeres of an 8-cell stage embryo gives rise to the pronephric anlagen among other ventrolateral tissues. In all subsequent injection experiments in this chapter, mRNA will be injected in one V2 ventral blastomere of 8-cell embryos with the aim of specifically targeting the pronephric area. To complement these experiments, we also analysed the effects of *Xtwnt9b* over-expression when *Xtwnt9b* mRNA is injected into the animal pole of 2-cell stage embryos which later on in development becomes epidermis (Urban et al., 2006). This experiment was designed to investigate whether signalling from epidermis overlying the pronephric region could influence pronephros development. Since only a partial coding sequence of *X. tropicalis wnt9a* has been identified, it is not yet possible to carry out functional studies on *Xtwnt9a*.

3.4.1 *Xtwnt9b* belongs to the canonical *wnt* class of molecules.

McMahon and Moon (1989), observed that over-expressing *wnt1* in ventral blastomeres of early *Xenopus* embryos elicits a duplication of the embryonic axis. Funayama et al. (1995) showed that this axis induction was triggered by the activation of the ß-catenin in wnt1/wg signalling. We used this axis induction assay to indicate whether *Xtwnt9b* belongs to the canonical or non-canonical class of wnt signalling molecules. 1or 2ng of *in vitro* transcribed *Xtwnt9b* mRNA was injected into one ventral blastomere at the 4 or 8-cell stage *X. laevis* embryos. Figure 3.11, panel A shows that embryos injected with *ß-GAL* lineage tracer alone resulted in normal axis formation (Fig 3.11 a). However, *X. laevis* embryos injected with 2ng of *Xtwnt9b* mRNA into one ventral blastomere at the 4-cell stage and left to develop

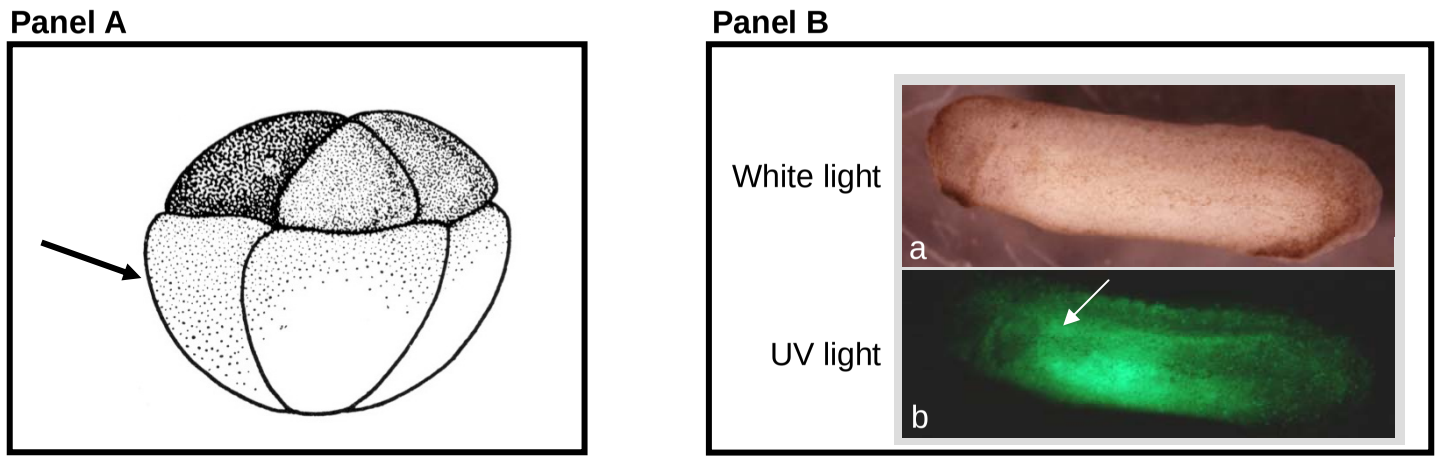

Figure 3.10 Injection of targeted *GFP* mRNA injection in 8-cell stage embryos and followed later on in development. Panel A shows a dorso-lateral view of a 8-cell embryo indicating the injection point in the equatorial region of one of the two V2 ventral blastomeres (black arrow). Panel B shows ventral blastomere V2-targeted *GFP*-injected embryo exposed to white and UV lights showing fluorescence in pronephros area (white arrow).

Panel A

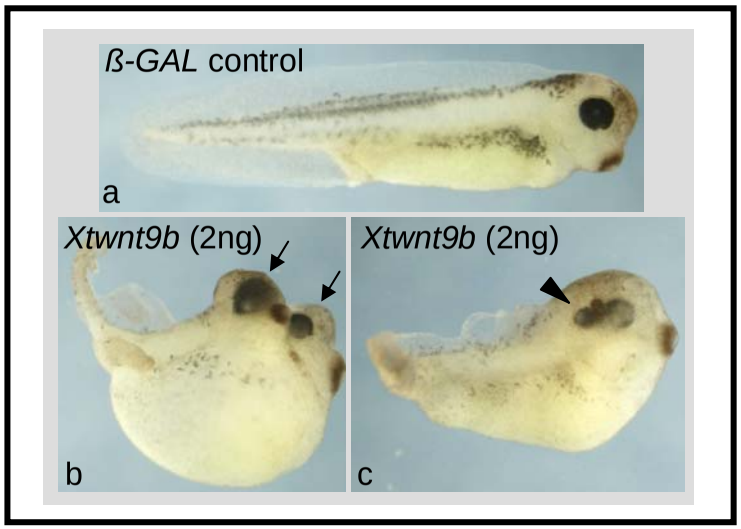

Panel B

Embryo phenotype ► / *Xtwnt9b* over-expression ▼	Normal embryos	Defective eye and short axis	Second axis formed
2ng in one ventral blastomere of 4-cell stage (n=29)	-	4 (14%)	25 (86%)
2ng in one V2 blastomere of 8-cell stage (n=40)	26 (65%)	12 (30%)	2 (5%)
1ng in one V2 blastomere of 8-cell stage (n=76)	50 (66%)	-	26 (34%)

Figure 3.11 *Xtwnt9b* is capable of inducing a second axis when over-expressed in the ventral blastomere of 4-cell and 8-cell stage embryos. Panel A shows *X. laevis* embryos injected with 2ng of *Xtwnt9b* mRNA in one ventral blastomere at 4-cell stage and left to develop until stage 39. Embryos injected with *ß-GAL* alone show normal axis formation (a). Embryos over-expressing *Xtwnt9b* develop a second axis (b, arrows) or show abnormal eye formation accompanied with shorted axis (c, arrowhead). Panel B gives a numerical summary of *Xtwnt9b* over-expression phenotypes.

until stage 39 resulted in 86% of embryos developing a complete secondary axis and showing double heads (arrows) with duplicated cement glands and eyes (Fig 3.11 b). 14% of such embryos showed disturbed axis formation by exhibiting ectopic eye formation (arrowhead) accompanied by a shorted axis (Fig 3.11 c). Figure 3.11, panel B provides a numerical summary of the data obtained following *Xtwnt9b* over-expression into 4 or 8-cell stage embryos. Over-expression of 2ng of *Xtwnt9b* mRNA into one V2 blastomere at the 8-cell stage resulted in 65% of the embryos showing a normal axis formation while 30% of the embryos showed defective eyes and shortened axis and 5% of the embryos formed a complete secondary axis. Injection of 1ng of *Xtwnt9b* into one V2 blastomere at the 8-cell stage embryos resulted in 66% of the embryos developing a complete normal anterior/posterior axis and 34% of such embryos showing a duplicated axis.

In conclusion, we showed that *Xtwnt9b* can induce a secondary axis when over-expressed into one ventral blastomere at the 4 or 8-cell stage *Xenopus* embryos. This result indicates that *Xtwnt9b* possesses one of the characteristics of the canonical class of *wnt* signalling molecules acting through the ß-catenin and the transcription factor TCF pathway. Since injection of 2ng of *Xtwnt9b* into one ventral blastomere at the 4-cell stage embryos resulted in higher number of embryos developing a second axis compared to those injected at the 8-cell stage, *Xtwnt9b* functional studies to investigate pronephros development would be more easily carried out if mRNA is injected into one V2 ventral blastomere at the 8-cell stage. Embryos injected in this way will be more phenotypically normal and the results therefore will be easier to interpret.

3.4.2 Over-expression of *Xtwnt9b* into the V2 blastomere results in abnormal pronephros formation.

In order to examine the role of *Xtwnt9b* in *X. laevis* pronephros formation, *Xtwnt9b* mRNA was over-expressed into one V2 blastomere of 8-cell stage *X. laevis* embryos, which specifically targets the pronephric region. Figure 3.12 shows that *Xenopus* embryos previously injected into the V2 blastomere with *Xtwnt9b* mRNA develop an abnormal pronephros. Figure 3.12, panel A shows a control *ß-GAL* embryo immuno-stained with the specific pronephric proximal tubule antibody, 3G8, stained in purple and the specific pronephric intermediate and distal tubule antibody, 4A6, stained in

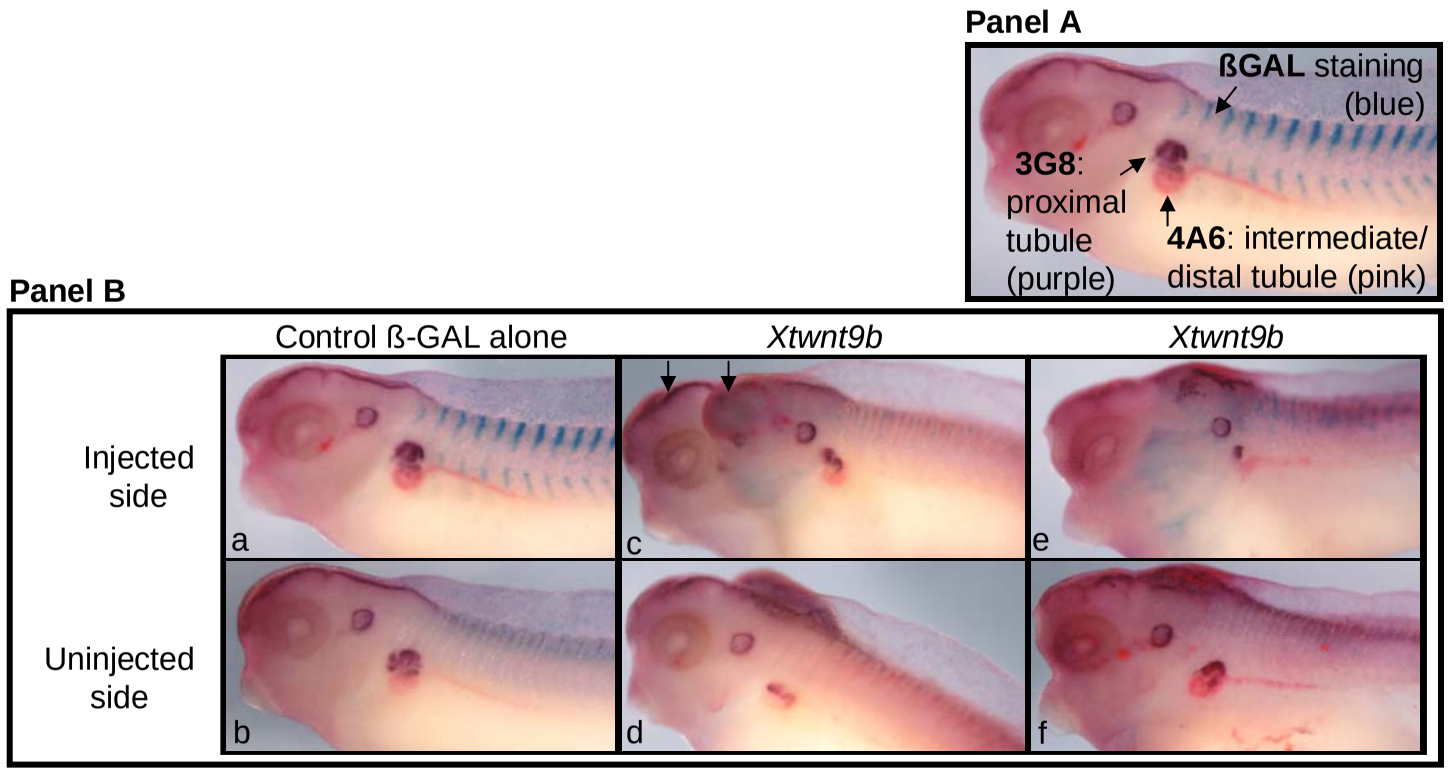

Figure 3.12 *Xenopus* embryos previously injected into the V2 blastomere with *Xtwnt9b mRNA* develop an abnormal pronephros. Panel A shows a control *ß-GAL* embryos immunostained with the specific pronephric proximal tubule antibody, 3G8, stained in purple and the specific pronephric intermediate and distal tubule antibody, 4A6, stained in pink. The lineage tracer *ß-GAL* stained the somites in blue resulting from mRNA injection into one V2 blastomere at the 8-cell stage embryo. Panel B shows that embryos injected with *ß-GAL* alone develop normal proximal, intermediate and distal tubule (a, b). Injection of *Xtwnt9b* mRNA in V2 blastomere often results in the formation of a second axis (arrows in c). Therefore, the pronephros developing on the second axis appears smaller due to the smaller size of the second body axis formed (c). On the uninjected side, pronephros formation is also affected (d). In embryos where the axis is normal injection of *Xtwnt9b* results in reduced proximal, intermediate and distal tubule on the injected side (e), while the pronephros on the uninjected side remains fairly normal (f).

pink. The lineage tracer *ß-GAL* stained the somites in blue indicating correct targeting of mRNA injection into one V2 blastomere at the 8-cell stage embryo. Figure 3.12, panel B shows that embryos injected with *ß*-GAL alone develop a normal pronephros (a, b). Injection of *Xtwnt9b* mRNA in V2 blastomere often results in the formation of a second axis (arrows in c). Therefore, the pronephros developing on the second axis appears smaller due to the smaller size of the second body axis formed (c). On the uninjected side, pronephros formation is also affected and appears reduced (d). In embryos showing a normal axis, injection of *Xtwnt9b* mRNA results in reduced proximal, intermediate and distal tubules on the injected side (e), while the pronephros on the uninjected side remains fairly normal (f). Embryos injected with 1 to 2ng of *Xtwnt9b* mRNA into one V2 blastomere at the 8-cell stage and left to develop until stage 40 were analysed for pronephros phenotype. Embryos presenting extreme defects in anterior-posterior axis formation such as duplicate axis or shortened axis were removed from this analysis as this will by itself cause abnormal kidney reduction. Equally, embryos showing abnormal pronephros formation on the uninjected side were rejected from this analysis. Figure 3.13 gives the number and the percentage of embryos injected with 1 to 2ng of *Xtwnt9b* mRNA into one V2 blastomere at 8-cell stage and showing fairly normal axis formation and pronephros phenotype on the injected side only. Table 3.13.1 and graph 1 show that 90% and 48% of embryos injected with 2ng and 1ng of *Xtwnt9b* mRNA respectively had a completely normal morphology, 13% and 38% of embryos injected with 1ng of *Xtwnt9b* showed a slightly bent axis and abnormal head formation (abnormal large head and fused, frontal eye) respectively. Figure 3.13, table 3.13.2 and graphs 2 and 3 show that 100% of the embryos injected with *ß*-GAL alone develop normal pronephric tubules. 52% and 70% of embryos over-expressing 1 and 2ng of *Xtwnt9b* mRNA respectively show reduced proximal tubule. 20% of embryos over-expressing 2ng of *Xtwnt9b* mRNA show abnormal enlarged, disorganised proximal tubule, while 17% of embryos over-expressing 1ng of *Xtwnt9b* mRNA did not develop any proximal tubule. Similarly, most of the embryos over-expressing 1 to 2ng of *Xtwnt9b* mRNA developed reduced intermediate/ distal tubule, 22% and 10% of embryos injected with 1ng and 2ng of *Xtwnt9b* mRNA respectively did not form any intermediate/ distal tubule and 10% of embryos over-expressing 2ng of *Xtwnt9b* mRNA show abnormal enlarged tubules.

Figure 3.13 Numerical and graphical representation of the pronephros phenotype in *X. laevis* embryos over-expressing 1 to 2ng of *Xtwnt9b* mRNA. Embryos were injected into one V2 ventral blastomere at the 8-cell stage embryo and left to develop until stage 40 before being analysed by antibody staining using the specific proximal tubule antibody 3G8 and the specific intermediate and distal tubule antibody 4A6.

		Embryo morphology		
mRNA injected		Normal	Bent	Abnormal head
ß-GAL	n=46	54	0	0
	%	**100**	**0**	**0**
Xtwnt9b (1ng)	n=23	11	3	9
	%	**48**	**13**	**39**
Xtwnt9b (2ng)	n=10	9	0	1
	%	**90**	**0**	**10**

Table 3.13.1 Morphology of embryos injected with 1 to 2ng of *Xtwnt9b* mRNA into one V2 blastomere at the 8-cell stage and analysed for pronephros phenotype.

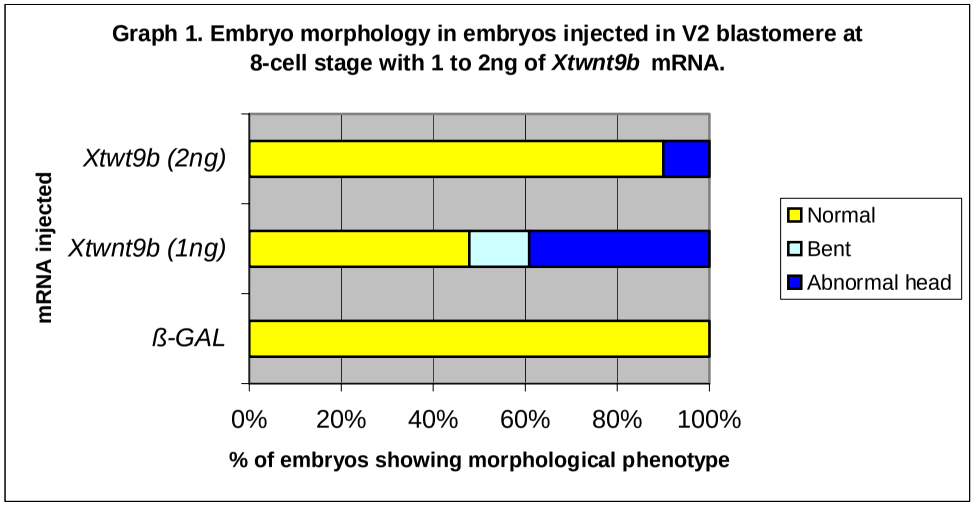

Graph 1 shows the morphology of embryos injected with 1 to 2ng of *Xtwnt9b* mRNA into one V2 blastomere at the 8-cell stage and analysed for pronephros phenotype.

mRNA injected		Proximal tubule morphology: Injected side Normal	Red.	Enl.	Abs.	Uninjected side Normal	Intermediate and distal tubule morphology: Injected side Normal	Red.	Enl.	Abs.	Uninjected side Normal
ß-GAL	n=46	46	0	0	0	46	46	0	0	0	46
	%	**100**	**0**	**0**	**0**	**100**	**100**	**0**	**0**	**0**	**100**
Xtwnt9b (1ng)	n=23	6	12	1	4	23	4	13	1	5	23
	%	**26**	**52**	**4**	**17**	**100**	**17**	**57**	**4**	**22**	**100**
Xtwnt9b (2ng)	n=10	0	7	2	1	10	2	6	1	1	10
	%	**0**	**70**	**20**	**10**	**100**	**20**	**60**	**10**	**10**	**100**

Key: Red.: Reduced. Enl.: enlarged. Abs.: absent.

Table 3.13.2 Number and percentage of embryos showing pronephros phenotype in embryos injected in V2 blastomere of 8-cell stage with 1 to 2ng of *Xtwnt9b* mRNA.

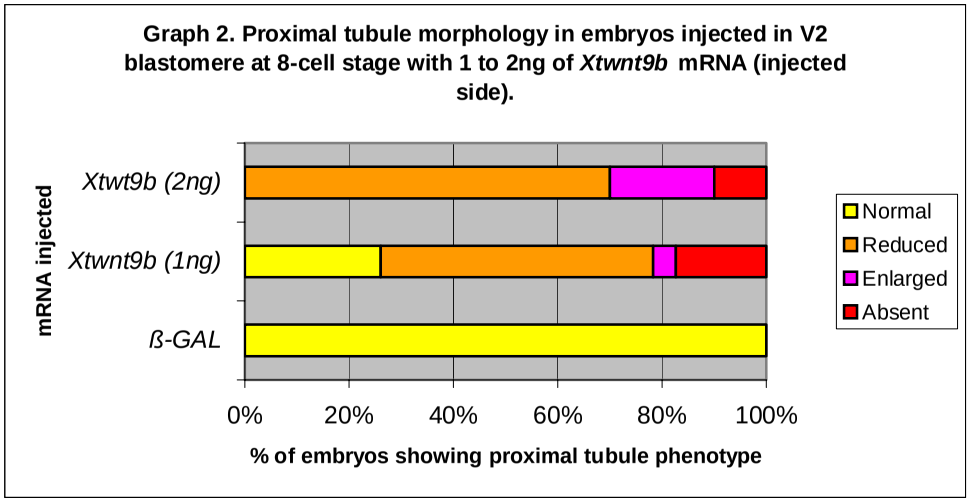

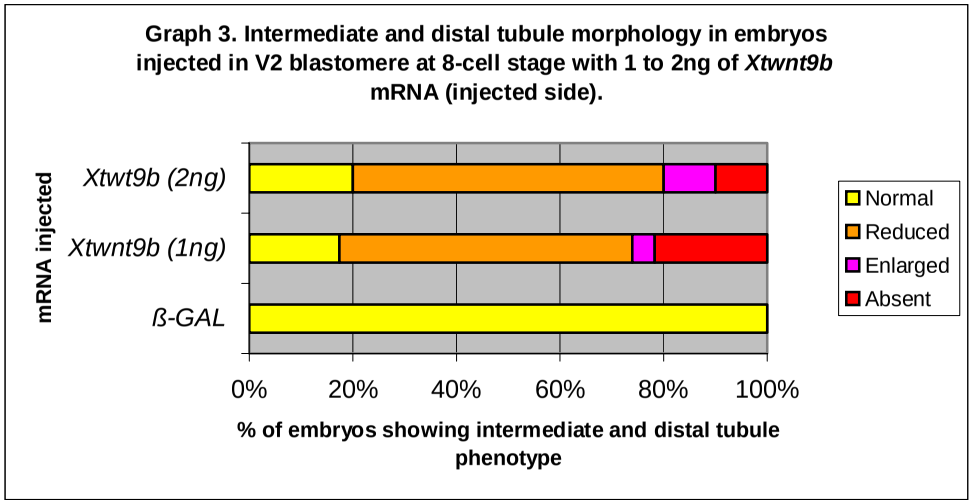

Graph 2 and 3 show the proximal tubule and the intermediate/ distal tubule phenotype in embryos injected in V2 blastomere of 8-cell stage with 1 to 2ng of *Xtwnt9b* mRNA.

To conclude, over-expression of *Xtwnt9b* mRNA into one V2 ventral blastomere at the 8-cell stage affects pronephros formation. Analysis suggests that the major phenotype observed, results in reduced proximal and intermediate/ distal tubules. However, absence of tubule is more frequently observed when 1ng of *Xtwnt9b* mRNA was injected and abnormal enlarged tubule is more often seen in embryos over-expressing 2ng of *Xtwnt9b* mRNA. However, the difference in phenotype is unlikely to be significant. In an attempt to overcome the gross axis formation defects caused by injection of *Xtwnt9b* mRNA into V2 ventral blastomere and with the aim of verifying that *Xtwnt9b* disturbs the kidney formation, *Xtwnt9b* mRNA was injected into the animal pole region of one cell of 2-cell stage embryos which will later in development give rise to the epidermis, some of which will overlay the pronephros region.

3.4.3 Over-expression of *Xtwnt9b* in epidermis results in abnormal pronephros formation.

Thus, with the aim of diminishing the gross morphological effects caused by the over-expression of *Xtwnt9b* in ventral blastomere, 0.25 to 1ng of *Xtwnt9b* mRNA was over-expressed in the animal pole of one cell of 2-cell stage *Xenopus* embryos. The animal pole gives rise to epidermal tissue that covers the entire embryo including the pronephric region. Figure 3.14 shows embryos that over-express *Xtwnt9b* in the epidermis also develop an abnormal pronephros in the absence of a gross axis phenotype. Embryos were injected in the animal pole of one blastomere at the 2-cell stage with *GFP* alone or with *GFP* and 0.25 to 1ng of *Xtwnt9b* mRNA and left to develop until stage 40 before being assayed by immuno-staining. Figure 3.14, panel A shows a normal *Xenopus* embryos at stage 40 stained in purple with the specific pronephric proximal tubule antibody, 3G8, and in pink with the specific pronephric intermediate and distal tubule antibody, 4A6. Figure 3.14, panel B shows that injection of *GFP* mRNA alone does not disturb pronephric development (a-b). However, on the injected side, injection of 0.25 to 0.5ng of *Xtwnt9b* mRNA shows a concentration dependent reduction of the pronephric proximal and intermediate/ distal tubules (c and e). On the uninjected side, the morphology of the pronephric tubules remains normal when embryos over-express 0.25 to 0.5ng of *Xtwnt9b* (d and f). Injection of 1ng of *Xtwnt9b* results in a large proportion of embryos not

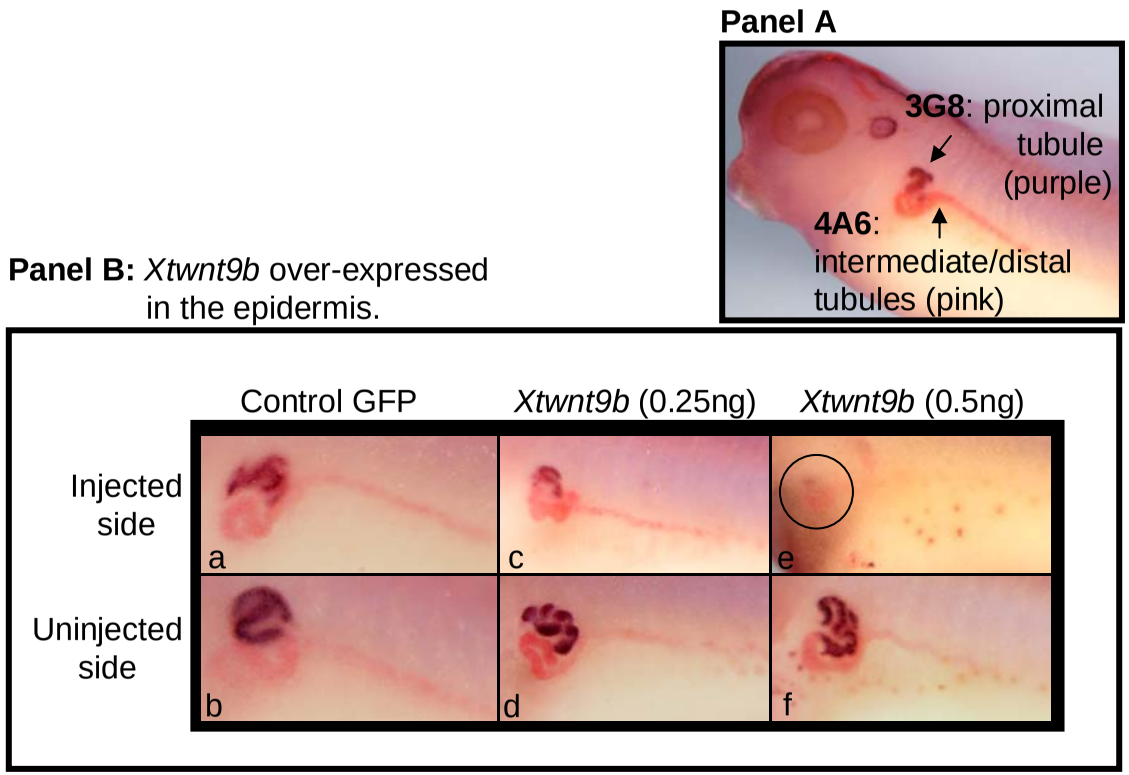

Figure 3.14 Embryos over-expressing *Xtwnt9b* in the epidermis develop an abnormal pronephros. Embryos were injected in the animal pole of one blastomere at the 2-cell stage with *GFP* alone or with *GFP* and 0.25 to 0.5ng of *Xtwnt9b* mRNA. Embryos were left to develop until stage 40 before being assayed by immunostaining. Panel A shows a normal *Xenopus* embryos at stage 40 stained with the specific pronephric proximal tubule antibody, 3G8, stained in purple and the specific pronephric intermediate and distal tubule antibody, 4A6, stained in pink. Panel B shows that injection of *GFP* mRNA alone does not disturb pronephric development (a-b). However, on the injected side, injection of 0.25 to 0.5ng of *Xtwnt9b* mRNA show increasing reduction of pronephric tubules as the message concentration increases (c and e). On the uninjected side, the morphology of the pronephric tubules remains normal when embryos over-express 0.25 to 0.5ng of *Xtwnt9b* (d and f).

developing any pronephric structure on the injected side but also showing abnormal pronephros morphology on the uninjected side (data not shown).

Figure 3.15 shows tables of numbers and graphical representations of the pronephros phenotype in *X. laevis* embryos injected with 0.25 to 1ng of *Xtwnt9b* mRNA into the animal pole of one cell of 2-cell stage embryos, left to develop until stage 40 before being analysed for pronephros phenotype. Embryos showing severe axis defects or abnormal kidney formation on the uninjected side were rejected from this analysis. Figure 3.15, table 3.15.1 and graph 1 show that morphologically, embryos injected with *Xtwnt9b* mRNA into the animal pole of one cell of 2-cell stage embryos develop an abnormal head (predominantly abnormal eye formation). Some embryos over-expressing 1ng of *Xtwnt9b* showed signs of kidney failure by showing formation of oedema. Figure 3.15, table 3.15.2 and graphs 2 and 3 show number and percentage of embryos showing a pronephros phenotype. Most of the embryos injected with 0.25 to 1ng of *Xtwnt9b* mRNA show reduced proximal tubule (67% and 47% respectively). 17% of embryos injected with 0.25ng of *Xtwnt9b* and 41% of embryos injected with 1ng of *Xtwnt9b* did not form any proximal tubule structures at all, suggesting an mRNA dose-dependent effect. Intermediate and distal tubule formation was also affected. In embryos injected with 0.25ng of *Xtwnt9b*, intermediate and distal tubules were reduced in 42%, enlarged in 17% and absent in 25%. Injection with 1ng of *Xtwnt9b* mRNA show similar results.

To conclude, over-expressing 0.25 to 1ng of *Xtwnt9b* mRNA in the animal pole of one cell of 2-cell stage *Xenopus* embryo affects the normal development of the embryos. Embryos developed abnormal head structure and oedema, but possessed a normal anterior-posterior axis. Embryos developed an abnormal pronephros and the proximal, intermediate/ distal tubules are reduced in a dose-dependent manner or absent in the most extreme case. Would inhibition of *Xtwnt9b* also affect pronephros development?

Figure 3.15 Numerical and graphical representation of the pronephros phenotype in *X. laevis* embryos over-expressing 0.25 to 1ng of *Xtwnt9b* mRNA. Embryos were injected into one animal pole of 2-cell embryo and left to develop until stage 40 before being analysed by antibody staining using the specific proximal tubule antibody 3G8 and the specific intermediate and distal tubules antibody 4A6.

		Embryo morphology				
mRNA injected		Normal	Bent	Shorted axis	Abnormal head	Abnormal ventral st.
GFP (1ng)	n=18	18	0	0	0	0
	%	**100**	**0**	**0**	**0**	**0**
Xtwnt9b	n=12	3	1	3	5	0
(0.25ng)	%	**25**	**8**	**25**	**42**	**0**
Xtwnt9b	n=17	0	1	1	13	2
(1ng)	%	**0**	**6**	**6**	**76**	**12**

Table 3.15.1 Morphology of embryos over-expressing 0.25 to 1ng of *Xtwnt9b* mRNA in the epidermis and analysed for pronephros phenotype.

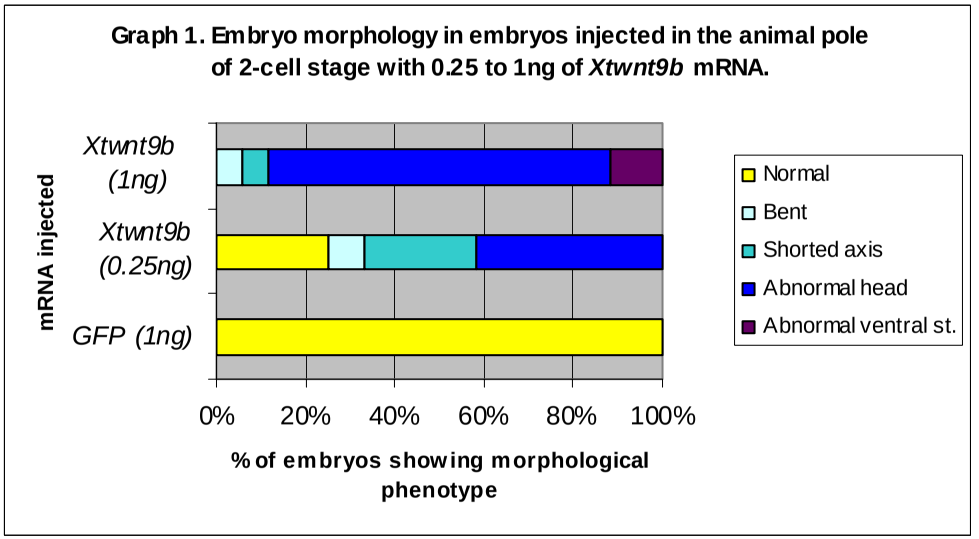

Graph 1 shows the morphology of embryos over-expressing 0.25 to 1ng of *Xtwnt9b* mRNA in the epidermis and analysed for pronephros phenotype.

mRNA injected		Proximal tubule morphology: Injected side Normal	Red.	Abs.	Uninjected side Normal	Intermediate and distal tubule morphology: Injected side Normal	Red.	Enl.	Abs.	Uninjected side Normal
GFP (1ng)	n=18	18	0	0	18	18	0	0	0	18
	%	**100**	**0**	**0**	**100**	**100**	**0**	**0**	**0**	**100**
Xtwnt9b (0.25ng)	n=12	2	8	2	12	2	5	2	3	12
	%	**17**	**67**	**17**	**100**	**17**	**42**	**17**	**25**	**100**
Xtwnt9b (1ng)	n=17	2	8	7	17	3	4	5	5	17
	%	**12**	**47**	**41**	**100**	**18**	**24**	**29**	**29**	**100**

Key: Red.: Reduced. Enl.: enlarged. Abs.: absent.

Table 3.15.2 Number and percentage of embryos showing pronephros phenotype in embryos injected in the animal pole of 2-cell stage with 0.25 to 1ng of *Xtwnt9b* mRNA.

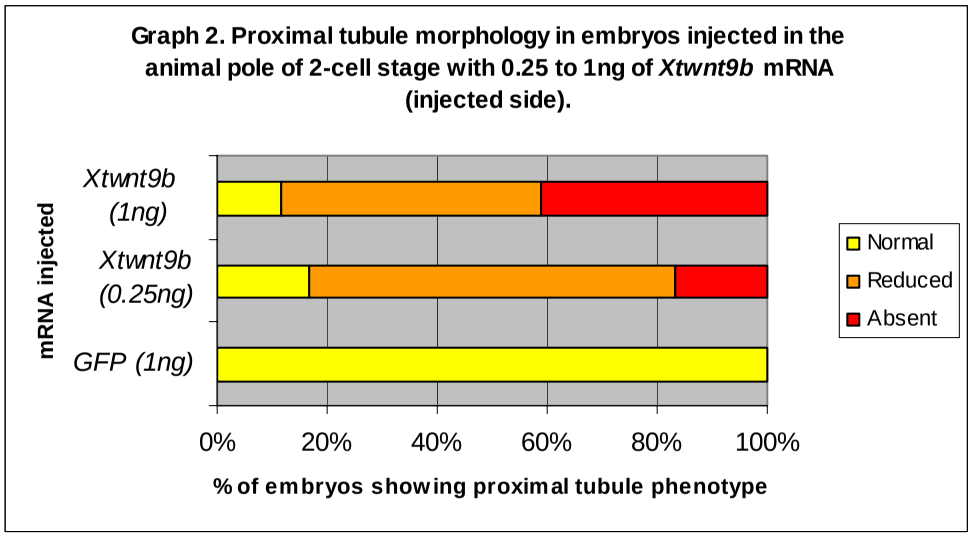

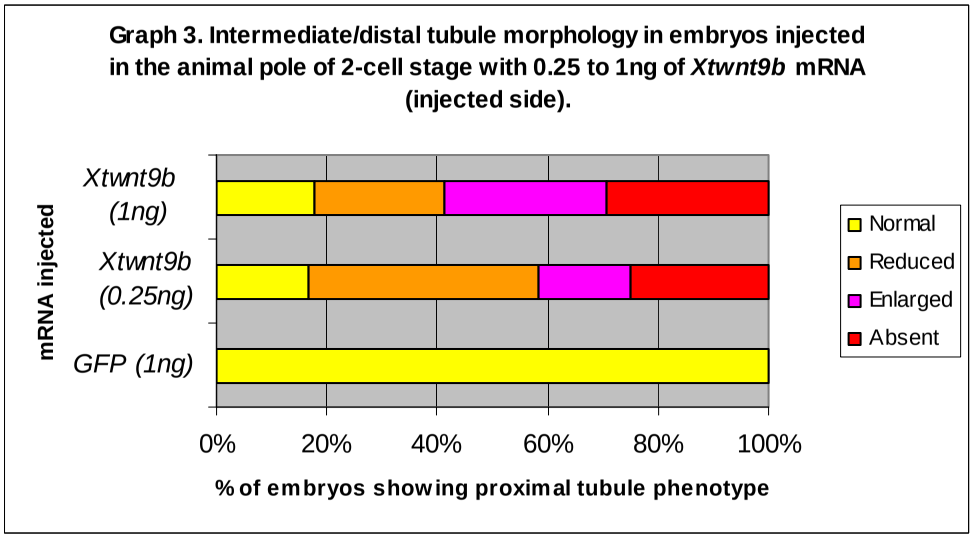

Graph 2 and 3 show the proximal tubule and the intermediate/ distal tubules phenotype in embryos injected in the animal pole of 2-cell stage with 0.25 to 1ng of *Xtwnt9b* mRNA.

3.5 Inhibition of function of *Xlwnt9a* and *Xlwnt9b* in *X. laevis* embryos using antisense morpholinos.

3.5.1 Design of *Xlwnt9a* and *Xlwnt9b* antisense morpholinos.

In order to investigate the phenotypic consequences when *Xlwnt9a* and *Xlwnt9b* are inhibited, a knock-down strategy using antisense morpholinos was carried out in *X. laevis* embryos. We used *Xlwnt9a* and *Xlwnt9b* sequences identified from generating *in situ* probes to perform 5' RACE PCR to identify the 5'UTRs and the beginning of the coding sequence including the ATG codon in both *Xlwnt9a* and *Xlwnt9b*. Subsequently, 25nt *Xlwnt9a* and *Xlwnt9b* antisense morpholololinos were designed by Gene Tools that will bind around the ATG region and block transcription of *Xlwnt9a* and *Xlwnt9b* within the cell.

5' RACE PCR was carried out following the manufacturer's instructions (Invitrogen). Table 3.5.1 shows the gene specific primers (GSP) designed from *Xlwnt9a* and *Xlwnt9b* sequences previously identified from generating *in situ* hybridization probes (chapter 3, section 3.3.1). According to the manufacturer's instructions, GSP1 primers were designed to anneal at least 300bp from the mRNA 5'-end and GSP2 and 3 are located 5' to GSP1. 5' RACE PCR was carried out using an adult *X. laevis* pancreas RNA sample, as it was previously shown that both *Xlwnt9a* and *Xlwnt9b* are abundantly expressed in the pancreas (chapter 3, section 3.3.4). Figure 3.16 shows *Xlwnt9b* partial DNA and its conceptual translation. Nucleotide sequence is assembled from novel sequence data obtained during the production of *in situ* probes (previously not detailed) and from novel 5'UTR RACE PCR amplification. *Xlwnt9b* partial DNA sequence includes 86 base pairs of the 5'UTR but lacks the end of the 3' coding region and the 3'UTR. The gene specific primers (GSP), the ATG position and the morpholino oligo sequence are indicated. The sequence of the *Xlwnt9b* antisense morpholino designed is 5'-GTTGTGCTGAGCTTCTCCTCATCTC-3'. There was an unintentional mismatch created during the design (A was replaced by G at position 4 in the morpholino sequence). The *Xlwnt9b* mRNA partial coding sequence was also conceptually translated to give a 293 amino acid long protein. This can be used for protein sequence comparison. Figure 3.17 shows *Xlwnt9a* partial DNA and its conceptual translation. Nucleotide sequence is assembled from novel sequence data obtained during the production of *in situ* probes (previously not

	Xlwnt9a	*Xlwnt9b*
GSP1	5’-GGTGCAGTTCCAGCGCTCAA-3’	5’-CCTCTGTCGAAGGAAGTTCT-3’
GSP2	5’-TCGGCACATCCTGCGTTGCT-3’	5’-GCAGGAATCGAGTGCTGTGT-3’
GSP3	5’-TCGGCACATCCTGCGTTGCT-3’	5’-AGTGCTGTGTCGGAGGTTGT-3’

Table 3.5.1 Gene specific primers (GSP) designed from *Xlwnt9a* and *Xlwnt9b* sequences previously identified from generating *in situ* hybridization probes designed to amplify by 5’ RACE PCR the 5’UTR *of XlWnt9a* and *XlWnt9b*. As according to manufact user’s instructions, GSP1 primers are designed to anneal at least 300bp from the mRNA 5’-end and GSP2 and 3 are located 5’ to GSP1.

Xlwnt9b mRNA, partial coding sequence.

cagccgtttgaagtgaaggagcggacagtccggtgcattgggcagtgggagagaaggaga***gaga***
tgaggagaagctcagcataaca**ATG**CCCACCGACCCCTGTCTGGCCGACCTCTGCCTCCCGCTC
CTGCTGCTGCTGATCACTCCCCTCCTGCCGCCGACCGGAGCCTATTTCGGTCTGACCAGCAAAG
AGTCTCTCTCGCTCTTCACCTCCCCGGCCCCCATAATCAGCAGCACCCACAGCCGACCCCACCT
GAAACACTGCGACCTGCTGCCCCTGACCCGGCGCCAGAAACGGCTGTGCCGCAAGGAACCAGGA
CTGGCCGAGGCGCTGAGAGAAGCCGTGCGACTGGGGGTCGTAGAGTGTCAGTTCCAGCTGCGGA
ACGAACGTTGGAACTGCAGTCTCCAGGAAAGGGGGACTCTCCTGAAAAGAGGTTTTAAAGAGAC
AGCATTCCTGTATGCCAATTCAGCTGCCTCCCTCACCCATTCCCTAGCGAAGGCCTGCAGTGGG
GGCAGAATGGAGCGATGTACCTGTGACGACTCCCAAGGCCTGGAGAGCCAGCGGGCTTGGCAGT
GGGGTGTTTGTGGGG**ACAACCTCCGACACAGCACTCGATTCCTGC**AGAACTTCCTTCGACAGAG
GAAAGGGGGGAAAGACGCACGGGCTAAGATGGATGTTCATAACAGCAACGCAGGCATTAAATCT
GTAAAGAGTGGATTAAAGACCACGTGTAAATGCCACGGGGTGTCCGGCTCCTGCGCTGTCCGCA
CATGTTGGAAGCAACTCTCTCCTTTCCATGAAACAGGAGCGCTGCTGAAAGCCAAGTATGAAAA
CGCCATAAAGATCCTTGGGGCCTCCAATGAGGCGGTGGGAGGCCATGAGACCCCGGGACAGTTA
TTCGGTGGGCGTCACACCCGCTCTACTGACTTCTTATACCTGGAGGAGTCACCCAACTTCTGCA
GGCCAAG

Xlwnt9b (293aa).

MPTDPCLADLCLPLLLLLITPLLPPTGAYFGLTSKESLSLFTSPAPIISSTHSRPHLKHCDLLP
LTRRQKRLCRKEPGLAEALREAVRLGVVECQFQLRNERWNCSLQERGTLLKRGFKETAFLYANS
AASLTHSLAKACSGGRMERCTCDDSQGLESQRAWQWGVCGDNLRHSTRFLQNFLRQRKGGKDAR
AKMDVHNSNAGIKSVKSGLKTTCKCHGVSGSCAVRTCWKQLSPFHETGALLKAKYENAIKILGA
SNEAVGGHETPGQLFGGRHTRSTDFLYLEESPNFCRP

Figure 3.16 Novel *Xlwnt9b* partial DNA and protein sequences. The *Xlwnt9b* partial DNA sequence includes 86 base pairs of the 5'UTR but lacks the 3' end of the coding region and the 3'UTR. Sequence amplified by 5'RACE PCR is highlighted in yellow and sequence previously identified from *in situ* probe generation is left in white. Bold, underlined, red nucleotides indicate the GSP1 location and bold, underlined black nucleotides indicate location of GSP2 and GSP3, that are in that case, overlapping. Starting codon, ATG, is highlighted in grey. Italic, bold underlined nucleotides indicate were *XlWnt9b* antisense morpholino was designed. The morpholino oligo sequence is 5'-GTTGTGCTGAGCTTCTCCTCATCTC-3'. The *Xlwnt9b* mRNA, partial coding sequence was translated to give a 293 amino acid partial protein.

Xlwnt9a mRNA, partial coding sequence.

ccaacatcaacgaaatggtcagccgtggagctg***cagcaaa***ATG***CTGGATGGACACCTT***GTTC
TGGGATGGCTATCAGTTGCCCTAGTAGCCCTCCACTGCCTCGGGCCGGCGGCTGCTAACTTC
GGGCTGACAGGGAATGAACCATTGACCATCCTCCCTCTGACCTCAGAAACGGAGGAAGCTGC
AGTGAAGGCCCATTACAAAATCTGTGACCGGCTTAAGCTTGAGCGGA**AGCAACGCAGGATGT**
GCCGACGAGACCCGGGGGTGGCCGAGACCCTTATAGAGGCCATTAGCATGAGTGCGCAGGAG
TGCGAGTACCAGTTTCACT**TTGAGCGCTGGAACTGCACC**CTGGAAGGACGATACCGGGCCAG
TTTACTGAAGAGAGGTTTTAAGGAAACGGCATTCCTTTACGCCATCTCCTCAGCAGGACTGA
CCCATGCAATGGCCAAGGCATGCAGCGCAGGTCGCATGGAACGCTGCACGTGTGACGAAGCT
CCTGACCTGGAGAACAGAGAGGCCTGGCAGTGGGGGGGCTGTGGAGACAACCTCAAGTACAG
CAACAAGTTTGTTAGGGAGTTTCTGGCAAATAAGTCCAGCAAGGATCTGCGGGCAAGAGTGG
ATTTACACAATACCAACGTGGGGATTAAGGTTATCAAAGCTGGAGTTAAGACCACATGCAAG
TGCCACGGAGTCTCTGGATCTTGTACAGTTCGCACATGTTGGAGACAATTGTCACCTTTTCA
TGAAATTGGGAAACAACTGAAGCAAAAGTACGAGACTTCACTAAAAGTAGGGAGCACTACTA
ACGAAGCTACTGGAGAAGGGGACATTTCTCCACCCAAAAAGCCAGTTGCTGGCCACAGCGAC
CAAATTCCAAGGACTACAGATTTAATATACATTGACGATTCACCAAGTTTTTGTCGNATGAG
CAAGTATCTCCTGGCACTT

Xlwnt9a (303aa).

MLDGHLVLGWLSVALVALHCLGPAAANFGLTGNEPLTILPLTSETEEAAVKAHYKICDRLKL
ERKQRRMCRRDPGVAETLIEAISMSAQECEYQFHFERWNCTLEGRYRASLLKRGFKETAFLY
AISSAGLTHAMAKACSAGRMERCTCDEAPDLENREAWQWGGCGDNLKYSNKFVREFLANKSS
KDLRARVDLHNTNVGIKVIKAGVKTTCKCHGVSGSCTVRTCWRQLSPFHEIGKQLKQKYETS
LKVGSTTNEATGEGDISPPKKPVAGHSDQIPRTTDLIYIDDSPSFC?MSKYLLAL

Figure 3.17 Novel *Xlwnt9a* partial DNA and protein sequences. The *Xlwnt9a* partial DNA sequence includes 40 base pairs of the 5'UTR but lacks the 3'end of the coding region and the 3'UTR. Sequence amplified by 5'RACE PCR is highlighted in yellow and sequence previously identified from *in situ* probe generation is left in white. Bold, underlined, red nucleotides indicate the GSP1 position and bold, underlined black nucleotides indicate position of GSP2 and GSP3, which are in that case, the same primers. Starting codon, ATG, is highlighted in grey. Italic, bold underlined nucleotides indicate were *XlWnt9a* antisense morpholino was designed. The morpholino oligo sequence is 5'-AAGGTGTCCATCCAGCATTTTGCTG- 3'. The *Xlwnt9a* mRNA, partial coding sequence was translated to give a 303 amino acid partial protein.

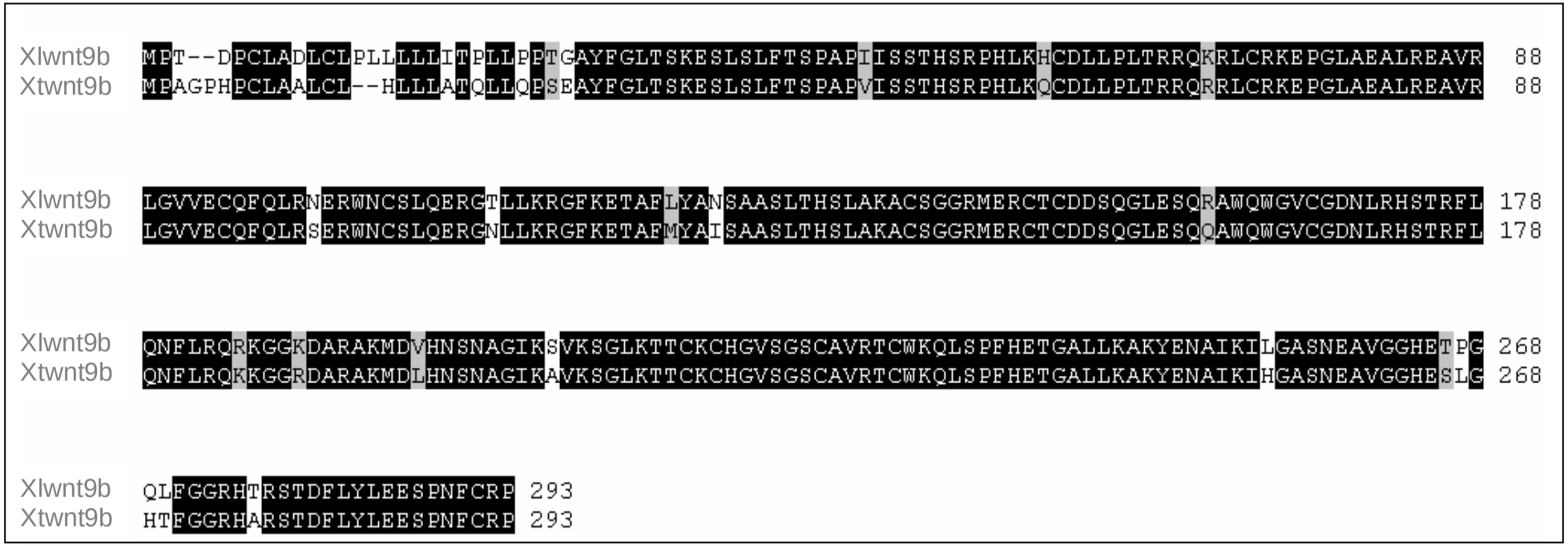

Key: Dashes indicate gaps in the alignment. Black box indicates identical amino acids, grey box indicates chemically similar amino acids and white box indicate dissimilar amino acids.

Figure 3.18 Amino acid sequences alignment shows that the newly identified Xlwnt9b protein is highly similar to its Xtwnt9b paralog. The first 293 amino acids protein sequences of Xlwnt9b and Xtwnt9b were aligned and showed 89% of identity in their amino acids sequence.

Key: Dashes indicate gaps in the alignment. Black box indicates identical amino acids, grey box indicates chemically similar amino acids and white box indicate dissimilar amino acids.

Figure 3.19 Amino acid sequences alignment shows that the newly identified Xlwnt9a protein is highly similar to its Xtwnt9a paralog. The first 302 amino acids protein sequences of Xlwnt9b and 256 of Xtwnt9b were aligned and showed 96% of identity in their amino acids sequence.

detailed) and from novel 5'UTR RACE PCR amplification. The *Xlwnt9a* partial DNA sequence includes 40 base pairs of the 5'UTR but lacks the end of the 3' coding region and the 3'UTR. The gene specific primers (GSP), the ATG position and the morpholino oligo sequence are indicated. The sequence of the *Xlwnt9a* antisense morpholino designed is 5'-AAGGTGTCCATCCAGCATTTTGCTG- 3'. The *Xlwnt9a* mRNA, partial coding sequence was conceptually translated to give a 303 amino acid long protein. This can be used for protein sequence comparison. The *Xlwnt9a* and *Xlwnt9b* amino acid sequences were analysed for similarity with their respective *X. tropicali*s orthologs. Figure 3.18 and 3.19 shows that at protein level *X. laevis* and *X. tropicalis* wnt9b are 89% identical and that the *X. laevis* and *X. tropicalis* wnt9a are 96% identical. Moreover, BLAST search shows that protein Xlwnt9b is 64% identical to *Gallus gallus* wnt9b protein and 63% identical to the human and mouse Wnt9b proteins (data not shown). Similarly, Xlwnt9a is 87%, 79% and 78% identical to chicken, mouse and human wnt9a proteins.

To conclude, 5'UTR RACE PCR has now allowed the amplification and identification of sequence around the ATG region of *Xlwnt9a* and *Xlwnt9b* and allowed the design of antisense oligo morpholino which can be used in knockdown experiments.

3.5.2 Inhibition of *Xlwnt9a* and *Xlwnt9b* using antisense oligo morpholino.

In the aim of analysing what effects could result from inhibiting the function of *Xlwnt9a* and *Xlwnt9b* during pronephros formation, 15ng of *Xlwnt9a* and *Xlwnt9b* antisense morpholinos was injected, together or separated, into one V2 blastomere at the 8-cell stage. Embryos were left to develop until stage 41 before being subjected to antibody staining using the pronephric tubule antibodies 3G8 and 4A6. So far, we have not been able to show that inhibition of *Xlwnt9a* and *Xlwnt9b* function using the antisense morpholinos has an effect on pronephros formation, since pronephric tubules appear perfectly morphologically normal. This experiment has been currently repeated by doubling the amount of antisense morpholinos.

3.6 Discussion.

3.6.1 Identification of *Xlwnt9a* and *Xlwnt9b* genes.

A combination of RT-PCR and 5'RACE PCR has allowed the identification of the novel *Xlwnt9a* and *Xlwnt9b* genes not previously described. However, only partial sequences of the two genes have been identified and further work including 3'RACE PCR would have to be performed in order to identify the 3'-end coding region and 3'UTR of each gene.

The first 293 amino acids of Xlwnt9b protein identified showed 89% identity with Xtwnt9b and 67% identity with human and mouse wnt9b proteins (data not shown). The first 303 amino acids of Xlwnt9a protein identified showed 96% and 85% identity with Xtwnt9a and the mammalian wnt9a proteins respectively (data not shown). The high percentage of similarity in wnt9a and wnt9b amino acids sequences respectively between the *X. laevis* and the other species suggests that we have identified the Xlwnt9a and Xlwnt9b orthologous genes of the *X. tropicalis*, human and mouse wnt9a and wnt9b respectively.

The *Xlwnt9a* and *Xlwnt9b* proteins showed 53.8% identity over the length of 279 amino acids with 15 gaps and 71.7% similarity (data not shown). According to Doolittle (1981), homologous genes are identified when over 25% of amino acids are identical within protein sequences. Therefore, our result suggests that *Xlwnt9a* and *Xlwnt9b* are paralogous genes and are derived from a genome duplication event.

As it was mentioned by Garriock et al. (2007), *X. tropicalis* has a duplicated *Xtwnt9b* gene present in the genome. Xtwnt9b and the duplicated copy Xtwnt9b2 are 98% identical in their nucleotide and protein sequences. Our genomic study shows that *Xtwnt9b* is contained in scaffold 43 while *X. tropicalis Xtwnt9b2* belongs to scaffold 14668. BLAST search showed that Xlwnt9b is 89% identical to the both Xtwnt9b and Xtwnt9b2 protein sequences. Because there is no genomic resource available for *X. laevis*, we cannot confirm the presence a second *Xlwnt9b* copy in the *X. laevis* genome.

3.6.2 Expression of *wnt9a* and *wnt9b* in *X. laevis* and *tropicalis* embryos and adult organs.

The use of specific *X. laevis* and *X. tropicalis wnt9a* and *wnt9b in situ* probes in a large range of developmental stages of *X. laevis* and *X. tropicalis* embryos (from stage 20 to stage 40) has confirmed the *in situ* analysis of Garriock et al (2007) and shows the expression of *wnt9a* in the pronephros and the lung and the expression of *wnt9b* in the eye and the branchial arches of the both frog species. Additionally to Garriock et al (2007), both *wnt9a* and *wnt9b* genes have also been detected in the heart of *X. laevis* and *X. tropicalis* embryos from stage 35 onwards.
Interestingly, we report the expression of *wnt9b* in the developing pronephros. Expression of *wnt9a* and *wnt9b* in the embryonic kidney coincides perfectly with the initial zygotic expression of both genes in whole *X. laevis* embryos at stage 13, the stage at which the *Xenopus* pronephros is specified (Brennan et al., 1998, 1999). Moreover, renal expression of *wnt9a* and *wnt9b* strongly persists in the adult frog consistent with studies in mouse in which *wnt9b* has been shown to be strongly expressed in the adult kidney (Qian et al., 2003). In addition, in *X. laevis* and *X. tropicalis* adult organs, both genes are highly detected in the pancreas, the reproductive organs and less strongly in the eye, the brain and the heart. *wnt9a* only is expressed in the lung of both species.

3.6.3 *wnt9b* belongs to the class of canonical *wnt* molecules.

Shimizu et al. (1997) showed that the stabilisation of *ß-catenin* by *wnt* is strongly correlated with their ability to transform C57MG cells in culture. In order to identify whether or not *wnt9b* belongs to the class of canonical *wnt* molecules, Qian et al. (2003) tested the transformation potential of *wnt9b* on C57MG mouse mammary epithelial cells and showed that *wnt9b* can only moderately transform the cell morphology from epithelial to fibroblastic and that *wnt9b* does not affect the cell growth characteristics. Because *wnt9b* does not strongly transform C57MG cells, it was thought that either *wnt9b* could act independently of the canonical *wnt/ß-catenin* pathway or that there is a *wnt* antagonist present in C57MG cells. Similarly, Carroll et al., (2005) showed that *wnt9b* can stabilise *ß-catenin* in responsive tissue culture cells. However, they showed that the well-characterised canonical *wnt1* can rescue

all aspects of *wnt9b* deficiency, implicating a canonical *wnt* activity. Our data provide additional evidence for *wnt9b* belonging to the class of canonical *wnt* molecule, as it is shown in this chapter that *Xtwnt9b* can induce a second axis when over-expressed in one ventral blastomere of 4 or 8-cell stage *Xenopus* embryos, a classic test of canonical *wnt* signalling.

3.6.4 *Xtwnt9b* plays a role in pronephros formation.

In order to investigate whether or not *Xtwnt9b* plays a role in pronephros formation, mis-expression studies were carried out in *X. laevis* embryos. Results show that over-expression of 0.25 to 2ng of *Xtwnt9b* mRNA, injected in one V2 blastomere at the 8-cell stage or into the animal pole of one blastomere at the 2-cell stage, results in the majority of embryos showing drastic reduction of the pronephric proximal, intermediate and distal tubules. Also, injection of 2ng of *Xtwnt9b* into one V2 blastomere at the 8-cell stage causes disturbance in cell movement and tubules appear abnormally enlarged and disorganised, whereas, injection in the same blastomere with 1ng of message leads to larger number of embryos showing absence of tubule. This observation needs to be confirmed as the number of embryos assayed in this experiment is small due to the difficulty in getting injected embryos developing with a normal anterior-posterior axis. Embryos injected with 0.25 to 1ng of *Xtwnt9b* mRNA show that tubules form abnormally in a dose-dependent manner as more embryos show absence of tubules as the message concentration increases. More importantly, disorganised intermediate/distal tubules were observed in approximately 30% of the embryos, indicating that *Xtwnt9b* might act as a pronephric organiser. Results suggesting that *Xtwnt9b* plays a role in *Xenopus* kidney formation correlate with studies carried out in mouse embryos. Carroll et al., (2005) have shown that *Wnt9b* is expressed throughout the Wolffian duct epithelium and in the ureteric bud and is involves in multiple aspects of metanephros formation by acting as a general organisation signal for the elaboration of several distinct components of the mouse urogenital system. In this study, *Wnt9b* has also been shown to be linked to *Wnt4* in the process of tubulogenesis. This last result strongly suggests the involvement of more than one *wnt* molecule having a role to play in kidney formation. In order to further establish the molecular mechanisms governing

the kidney formation, we were next interested in identifying which key *wnt* molecules might be involved in *X. laevis* pronephros formation.

Chapter 4 Identification of the *wnt* signalling molecules potentially involved in *X. laevis* pronephros formation.

4.1 Introduction.

The pronephros is located between the somites and the lateral plate of post-gastrula-stage embryo (Hausen and Riebesel, 1991). In 1999, Seufert et al., demonstrated that the tissue responsible for the induction of the intermediate mesoderm to become kidney in normal development is the anterior somites. However, little is know about the genes in the somites that give the inductive signal and the genes in the presumptive pronephric anlagen that respond to that signal. There is numerous evidence in the literature showing that the *wnt* signalling molecules are involved during developmental pocesses, including the kidney formation. *wnt4* has been shown to be critically required during *Xenopus* tubulogenesis (Saulnier et al., 2002). Perturbation of *wnt9b* results in formation of smaller pronephros (chapter 3). With the aim of identifying candidate genes being directly involved in the signalling events controlling pronephros formation, two direct screens of known *wnt* and other signalling molecules were carried out. The first screen analysed isolated pronephric anlagen of *X. laevis* embryos from stage 12.5 to stage 35 and the second screen looked at anterior versus posterior somites of *X. laevis* embryos at stage 17.

4.2 Temporal expression of known developmental signalling molecules screened in isolated *Xenopus* pronephric anlagen.

4.2.1 Localisation and dissection of pronephric anlagen during early stages of *X. laevis* development.

In *X. laevis*, all components of the pronephric kidney are derived from the intermediate mesoderm (Brändli et al., 1999). Figure 4.1 shows a diagram of the localisation and dissection of presumptive pronephric anlagen or the pronephros, in *X. laevis* embryos from stage 12.5 to stage 35. Embryos are shown in chronological order of developmental stage from left to right with anterior to the top and the

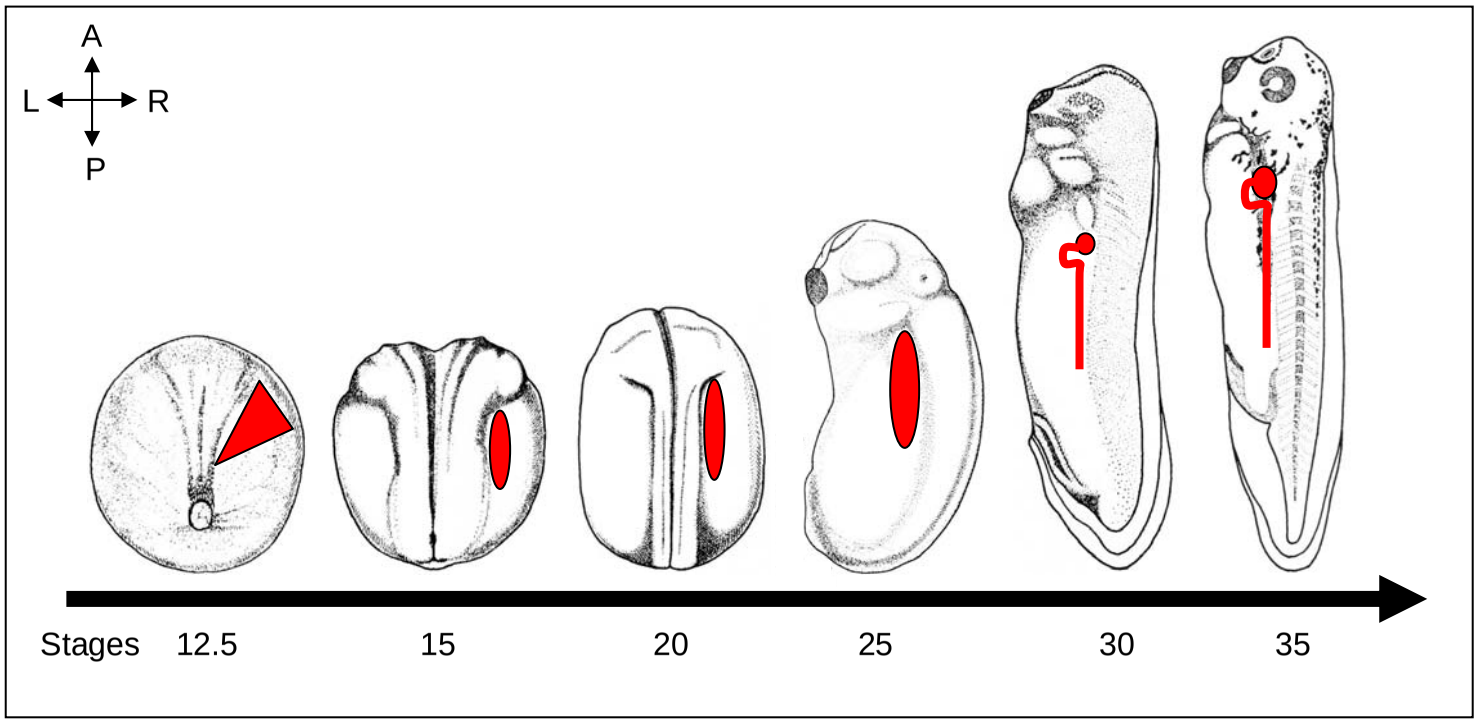

Figure 4.1 Diagram representing the pronephros anlagen dissections in *X. laevis* embryos from stage 12.5 to stage 35. Embryos are shown in chronological order of developmental stage from left to right with anterior to the top and the posterior to the bottom of the picture. In each embryo, the red shape indicates where the pronephros anlagen or pronephros was dissected.

posterior to the bottom of the picture. In each embryo, the red shape indicates from which region the pronephric anlagen was dissected. The earliest stage that the presumptive pronephric anlage could accurately be dissected from is in gastrulating embryos at stage 12.5, at the exact time that the pronephric tubules are specified (Brennan et al., 1998). In embryos at stage 12.5, the presumptive pronephric tissue is located between the somites and the lateral plate. These dissections contain epidermal and non pronephric intermediate mesoderm as this cannot be separated at this stage. The second stage chosen for dissecting the pronephros anlage is in early neurulating embryos at stage 15, when the pronephric intermediate tubule had specified (Brennan et al., 1998). This sample, too, contains the same additional tissues. In embryos at stage 15, the presumptive kidney is located underneath the presumptive somites. The third stage of dissection chosen is stage 20-21 which marks the first morphological indication of *Xenopus* pronephros development (Vize et al., 1997). At stage 20-21 the pronephros is located below somites 3 to 5 and can be dissected away from epidermis and other intermediate mesoderm. The fourth stage of pronephros dissection chosen is in early tailbud at stage 25. At this stage the pronephros extends in posterior position below somite 6. The next dissection was from embryos at stage 30. At this stage, a lumen has formed in the anterior portion of the anlage (Vize et al., 1997), and the pronephric anlage continues to extend caudally. The last stage of dissection chosen was stage 35 when the pronephros is potentially functional (Brennan et al., 1998) and just before the caudal extension of the tubule/distal tubule fuses with the rectal diverticulum (connecting tubule) (Brändli, 1999, Reggiani et al., 2008). Once multiple dissections of isolated presumptive pronephros or pronephric anlagen of *X. laevis* embryos from stage 12.5 to stage 35 were completed, total RNA was extracted from each sample, cDNA prepared and subjected to RT-PCR analysis.

4.2.2 Temporal expression of *wnt* signalling molecules screened in isolated *Xenopus* pronephric anlagen.

With the aim of identifying which canonical and non-canonical *wnt* candidate genes might be directly involved in the signalling events controlling pronephros formation, a direct screen was carried out. RT-PCR analysis was carried out from six different stages of isolated pronephric anlagen of *X. laevis* embryos from stages 12.5 to 35

using specific w*nt* gene primers. Figure 4.2 shows the expression of *wnt* signalling molecules expressed in isolated *Xenopus* pronephric anlagen. *odc* is expressed continuously from stage 12.5 to 35 and was used to equalize the cDNA input into the RT-PCR samples. The expression profiles of the *wnt* molecules identified within the pronephric anlagen are grouped in the chronological order of their expression pattern and are divided into three expression pattern groups. Group A contains only the canonical *wnt8,* expressed during the early stages of pronephros development only, from stages 12.5 to 20. Group B consists of *wnt11b, wnt5a, wnt9b, wnt4, wnt9a* and *wnt6* which are expressed throughout pronephros formation. Although non-canonical *wnt11b* (according to new nomenclature, Garriock et al., 2007, previously described as *wnt11*) is expressed in the pronephros from the earliest stage tested, stage 12.5 until the last stage tested, stage 35, it is more strongly expressed during the latest stages, stages 25 to 35. Non-canonical *wnt5a* is strongly expressed in the early stages of pronephros development, stages 12.5 and 15 and also in the last stage tested stage 35. At stages 20 to 30, *wnt5a* is more weakly expressed. Canonical *wnt9b* is weakly detected in the pronephros at stage 15, with significant expression from stage 20, and remains constant until stage 35. The canonical/ non-canonical *wnt4* is expressed weakly in the pronephros at stage 15 and 20, and is more strongly and constantly expressed in the pronephros from stage 25 to 35. *wnt9a* is expressed in the pronephros anlagen from stage 15 until stage 35 and appears to be up-regulated twice, once at stage 25 and once at stage 35. Canonical *wnt6* is weakly expressed throughout the pronephros development from stage 15 to stage 35. Finally, group C shows *wnt11* and *wnt7b* being expressed within the pronephros only during later stages of development. The non-canonical *wnt11* (according to new nomenclature, Garriock et al., 2007, previously described as *wnt11-R*) is weakly expressed in the pronephros at stage 25 and more strongly at stage 30 to 35. Canonical *wnt7b* is expressed in the pronephros from stages 25 and is up-regulated at stage 35, the last stage tested.

In conclusion, all the *wnt* molecules tested are expressed in the developing pronephros. Interestingly, although the *wnt* molecules can be classified in three different patterns of temporal expression, individual *wnt* molecules seem to show characteristic temporal expression patterns within the developing pronephros which are not dependent on the canonical or non-canonical classes to which they belong.

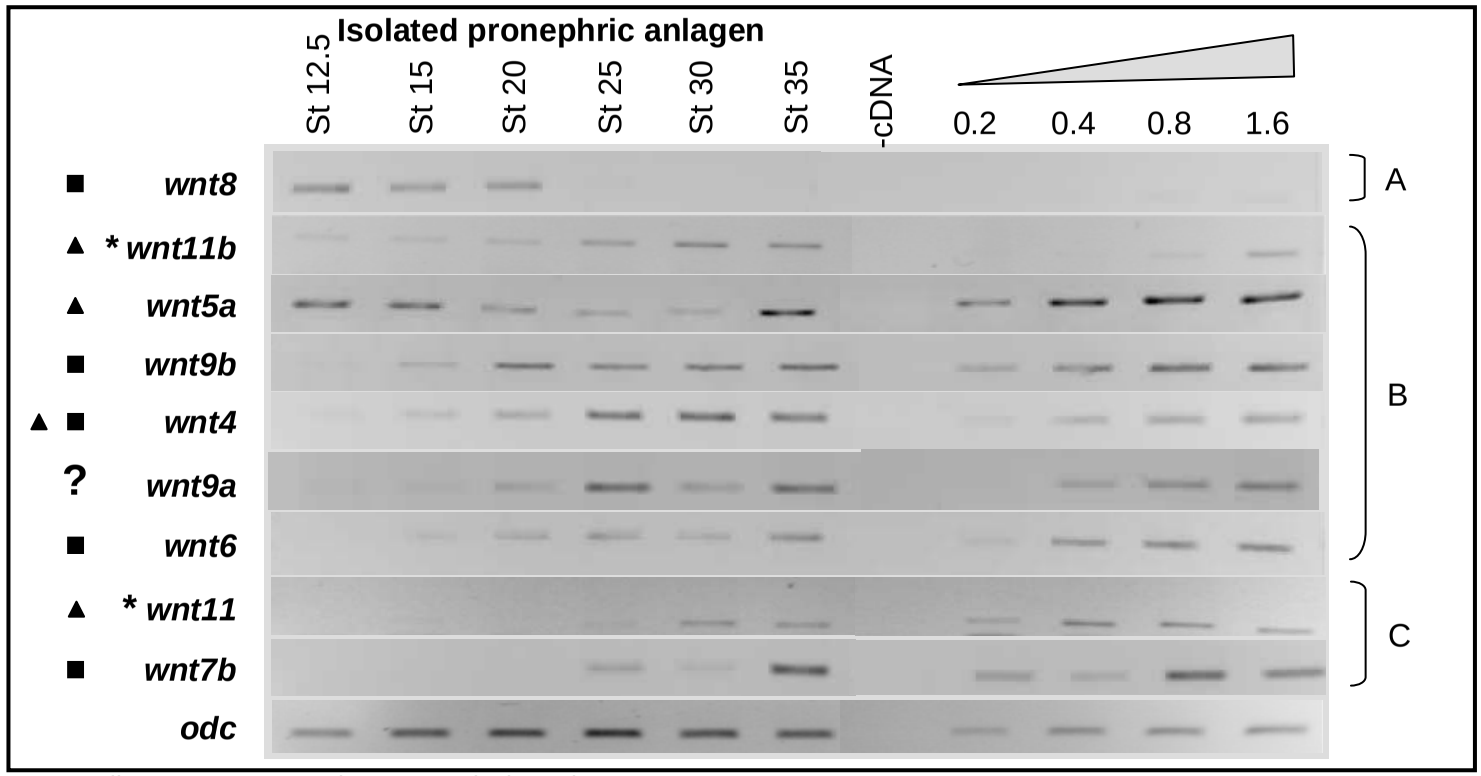

* According to new nomenclature, Garriock et al., 2007.

Figure 4.2 Identification of *wnt* signalling molecules expressed in isolated *X. laevis* pronephric anlagen. (■) indicates the canonical *wnt* molecules, (▲) indicates the non-canonical *wnt* molecules and (**?**) indicates unknown whether the *wnt* molecule is canonical or non-canonical. Pronephric anlagen from six different stages, stage 12 to 35, were dissected. Total RNA was extracted from each sample before being subjected to RT-PCR analysis. *odc* was used for equalizing cDNA samples. The triangle illustrates sequentially increasing cDNA inputs of whole embryo cDNA. The *wnt* molecules tested within the pronephric anlagen are classified in chronological order of their expression and divided in three expression pattern groups. Group A (*wnt8* only) shows expression during early stages only from stages 12 to 20. Group B (*wnt11b, wnt5a, wnt9b, wnt4, wnt9a and wnt6)* shows expression throughout pronephros formation from stage 12 or 15 until stage 35. Finally, group C (*wnt11* and *wnt7b*) shows expression within the pronephros during later stages of development, from stage 25 until stage 35, the last stage tested.

4.2.3 Temporal expression of other signalling molecules screened in isolated *X. laevis* pronephric anlagen.

We now know that *wnt* molecules are present very early on during pronephros formation (section 4.2.2). However, it has been shown that *wnt* signalling pathways interact with other signalling molecules pathway during development. For example, Hoppler and Moon (1998) showed that *bmp2, bmp4*, members of the TGF-ß-superfamily, regulate *wnt8* expression in the *Xenopus* gastrula. In addition, Galceran et al. (2004) showed that *wnt* signalling can affect the notch pathway in vertebrate somitogenesis. Therefore, we investigated which of these other signalling molecules are also expressed during early pronephros formation. Figure 4.3 shows *X. laevis* isolated pronephros anlagen from stage of development 12.5 to 35 tested by RT-PCR for the presence of some signalling molecules potentially involved in pronephros formation. The signalling molecules tested are grouped by chronological order of their expression. *odc* is expressed continuously from stage 12.5 to 35 and was used to equalize the cDNA input into the RT-PCR samples. There are three distinct major groups. First of all, group A, which only contains *bmp7,* is expressed in the dissected pronephric anlage at stage 12.5 only. The second group of signalling molecules, group B contains *jag1, dll1, notch-1, epha7, bmp4*, *hgf* and *fst* expressed throughout pronephric development from stage 12.5 or 15 to 35. Members of group B show an up-regulation at stage 25, when the pronephros starts to differentiate. *jag1* (previously called *XSerrate-1*) is expressed through pronephros formation from stage 12.5 to stage 35 with a strong up-regulation from stage 25 to 35. *dll1* (previously called *Xdelta-1)* is also expressed throughout early kidney development, and shows a clear up-regulation at stage 25 followed by a subsequent decrease in expression. *notch1* follows the same pattern. *Epha7* (previously called *Pagliaccio)* is expressed all way through pronephros development. *Epha7*is very weakly expressed between stages 12 to 20, becomes especially strong at stage 25 and expression remains robust during stages 30 to 35. *bmp4* is expressed continuously at very low level all way through pronephros formation without showing any differential expression. *hgf (hepatocyte growth factor)* is expressed from stage 15 to stage 35 and is up-regulated between stages 15 to 20 in the pronephric anlagen. *fst* (previously called *Follistatin*) starts to be expressed at stage 15, is strongly up-regulated at stage 25 and 30 followed by a gradual decrease of its mRNA expression to stage 35. Finally, group C

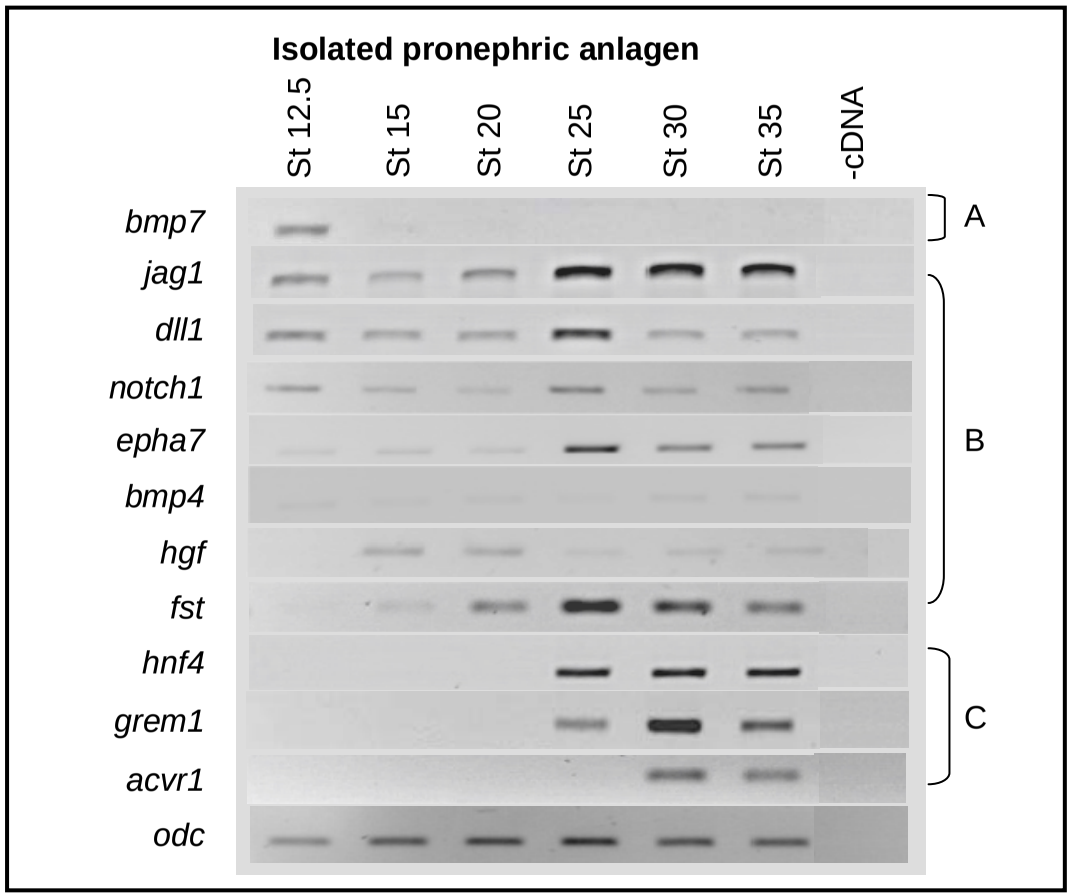

Figure 4.3 Analysis of some non-*wnt* signalling molecules expressed in *X. laevis* pronephric anlagen. Pronephric anlagen from six different stages, stage 12 to 35, were dissected. Total RNA was extracted from each sample before being subjected to RT-PCR analysis. *odc* was used for equalizing cDNA samples. The signalling molecules tested within the pronephric anlagen are classified in chronological order of their expression and divided in three expression pattern groups. Group A (*bmp* only) shows expression at stage 12 only. Group B (*jag1, dll1, notch1, epha7, bmp4, hgf and fst)* shows expression throughout pronephros formation from stage 12 or 15 until stage 35. Finally, group C (*hnf4* , *grem1* and *acvr1*) shows expression within the pronephros during later stages of development, from stage 25 or 30 until stage 35, the last stage tested.

shows clear onset of expression within pronephros development at or after stage 35. *hnf4* expression is exclusively restricted to stages 25 to 35. *grem1* (previously called *Gremlin)* is expressed between stages 25 and 35 with a strong up-regulation at stage 30. *acvr1* (previously called *Activin-A receptor type 1*) is expressed late in the pronephric anlagen dissections, at stage 30 to 35.
Taken together, studies of expression of signalling molecules within pronephric anlagen can provide information on potential signalling networks involved in early pronephrogenesis.

4.3 Expression of signalling molecules in *X. laevis* somites.

4.3.1 Dissection of anterior and posterior somites in *X. laevis* stage 17 embryos.

Seufert et al., in 1999, demonstrated that dorsal tissues, especially the anterior somites, are responsible for the establishment of the intermediate mesoderm and the induction of the embryonic *Xenopus* kidney. Nonetheless, the inductive signalling molecules necessary for pronephric specification deriving from the somites have not yet been identified. We have chosen to analyse the expression of *wnt* and other signalling molecules present at stage 17 in *X. laevis* anterior and posterior somites in order to identify potential candidates. In fact, stage 17 is the earliest stage at which the somites could be accurately dissected and this stage has been shown to have activity in a Holtfreter sandwich assay for nephrogenesis (chapter 5). Figure 4.4 illustrates the somite dissections in *X. laevis* embryos at stage 17 used to extract RNA for these analyses. The embryo is shown in dorsal view with the anterior to the top and the posterior to the bottom of the picture. The red square indicates where the anterior somites were dissected which corresponds to somite 3-5. The orange square indicates the position from which the posterior somites were taken, unsegmented at this stage. Both left and right sides of the embryo were used for dissecting anterior and posterior somites. Once enough material was dissected, total RNA was extracted from each sample and cDNA templates were used in RT-PCR analysis.

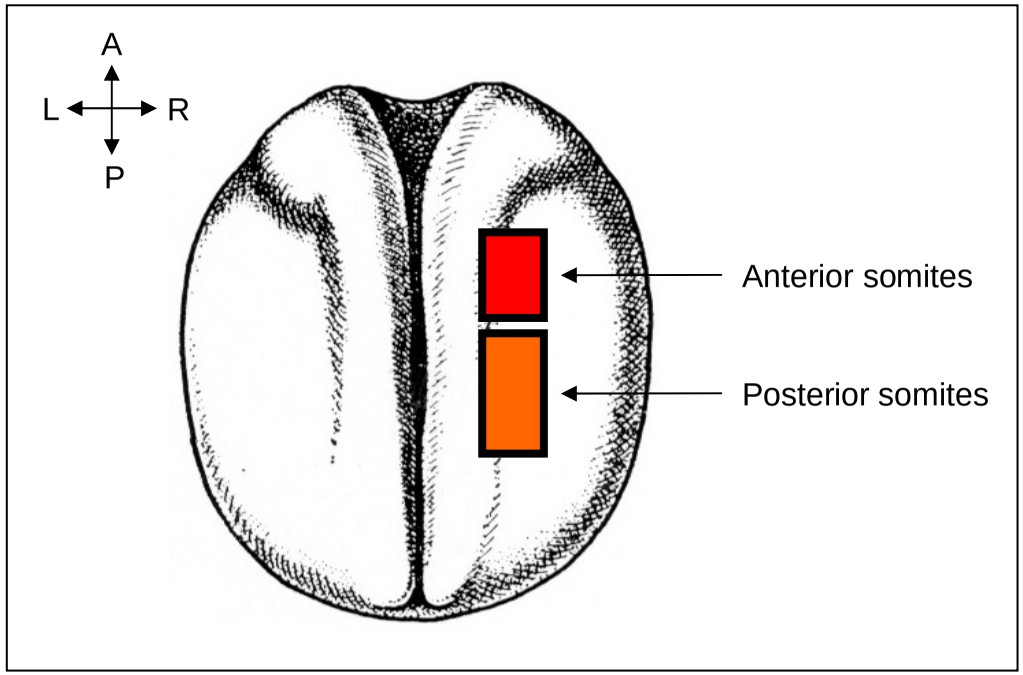

Figure 4.4 Diagram illustrating the somite dissections in *X. laevis* embryos at stage 17. The embryo is shown in dorsal view with the anterior to the top and the posterior to the bottom of the picture. The arrows indicate the anterior somites (red square) and the posterior somites (orange square). Both left and right sides of the embryo were dissected.

4.3.2 Expression of *wnt* signalling molecules in *X. laevis* isolated anterior and posterior somites.

From the literature, *wnt3A* has been shown to be expressed during somitogenesis in vertebrates (Dunty et al., 2008) and *wnt11b* is expressed in the somites of *Xenopus* embryos (Ku and Melton, 1993). We have extended this work, and by RT-PCR, have analysed the expression of *wnt* molecules in anterior and posterior somites in *Xenopus* embryos at stage 17. Figure 4.5 shows isolated anterior and posterior somites from stage 17 *X. laevis* embryos tested by RT-PCR for the presence of canonical and non-canonical *wnt* signalling molecules. *eef1a1* was used to equalize cDNA input into the RT-PCR samples. The grey triangle illustrates sequentially increasing cDNA inputs of stage 17 whole embryo cDNA. Expression of *wnt* signalling molecules into the somites can be divided in to four groups. The first one, group A, shows *wnt11* and *wnt9b* being more expressed in the anterior somites than in the posterior somites. The non-canonical *wnt11* (according to new nomenclature, Garriock et al., 2007, previously described as *wnt11-R*) is reasonably strongly expressed in anterior somites and only weakly expressed in the posterior somites. However, the canonical *wnt9b* shows a weak expression in the anterior somites and is absent in the posterior somites. *wnt9b* is in fact, weakly expressed in whole embryo at stage 17. The second group, group B shows *wnt11b* and *wnt4* that are equally expressed in both tissues. The non-canonical *wnt11b* (according to new nomenclature, Garriock et al., 2007, previously described as *wnt11*) actually shows the same intensity of expression in anterior and posterior somites and is strongly expressed in the whole embryo at stage 17. The canonical/non-canonical *wnt4* follows exactly the same expression pattern as *wnt11b*. The third group, group C, shows *wnt8* and *wnt5a* more expressed in the posterior somites than in the anterior somites. The canonical *wnt8* shows weak expression in the posterior somites and in whole embryo at stage 17 and is nearly undetectable in anterior somites. However, the non-canonical *wnt5a* is intensively expressed in the posterior somites and in whole embryo at stage 17 and is almost absent from the anterior somites. The final group, group D shows the canonical *wnt7b*, *wnt9a* and *wnt6* that are not expressed in the somites at all and that are not expressed in whole embryos at stage 17. However, a positive control should have been included to validate *wnt9a* and *wnt6* PCR reactions.

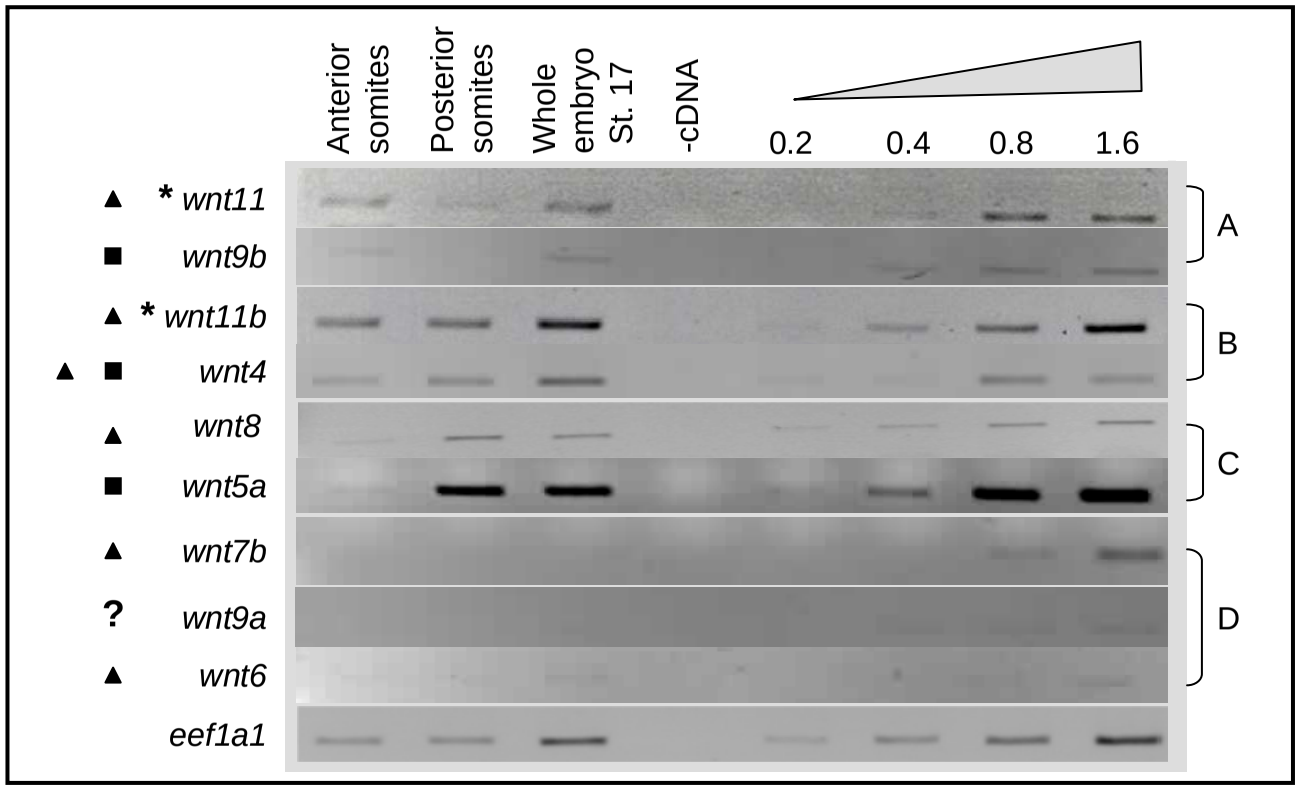

* According to new nomenclature, Garriock et al., 2007.

Figure 4.5 Identification of *wnt* signalling molecules expressed in *X. laevis* anterior and posterior somites. (▲) indicates the canonical *wnt* molecules, (■) indicates the non-canonical *wnt* molecules and (**?**) indicated unknown whether the *wnt* molecule is canonical or non-canonical. Anterior and posterior somites were dissected from stage 17 *Xenopus* embryos. Total RNA was extracted from each sample before being subjected to RT-PCR analysis. *eef1a1* was used for equalizing cDNA samples. The grey triangle illustrates sequentially increasing cDNA inputs of whole embryo cDNA. Group A (*wnt11* and *wnt9b)* are more expressed in the anterior somites than in the posterior somites. Group B *(wnt11b* and *wnt4)* are equally expressed in both tissues. Group C (*wnt8* and *wnt5a)* are more expressed in the posterior somites than in the anterior somites. Lastly, group D (*wnt7b*, *wnt9a* and *wnt6)* are not expressed in the somites at stage 17. Although, a positive control should have been included to validate *wnt9a* and *wnt6* PCR reactions .

To conclude, the non-canonical *wnt* molecules, *wnt11, wnt11b wnt5a* and the canonical/non-canonical *wnt4* are expressed in the somites in *Xenopus* embryos at stage 17, whereas the canonical *wnt*, *wnt9b, 8, 7b, 9a* and *6* are weakly expressed or absent in such tissues. Since Seufert et al. showed that the anterior somites are the tissue responsible for kidney induction, the *wnt* molecules with a potential inducing role in kidney formation would be those expressed in the anterior somites such as *wnt11, 9b, 11b,* and *4*.

4.3.3 Expression of other signalling molecules in *X. laevis* isolated anterior and posterior somites.

Because *wnt* molecules interact with other signalling pathways during early development, anterior and posterior somites of *Xenopus* embryos at stage 17 have been analysed for the presence of additional signalling molecules. Figure 4.6 shows the expression of signalling molecules in isolated anterior and posterior somites. *eef1a1* is expressed at stage 17 and was used to equalize the cDNA input into the RT-PCR samples. There are three distinct major groups. The first group, group A, shows that *fst, hgf* and *epha7* are more expressed in anterior somites than in posterior somites. *fst* is strongly expressed in anterior somites and is absent from posterior somites at stage 17. *hgf* is weakly expressed in anterior somites and is absent from posterior somites. *epha7* is reasonably strongly expressed in anterior somites and only weakly expressed in posterior somites at stage 17. The second group, group B, contains *notch1*, which is expressed weakly in both anterior and posterior somites. The third group, group C, contains *bmp4* whose expression is absent in anterior somites and which shows weak expression in posterior somites only. *bmp7* is not expressed in somites in embryos at stage 17. *myf5*, a marker of developing somites was used to validate the specificity of somites dissections and here confirming that only posterior somites are expressing *myf5*.

Knowing the important role of the anterior somites tissue in giving an inductive signal to the intermediate mesoderm to become kidney (Seufert et al., 1999), the candidate signalling molecules identified as potential inducers are the genes expressed in the anterior somites at stage 17 such as *fst*, *hgf, epha7* and *notch1*.

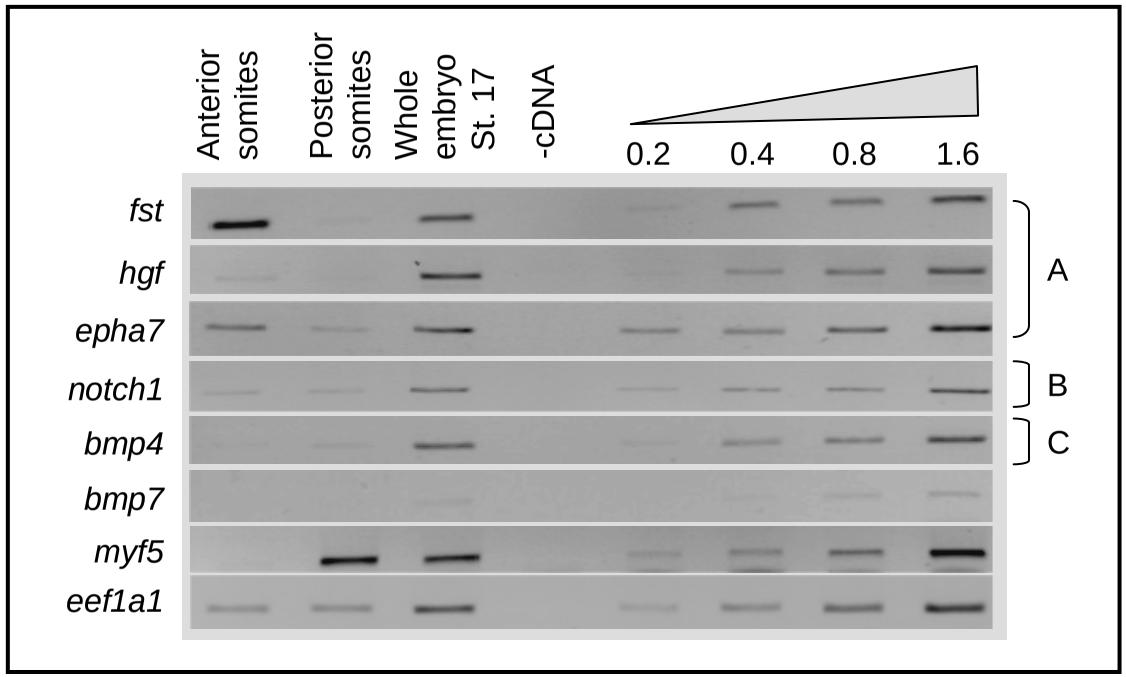

Figure 4.6 Analysis of some non-*wnt* signalling molecules expressed in *X. laevis* somites. Anterior and posterior somites were dissected from stage 17 *Xenopus* embryos. Total RNA was extracted from each sample before being subjected to RT-PCR analysis. *eef1a1* was used for equalizing cDNA samples. The triangle illustrates sequentially increasing cDNA inputs of whole embryo cDNA. Group A (*fst, hgf* and *epha7)* is more expressed in anterior somites than in posterior somites. Group B (*notch1 only)* is expressed in both anterior and posterior somites. However, group C (*bmp4 only)* is expressed in posterior somites only. *bmp7* is not expressed in somites in embryos at stage 17. *myf5*, a marker of developing somites was used to validate the specificity of somites dissections and here confirming that only posterior somites are expressing *myf5*.

4.4 Discussion.

4.4.1 Control of somite tissue maturity prior analysis of gene expression.

In order to analyse the signalling molecules expressed in anterior and posterior somites at stage 17, we first controlled for the maturity of the tissue by analysing the expression of the transcription factor *myf5.* In fact, the wave of differentiation of the somites goes from anterior to posterior and our results show that *myf5* is strongly expressed in the posterior somites only. In *Xenopus,* it has been established that *myf5* transcripts are restricted to posterior part of the somitic mesoderm only (Mei et al., 2001) and therefore *myf5* constitute an excellent control in this experiment confirming the level of differentiation between the anterior and posterior somite tissues. However, a more general somite marker, such as cardiac-actin, should have been included in order to control the muscle specificity of both anterior and posterior somites samples.

4.4.2 The different phases of kidney development are characterised by waves of signalling molecules expression.

Results show that signalling molecules screened in isolated pronephric anlagen can be mainly separated into two groups.

The first group shows *bmp7* expressed at stage 12.5 only. *bmp7* has been shown to act as an essential signalling molecule during mammalian kidney development (Dudley et al., (1995), Takahashi and Ikeda, (1996), Piscione et al., (2001)) but its role in *Xenopus* kidney development has not been yet elucidated. Our result suggests that *bmp7* is either expressed very early in isolated pronephric anlagen (stage 12.5) and plays a very important role as a pronephric inducer or is expressed in the epidermis only. Since the epidermis is difficult to dissociate from the pronephric anlagen at this early stage of development, expression of *bmp7* in pronephric anlagen at stage 12.5 remains of unlikely significance.

The second group B shows genes expressed throughout pronephros formation and up-regulated at stage 25. But, equalization of the cDNA input into the RT-PCR samples using *odc* expression shows that *odc* signal at stage 25 is slightly stronger than *odc* signal of other stages, which may explain the apparent increase of genes

signal at stage 25. However, expression of known transcription factors during *Xenopus* pronephros formation was also carried out and results showed a similar up-regulation of activity for transcription factors at stage 25 (data not shown). This result suggests that a genuine change of gene expression is happening during pronephros development at stage 25 which probably correlates with morphological changes within the forming embryonic kidney. Nevertheless, recent studies have demonstrated that the notch signalling pathway (including notch1 receptor and ligands jag1 (serrate1) and dll1 (delta1)) is involved in the cell fate decisions that occur as a normal part of the formation of the pronephros (McLaughlin, 2000). Our results confirm the presence of notch signalling within the developing pronephros. e*pha7*, member of the *eph* family has been shown to be expressed in *Xenopus* pronephric tubules at stage 26 (Winning and Sargent, 1994). Our results confirm that *epha7*is strongly expressed in pronephros around stage 25 but also shows it to be continuously expressed from stage 12.5 to stage 35. The strong up-regulation observed at stage 25 suggests a specific role at this time. In the normal mouse embryo, *bmp4* is expressed in mesenchymal cells surrounding the Wolffian duct (WD) and ureter stalk conferring a function in the early morphogenesis of the kidney and urinary tract (Miyazaki et al., 2000). Our result suggests that *bmp4* might also play a role in *Xenopus* early kidney formation. *hgf* has been identified as an inducer of epithelial tubulogenesis in MDCK cell line (Brändli, 1999) and in *Xenopus, hgf* has been shown to be expressed in mesenchymal cells (Nakamura et al., 1995). The up-regulation observed between stages 15 and 20 suggests that *hgf* might play a role in tubule formation in *Xenopus* pronephros. In *Xenopus* embryos, *fst* is transiently expressed in the pronephros around stage 24 but its role in kidney development is still unknown (Hemmati-Brivanlou et al., 1994). Here, we have confirmed that *fst* is strongly expressed within pronephros between stages 25 and 30 suggesting a role in pronephros morphogenesis.

To conclude, *jag1, dll1, notch1, epha7, bmp4, hgf and fst* being expressed from the earliest stages of pronephros development, stages 12.5 and 15, suggests that these signalling molecule could potentially plays a role in the specification of the pronephric tissue. Moreover, *notch1, fst, hgf* and *epha7* are expressed in the anterior somites in *Xenopus* embryos at stage 17.

Finally, group C shows genes expressed at variable stages of development. *hnf4* is detected in *Xenopus* pronephric proximal tubules but not in intermediate and distal

tubules at stage 29 (Holewa et al., 1997). Moreover, mutations in the human genes encoding the tissue-specific *hnf1 (α - ß)* and *hnf4* are responsible for maturity onset diabetes of the young (MODY) and cause defective development of the kidney (Ryffel et al., 2001, Thomas and al., 2001, Yamagata et al., 1996). Our results show a constant expression of *hnf4* between stages 25 and 35 suggests that *hnf4* might have a role in tubule specification. g*rem,* a *dan* family member, antagonises *bmp* and *nodal* signalling, is expressed at stage 27 in intermediate and distal tubules (Hsu et al., 1998). The strong up-regulation observed at stage 30 within pronephric anlagen is explained by the role of g*rem* in pronephric intermediate and distal tubules formation. Finally, our results show that *acvr1* is expressed at stage 30 and 35 in pronephric anlagen suggesting a role in late pronephros differentiation.

To conclude, expression of *hnf4a, grem* and *acvr1* from stage 25 onwards, suggests that these signalling molecules might be involved in the pronephric tubules differentiation mainly.

It would have been very interesting to study the expression of the *fgf* signalling molecules as it was shown that in *Xenopus* embryos, *fgf8* acts as one of the potential mediators of *hedgehog* and plays a critical role in the earliest stages of pronephric tubules development (Urban et al., 2006). However, this was not carried out.

4.4.3 Identification of the *wnts* signalling molecules in the pronephric anlagen at the right time and place to have a role to play in pronephric development.

Analyses of expression of *wnt* signalling molecules in the developing *Xenopus* pronephros and somites at stage 17 suggest that pronephros formation and organogenesis could result from the interaction of complex molecular signalling networks. The RT-PCR analyses have shown that the nine *wnt* molecules tested are expressed at various key points during pronephros formation and we hypothesise that they are therefore playing a role in the process. *wnt8* is expressed from the earliest stage tested, stage 12.5 and until stage 20 only, suggesting that *wnt8* could play a role in the early induction of the pronephric anlagen. *wnt11b, wnt5a, wnt9b, wnt4, wnt9a* and *wnt6* show expression all the way through pronephros development, indicating that these *wnt* molecules might be involved in the early induction and the patterning of the embryonic kidney tissues. *wnt11* and *wnt7b* are expressed relatively late within the pronephros, from stage 25 onwards, indicating that *wnt11* and *wnt7b* might be

involve in the differentiation of the pronephric components. However, *wnt6, wnt7b* and *wnt9a* are not expressed in the somites at stage 17. This leaves *wnt11, wnt9b, wnt11b, wnt4* and the less expressed *wnt8* and *wnt5a,* as the candidates genes expressed in the anterior somites, which might induce pronephros formation (Seufert et al.).

It would have been very interesting to study the expression of *wnt2* and *wnt3a* within the developing *Xenopus* pronephros and somites as it was shown that in mouse embryos, canonical *Wnt3A* coordinates mesoderm formation (Dunty et al., 2008) and *Wnt2* acts during metanephric morphogenesis (Lin et al., 2001).

Thus, study of expression of *wnt* signalling molecules within the forming embryonic kidney has revealed that all nine *wnt* molecules tested are expressed differentially during pronephros formation. It also clearly apparent that both canonical and non-canonical *wnt* molecules are required for normal pronephros formation but their role has not yet been clearly elucidated. Because of the spatial and temporal characteristics of *wnt11b,* being expressed in anterior somites at stage 17 and in pronephric anlagen from the earliest stage (stage 12.5), *wnt11b* is the most attractive candidate gene for analysis in the pronephrogenesis assay. However, in chapter 5, both the non-canonical and canonical *wnt* molecules will be tested in a pronephros induction assay.

Chapter 5 A direct assay of pronephrogenesis using the Holtfreter sandwich cultures.

5.1 Introduction.

With the aim of analysing tissue interaction and the role of candidate *wnt* signalling molecules (identified in Chapter 4) in *Xenopus* pronephrogenesis, *in vitro* explant cultures, named Holtfreter sandwich cultures, were carried out. This chapter firstly describes the set up and the validation of this original induction assay. Subsequently, both non-canonical and canonical *wnt* molecules were tested for their potential activity in inducing pronephric tubules in embryonic explants inside *wnt*-expressing Holtfreter sandwich cultures.

5.2 Setting up an *in vitro* model for pronephrogenesis.

5.2.1 Assembly of Holtfreter sandwich cultures.

The Holtfreter sandwich assay requires fine dissection of embryonic material and was accomplished together with Professor E.A. Jones. Figure 5.1 panel A shows dissection of explants. First of all, ectoderm animal caps were dissected from embryos at stage 9 (figure 5.1 panel A, a). Embryos were either control uninjected embryos or were over-expressing the *wnt* signalling molecules of interest. These ectoderm animal caps were used to wrap the potential pronephric tissues, intermediate mesoderm and somitic mesoderm. Secondly, unspecified intermediate mesoderm was dissected from normal embryos at stage 10.5-11, in a wedge of 60° to 70° from the vertical midline (figure 5.1 panel A, b). Finally, presumptive anterior somitic tissue was removed from normal embryos at stage 17 (figure 5.1 panel A, c). When it was technically possible, somitic tissues were dissected from both sides of the donor embryos. For all dissections, staging of embryos was performed according to the normal table of Nieuwkoop and Faber, 1999 and for further method refer to chapter 2.

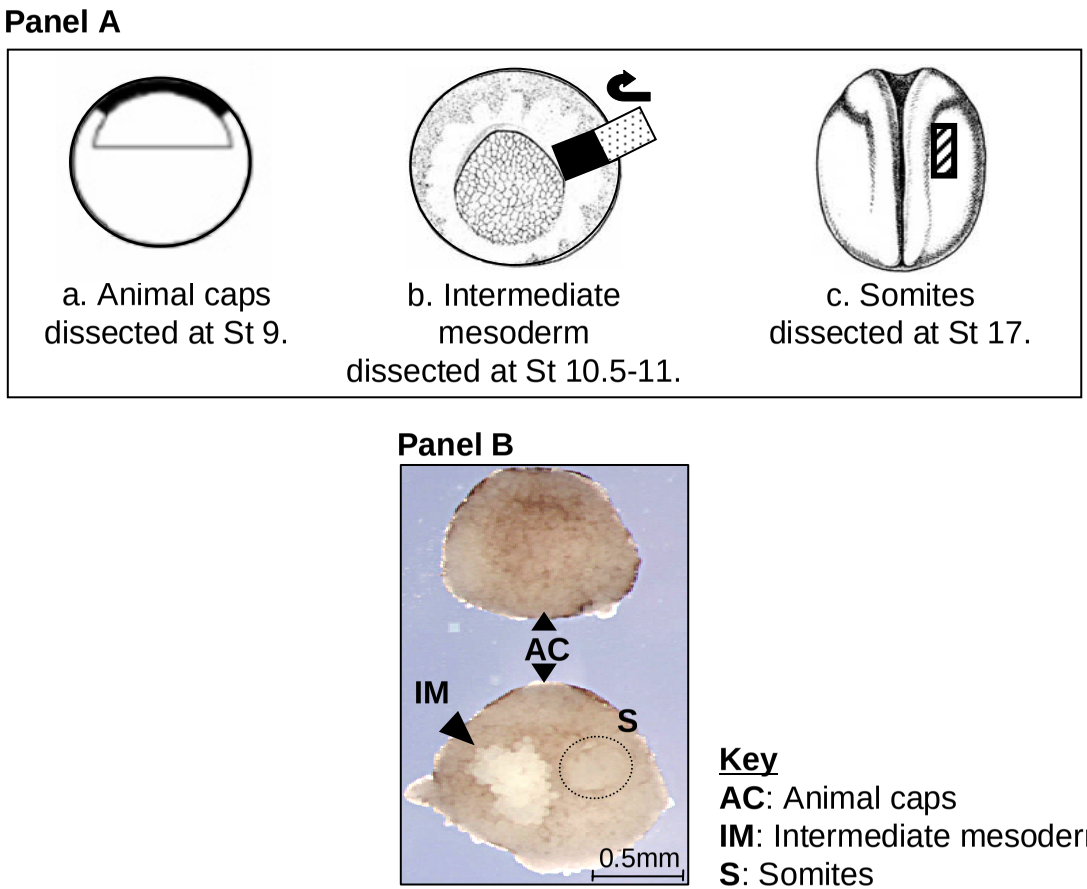

Figure 5.1 Dissection of explants and assembly of Holtfreter sandwich cultures. Panel A shows dissections of explants. Animal caps are dissected from embryos at stage 9 (a). The intermediate mesoderm is removed from the overlying epidermis from normal embryos at stage 10.5-11, in a wedge of 60° from the vertical midline (b). Finally, the somites are dissected from embryos at stage 17 (c). Panel B shows a sandwich assembly with intermediate mesoderm (IM) and somites (S) placed together in a first animal cap. A second animal caps was used to close the sandwich culture.

Once dissections of animal poles, intermediate mesoderm and somitic mesoderm were completed, embryonic explants were assembled to form sandwich cultures. Figure 5.1 panel B shows a photograph of a sandwich assembly. Intermediate mesoderm and somites lie next to each other inside a first animal cap. Intermediate mesoderm looks much whiter in colour than somitic mesoderm. A second animal cap was used to cover and seal the Holtfreter sandwich culture. Cultures were allowed to develop until stage 40-41 equivalent according to control embryos of the same stage as those used for the intermediate mesoderm dissection, before being subjected to immuno-staining for the presence of pronephric structures using the specific pronephric proximal tubule antibody 3G8 and the specific intermediate/ distal tubule antibody 4A6.

5.2.2 Animal caps over-expressing *wnt* molecules analysed by RT-PCR for the presence of pronephric and other genes.

In order to validate the Holtfreter sandwich cultures, investigating whether *wnt* signalling molecules over-expressed in animal caps can give an inductive signal to the unspecified intermediate mesoderm to differentiate into pronephros, it was important to verify that *wnt* signalling molecules do not have the ability to induce formation of pronephric or other tissues when cultured on their own. Therefore, animal caps over-expressing *wnt* molecules were analysed by RT-PCR for the presence of epidermis, kidney, muscle and nervous system tissues.

5.2.2.1 Overall morphology of animal caps expressing *wnt* signalling molecules.

In order to verify that *wnt* signalling molecules do not have the potential to induce formation of differentiated tissue when over-expressed in animal caps and cultured on their own, single cell *X. laevis* embryos were injected with 2ng of either *wnt4*, *wnt5a*, *wnt6*, *wnt7b*, *wnt8*, *wnt11b* or *wnt11* mRNA. After over-night incubation, animal caps were dissected and left to develop until stage 30-32 equivalent relative to undissected embryos. Animal caps over-expressing *wnt* molecules are round and are morphologically identical to normal animal caps, therefore their morphology is non informative (data not shown). However, the stage 30-32 equivalent embryos over-expressing members of the non-canonical *wnt* family have abnormal morphology

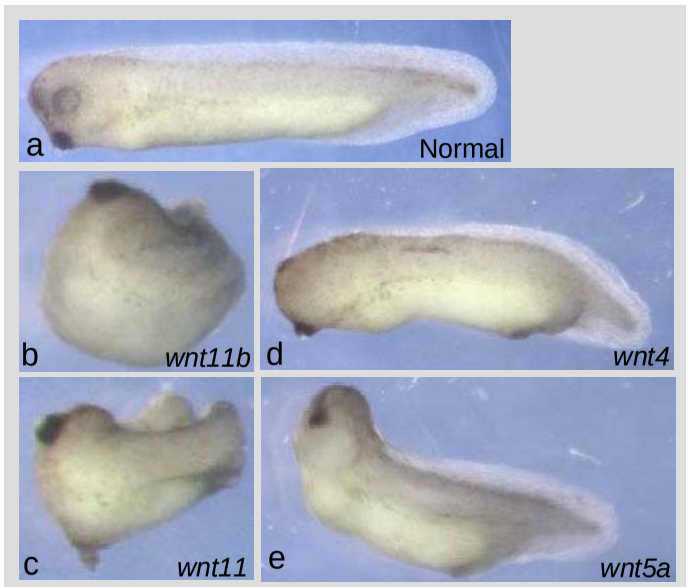

Figure 5.2 Morphological analysis of *X. laevis* embryos over-expressing *wnt* molecules. Single cell *X. laevis* embryos were injected with 2ng of either *wnt4*, *wnt5a*, *wnt11b* or *wnt11* mRNA. After over-night incubation, animal caps were dissected and left to develop until stage 30-32 equivalent. Animal caps over-expressing *wnt* molecules are round and are morphologically identical to normal animal caps, therefore their morphology is non informative (data not shown). However the stage 30-32 equivalent embryos over-expressing members of the non-canonical *wnt* family have abnormal morphology (b, c, d and e) when compared to normal embryos (a). This indicates that the mRNA messages are biologically active even if there are no apparent morphological differences between the animal caps over-expressing the *wnt* genes and normal control caps.

(Fig 5.2 b, c, d and e) when compared to normal embryos (Fig 5.2 a). Embryos injected with 2ng of *wnt11b* or *wnt11* mRNA show mainly abnormal anterior-posterior axis formation (Fig 5.2 b and c). Embryos over-expressing 2ng of *wnt4* have normal anterior-posterior axis and head but are abnormal in their ventral part (Fig 5.2 d). Embryos over-expressing 2ng of *wnt5a* show defective head formation (Fig 5.2 e). Finally, over-expression of 2ng of the canonical *wnt* molecules (*wnt6*, *wnt7b* and *wnt8*) resulted in such toxic effects that the embryos did not survive (data not shown). This indicates that the mRNA messages are biologically active even if there are no apparent morphological differences between the animal caps over-expressing *wnt* genes and the normal control caps.

5.2.2.2 Animal caps over-expressing *wnt* molecules do not induce nervous system, kidney or muscle markers.

Prior to the setting up of the *wnt* Holtfreter sandwich culture experiment, the ability of *wnt* molecules to form pronephric tissues when over-expressed in animal caps was tested. Single cell *X. laevis* embryos were injected with 2ng of either *wnt4*, *wnt5a*, *wnt6, wnt7b, wnt8*, *wnt11b* or *wnt11* mRNA. Animal caps were dissected at stage 9 and left to develop until stage equivalent 21. Total RNA was extracted from each sample before being subjected to RT-PCR analysis (Fig 5.3). *eef1a1* was used to equalize the cDNA samples. The triangle illustrates sequentially increasing cDNA inputs of whole embryo cDNA. Primers for specific tissues markers were used to test the presence of epidermis, kidney, muscle and nervous system in animal caps over-expressing *wnt* molecules. All markers tested are expressed in whole *Xenopus* embryos at stage 21. Animal caps over-expressing *wnt* molecules contain epidermal tissue as shown by the expression of *cytokeratin*, *bmp4* and *bmp7* in all samples. However, animal caps over-expressing *wnt* molecules show that none of the pronephric markers tested, such as tubules markers *lhx1* (previously called *lim1*), *pax2, pax8* and glomus marker *wt1,* can be detected. Animal caps over-expressing *wnt* molecules are not capable of forming muscle tissue either, since expression of *myf5, myod1* and *actc1* (cardiac actin) is absent from all samples. Heart marker *nkx2-5* is expressed in animal caps over-expressing *wnt4, 5a, 6*, *7b* and *11* but is also expressed in normal animal caps, suggesting that *nkx2-5* is also expressed in epidermal tissue. Animal caps over-expressing *wnt* molecules and cultured on their

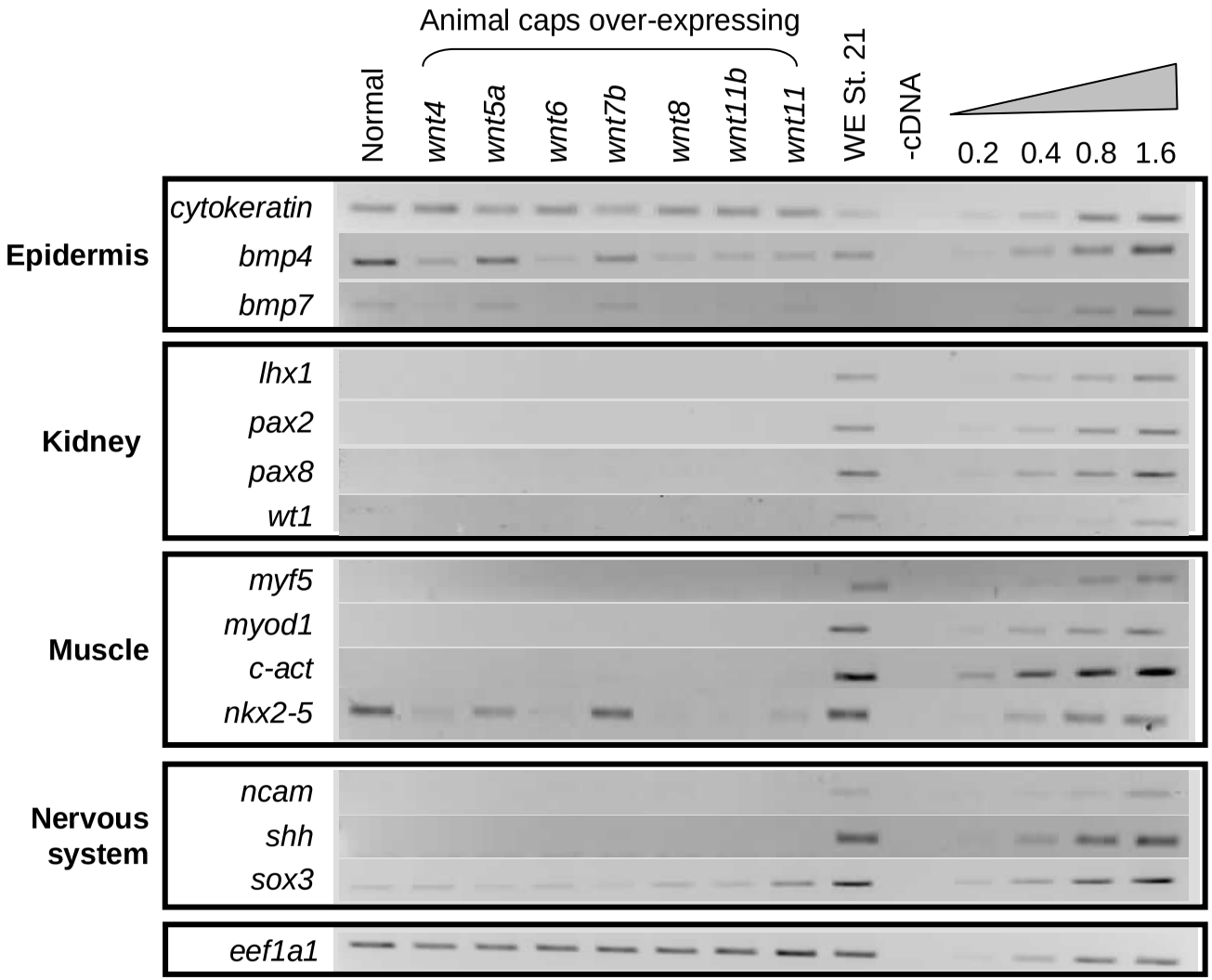
Animal caps over-expressing
Normal
wnt4
wnt5a
wnt6
wnt7b
wnt8
wnt11b
wnt11
WE St. 21
-cDNA
0.2
0.4
0.8
1.6
Epidermis
cytokeratin
bmp4
bmp7
Kidney
lhx1
pax2
pax8
wt1
Muscle
myf5
myod1
c-act
nkx2-5
Nervous system
ncam
shh
sox3
eef1a1

Figure 5.3 Animal caps over-expressing *wnt* molecules do not induce nervous system, kidney or muscle markers. Single cell *X. laevis* embryos were injected with 2 ng of either *wnt4*, *wnt5a*, *wnt6, wnt7b, wnt8*, *wnt11b* or *wnt11* mRNA. Animal caps were dissected at stage 9 and left to develop to stage equivalent 21 whole embryo (WE). Total RNA was extracted from each sample before being subjected to RT-PCR analysis. *eef1a1* was used to equalize the cDNA samples. The triangle illustrates sequentially increasing cDNA inputs of whole embryo cDNA. Primers for specific tissues markers were used to test the presence of epidermis, kidney, muscle and nervous system in animal caps over-expressing *wnt* molecules. Animal caps over-expressing *wnt* molecules contain epidermis tissue but do not show the presence of kidney, muscle or nervous system tissues.

own do not lead to the formation of nervous system, since *ncam* and *shh* are not expressed in such samples. *sox3* is expressed in all samples including the normal animal caps suggesting that *sox3* is also expressed at low level in epidermis.
In conclusion, animal caps over-expressing *wnt* molecules are constituted of epidermal tissue only and do not have the ability on their own to form other tissues such as kidney, muscle or nervous system. Therefore, *wnt* molecules can now be tested for kidney induction in a Holtfreter sandwich.

5.2.3 The general morphology of Holtfreter sandwich cultures before immuno-assay.

Figure 5.4 shows the general morphology of Holtfreter sandwich cultures developed until stage 41-43 equivalent, according to control embryos of the same developmental stage as those used for the intermediate mesoderm dissection, and before the pronephric immuno-staining process. Each experiment involves an extensive series of control sandwiches. A background sandwich culture controlling the level of pronephros development is established from intermediate mesoderm cultured alone inside two normal animal caps (Fig 5.4 panel a) and verifies that no pronephros can be formed with such a combination. The background sandwich cultures show a rounded shape but clearly contain mesodermal structures. A positive control is composed of intermediate mesoderm and somitic mesoderm cultured inside two normal animal caps (Fig 5.4 panel b) and verifies that pronephros can form (Seufert et al., 1999). The positive control sandwich cultures also look fairly round and clearly show mesodermal activity. The test experiments involve intermediate mesoderm cultured inside two animal caps over-expressing 2ng of the test *wnt* mRNA. Commonly, the positive control sandwich cultures and the animal caps over-expressing the non-canonical *wnt5a, wnt11b*, *wnt11*, (and *wnt4*, data not shown) cultured with intermediate mesoderm showed few pigmented cells which could results from neural crest tissue formation since neural crest cells are the embryonic precursors of pigment cells (Tucker R. P., 1996), but exhibited the same common fairly round and "bubbly" morphology (Fig 5.4 panel c, d and e, respectively). This is in contrast to animal caps over-expressing the canonical *wnt* molecules and cultured with intermediate mesoderm. When intermediate mesoderm was cultured inside two animal caps over-expressing 2ng of *wnt6*, the sandwich cultures developed eye-like structures as shown by the arrow (Fig 5.4 f). Animal caps

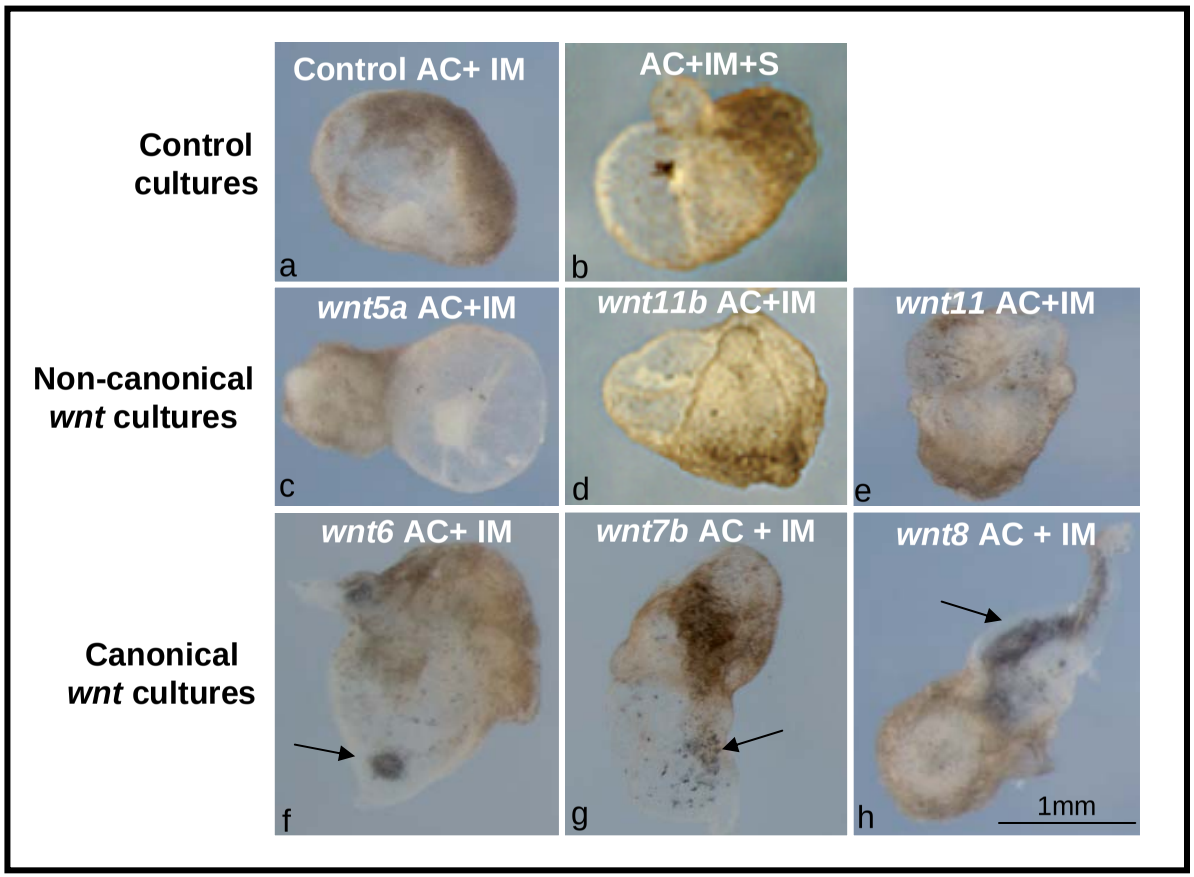

Key: AC, animal cap. O/E, over-expressing. IM, intermediate mesoderm. S, somite.

Figure 5.4 The general morphology of Holtfreter sandwich cultures before immuno-assay. Sandwich cultures were allowed to develop until stage 41-43 equivalent according to control embryos of the same developmental stage as those used for the intermediate mesoderm dissection. Intermediate mesoderm alone cultured in normal animal caps give sandwich cultures with a rounded shape which clearly contain mesodermal structures (panel a). Panel (b) shows the positive control containing intermediate mesoderm and somites cultured together in normal animal caps and also shows mesodermal activity. Panels (c, d and e) show animal caps over-expressing non-canonical *wnt5a, wnt11b* and *wnt11* respectively and cultured with intermediate mesoderm. Such cultures show comparable morphology to the positive sandwich culture. However, when intermediate mesoderm was cultured inside two animal caps over-expressing 2ng of *wnt6*, the sandwich cultures developed eye-like structures as shown by the arrow (f). Animal caps over-expressing 2ng of *wnt7b* and cultured with intermediate mesoderm show the presence of pigmented cells (possibly melanocytes), as indicated by the arrow (g). Animal caps over-expressing 2ng of *wnt8* and cultured with intermediate mesoderm form extended axial structures that resemble tail-like structures as shown by the arrow (h).

over-expressing 2ng of *wnt7b* and cultured with intermediate mesoderm show the presence of pigmented cells (possibly melanocytes), as indicated by the arrow (Fig 5.4 g). Finally, animal caps over-expressing 2ng of *wnt8* and cultured with intermediate mesoderm form extended axial structures that resemble tails (Fig 5.4 h, arrow).

To conclude, the control sandwich cultures and the non-canonical *wnt* sandwich cultures show a highly similar rounded morphology. Animal caps over-expressing canonical *wnt* signalling molecules and cultured with intermediate mesoderm, however, seems to develop dorsal tissues that contains some nervous tissue. All Holtfreter sandwich cultures were then subjected to 3G8/ 4A6 antibody staining for the presence of pronephric tubules.

5.2.4 Somites can induce pronephros from intermediate mesoderm in explants cultures.

Dissections of embryonic explants were achieved as described in section 5.2.1 and cultures were allowed to develop until stage 40 equivalent according to control embryos used for the intermediate mesoderm dissection, when the pronephric tubules have fully specialized. Figure 5.5 shows combination of sandwich cultures assayed for double antibody staining. Proximal tubules were visualised using the specific pronephric tubules antibody 3G8 and an FITC-conjugated secondary antibody fluorescing under UV light (Fig 5.5 e). At stage 40, proximal tubules look like connected T-shaped tubes, and the staining pattern expands with the expansion of the lumen of the tubules, along which the staining is localised (Fig 5.5 e and Brennan et al., 1998). Intermediate and distal tubules were visualised using the specific intermediate/distal pronephric tubules antibody 4A6 and a TRITC-conjugated secondary antibody fluorescent under UV light (Fig 5.5 j). Intermediate and distal tubules immunostain as continuous wide sheet, the staining is seen over the entire surface of the cells and the tube lumen is not visible (Fig 5.5 j and Brennan et al., 1998). Immuno-staining with 3G8/FITC and 4A6/TRITC gives an accurate method of distinguishing pronephric proximal tubules from pronephric intermediate and distal tubules. Two animal caps cultured on their own do not have the ability to form pronephric tubules (Fig 5.5 a and f). Intermediate mesoderm cultured inside two animal caps does not result in the formation of tubules (Fig 5.5 b and g). Two animal

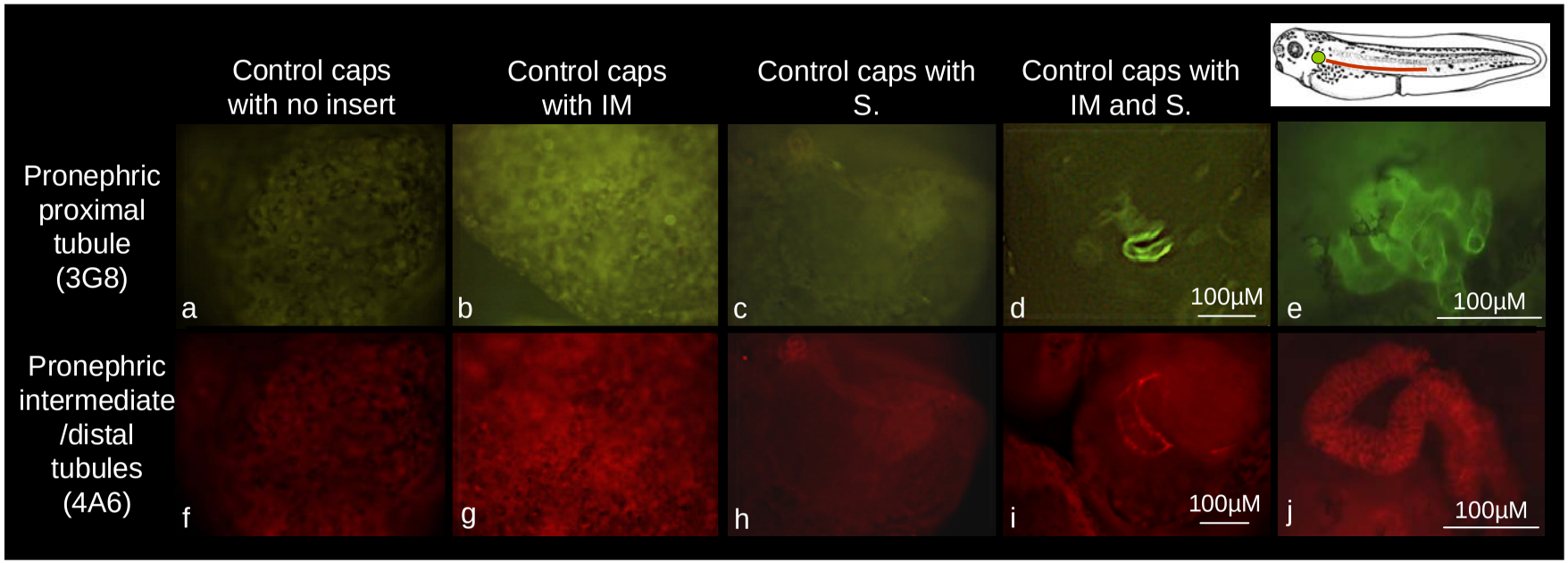

KEY S: somites. **IM**: intermediate mesoderm.

Figure 5.5 Somites can induce pronephros in explant cultures. The sandwich cultures combinations showed above were assayed for the presence of pronephric proximal tubules using the specific antibody 3G8 and for pronephric intermediate/distal tubules using the specific antibody 4A6. Two animal caps cultured together do not give any tubule structure (a, f). Two animal caps containing intermediate mesoderm alone do not give rise to pronephric structures (b, g). Two ectodermal wraps containing somites alone do not result in tubules formation (c, h). However, intermediate mesoderm and somites wrapped together into two animal caps can develop pronephric distal tubules (d) and pronephric intermediate/ distal tubules (i). Whole embryos immuno-stained at stage 40 show proximal tubule morphology (e) and intermediate/distal morphology (j).

caps containing somitic mesoderm only do not give rise to any pronephric structures (Fig 5.5 c and h). Nevertheless, intermediate mesoderm and somitic mesoderm cultured together into two animal caps result in the formation of tubule structures (Fig 5.5.d and i).

The numerical results of the assay are shown in table 5.1. We show that undifferentiated intermediate mesoderm cultured together with presumptive anterior somites have the capability to form proximal tubules in 25% of the cases (23/92 sandwich cultures) and intermediate/distal tubules in 13% of the cases (11/85 sandwich cultures). Two ectodermal caps cultured on their own never give tubules structures (0%) and therefore provide an inert wrap for the culture of embryonic explants. We have shown that undifferentiated intermediate mesoderm (stage 10.5-11), the tissue from which the pronephros is derived, does not have the ability on its own to develop pronephric tubules when cultured in inert ectodermal wraps. However, a small percentage of approximately 6% (8/108 sandwich cultures) of intermediate mesoderm cultured inside two caps showed tubules structures. This could be due to technical difficulties of dissecting the intermediate mesoderm standing between the somites and the lateral plate and occasionally including presumptive somite with the intermediate mesoderm. Somitic mesoderm cultured inside two animal caps is not capable of inducing pronephric structure. However, a small percentage of 3% of sandwich cultures showed tubules (approximately 1/38 sandwich cultures). Technical difficulties arising from dissecting somite away from presumptive pronephros could be the reason for this. So far, we have confirmed that the anterior somites are the tissue responsible for inducing the intermediate mesoderm to become kidney and we hypothesise that signalling molecules secreted from the anterior somites would be the key molecules. Therefore, we have decided to test the ability of the *wnt* signalling molecules to induce pronephros formation in this *in vitro* nephrogenesis culture assay.

		Cultures assayed for 3G8 staining				Cultures assayed for 4A6 staining			
	Sandwich combinations	Number of repeats	Total number of cultures	Number of sandwich positive for 3G8 staining	% of cultures forming tubule	Number of repeats	Total number of cultures	Number of sandwich positive for 4A6 staining	% of cultures forming tubules
Control	C+	6	92	23	25	5	85	11	13
	AC alone	3	22	0	0	2	20	0	0
	AC+ IM	8	108	6	6	8	108	5	5
	AC+ S	3	38	1	3	2	31	1	3
Non-canonical *wnt* molecules	*wnt4* AC alone	1	3	0	0	1	3	0	0
	wnt4 AC+ IM	2	23	2	9	2	23	2	9
	wnt5a AC+ IM	1	20	1	5	1	20	1	5
	wnt11b AC alone	6	41	0	0	5	39	0	0
	wnt11b AC+ IM	9	137	31	23	8	124	25	20
	wnt11 AC alone	1	11	0	0	1	11	0	0
	wnt11 AC+ IM	4	83	14	17	4	83	14	17
	AC+IM+*dnwnt11b* S	4	35	12	34	3	32	9	28
Canonical *wnt* molecules	*wnt6* AC alone	1	4	1	25	1	4	0	0
	wnt6 AC+ IM	4	64	26	41	4	64	42	66
	wnt7b AC+ IM	2	16	2	13	2	16	2	13
	wnt8 AC+ IM	1	17	6	35	1	17	4	24

Key: C+: AC+ IM+ S. AC: Animal caps. IM: Intermediate mesoderm. S: Somites.

Table 5.1 showing a summary of the number of controls and *wnt* sandwich cultures assayed for presence of pronephric tubules using the specific antibodies 3G8/4A6. Sandwich were set as described in chapter 5, section 5.3.1. Results show the number of positive cultures forming tissue per immunoassay and the calculated percentage.

5.3 Holtfreter sandwich cultures to test the *wnt* molecules in forming pronephros.

5.3.1 Both non-canonical *wnt11b* and *wnt11* can induce pronephric tubule formation in explants cultures.

According to chapter 4 sections 4.2.2 and 4.3.2, *wnt11b* and *wnt11* are both expressed in anterior somites and during pronephros development in early *X. laevis* embryos. Therefore, *wnt11b and wnt11* constitute potential pronephric inducers, this hypothesis has been directly investigated using the Holtfreter sandwich cultures.
Embryos were injected at the one-cell stage with 2ng of *wnt11b* or *wnt11* mRNA. After over-night incubation, animal caps were removed and sandwich cultures assembled with or without stage 10.5-11 intermediate mesoderm. The rational of this experiment is that if either of these *wnt* molecules are the natural inducing molecule, secretion from the over-expressing animal caps will induce the uncommitted intermediate mesoderm to pronephric tissue. Sandwich cultures were fixed at stage 40 equivalent and immuno-assayed for the presence of pronephric proximal tubules using the 3G8/FITC antibody combination and pronephric intermediate/distal tubules using the 4A6/TRITC antibody combination. As shown previously, the positive control constituted of intermediate mesoderm co-cultured with anterior somites inside two normal animal caps is capable of generating pronephric tubules. Figure 5.6 shows that two animal caps over-expressing *wnt11b* or *wnt11* mRNA cultured on their own and do not have the ability to form any pronephric structure (Fig 5.6.a and b, e and f respectively). However, two caps over-expressing *wnt11b* and cultured with intermediate mesoderm have the ability to form pronephric proximal tubules (Fig 5.6 c) and intermediate/ distal tubules (Fig 5.6 d). Similarly, when two animal caps over-expressing *wnt11* were cultured with unspecified intermediate mesoderm, pronephric tubules were formed (Fig 5.6 g, h).
Table 5.1 shows number of caps over-expressing *wnt11b* and *wnt11* cultured with or without intermediate mesoderm assayed for the presence of pronephric tubules. None of the animal caps over-expressing *wnt11b* formed pronephric tubules (0/40). However, animal caps over-expressing *wnt11b* and cultured with intermediate mesoderm developed proximal tubule structure in 23% of the cases (31/137) and formed intermediate/ distal tubules tissue in 20% (25/124). Despite their small total

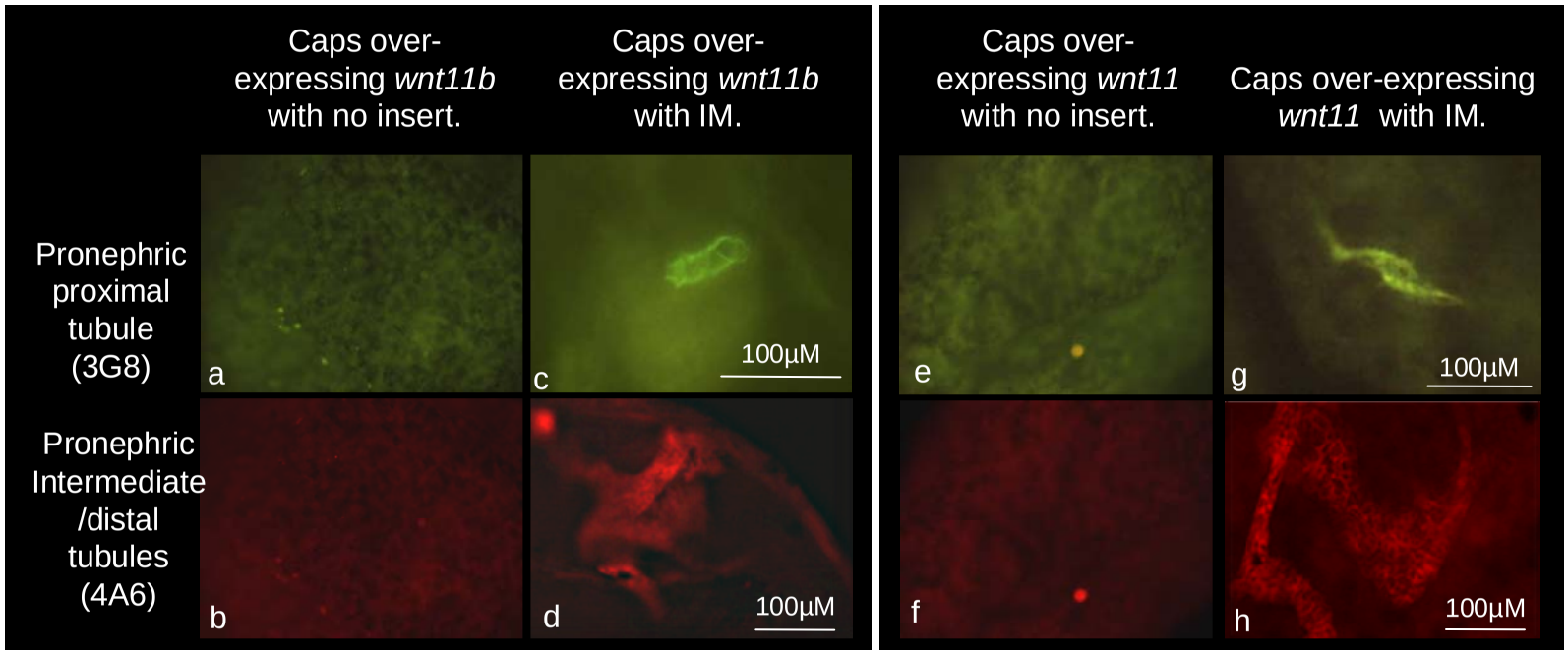

KEY IM: Intermediate mesoderm.

Figure 5.6 *wnt11b* and *wnt11* can induce pronephros formation when cultured with unspecified intermediate mesoderm alone. Embryos were injected at the one-cell stage with 2ng of *wnt11b* or *wnt11* mRNA. After over-night incubation, animal caps were removed and sandwich cultures assembled with or without stage 10.5-11 intermediate mesoderm. Sandwich cultures were fixed at stage 40 equivalent and immuno-assayed for the presence of pronephric proximal tubules using the 3G8 antibody and pronephric intermediate/distal tubules using the 4A6 antibody. Two caps over-expressing *wnt11b* cultured without insert do not have the ability to form tubules (a, b). However, two caps over-expressing *wnt11b* and cultured with intermediate mesoderm form pronephric tubules (c, d). Similarly, two animal caps over-expressing *wnt11* cultured with no insert can not form pronephric structures (e, f) but when two animal caps over-expressing *wnt11* were cultured with unspecified intermediate mesoderm, pronephric tubules were formed (g, h).

number, caps over-expressing *wnt11* cultured on their own never developed any tubules (0/11). When animal caps over-expressing *wnt11* were cultured in the presence of intermediate mesoderm, 17% of the sandwich cultures developed pronephric tubules tissue (14/83 for each tubular structure).
In conclusion, undifferentiated intermediate mesoderm which received either *wnt11b* or *wnt11* signal can differentiate into pronephric proximal, intermediate and distal tubules, suggesting that both *wnt11b* and *wnt11* could play an important role in *Xenopus* pronephros induction having at least the necessary biological activity either directly or indirectly.
We were next interested to know whether the inductive pronephric signal given by *wnt11b* could be blocked by its dominant negative (*dnwnt11b*).

5.3.2 Somites over-expressing the *dnwnt11b* cultured with intermediate mesoderm inside normal animal caps surprisingly form pronephric tubules.

In order to test that *wnt11b,* normally strongly expressed in the somites, could be the signalling molecule responsible for giving the signal to the intermediate mesoderm to differentiate into kidney, an experiment was designed to block *wnt11b* signalling from the somites. The *dnwnt11b* mRNA was injected into the one-cell stage *Xenopus* embryos, so that some of it would later in development be expressed in the somites. At stage 17, the stage at which the anterior somites were dissected from, the morphology of embryos over-expressing the *dnwnt11b* was very affected and embryos showed signs of gastrulation defects (Chapter 6). This indicated that *dnwnt11b* message was active. However, because the embryos were so morphologically abnormal, it was rather difficult to carry out the somite dissection. Dissected anterior somites over-expressing *dnwnt11b* were cultured together with stage 11.5 intermediate mesoderm inside two normal animal caps. Sandwich cultures were left to develop until stage 40 equivalent and immuno-assayed with the pronephric antibodies 3G8 and 4A6.
Very surprisingly, results showed that pronephric tubules can form in such sandwich cultures at an even greater frequency than the animal caps over-expressing *wnt11b* cultured with intermediate mesoderm alone and with a greater frequency than the positive control itself. Table 5.1 shows that 34% (12/35) and 28% (9/32) of Holtfreter sandwich cultures composed of somites over-expressing the *dnwnt11*

cultured with unspecified intermediate mesoderm inside two normal animal caps can form proximal and intermediate/distal pronephric tubules respectively. In conclusion, very surprisingly, blocking *wnt11b* signal in the somites using the *dnwnt11b* results in enhanced pronephros formation in Holtfreter sandwich cultures.

5.3.3 Non-canonical *wnt4* cannot induce pronephric tubules in explant cultures.

According to chapter 4, section 4.2.2, *wnt4* is expressed in the developing pronephros from stage 15 until stage 35 and it has also been shown to play a role in tubulogenesis later in *Xenopus* pronephros formation (Saulnier et al., 2002). Moreover, since *wnt4* is expressed equally in the anterior and posterior somites in *Xenopus* embryos at stage 17 (Chapter 4, section 4.3.2), it therefore constitutes a very interesting candidate for the pronephrogenesis assay. 2ng of *wnt4* mRNA was injected into the animal pole of one-cell stage *Xenopus* embryos. Sandwich cultures were assembled in an identical way to that previously described, cultured and immunostained for the presence of pronephric tubules using the specific 3G8/FITC and 4A6/TRITC antibodies. The result shows that animal caps over-expressing 2ng of *wnt4* cultured on their own survived poorly and did not form any tubule structures, however, the same animal caps cultured with unspecified intermediate mesoderm formed pronephric tubules in 9% of the sandwich (2/23) (table 5.2). Statistical analyses show that *wnt4* does not significantly induce pronephros in *in vitro* cultures (section 5.3.6).

In conclusion, since *wnt4* can induce pronephros in Holtfreter sandwich at low frequency only, we suggest that *wnt4* does not act as a pronephros inducer, and carries out other functions in kidney formation. However, since small numbers of sandwich cultures have been assayed in this experiment, this result remains to be confirmed.

5.3.4 Non-canonical *wnt5a* cannot induce pronephric tubules in explant cultures.

wnt5a has been shown to be expressed all way through pronephros formation from the earliest stage tested, stage 12.5, until the latest stage tested, stage 35 (Chapter 4, section 4.2.2). Interestingly, *wnt5a* is not expressed in the anterior somites at stage 17 (Chapter 4, section 4.3.2). Because *wnt5a* is strongly detected in the posterior

somites only, it is very unlikely that *wnt5a* would be capable of inducing pronephros (Seufert et al., 1999). Animal caps over-expressing 2ng of *wnt5a* mRNA were cultured in the presence of unspecified intermediate mesoderm as previously described. Results show that only 5% (1/20) of the cultures over-expressing *wnt5a* were capable of developing pronephric structures (table 5.2) and this result is shown to be statistically non significant (section 5.3.6). In conclusion, *wnt5a* does not have the ability to induce pronephros in *in vitro* Holtfreter cultures.

5.3.5 Canonical *wnt6* and *wnt8* can induce pronephric tubules in explant cultures.

According to Chapter 4 sections 4.2.2 and 4.3.2, canonical *wnt6* is expressed throughout pronephros formation as early as stage 15 and until stage 35, the latest stage tested. However, *wnt6* cannot be detected in anterior or posterior somites in embryos at stage 17 and therefore is very unlikely to constitute a pronephric inducer (Seufert et al., 1999). On the other hand, canonical *wnt8* was detected within the pronephric anlagen very early, from stage 12.5 until stage 20 only and was detected more strongly in the posterior somites than in the anterior somites in embryos at stage 17. Because *wnt8* is expressed very early and shortly in the developing pronephros and because it is not expressed in the anterior somites, the tissue responsible for pronephros induction (Seufert et al., 1999), *wnt8* does not meet the required criteria of for the pronephric inducer. Nevertheless, the capability of both canonical *wnt6* and *wnt8* to induce pronephros in Holtfreter sandwich cultures was tested. Embryos were injected at the one-cell stage with 2ng of *wnt6* or *wnt8* mRNA. Sandwich cultures were set up as previously described and were fixed at stage 43 equivalent and immunoassayed for the presence of pronephric proximal tubules using the 3G8 antibody and pronephric intermediate/distal tubules using the 4A6 antibody. Surprisingly, two animal caps over-expressing *wnt6* and cultured with unspecified intermediate mesoderm can form proximal tubules (Fig 5.7 a and c) and also intermediate/distal tubules (Fig 5.7 b and d). Table 5.1 shows that *wnt6* over-expressed in animal caps and cultured with intermediate mesoderm forms pronephric tubules in a very high frequency, 41% (26/64) of the cultures formed proximal tubules and 66% (42/64) of the cultures formed intermediate/distal tubules. Animal caps over-expressing *wnt6* and cultured on their own were shown to be able to spontaneously form proximal tubule (25%, 1/4) but not intermediate/distal tubules.

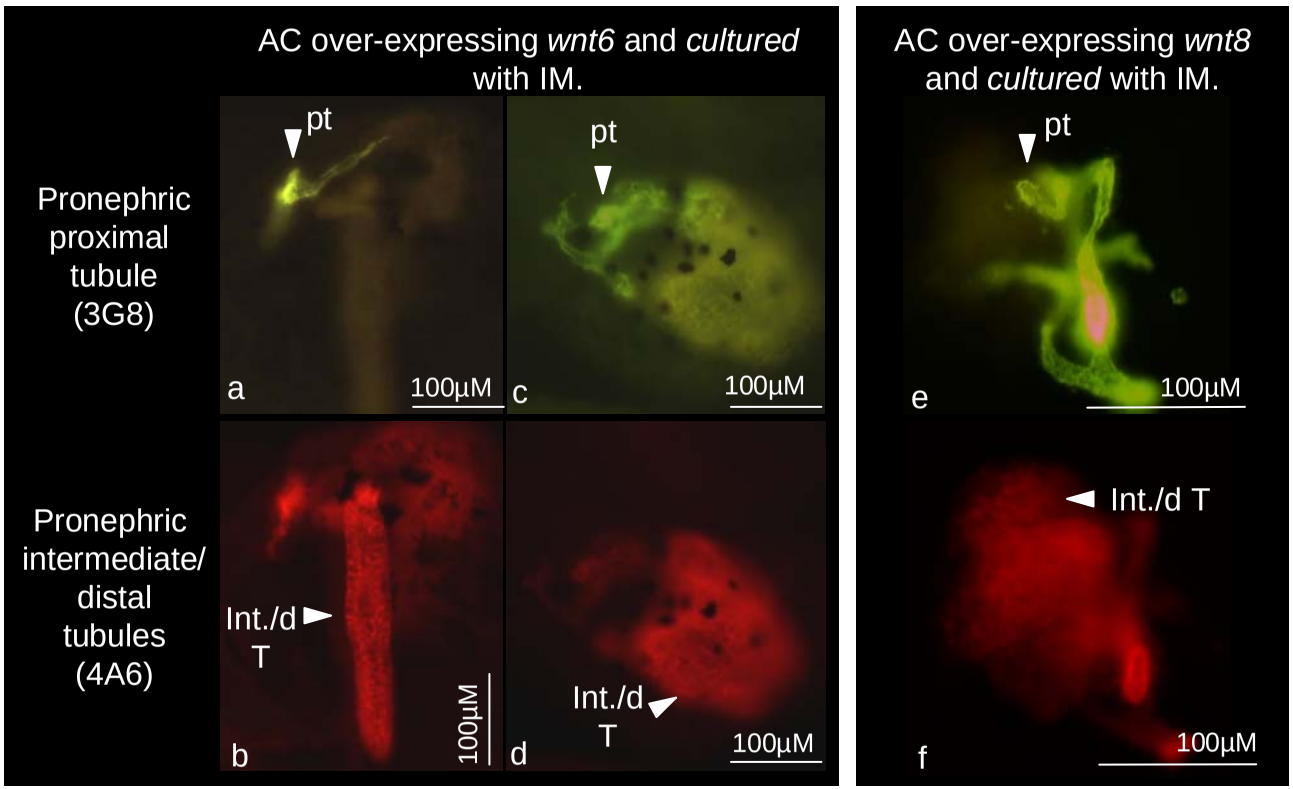

Key: **AC:** Animal caps. **IM**: Intermediate mesoderm.

Figure 5.7 Canonical *wnt6* and *wnt8* over-expressed in animal caps and cultured with unspecified intermediate mesoderm alone can *in vitro* induce pronephros formation. Embryos were injected at the one-cell stage with 2ng of *wnt6* or *wnt8* mRNA. Sandwich cultures were set up as previously described and were fixed at stage 43 equivalent and immunoassayed for the presence of pronephric proximal tubules using the 3G8 antibody and pronephric intermediate/distal tubules using the 4A6 antibody. Two caps over-expressing *wnt6* and cultured with intermediate mesoderm form proximal tubules (pt) (a and c) and also intermediate/distal tubules (int./d T) (b and d). Similarly, two animal caps over-expressing *wnt8* cultured with unspecified intermediate mesoderm produce pronephric proximal tubules (e) and intermediate/distal tubules (f).

This result is shown to be statistically not significant (section 5.3.7). Similarly, two animal caps over-expressing *wnt8* and cultured with unspecified intermediate mesoderm can produce pronephric proximal tubules (Fig 5.7 e) and intermediate/distal tubules (Fig 5.7 f). Results showed that such cultures can form proximal tubules in 35% (6/17) of the cases and intermediate/distal tubules in 24% (4/17) of the cases.

In conclusion, results show that unexpectedly, canonical *wnt6* and *wnt8* are both capable of inducing pronephric tubules when over-expressed in animal caps and cultured with intermediate mesoderm despite their normal expression patterns which were not consistent with a role in somite signalling or pronephrogenesis.

5.3.6 Canonical *wnt7b* cannot induce pronephric tubules in explant cultures.

From Chapter 4 sections 4.2.2 and 4.3.2, *wnt7b* does not start to be expressed within the developing pronephros before stage 25, and its expression remains weak until stage 35, the latest stage tested. Also, *wnt7b* is not expressed in the somites in embryos at stage 17. These results suggest that *wnt7b* is an unlikely candidate for pronephric induction, but even so, its capability to induce pronephros formation in Holtfreter sandwich cultures was tested. Embryos were injected at the one-cell stage with 2ng of *wnt7b* mRNA. Sandwich cultures were set up as previously described and were fixed at stage 43 equivalent and immunoassayed for the presence of pronephric proximal tubules using the 3G8 antibody and pronephric intermediate/distal tubules using the 4A6 antibody. Table 5.1 shows that *wnt7b* is capable of inducing pronephric tubules in only 13% (2/16) of the cultures and this result is shown to be statistically not significant (section 5.3.6).

To conclude, analysis of *wnt7b* Holtfreter sandwich cultures have now confirmed that *wnt7b,* normally expressed only very late within the developing pronephros and not expressed at all in the somites, does not act as a pronephric inducer in *in vitro* nephrogenesis assay.

5.3.7 Statistical analysis shows that some but not all *wnt* molecules can significantly induce pronephric tubules in *in vitro* Holtfreter sandwich cultures.

A chi-squared test (χ^2) was performed in order to determine whether *wnt* molecules could significantly induce pronephros formation in Holtfreter sandwich cultures. The chi-squared test allows a comparison of the observed number of Holtfreter sandwich cultures assayed for pronephric tubules formation when *wnt* molecules were over-expressed in animal caps and cultured with unspecified intermediate mesoderm with a theoretically expected distribution. The null hypothesis (H_0) is that pronephros formation in Holtfreter sandwich cultures is not dependent on *wnt* signalling molecules over-expressed in the animal caps. For each assay, the χ^2 value determines whether the difference in tubule formation between *wnt* sandwich cultures and the background control (normal animal caps cultured with intermediate mesoderm) was significant. Thus, the χ^2 calculated value is compared with tabulated value for one degree of freedom at 95% probability. When the χ^2 calculated value exceeds the tabulated value of 3.8 then pronephric tubule formation is dependent on the over-expression of the tested *wnt* molecule and therefore the null hypothesis is rejected. Tables 5.2 and 5.3 give the details of χ^2 calculations for the formation of proximal tubules and intermediate/ distal tubules respectively. Figure 5.8 shows the χ^2 value of sandwich cultures when assayed for proximal tubule formation and compared to the tabulated value of 3.8. Complementary to this, figure 5.9 shows χ^2 value of sandwich cultures when assayed for intermediate/ distal tubules formation and compared to the tabulated value of 3.8. The result of this analysis shows that the positive control (animal caps cultured with intermediate mesoderm and somites) can significantly form proximal and intermediate/distal tubules with χ^2 values of approximately 15 and 5 respectively. Animal caps cultured with somites alone cannot significantly form pronephric tubules confirming that somites on their own cannot induce kidney. Formation of tubules at low frequency in *wnt4* and *wnt5a* Holtfreter sandwich cultures is not dependent on the over-expression of *wnt4* and *wnt5a* genes with χ^2 values below 3.8. This result suggests that the very few pronephric tubules forming in such samples might result from dissection artefacts which occasionally gave false positive results. However, formation of pronephric tubules in *wnt11b* and *wnt11* Holtfreter sandwich cultures is significant and clearly dependent on the inducing signal that both genes give when translated in the animal cap tissue to the

Table 5.2 Statistical analyses show that some *wnt* molecules but not all can significantly induce proximal tubule formation in Holtfreter sandwich cultures. Chi Square test allows comparing the observed number of Holtfreter sandwich cultures assayed for tubule formation when *wnt* molecules were over-expressed in animal caps and cultured with unspecified intermediate mesoderm with a theoretically expected distribution. For each assay, x^2 value determines whether the difference in tubule formation between *wnt* sandwich cultures and the background control (AC+ IM) was significant. Thus, x^2 calculated value is compared with tabulated value for one degree of freedom at 95% probability. When the x^2 calculated value exceeds the tabulated value of 3.8 then tubule formation is related to the over-expression of the tested *wnt* molecule.

Sandwich combinations	O (+)	O (-)	Total	E (+)	E (-)	Total	$\chi^2 = \Sigma (O-E)^2/E$	Significant if $\chi^2>3.8$
C+	23	69	92	13.340	78.660	92		
AC+ IM	6	102	108	15.660	92.340	108	**15.146**	yes
Σ	29	171	200	29.000	171.000	200		
AC+ S	1	37	38	1.822	36.178	38		
AC+ IM	6	102	108	5.178	102.822	108	**0.526**	no
Σ	7	139	146	7.000	139.000	146		
wnt4 AC+ IM	2	21	23	1.405	21.595	23		
AC+ IM	6	102	108	6.595	101.405	108	**0.324**	no
Σ	8	123	131	8.000	123.000	131		
wnt5a AC+ IM	1	19	20	1.094	18.906	20		
AC+ IM	6	102	108	5.906	102.094	108	**0.009**	no
Σ	7	121	128	7.000	121.000	128		
wnt11b AC + IM	31	106	137	20.690	116.310	137		
AC+ IM	6	102	108	16.310	91.690	108	**13.728**	yes
Σ	37	208	245	37.000	208.000	245		
wnt11 AC + IM	14	69	83	8.691	74.309	83		
AC+ IM	6	102	108	11.309	96.691	108	**6.405**	yes
Σ	20	171	191	20.000	171.000	191		
AC+IM+*dnwnt11b* S	12	23	35	4.406	30.594	35		
AC+ IM	6	102	108	13.594	94.406	108	**19.826**	yes
Σ	18	125	143	18.000	125.000	143		
wnt6 AC alone	1	3	4	0.250	3.750	4		
AC+ IM	6	102	108	6.750	101.250	108	**2.488**	no
Σ	7	105	112	7.000	105.000	112		
wnt6 AC+ IM	26	38	64	11.907	52.093	64		
AC+ IM	6	102	108	20.093	87.907	108	**32.636**	yes
Σ	32	140	172	32.000	140.000	172		
wnt7b AC+ IM	2	14	16	1.032	14.968	16		
AC+ IM	6	102	108	6.968	101.032	108	**1.114**	no
Σ	8	116	124	8.000	116.000	124		
wnt8 AC + IM	6	11	17	1.632	15.368	17		
AC+ IM	6	102	108	10.368	97.632	108	**14.968**	yes
Σ	12	113	125	12.000	113.000	125		

Key:**C+** : AC+ IM+ S. **AC**: Animal caps. **IM**: Intermediate mesoderm. **S**: Somites
O: Observed number of cultures forming or not proximal tubule.
E (+) / **(-)**: Expected number of cultures forming or not proximal tubule.

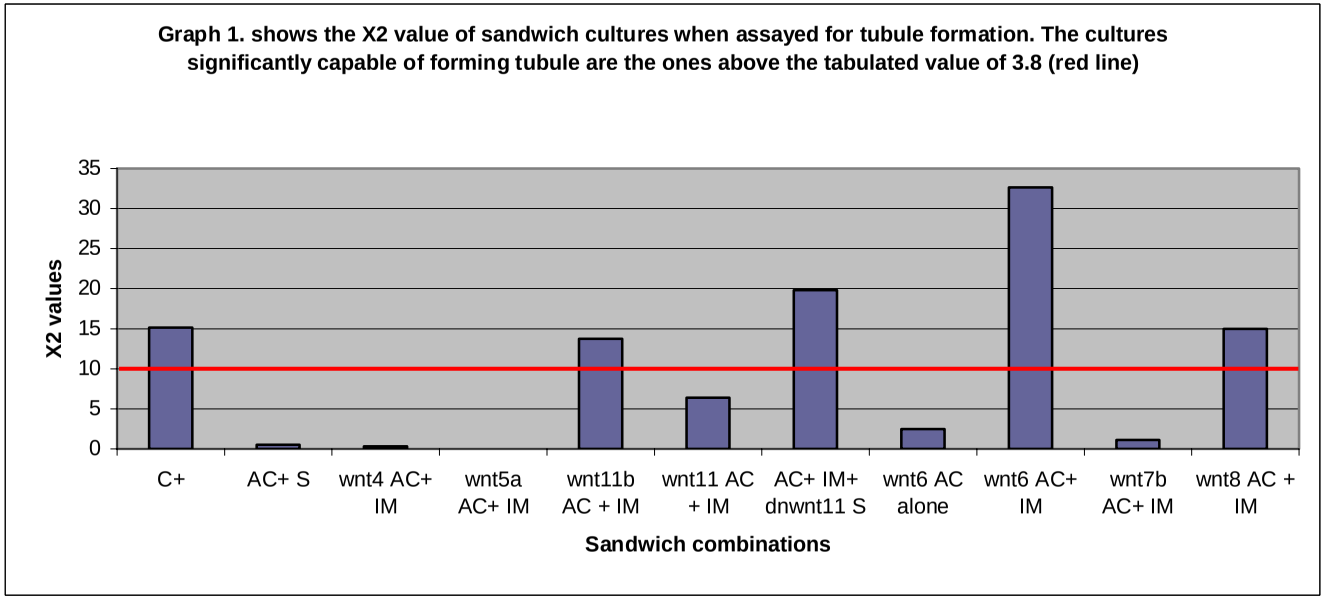

Figure 5.8 Statistical analyses show that some but not all *wnt* molecules can significantly induce proximal tubule formation in Holtfreter sandwich cultures. Graph 1 compare the calculated χ^2 values of control and *wnt* sandwich cultures assayed for proximal tubule formation. Unspecified intermediate mesoderm was cultured inside two animal caps over-expressing a member of the *wnt* molecules family or inside normal animal caps in the case of the background control. Sandwich cultures were assayed by antibody staining using the specific proximal tubule marker, 3G8. When a χ^2 calculated value exceeds the tabulated value of 3.8 (red line) then tubule formation is related to the over-expression of the tested *wnt* molecule. Table 5.2 gives the details of χ^2 calculations.

Table 5.3 Statistical analyses show that some *wnt* molecules but not all can significantly induce intermediate/distal tubules formation in Holtfreter sandwich cultures. Chi Square test allows comparing the observed number of Holtfreter sandwich cultures assayed for intermediate/distal tubules formation when *wnt* molecules were over-expressed in animal caps and cultured with unspecified intermediate mesoderm with a theoretically expected distribution. For each assay, x^2 value determines whether the difference in tubules formation between *wnt* sandwich cultures and the background control (AC+ IM) was significant. Thus, x^2 calculated value is compared with tabulated value for one degree of freedom at 95% probability. When the x^2 calculated value exceeds the tabulated value of 3.8 then intermediate/ distal tubules formation is related to the over-expression of the tested *wnt* molecule.

Sandwich combinations	O (+)	O (-)	Total	E (+)	E (-)	Total	$\chi^2 = \Sigma (O-E)^2/E$	Significant if
C+	12	73	85	7.487	77.513	85		
AC+ IM	5	103	108	9.513	98.487	108	**5.33**	yes
Σ	17	176	193	17.000	176.000	193		
AC+ S	1	30	31	1.338	29.662	31		
AC+ IM	5	103	108	4.662	103.338	108	**0.114**	no
Σ	6	133	139	6.000	133.000	139		
wnt4 AC+ IM	2	21	23	1.229	21.771	23		
AC+ IM	5	103	108	5.771	102.229	108	**0.619**	no
Σ	7	124	131	7.000	124.000	131		
wnt5a AC+ IM	1	19	20	0.938	19.063	20		
AC+ IM	5	103	108	5.063	102.938	108	**0.005**	no
Σ	6	122	128	6.000	122.000	128		
wnt11b AC + IM	25	99	124	16.034	107.966	124		
AC+ IM	5	103	108	13.966	94.034	108	**12.368**	yes
Σ	30	202	232	30.000	202.000	232		
wnt11 AC + IM	14	69	83	8.257	74.743	83		
AC+ IM	5	103	108	10.743	97.257	108	**7.844**	yes
Σ	19	172	191	19.000	172.000	191		
AC+ IM+*dnwnt11b* S	9	23	32	3.200	28.800	32		
AC+ IM	5	103	108	10.800	97.200	108	**15.141**	yes
Σ	14	126	140	14.000	126.000	140		
wnt6 AC alone	0	4	4	0.179	3.821	4		
AC+ IM	5	103	108	4.821	103.179	108	**0.193**	no
Σ	5	107	112	5.000	107.000	112		
wnt6 AC+ IM	42	22	64	17.488	46.512	64		
AC+ IM	5	103	108	29.512	78.488	108	**75.289**	yes
Σ	47	125	172	47.000	125.000	172		
wnt7b AC+ IM	2	14	16	0.903	15.097	16		
AC+ IM	5	103	108	6.097	101.903	108	**1.621**	no
Σ	7	117	124	7.000	117.000	124		
wnt8 AC + IM	4	13	17	1.224	15.776	17		
AC+ IM	5	103	108	7.776	100.224	108	**7.053**	yes
Σ	9	116	125	9.000	116.000	125		

Key:**C+** : AC+ IM+ S. **AC**: Animal caps. **IM:** Intermediate mesoderm. **S**: Somites
O: Observed number of cultures forming or not intermediate/distal tubules.
E (+) / **(-)**: Expected number of cultures forming or not intermediate/distal tubules.

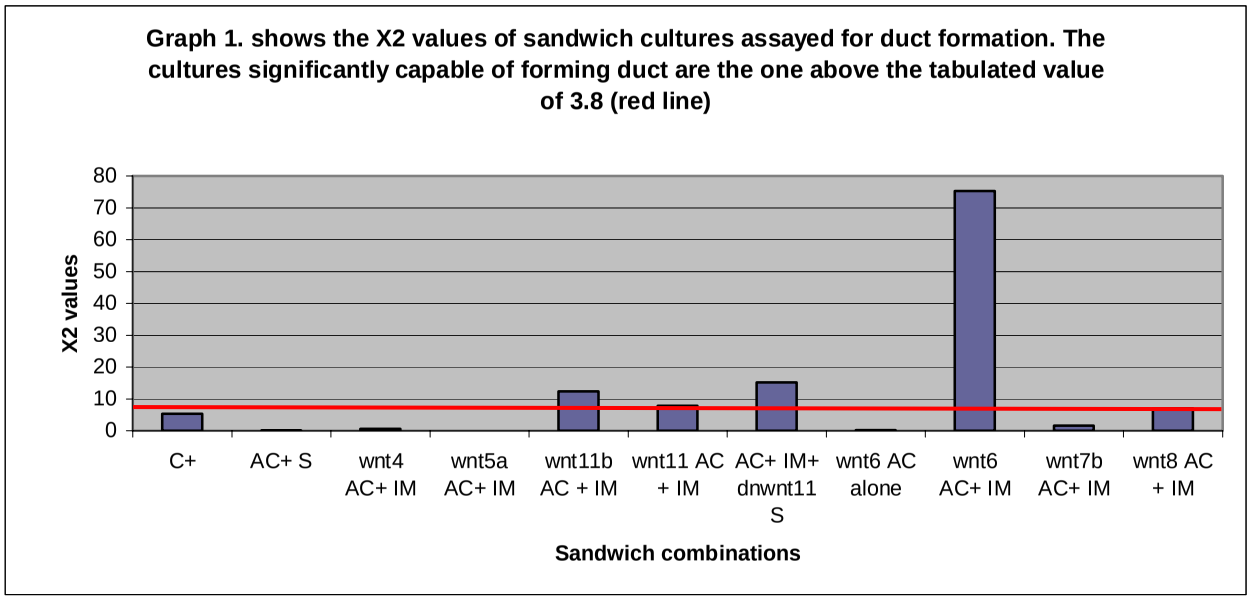

Figure 5.9 Statistical analyses show that some but not all *wnt* molecules can significantly induce intermediate/distal tubules formation in Holtfreter sandwich cultures. Graph 1 compare the calculated χ^2 values of control and *wnt* sandwich cultures assayed for intermediate/ distal tubules formation. Unspecified intermediate mesoderm was cultured inside two animal caps over-expressing a member of the *wnt* molecules family or inside normal animal caps in the case of the background control. Sandwich cultures were assayed by antibody staining using the specific intermediate/distal tubules marker, 4A6. When a χ^2 calculated value exceeds the tabulated value of 3.8 (red line) then tubules formation is related to the over-expression of the tested *wnt* molecule. Table 5.3 gives the details of χ^2 calculations.

intermediate mesoderm resulting in differentiation of kidney, as shown by χ^2 values exceeding the tabulated value of 3.8. In the same way, somites over-expressing *dnwnt11b* cultured with intermediate mesoderm inside normal animal caps can significantly form proximal tubule and intermediate/distal tubules with χ^2 values of 19.826 and 15.141 respectively.

Results concerning the canonical *wnt* sandwich cultures indicate that *wnt6* can highly significantly induce pronephric proximal tubule formation when over-expressed in animal caps and cultured with unspecified intermediate mesoderm with a χ^2 value of 32.636, much higher than the significance tabulated value of 3.8. In an even more spectacular manner, such sandwich cultures were capable of forming intermediate/distal tubules with a χ^2 value that equalled 75.289. However, pronephric tubules forming at low frequency when animal caps were over-expressing *wnt6* and cultured on their own, is revealed as not statistically significant with a χ^2 value of 2.488 and 0.193 for proximal and intermediate/distal tubules respectively. All together, these results indicate that the null hypothesis (H_0) is rejected and formation of both proximal and intermediate/distal tubules is strictly related to the pronephric inducing activity that *wnt6* confers to the intermediate mesoderm when cultured in a Holtfreter sandwich culture manner. Similarly, although not as strong, formation of pronephric tubules in *wnt8* Holtfreter sandwich cultures is significant and strictly due to the inductive signal that *wnt8* gives to the intermediate mesoderm to differentiate into kidney (χ^2 values equal 14.968 and 7.053 for proximal and intermediate/distal tubules respectively). Finally, results show that the low frequency of pronephros formation in *wnt7b* Holtfreter sandwich is not statistically significant, with χ^2 values below the tabulated value of 3.8 (1.114 and 1.621 for proximal and intermediate/distal tubules respectively), indicating that *wnt7b* does not act as a inducer in pronephros formation.

To conclude, Holtfreter sandwich cultures have been used to replace the natural source of pronephric-inducing signal, the anterior somites, by an over-expression of mRNA of candidate *wnt* signalling molecules in animal caps, cultured with intermediate mesoderm. These show that the non-canonical *wnt11b* and the closely related *wnt11* are capable of giving such signal and significantly induce formation of pronephric proximal and intermediate/distal tubules, whereas non-canonical *wnt4* and *wnt5a* cannot induce pronephros formation. Moreover, the canonical *wnt*

molecules, *wnt6* and *wnt8* have been shown to be highly significantly capable of inducing pronephric tubules formation when over-expressed in animal caps and cultured with intermediate mesoderm, by a yet unknown mechanism. We suggest that formation of pronephros in such cultures is as a result of an indirect induction. These cultures, by external morphology, showed that before immunostaining they contained neural tissue. This observation leads to the hypothesis that *wnt6* and *wnt8* can, in the presence of intermediate mesoderm, induce the formation of most-dorsal structure, including nervous system and somites, that in turn can actively induce pronephric tubule formation. However, although there is evidence of pigmented neural crest derivates in *wnt7b* Holtfreter sandwich cultures, this does not seem to be sufficient to induce pronephric structures either directly or indirectly. We next tried to investigate this hypothesis.

5.4 *wnt* Holtfreter sandwich cultures assayed for somite formation.

In order to gain more information on the process of pronephric tubules formation in Holtfreter sandwich cultures, we hypothesised that formation of pronephric tubules in *wnt* Holtfreter sandwich cultures could result from formation of somites which themselves are able to induce pronephric tissue. Thus, Holtfreter sandwich cultures were constructed as described in Chapter 5, section 5.2.1 and were left to develop until stage 40 equivalent before being subjected to antibody staining using the specific muscle antibody 12/101 and detected using a secondary antibody, coupled to Alexa fluor 205. Table 5.4 shows a summary of the number of controls and specific *wnt* sandwich cultures assayed for presence of somites and table 5.5 gives the corresponding calculated chi-squared (χ^2) values. For each assay, the χ^2 value determines whether the difference in somites formation between *wnt* sandwich cultures and the background control (AC+ IM) was significant. The null hypothesis is that over-expression of *wnt* molecules in animal caps cultured with intermediate mesoderm will induce formation of somite. Thus, χ^2 calculated value is compared with tabulated value for one degree of freedom at 95% probability. When the χ^2 calculated value exceeds the tabulated value of 3.8 then somite formation is related to the over-expression of the tested *wnt* molecule and the null hypothesis is rejected. Table 5.4 shows that 88% of the control positive sandwich kept their somite tissues initially cultured with intermediate mesoderm, and this result is highly significantly

		Cultures assayed for 12/101 staining			
	Sandwich combinations	Number of repeats	Total number of sandwich cultures	Number of sandwich positive for 12/101 staining	% of cultures forming somite
Control	C+	2	34	30	88
	AC+ IM	2	21	4	19
Non-canonical *wnt*	*wnt11b* AC alone	2	15	2	13
	wnt11b AC+ IM	4	53	20	38
	wnt11 AC+ IM	1	21	8	38
Canonical w*nt*	*wnt6* AC alone	2	8	4	50
	wnt6 AC+ IM	4	44	18	41
	wnt7b AC+ IM	1	8	1	13

Key: **C+** : AC+ IM+ S. **AC**: Animal caps. **IM**: Intermediate mesoderm. **S**: Somites

Table 5.4 showing a summary of the number of controls and *wnt* sandwich cultures assayed for presence of somites using the specific antibody 12/101. Sandwich were set as described in chapter 5, section 5.2.1. Results show the number of positive cultures forming tissue per immunoassay and the calculated percentage.

Table 5.5 Statistical analyses show that some *wnt* molecules but not all can significantly induce somites formation in Holtfreter sandwich cultures. Chi Square test allows comparing the observed number of Holtfreter sandwich cultures assayed for somites formation when *wnt* molecules were over-expressed in animal caps and cultured with unspecified intermediate mesoderm with a theoretically expected distribution. For each assay, x^2 value determines whether the difference in somites formation between *wnt* sandwich cultures and the background control (AC+ IM) was significant. Thus, x^2 calculated value is compared with tabulated value for one degree of freedom at 95% probability. When the x^2 calculated value exceeds the tabulated value of 3.8 then somites formation is related to the over-expression of the tested *wnt* molecule.

Sandwich combinations	O (+)	O (-)	Total	E (+)	E (-)	Total	$\chi^2 = \Sigma (O-E)^2/E$	Significant if $\chi^2 > 3.8$
C+	30	4	34	20.400	13.600	34		
AC+ IM	3	18	21	12.600	8.400	21	**29.578**	yes
Σ	33	22	55	33.000	22.000	55		
wnt11b AC alone	2	13	15	2.083	12.917	15		
AC+ IM	3	18	21	2.917	18.083	21	**0.007**	no
Σ	5	31	36	5.000	31.000	36		
wnt11b AC + IM	20	33	53	16.473	36.527	53		
AC+ IM	3	18	21	6.527	14.473	21	**3.861**	yes
Σ	23	51	74	23.000	51.000	74		
wnt11 AC + IM	8	13	21	5.500	15.500	21		
AC+ IM	3	18	21	5.500	15.500	21	**3.078**	no
Σ	11	31	42	11.000	31.000	42		
wnt6 AC alone	4	4	8	1.931	6.069	8		
AC+ IM	3	18	21	5.069	15.931	21	**4.035**	yes
Σ	7	22	29	7.000	22.000	29		
wnt6 AC+ IM	19	25	44	14.892	29.108	44		
AC+ IM	3	18	21	7.108	13.892	21	**5.301**	yes
Σ	22	43	65	22.000	43.000	65		
wnt7b AC+ IM	1	7	8	1.103	6.897	8		
AC+ IM	3	18	21	2.897	18.103	21	**0.015**	no
Σ	4	25	29	4.000	25.000	29		

Key: **C+** : AC+ IM+ S. **AC**: Animal caps. **IM**: Intermediate mesoderm. **S**: Somites.
O: Observed number of cultures forming or not somites.
E (+) / (-): Expected number of cultures forming or not somites.

since the χ^2 value is approximately 30. A small percentage, 19%, of the background control sandwich cultures (animal caps cultured with intermediate mesoderm alone) showed formation of somites and this result illustrates the difficulty of dissecting thin embryonic pieces of intermediate mesoderm without occasional contamination of unwanted somitic material. Similarly, 13% of animal caps over-expressing *wnt11b* and cultured on their own, formed some muscle tissue. However, statistically, this result is not significant. 38% of the animal caps over-expressing *wnt11b* and cultured with intermediate mesoderm formed somitic tissue and the corresponding χ^2 value for this result is just above the tabulated value of 3.8. Similarly, 38% of the animal caps over-expressing *wnt11* and cultured with intermediate mesoderm formed muscle tissue but this time the corresponding χ^2 value for this result is just below the tabulated value of 3.8. In order to assess whether the positive sandwich cultures were due to the presence of muscle tissue, a small sample of 24 animal caps over-expressing *wnt11b* and cultured with intermediate mesoderm, were assayed by triple antibody staining using the pronephric tubules antibodies 3G8/ 4A6 and the somite antibody 12/101 (data not shown). A detailed analysis revealed that 6 sandwich cultures formed both tubules and somites but 7 sandwich cultures formed pronephros without forming any somite tissues and also 4 sandwiches formed somite but did not form any pronephric tubules. 7 sandwich cultures were negative for both tissues. A similar result was found in animal caps over-expressing *wnt11* and cultured with intermediate mesoderm.

Concerning the canonical *wnt* sandwich cultures, results showed that 50% of the animal caps over-expressing *wnt6* and cultured on their own formed somitic tissue and the corresponding χ^2 value for this result is above the tabulated value of 3.8, suggesting that animal caps over-expressing *wnt6* and cultured on their own can form somitic tissue. However, the number of cultures assayed was very small (4/8) and increased numbers should be assayed. Nonetheless, 41% (18/44) of the animal caps over-expressing *wnt6* and cultured with intermediate mesoderm formed muscle tissue and showed a corresponding χ^2 value of 5.301. This result is convincingly significant and a small sample of 38 cultures was assayed by triple staining in order to detect the presence of pronephric proximal, intermediate/distal tubules and somites (data not shown). Results showed that 15 cultures scored positively for the presence of both pronephric tubules and somites, 12 cultures did not form any tissues, 3 cultures formed somites but no pronephros and finally 7 cultures formed pronephros without

somites. This observation suggests that formation of pronephros correlates at high frequency with formation of somites in *wnt6* Holtfreter sandwich cultures.

As expected the *wnt7b* Holtfreter sandwich cultures that did not form pronephric tubules, did not form somitic tissue neither, as only 13% of the cultures (1/8) (table 5.4) showed the presence of somites, a result that is statistically not significant (table 5.5).

To conclude, animal caps over-expressing *wnt11* and *wnt11b* cultured with intermediate mesoderm have also the capability of forming somitic muscle. However, formation of both tissues in *wnt11* and *wnt11b* Holtfreter sandwich cultures seems to be independent from one to another and we hypothesize that presence of somite tissue in such sandwich cultures arose from mis-dissection, because of the difficulty of dissecting such small pieces of embryonic material. We conclude that formation of somites in such sandwich cultures is unlikely to influence pronephric tubule formation. However, animal caps over-expressing *wnt6* cultured with intermediate mesoderm can form, at high frequency, both pronephric and somitic tissues. Furthermore, microscopic observations and statistical analyses suggest that formation of pronephros in such cultures is dependent on the formation of somites, as most of the cultures showed the simultaneous presence of both tissues. Thus, we hypothesised that formation of pronephric tubules in *wnt6* Holtfreter sandwich cultures might resulted from a secondary induction perhaps involving the formation of dorsal tissue such as the somites.

5.5 Sandwich cultures over-expressing *wnt11b* cultured with intermediate mesoderm induce specific pronephric markers.

With the aim of confirming pronephros formation and investigating the pronephric genes expressed in Holtfreter sandwich cultures, various sandwich combinations were set up. Expression of pronephric genes in animal caps over-expressing 2 or 3ng of *wnt11b* mRNA and cultured with unspecified intermediate mesoderm (referred as 2 and 3ng *wnt11b* sandwich in this section) was compared to normal animal caps cultured with intermediate mesoderm and somites (referred as positive control in this section). Since animal caps were being dissected, embryos could accommodate slightly more *wnt11b* mRNA. Sandwich cultures were set up as described in chapter 5, section 5.3.1 and were left to develop until stage 40 equivalent. Total RNA was

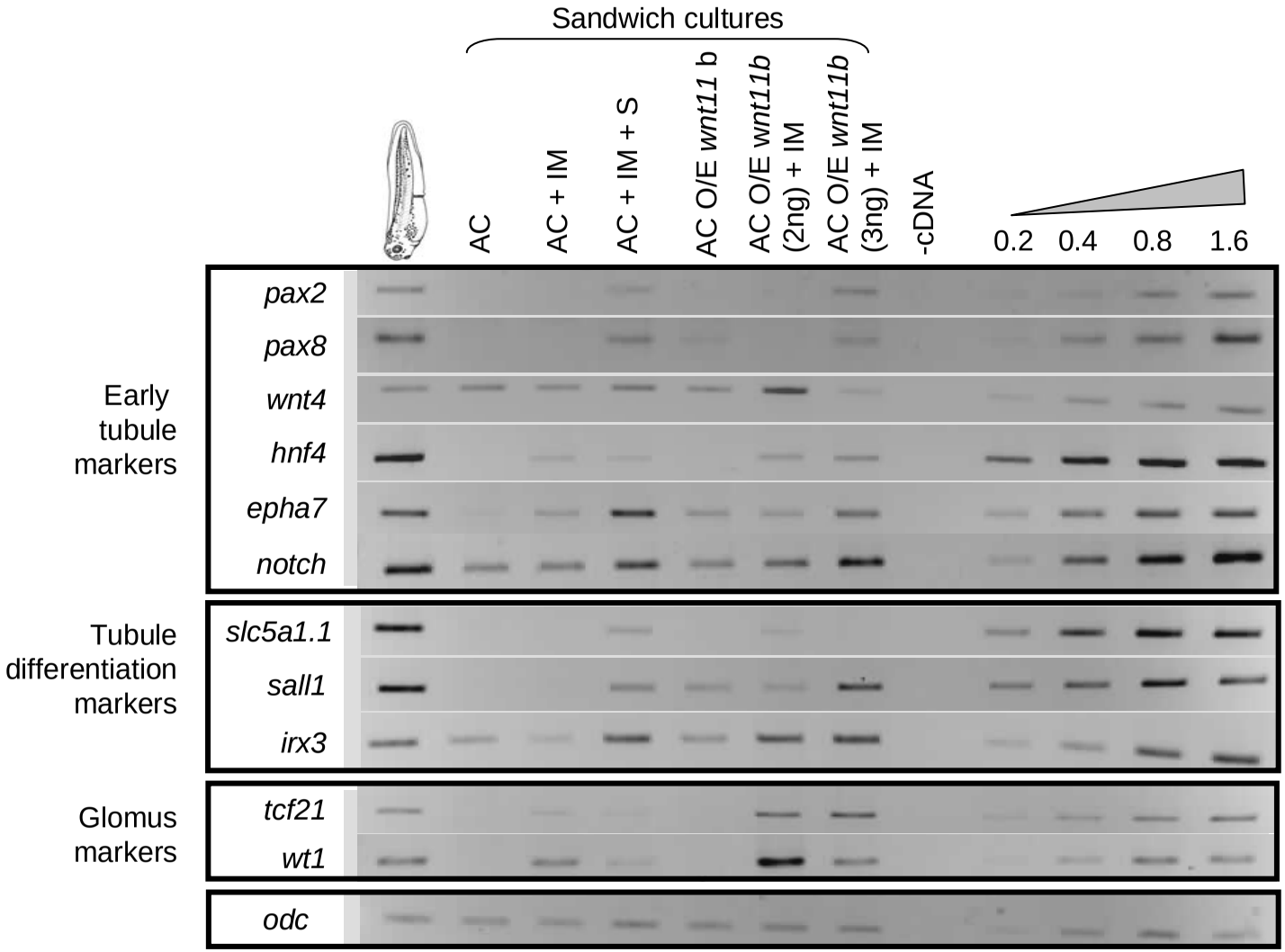

KEY **AC**: Animal caps. **IM**: Intermediate mesoderm. **S**: Somites. **O/E**: Over-expressing.

Figure 5.10 Pronephric markers are expressed in sandwich cultures over-expressing *wnt11b*. One-cell stage *X. laevis* embryos were injected or not with 2 or 3ng of *wnt11b* mRNA. After over-night incubation, animal caps were dissected from normal embryos and from embryos over-expressing *wnt11b*. Intermediate mesoderm was dissected from stage 10.5-11 embryos and somites were taken from stage 17 embryos. Sandwich combinations were set up as indicated on the figure. Cultures were allowed to develop until stage 40 equivalent. Total RNA was extracted from each sample before being subjected to RT-PCR analysis. *odc* was used to equalize the cDNA samples. The triangle illustrates sequentially increasing cDNA inputs of whole embryo cDNA. The animal caps over-expressing 2 or 3ng of *wnt11b* cultured with unspecified intermediate mesoderm show the presence of both tubules specification and differentiation markers. Moreover, the presence of glomus markers in such sandwich combinations indicates that *wnt11b* is also capable of inducing pronephric glomus in sandwich cultures.

extracted from each sample before being subjected to RT-PCR analysis. Figure 5.10 shows that pronephric markers are expressed in *wnt11b* sandwich cultures. *odc* was used to equalize the cDNA samples. The triangle illustrates sequentially increasing cDNA inputs of whole embryo cDNA.

Expression of the early proximal, intermediate and distal tubules markers *pax2* (Heller and Brändli, 1997) and *pax8* (Carroll and Vize, 1999) confirm the presence of pronephric tissue in the positive control and also in 2 and 3ng *wnt11b* sandwich cultures. Expression of *wnt4* (Saulnier et al., 2002) and *notch* (McLaughlin et al., 2000) is detected in all samples tested, therefore these markers are not informative in this experiment. However, *wnt4* expression is strongly up-regulated in 2ng *wnt11b* sandwich cultures and similarly, *notch* is strongly up-regulated in the positive control and in 3ng *wnt11b* sandwich cultures. Interestingly, *hnf4* mRNA (Ryffel, 2001) was detected in 2 and 3ng *wnt11b* sandwich cultures and not in animal caps over-expressing 2ng of *wnt11b* cultured on their own (referred as experimental control in this section) and only weakly in the positive control and in normal animal caps cultured with intermediate mesoderm alone (referred as background control in this section). Due to the role of *hnf4* in pronephros development, this result suggests specific pronephric activity occurring in *wnt11b* sandwich cultures. *epha7* (Winning and Sargent, 1994) is expressed in all samples except in the normal caps cultured on their own, indicating that *epha7* is not normally found in the epidermis. On the other hand, *epha7* is up-regulated in the positive control and in 3ng *wnt11b* sandwich cultures.

Tubule differentiation markers such as, *slc5a1.1* (previously called the sodium-dependent glucose cotransporter 1, *SGLT-1)*, (Nagata et al., 1999), *sall1* (Brändli , 1999) and *irx3* (Brändli , 1999) were also detected in the positive control and in *wnt11b* sandwich cultures. *slc5a1.1* shows expression in the positive control and in 2ng *wnt11b* sandwich cultures. *sall1* is expressed in the positive control and in all samples over-expressing *wnt11b.* Moreover*, sall1* expression is noticeable stronger in 3ng *wnt11b* sandwich than in 2ng *wnt11b* sandwich, suggesting that *sall1* could be activated downstream of *wnt11b* during pronephros differentiation. *irx3* is expressed in all samples tested but is up-regulated in the positive control and in *wnt11b* sandwich cultures, suggesting that such cultures contain differentiated pronephric tubules. In conclusion, expression of tubule differentiation markers in Holtfreter positive control sandwich cultures and *wnt11b* sandwich cultures suggests that such

cultures are capable of maturing primary pronephric components into differentiated proximal and intermediate/distal tubular structure, indicating that such *in vitro* cultures could possibly produce functional pronephric explants.

Finally, *wnt11b* is also capable of inducing the third pronephric component, the pronephric glomus in Holtfreter sandwich cultures, as expression of the pronephric glomus *tcf21* (previously called *XPod-1*, Simrick et al., 2005) and *wt1* (Carroll and Vize, 1996) is strongly up-regulated in *wnt11b* sandwich cultures.

To conclude, animal caps over-expressing 2 and 3ng of *wnt11b* cultured with unspecified intermediate mesoderm show the presence of pronephric proximal, intermediate/distal tubules and pronephric glomus. This result is very interesting since during development, the pronephric anlagen undergoes partitioning that specifies the three pronephric components (Taelman et al., 2006). In Holtfreter sandwich cultures, *wnt11b* can give a signal that will result in the formation of the components of a complete functional embryonic renal unit, a nephron. Whether this is capable of function is unknown but there is precedent for functional kidney induced in animal caps by activin and retinoic acid treatment (Moriya et al., 1993 and Chan et al., 1999).

5.6 Discussion.

5.6.1 Holtfreter sandwich cultures, an explant model to study pronephrogenesis, advantages and limitations.

One of the great advantages of the Holtfreter sandwich is that explants can respond specifically to the signalling molecule which induces pronephros formation. So far, we have shown that *wnt11* and *wnt11b* are both expressed in the somites and in the developing pronephros and can give a signal to the intermediate mesoderm to differentiate into kidney when over-expressed in animal caps. However, *wnt5a* which is also expressed in the developing somites and in the developing pronephros does not have this inductive property and therefore cannot induce pronephric tubules in explant sandwich cultures. Moreover, results of Chapter 4 showed that the signalling molecule *fst* (*follistatin*) is strongly expressed in the anterior somites and throughout pronephros formation with a strong up-regulation at stage 25. Even though, when *fst*

was assayed in Holtfreter sandwich cultures, no pronephric tubules were formed (data not shown).

On the other hand, Holtfreter sandwich cultures require fine dissections of embryonic material, which are subject to potential contamination of unwanted tissue, especially if animal caps are a little thickened as a result of the injection of *wnt* molecules. Consequently, mature sandwich cultures could give spontaneously false positive results for the presence of pronephric components. This is illustrated by the background seen when normal animal caps cultured with intermediate mesoderm alone form pronephric tubules at low frequency. So, this is a labour intensive and difficult technique. A small number of sandwich cultures can be set up at a time and the staging of the embryos used for dissected fragments is critical. For example, intermediate mesoderm dissected at stage 12.5 instead of stage 11.5 would form pronephric material in a false positive manner because at stage 12.5 the pronephric anlagen has already been specified. Explants are also difficult to culture to stages equivalent to 38-40, stages at which the pronephros has fully differentiated and antibodies 3G8 and 4A6 can accurately recognise their antigens. In multiple experiments by stage 38-40 many of the sandwich cultures had disintegrated and only a few survivors would therefore be available to process to antibody staining.

5.6.2 Somites over-expressing the *dnwnt11b* cultured with intermediate mesoderm inside normal animal caps still form pronephric components.

Our results showed that somites over-expressing *dnwnt11b* cultured with intermediate mesoderm inside normal animal caps does not result in blocking the pronephric inductive activity that could be generated by *wnt11b* but instead generated pronephros tubules in an even higher frequency than the positive control itself or the animal caps over-expressing *wnt11b* cultured with intermediate mesoderm. The *dnwnt11b* activity was verified (Chapter 6) and we therefore know that the mRNA message was active in the somites over-expressing the *dnwnt11b*. One potential explanation for why *dnwnt11b* injected somites in Holtfreter sandwich cultures can generate pronephric tubule at such a high frequently could be that inhibition of the non-canonical *wnt* signalling could enable activation of the canonical *wnt* signalling pathway. Cell line studies have shown that elevation of intracellular Ca^{2+} which results from *wnt11* treatment led to inhibition of canonical

signalling (Maye et al., 2004). Hypothetically, it could be possible that in the *in vitro* Holtfreter sandwich model, inhibition of the non-canonical *wnt11b* actually enables subsequent activation of the canonical pathway and that other canonical *wnt* molecules are responsible for the formation of the pronephros in Holtfreter sandwich set up with *dnwnt11b* somites. This argument is supported by the fact that some canonical *wnt* molecules such as *wnt6* and *wnt8* can greatly induce pronephros formation in Holtfreter *in vitro* cultures.

5.6.3 Animal caps over-expressing *wnt* molecules and tissue formation.

Before setting up the Holtfreter *in vitro* cultures, the model system used as a pronephrogenesis assay, it was important to verify that animal caps over-expressing *wnt* molecules were not capable of inducing tissue formation on their own. Results showed that animal caps over-expressing *wnt* molecules cultured to stage 21 equivalent and analysed by RT-PCR for presence of renal, muscular and nervous system tissues, could not form any tissues except epidermis. However, contrary to this first result, it was also shown that two animal caps over-expressing *wnt11b* or *wnt6* and cultured on their own until stage 40 equivalent and analysed by antibody staining using the somite antibody 12/101, occasionally formed somitic muscle at low frequency. This could be due to contamination of mesodermal tissue in the animal cap dissections caused by the thickened animal caps which results following *wnt* injection, which would be dorsalised following exposure to *wnts*. Also, animal caps over-expressing *wnt* molecules should perhaps have been cultured to stage 40 equivalent, leaving time for tissue to develop, before being subject to RT-PCR analysis for the presence of tissue markers.

5.6.4 *wnt11b* and *sall1* might share the same pathway in pronephros formation.

In mouse metanephros formation, in the process of ureteric branching, *gdnf* and *ret* cooperate in a positive feedback loop to maintain an appropriate balance of *wnt11* (Majumdar et al., 2003). Also *gdnf-ret-wnt11* and s*all1* might be playing a role in ureteric bud formation (Vainio and Lin, 2002). It has been shown that *sall1* acts upstream of the transcription factor *Emx2* and influences epithelial signalling through *wnt6* and *wnt4* (Vainio and Lin, 2002). In *Xenopus* embryos, using Holtfreter

cultures, we have shown that animal caps over-expressing *wnt11b* (closely related to *wnt11*) cultured with intermediate mesoderm and analysed by RT-PCR for the presence of pronephric differentiation markers, showed expression of *sall1*. *sall1* is more strongly expressed in animal caps over-expressing 3ng of *wnt11* than in the animal caps over-expressing 2ng of *wnt11b* and cultured with intermediate mesoderm. This result suggests that *wnt11b* and *sall1* might act in the same pathway in pronephros formation in *in vitro* pronephrogenesis assay.

5.6.5 Direct and indirect formation of pronephric tubules in Holtfreter sandwich cultures over-expressing *wnt* molecules.

Before assaying the *wnt* sandwich cultures for the presence of pronephric tubules and somites, morphological analyses revealed that non-canonical *wnt* sandwich cultures looked morphologically similar to the positive control, but that the canonical *wnt* sandwich showed neural-like structure. *wnt6* sandwich cultures seemed to form eye-like structures, *wnt7b* sandwich cultures showed pigmented cells and *wnt8* sandwich cultures showed tail-like structure, possibly containing notochord structure. To confirm these observations, canonical *wnt* Holtfreter sandwich cultures would need to be subjected to *in situ* hybridization using specific nervous tissue restricted markers, such as the neural crest marker, *slug* (Mayor et al., 1995), the neural tube marker *pax3* (Bang and al., 1997) and the eye marker *pax6* (Hirsch and Harris, 1997) and analysed for fine histology by sectioning and microscopy. Interestingly, each canonical *wnt* molecule tested in this assay seems to initiate the development of a particular type of neural tissue suggesting that, first of all the mRNA messages were active and secondly that each canonical *wnt* molecule over-expressed in animal caps conferred specific more dorsal properties to the intermediate mesoderm, which subsequently secondarily induced differently patterned neural tissue. Induction of neural crest cells, the embryonic precursors of pigmented cells, could give rise to the observed pigmentation (Tucker et al., 1996). Eye formation, which constitutes a highly specialised extension of the brain arises from a sequential induction of three tissues, the neural tube, the neural crest and the epidermis, could result in a similar manner (Chow and Lang, 2001).

A close examination of the *wnt* Hotfreter sandwich cultures has revealed that the non-canonical *wnt11b* and *wnt11* and the canonical *wnt6* and *wnt8* confer to the intermediate mesoderm the potential to differentiate into pronephric tubules when these *wnt* molecules were over-expressed in the animal caps. However, the formation of pronephric tubules in such sandwich cultures seems to be happening by different mechanisms depending on the nature of the *wnt* molecule over-expressed in the animal caps. Immunohistological analyses have revealed that *wnt6* sandwich cultures contain a significant amount of somitic material, whereas, *wnt11b* and *wnt11* sandwich cultures contain none or only a small portion of somitic tissue.

The *wnt6* sandwich cultures analysed for the simultaneous presence of both pronephric and somitic tissues showed that presence of somitic tissue is strongly associated with the presence of pronephric tubules. This result suggests that *wnt6* can indirectly induce pronephric tubules formation in Holtfreter sandwich cultures, by firstly inducing somite formation, presumably by dorsalising the intermediate mesoderm, that will in turn induce pronephros formation. This idea is supported by studies in chick embryos reporting that *wnt6* is expressed in the epidermis that covers the segmental plate and all somite during their entire development and acts as an epithelialisation factor inducing somite formation and somite-derived progenitors cells to form muscle cells (Geetha-Loganathan et al., 2006, Schmidt et al., 2004, Schubert et al., 2002, Rodríguez-Niedenführ et al., 2003). It is also possible that during the process of animal caps dissection, some mesoderm contaminates the explant and that over-expression of *wnt6* in the epidermis is enough to dorsalised mesoderm into muscle. The animal caps over-expressing *wnt6* are thickened and that could explain why at low frequency two animal caps over-expressing *wnt6* and cultured on their own can form somitic tissue.

The presence of somitic tissue in *wnt8* Holtfreter sandwich cultures was not investigated in this study. However, it is highly suspected that the significant formation of pronephric tissue in such cultures would also result from an indirect mechanism involving somite formation that induces induce kidney formation. It was shown that *wnt8* is expressed in *Xenopus* embryos, after the mid-blastula transition, in the prospective notochord cells and that it is able to divert the fate of these cells along a more ventral fate perhaps directing these cells to differentiate as muscle rather than notochord (Christian and Moon, 1992).

However, the *wnt11b* and *wnt11* sandwich cultures seem to induce kidney formation in *in vitro* cultures in a different manner than the canonical *wnt* molecules. *wnt11b* sandwich cultures analysed for the simultaneous presence of somitic and pronephric tissues showed that presence of somitic tissues does not necessary involve the presence of pronephric tubules and visa-versa. This result suggests that *wnt11b* and also most certainly the closely related *wnt11* can directly signal to the unspecified intermediate mesoderm to form pronephric tubules in Holtfreter sandwich cultures. Somites forming in such cultures would result from misdissection and does not seem to generate enough material to influence pronephros formation.

To conclude, *wnt* Holtfreter sandwich cultures have demonstrated that both canonical and non-canonical *wnt* signalling molecules are sufficient for pronephric tubules formation *in vitro*. With this observation in place, we decided to investigate the role of *wnt11b* and *wnt6* directly in pronephros formation in *Xenopus* embryos.

Chapter 6 *In vivo* function of non-canonical *wnt11b* and *wnt11* molecules in *X. laevis* pronephros development.

6.1 Introduction.

In order to clarify the exact temporal and spatial expression pattern of the two *Xenopus wnt11* genes whole-mount *in situ* hybridization was carried out using gene specific *wnt11* and *wnt11b in situ* hybridization probes. Secondly, because *wnt11b* is expressed throughout pronephric development and in the anterior somites (Chapter 4) and is capable of inducing pronephros formation in Holtfreter sandwich cultures (Chapter 5), its role in pronephros formation was investigated by gain and loss-of-function analyses.

6.2 *wnt11b* and *wnt11*, two closely related genes, have distinct spatial expression patterns in *Xenopus* embryos.

wnt11b was shown to be expressed around the closing blastopore during the late gastrula stage and in somitic muscle and in the first branchial arch during the early tadpole stages (Ku and Melton, 1993). *wnt11* mRNA transcripts were first detected in early *Xenopus* tadpole, in the brain, the neural tube, the branchial arches, the somites and the heart (Garriock et al., 2005). Moreover, in accordance with the *Xenopus wnt11* embryonic expression pattern (Garriock et al., 2005), in mouse, *wnt11* transcripts are first detected in the heart tube and in the somites in embryos of 8.25 days of gestation (Christiansen et al., 1995). In addition, *Wnt11* is expressed at the tip of the ureteric bud throughout mouse renal development (Yu et al., 2004) and is believed to play a role in regulating ureteric branching during metanephros formation. (Majumdar et al., 2003). However, neither of these publications give information about the specificity of whole-mount *in situ* hybridization probes used for detecting *wnt11b* and *wnt11* mRNA transcripts in *Xenopus* embryos, raising the issue that the probes used may detect both genes (Ku and Melton, 1993 and Garriock et al, 2005). Thus, we decided to confirm the expression pattern of both genes by designing gene specific *in situ* hybridization probes.

	wnt11b (XELWNT11)	*wnt11* (AY695415)	*3'-wnt11b* PCR amplification
wnt11 (AY695415)	65.3		
3'-wnt11b PCR amplification	98.7	30.1	
5'-wnt11 PCR amplification	17.9	98.9	39.3

Table 6.1 showing the percentage of DNA sequence identity between the PCR amplified *wnt11b* 3' *in situ* probe, the PCR amplified *wnt11* 5' *in situ* probe and the respective whole gene sequences deposited in GenBank. Since *wnt11b* and *wnt11* are 65.3% identical in their full length DNA sequences, 3'-*wnt11b* and 5'-*wnt11* specific gene sequences were amplified by PCR in order to generate gene-specific *in situ* probes.

6.2.1 Generation of *X. laevis wnt11* and *wnt11b in situ* probes.

In order to examine the specific temporal and spatial expression of *wnt11* and *wnt11b* in whole *X. laevis* embryos and since the two genes are 65% identical in their full length DNA sequences, specific primers were designed in the unique untranslated region (UTR) of both genes. 3' and 5'UTR gene-specific *in situ* probes were prepared by subcloning 5'UTR region of *wnt11* and 3'UTR region of *wnt11b* gene into the appropriate expression vector (chapter 2). PCR amplification products of 3' and 5'UTR regions were sequenced and alignments confirmed the correct amplification of sequence. Table 6.1 shows the results of alignment expressed as a percentage of identity between the two DNA sequences. Our analysis confirmed that *wnt11b* and *wnt11* are 65% identical in their full length DNA sequence, which correlated with the published percentage. The *wnt11b* and *wnt11* PCR amplifications are 98.7% and 98.9% identical to their published DNA sequence respectively. However the two *wnt11b* and *wnt11* PCR amplifications are only 39.3% identical. Also, PCR amplification products are undoubtedly gene specific since *wnt11* PCR amplification product is only 17.9% identical to *wnt11b* gene and *wnt11b* PCR amplification product is only 30.1% identical to *wnt11* gene. All together, results of the alignment suggest that the cloned *wnt11* and *wnt11b* PCR amplifications are highly specific to their respective genes and should yield unambiguous *in situ* data.

6.2.2 Temporal and spatial expression of *wnt11* and *wnt11b* in *Xenopus* embryo.

The expression plasmids pGEMT-wnt11b and pGEMT-wnt11 PCR containing respectively *wnt11b* PCR amplification and *wnt11* PCR amplification were used as template for generating DIG labelled sense and antisense *in situ* hybridization probes. Figure 6.1 shows the temporal and spatial expression of *wnt11b* and *wnt11* at key stages of *X. laevis* development. *wnt11b* mRNA transcripts are first detected during gastrulation in a ring around the blastopore (Fig.6.1.a). As neurulation occurs, *wnt11b* starts to be expressed in the somitic muscles (Fig.6.1.b). From early tailbud stage onwards, *wnt11b* is strongly expressed in the somites and in the branchial arches (Fig.6.1.c and d). Around stage 26, *wnt11b* is also detected in the developing pronephros (Fig 6.1 c). In contrast, *wnt11* is not expressed in gastrulating embryos (Fig.6.1.e). *wnt11* starts to be expressed during neurulation in the neural tube

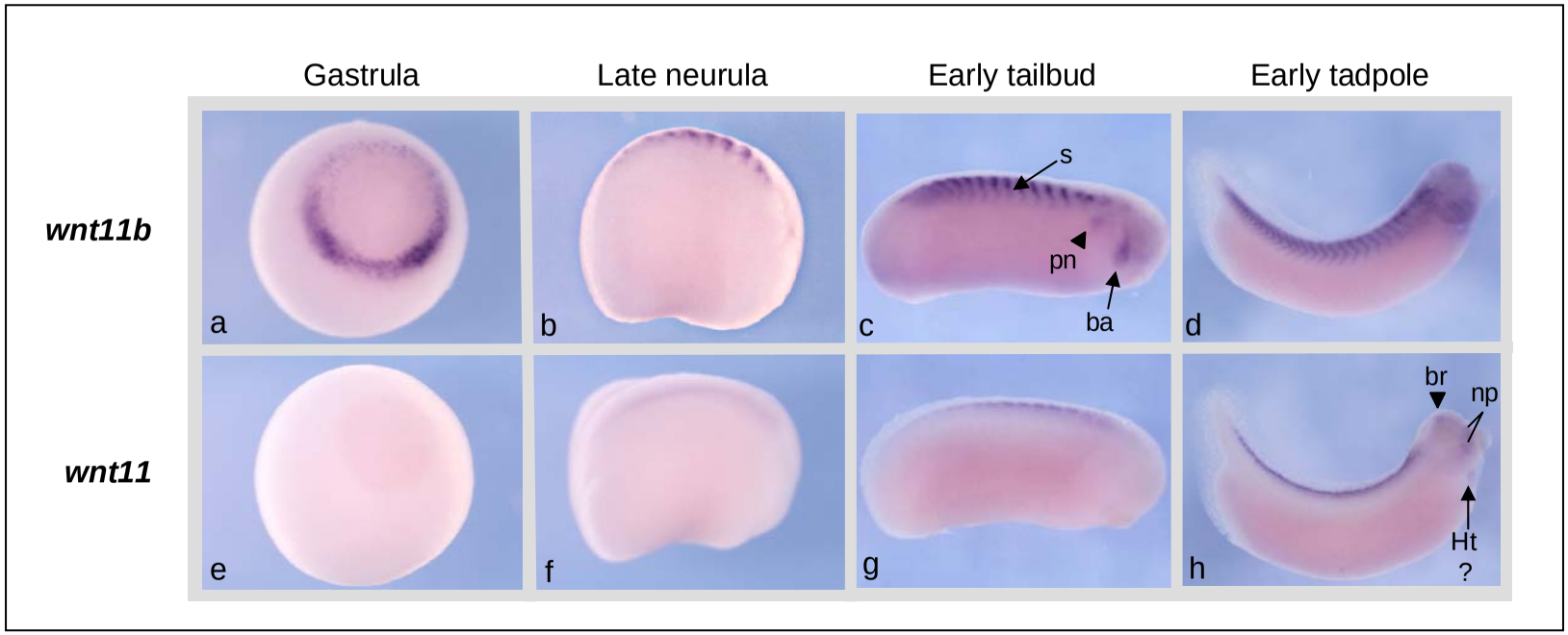

Key: s, somites. pn, pronephros. ba, branchial arches. br, brain. np, nasal placode. ht, heart.

Figure 6.1 The temporal and spatial expression of *wnt11b* and *wnt11* during *X. laevis* development. *In situ* hybridization analysis using the 3'UTR *wnt11b* and the 5'UTR *wnt11* DIG-labelled antisense probes in whole-mount *X. laevis* embryos shows that *wnt11b* is expressed around the blastopore during gastrulation (a), throughout the developing somites (b-d), in the branchial arches from early tailbud stage onwards (c and d) and is visible in the pronephros around stage 26 (c). However, *wnt11* is not expressed in *Xenopus* embryo at gastrula stage (e), but is expressed in the nervous system from late neurula onwards (f-h), at the very most dorsal tip of the somites from early tailbud stage onwards (g and h). At stage 33-34, *wnt11* is detected in the brain, the nasal placode and weakly in the heart (h).

(Fig.6.1.f) and remains strong until the early tadpole stage (Fig 6.1 g and h) until it also becomes visibly expressed at the most dorsal tip of the somites (Fig.6.1.g and h). At stage 33-34, *wnt11* is also detected in the brain, the nasal placodes and weakly in the heart (Fig 6.1 h).

In conclusion, the use of highly specific 3'UTR *wnt11b* and 5'UTR *wnt11 in situ* probes has allowed confirmation of the temporal and spatial expression pattern of both genes in *X. laevis* embryos. However, additionally to the published expression pattern (Ku and Melton, 1993) our result suggests that *wnt11b* is also expressed in the developing pronephros at stage 26. In contrast, to the published data (Garriock et al., 2005) *wnt11* is not expressed in the branchial arches and is visible at the very most dorsal tip of the somites in a very different expression pattern to that observed for *wnt11b*. I was next interested in investigating the role *in vivo* of *wnt11b* in pronephros formation.

6.3 *In vivo* function of *wnt11b* in *X. laevis* pronephros formation.

So far, *wnt11b* has been shown to be expressed in the developing pronephros and somites and to be capable of inducing pronephric tubules and glomus formation in *in vitro* explant cultures. Thus, we decided to investigate *in vivo* the functions of *wnt11b* in *Xenopus* pronephros formation by perturbing the normal function of *wnt11b* using various approaches such as over-expression, dominant-negative and antisense morpholinos knock-down.

6.3.1 Over-expression of *wnt11b* results in formation of abnormal pronephros.

6.3.1.1 Morphological phenotypes of *Xenopus* embryos over-expressing *wnt11b.*

During *Xenopus* development, *wnt11b* is necessarily required for normal gastrulation movements (Ku and Melton in 1993, Tada and Smith, 2000 and Smith et al., 2000). We examined the morphological consequences of microinjecting *wnt11b* mRNA into *X. laevis* embryos. 2.4ng of *wnt11b* mRNA message was injected into one-cell *Xenopus* embryos. Figure 6.2 shows the morphological defects of *wnt11b* injected embryos. Tadpoles were fixed at stage 41. Embryos injected with *GFP* mRNA alone showed

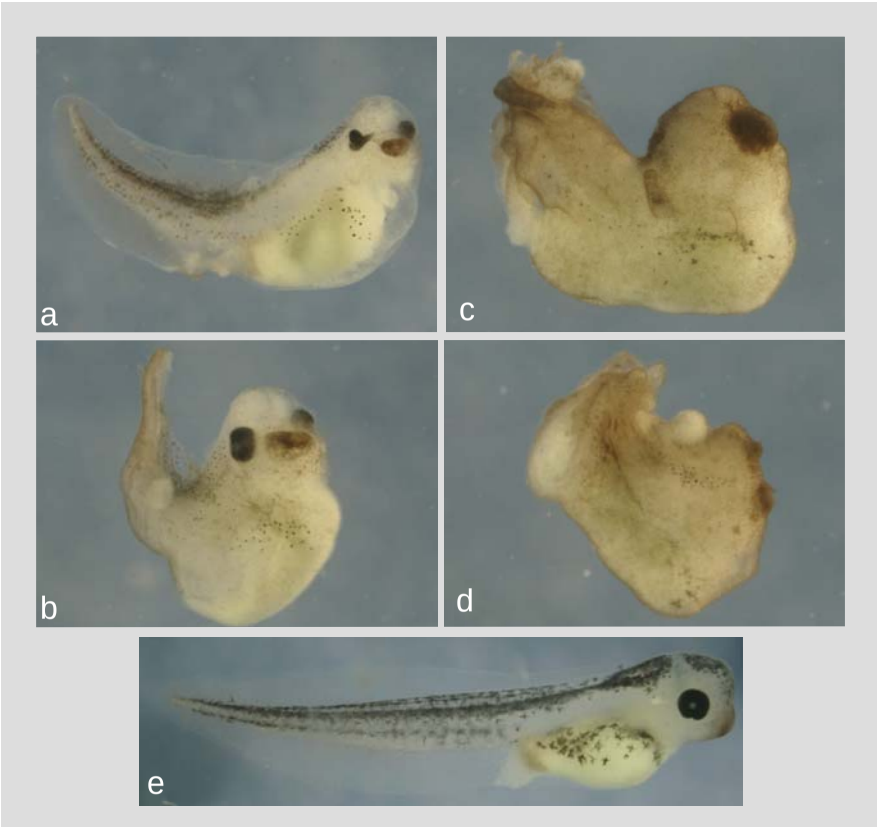

Figure 6.2 Morphological defects caused by *wnt11b* over-expression in *X. laevis* embryos. Embryos were injected with 2.4ng of *wnt11b* mRNA into the one-cell embryo and fixed at stage 41. Injection with *wnt11b* mRNA results in bent anterior-posterior axis (a), in short embryos with a relative lack of ventral structure (b), in embryos with an abnormal anterior-posterior axis and abnormal head formation (c) and in embryos with a completely disorganised axis, with lack of anterior and posterior structures (d), when compared to normal *GFP* injected embryos (e).

completely normal morphology and so provided the control experiment (Fig 6.2 a). Injection of 2.4ng of *wnt11b* resulted in a range of more or less severe abnormal morphology. Some embryos displayed a bent anterior-posterior axis accompanied with disturbances in the head and in the ventral structures (Fig 6.2 b). Some embryos had a very short anterior-posterior axis and were lacking substantial amounts of the ventral structures (Fig 6.2 c). Some other embryos over-expressing *wnt11b* showed very disturbed body axes and almost complete lack of head (Fig 6.2 d). The most severe phenotypes show completely abnormal embryos with no definable body axes and no clearly identifiable structures. In conclusion, injection of the *wnt11b* into the one-cell embryo causes dramatic defects on anterior-posterior axes, with subsequent lack of ventral structures. The causes of these abnormal phenotypes are almost certainly due to the role that *wnt11b* plays in regulating normal gastrulation movements during *Xenopus* development. Thus, restricting the over-expression of *wnt11b* into one blastomere during the early cleavage divisions reduces the effects on axis formation (data not shown), therefore resulting in much more normal embryos which could then be analysed for pronephros development.

6.3.1.2 Over-expression of *wnt11b* in V2 blastomere affects normal pronephros morphogenesis.

To investigate the role of *wnt11b* in pronephros development, 2.4ng of *wnt11b* mRNA was co-injected with cell-fate marker *GFP* into one ventral V2 blastomere of 8-cell stage embryo, with the aim of using the uninjected side as a contra-lateral control. Fate mapping of blastomeres at the 8-cell and 32-cell stages (see chapter 3, section 3.4 and figure 3.10 for the identification of the correct blastomere and delivery of specific mRNAs into presumptive kidney) allows us to identify the blastomere V2 of an 8-cell stage embryo to be the cell fated to contribute significantly to pronephric structures (Dale and Slack, 1987 and Moody, 1987). Embryos were left to develop until stage 40 and subjected to double antibody staining using the specific proximal tubule antibody 3G8 and the specific intermediate/distal tubules antibody 4A6 (Vize et al., 1995). Figure 6.3 shows that embryos injected with *GFP* mRNA alone develop normal tubule morphology on both the injected and uninjected sides (Fig 6.3 a-b) and therefore constitute the control experiment. Injection of 2.4ng of *wnt11b* results in reduction of pronephric

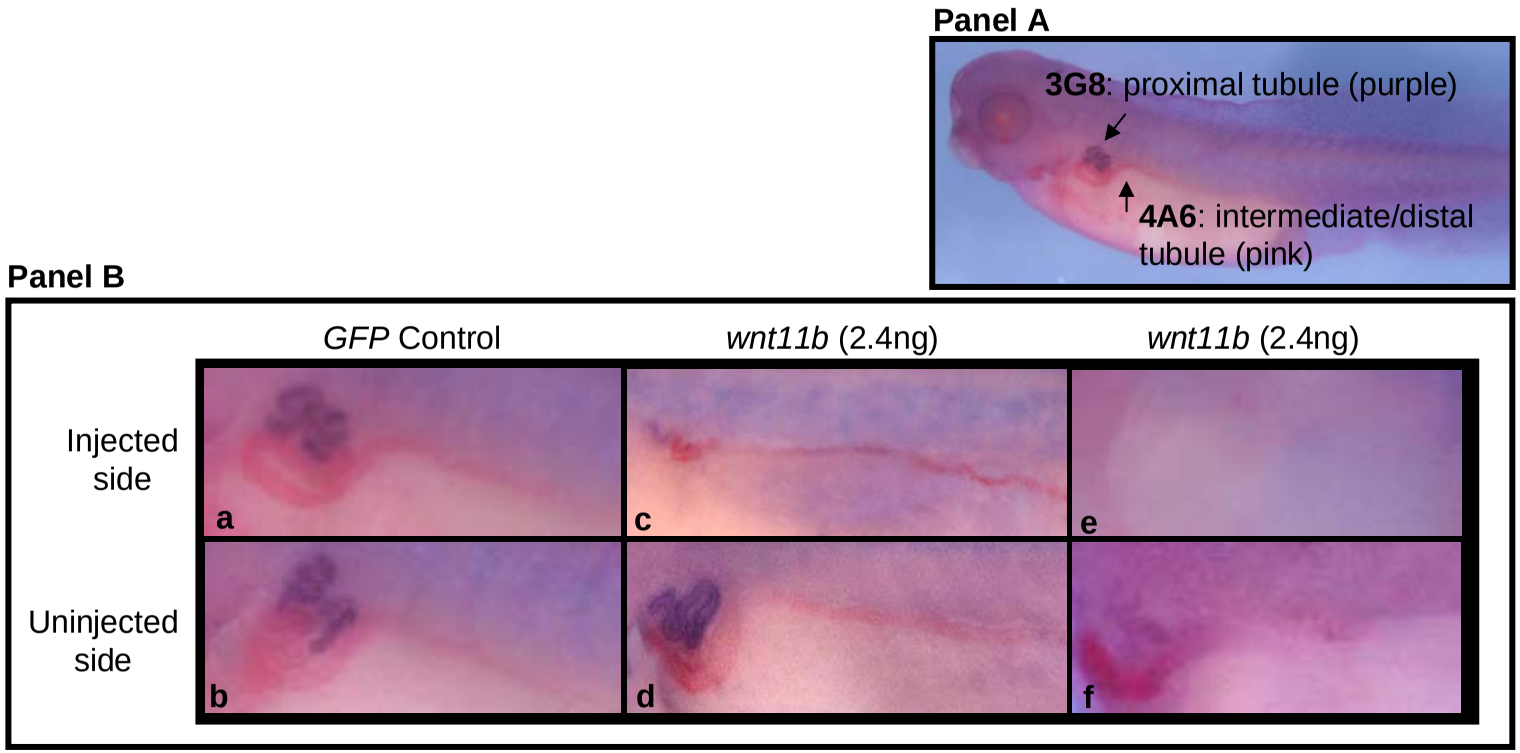

Figure 6.3 Embryos over-expressing *wnt11b* in one V2 blastomere develop abnormal pronephros. Embryos were injected in one V2 blastomere at the 8-cell stage with *GFP* mRNA and with or without 2.4ng of *wnt11b* mRNA. Embryos were left to develop until stage 40 before being assayed by immuno-staining. Panel A shows a normal *Xenopus* embryo at stage 40 stained in purple with the specific pronephric proximal tubules antibody, 3G8 and in pink with the specific pronephric intermediate/distal tubules antibody, 4A6. Panel B shows that injection of *GFP* mRNA alone does not disturb pronephric development (a-b). However, injection of 2.4ng of *wnt11b* mRNA can result in a reduction of pronephric tubules on the injected side (c) with normal pronephros morphology on the uninjected side (d). In extreme cases, *wnt11b* over-expression can result in an absence of pronephric tubules on the injected side (e) and reduced tubules on the uninjected side (d).

tubules on the injected side (Fig 6.3 c) and in normal tubule morphology on the uninjected side (Fig 6.3 d). The major pronephros phenotype resulting from injection of 2.4ng of *wnt11b* mRNA in V2 blastomere showed an absence of tubules on the injected side (Fig 6.3 e) and a reduction of tubules on the uninjected side (Fig 6.3 f), with intermediate/distal tubules looking shorter and straighter. A possible reason for abnormal pronephros formation on the uninjected side, is that most of the embryos injected with 2.4ng or even 1.6ng of *wnt11b* mRNA in one V2 blastomere developed abnormally showing abnormal anterior-posterior axis formation (data not shown). Organogenesis is affected by the embryo's morphology, which may explain why the pronephros developed abnormally on both the injected and uninjected sides. Less than 20% (data not shown) of the embryos injected with 1.6 and 2.4ng of *wnt11b* succeeded in forming a completely normal body axis and consequently no numerical data are presented for this experiment.

In order to analyse the effect of *wnt11b* on early pronephros differentiation, embryos were injected with 1.6ng of *wnt11b* mRNA in one V2 blastomere and left to develop until stage 28. Embryos were then subjected to *in situ* hybridization for pronephros phenotype using the pronephric markers *lhx1* and *pax8*. As described previously, some injected embryos developed abnormal anterior-posterior axis formation and showed abnormal pronephric anlagen on the uninjected side. However, the small number of embryos developing with a normal body axis, showed a reduction in the forming pronephric anlagen only on the injected side.

To conclude, the few embryos injected with *wnt11b* mRNA in V2 blastomere which showed normal anterior-posterior axis formation, developed reduced pronephric anlagen at stage 28 and reduced pronephric tubules at stage 40 on the injected side, suggesting that mis-expression of *wnt11b* deregulates normal pronephrogenesis, affecting pronephros terminal differentiation and possibly earlier development of the anlagen. With the aim of reducing the gross morphological defects caused by over-expression of *wnt11b* in the V2 blastomere, mRNA was injected in the animal pole of one cell of two-cell stage *X. laevis* embryos, which will later in development give rise to the epidermis, some of which will overlay the pronephric region.

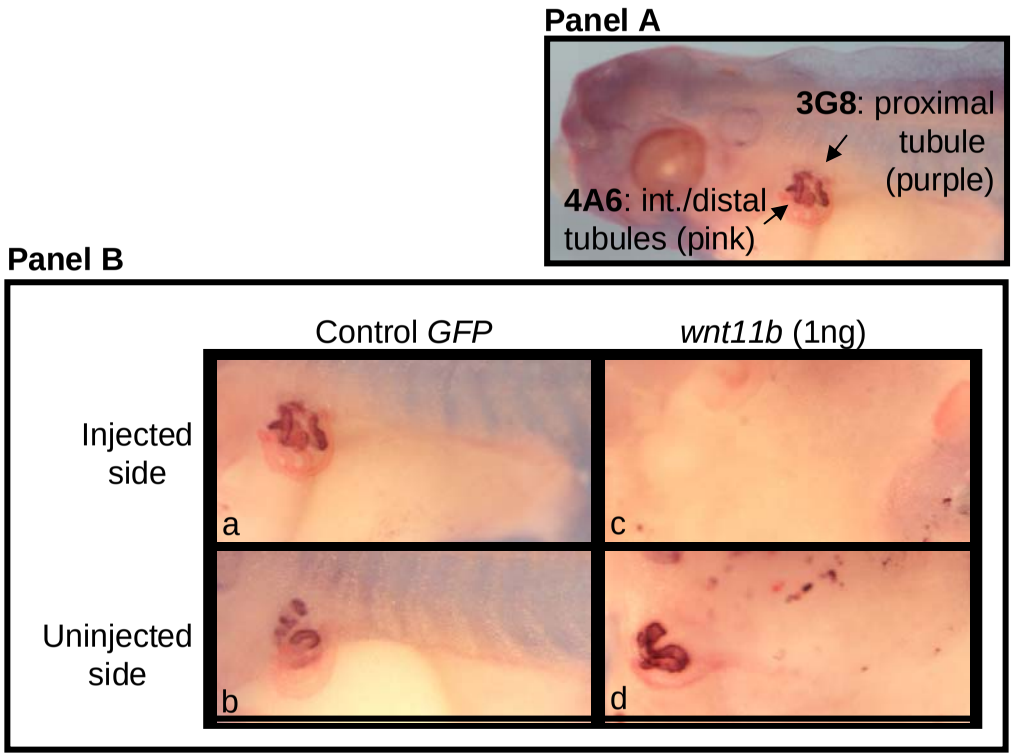

Figure 6.4 Embryos over-expressing *wnt11b* in the epidermis develop an abnormal pronephros. Embryos were injected in the animal pole of one blastomere at the 2-cell stage with *GFP* alone or with *GFP* and 1ng of *wnt11b* mRNA. Embryos were left to develop until stage 42 before being assayed for immuno-staining. Panel A shows a normal *Xenopus* embryos at stage 42 stained in purple with the specific pronephric proximal tubules antibody, 3G8 and in pink with the specific pronephric intermediate/distal tubules antibody, 4A6. Panel B shows that injection of *GFP* mRNA alone does not disturb pronephric development (a-b). However, injection of 1ng of *wnt11b* mRNA results in inhibition of kidney formation on the injected side (c) and in fairly normal pronephros morphology on the uninjected side (d).

Figure 6.5 Numerical and graphical representation of the pronephros phenotype in *X. laevis* embryos over-expressing 1ng of *wnt11b* mRNA. Embryos were injected into the animal pole of one cell at the 2-cell stage and left to develop until stage 42 before being analysed by antibody staining using the specific proximal tubule antibody 3G8 and the specific intermediate and distal tubules antibody 4A6.

		Embryo Morphology		
mRNA injected		Normal	Bent	Short axis
GFP	n= 33	33	0	0
	%	**100**	**0**	**0**
wnt11b (1ng)	n= 46	28	17	1
	%	**61**	**37**	**2**

Table 6.5.1 Morphology of embryos over-expressing 1ng of *wnt11b* mRNA in the epidermis and analysed for pronephros phenotype.

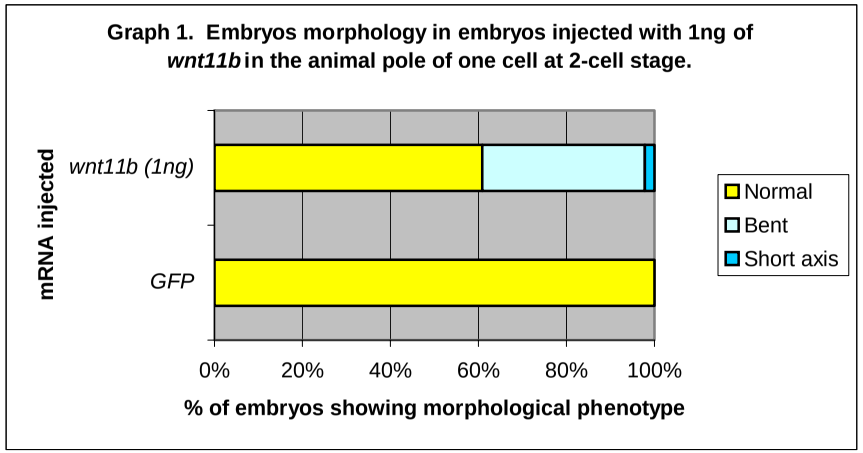

Graph 1 shows the morphology of embryos over-expressing 1ng of *wnt11b* mRNA in the epidermis and analysed for pronephros phenotype.

mRNA injected		Proximal tubule morphology: Injected side Normal	Reduced	Enlarged	Absent	Uninjected side Normal	Intermediate/distal tubule morphology: Injected side Normal	Reduced	Absent	Uninjected side Normal
GFP	n= 33	32	1	0	0	33	32	1	0	33
	%	**97**	**3**	**0**	**0**	**100**	**97**	**3**	**0**	**100**
wnt11b (1ng)	n= 46	0	16	4	26	46	2	19	25	46
	%	**0**	**35**	**9**	**57**	**100**	**4**	**41**	**54**	**100**

Table 6.5.2 Number and percentage of embryos showing pronephros phenotype in embryos injected in the animal pole of one cell at 2-cell stage with 1ng of *wnt11b* mRNA.

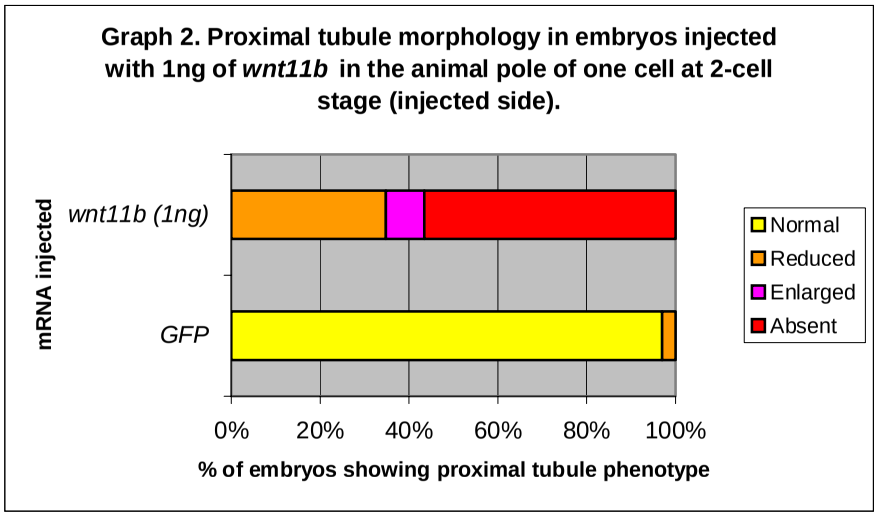

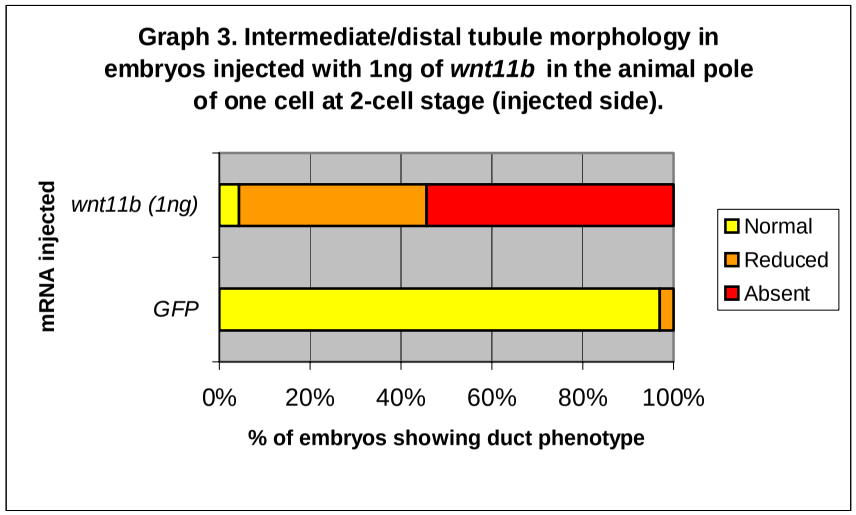

Graph 2 and 3 show the proximal tubule and the intermediate/distal tubules phenotype in embryos injected in the animal pole of one cell at 2-cell stage with 1ng of *wnt11b* mRNA.

6.3.1.3. Over-expression of *wnt11b* in the epidermis leads to abnormal kidney formation.

Injection of *wnt11b* mRNA in the V2 blastomere, often results in embryos developing with abnormal anterior-posterior axis and therefore with an abnormal pronephros on both the injected and the uninjected sides. As a consequence, it is difficult to interpret the result of the effects of *wnt11b* over-expression on kidney development. However, as it was shown in chapter 3, section 3.4, signalling from epidermis overlying the pronephric region can influence the pronephros development. Thus, 1ng of *wnt11b* mRNA was co-injected with *GFP* mRNA in the animal pole of one cell at the 2-cell stage embryo, which would later on in development give rise to epidermis some of which covers the pronephric region. Embryos were left to develop until stage 42 before being assayed for immuno-staining. Figure 6.4, panel A shows a normal *Xenopus* embryos at stage 42 stained in purple with the specific pronephric proximal tubules antibody, 3G8 and in pink with the specific pronephric intermediate/distal tubules antibody, 4A6. Figure 6.4, panel B shows that injection of *GFP* mRNA alone does not disturb the pronephros development (Fig 6.4 a-b). However, injection of 1ng of *wnt11b* mRNA results in inhibition of kidney formation on the injected side (Fig 6.4 c) and in fairly normal pronephric proximal, intermediate and distal tubules morphology on the uninjected side (Fig 6.4 d). Figure 6.5, table 6.5.1 and graph 1 show that 61% of the embryos analysed for pronephros morphology, when injected in the animal pole of one cell at 2-cell stage, developed normal body morphology. There was still a significant percentage (37%) of embryos developing with a distorted anterior-posterior axis, however, those embryos showed normal pronephros morphology on the uninjected side, and the ones that did not were rejected from this study. Only 2% of the embryos exhibited a short anterior-posterior axis, but again, showed normal pronephros morphology on the uninjected side. Figure 6.5, table 6.5.2 and graph 2 and 3 show that injection of *GFP* mRNA alone does not affect the normal development of the pronephric tubules (97% of the embryos developed normal pronephros on the injected side and 100% of the embryos showed normal pronephros morphology on the uninjected side). More than half of the embryos injected with 1ng of *wnt11b* mRNA in the animal pole of one cell at 2-cell stage did not form any proximal tubules or intermediate/distal tubules (57% and 54% respectively), while the pronephros on the uninjected side developed normally.

35% and 41% of the embryos over-expressing 1ng of *wnt11b* developed reduced pronephric proximal and intermediate/distal tubules respectively, 9% showed abnormal enlarged proximal tubule and 4% developed normal intermediate/distal tubules on the injected side. In conclusion, 1ng of *wnt11b* mRNA over-expressed in the epidermis of one side of the embryo affects pronephros formation and results show that mainly over-expression of *wnt11b* inhibits the pronephros formation. With the aim of exploring further the function of *wnt11b* in *Xenopus* pronephros development, we decided to inhibit *wnt11b* gene function by using a dominant-negative form of the gene.

6.3.2 Inhibition of *wnt11b* using a dominant-negative construct (*dnwnt11b*) leads to abnormal kidney development in *X. laevis* embryos.

6.3.2.1 *dnwnt11b* specificity and its biological activity.

In 2000, Tada and Smith investigated the function of *wnt11b* during *Xenopus* gastrulation movements. They constructed a C-terminally truncated form of the protein, dnwnt11b, (according to new nomenclature, Garriock et al., 2007) which might be expected to act in a dominant-negative fashion. Figure 6.6 shows a schematic representation of wild-type *wnt11b* and *dnwnt11b* which carries a C-terminal cystein region deletion. It was important to demonstrate that *dnwnt11b* mRNA is active in *X. laevis* embryos. Figure 6.7 shows that *dnwnt11b* can inhibit elongation in animal caps treated with activin. Animal pole explants previously injected with gradient concentration of *dnwnt11b* mRNA (0ng to 4.5ng) were cultured in Barth X buffer alone and in Barth X buffer containing 5 ng/ml of activin. Animal cap cultured in Barth X buffer alone stay perfectly round (Fig 6.7 a, c, e, g). However, normal animal caps elongate under the influence of the growth factor activin (Fig 6.7 b), and therefore constitute the positive control for this experiment. Injection of 1.1ng to 2.25ng of *dnwnt11b* mRNA reduces elongation of animal caps when compared to the control experiment (Fig 6.7 d, and f with b). Injection of 4.5ng of *dnwnt11b* results in inhibition of animal caps elongation (Fig 6.7 h). In conclusion, *dnwnt11b* prevents activin-induced elongation of isolated animal caps confirming that *dnwnt11b* mRNA is active in *Xenopus* embryos.

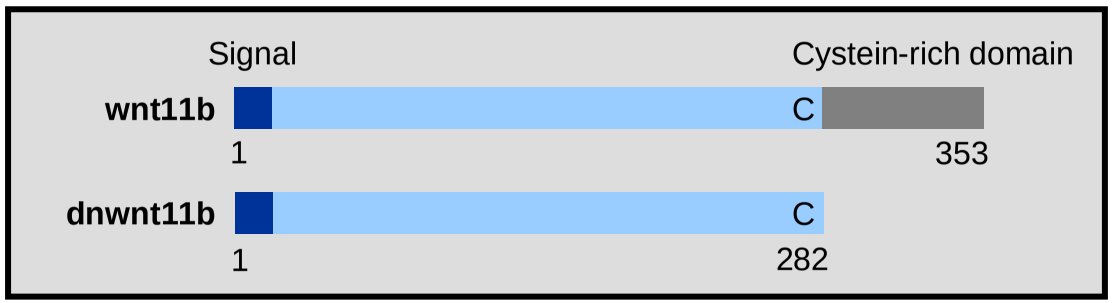

Figure 6.6 Construction of dominant-negative *wnt11b* (*dnwnt11b*), according to Smith at al., 2000. Deletion of the cystein-rich domain results in a dominantly active molecule, by a yet unknown mechanism.

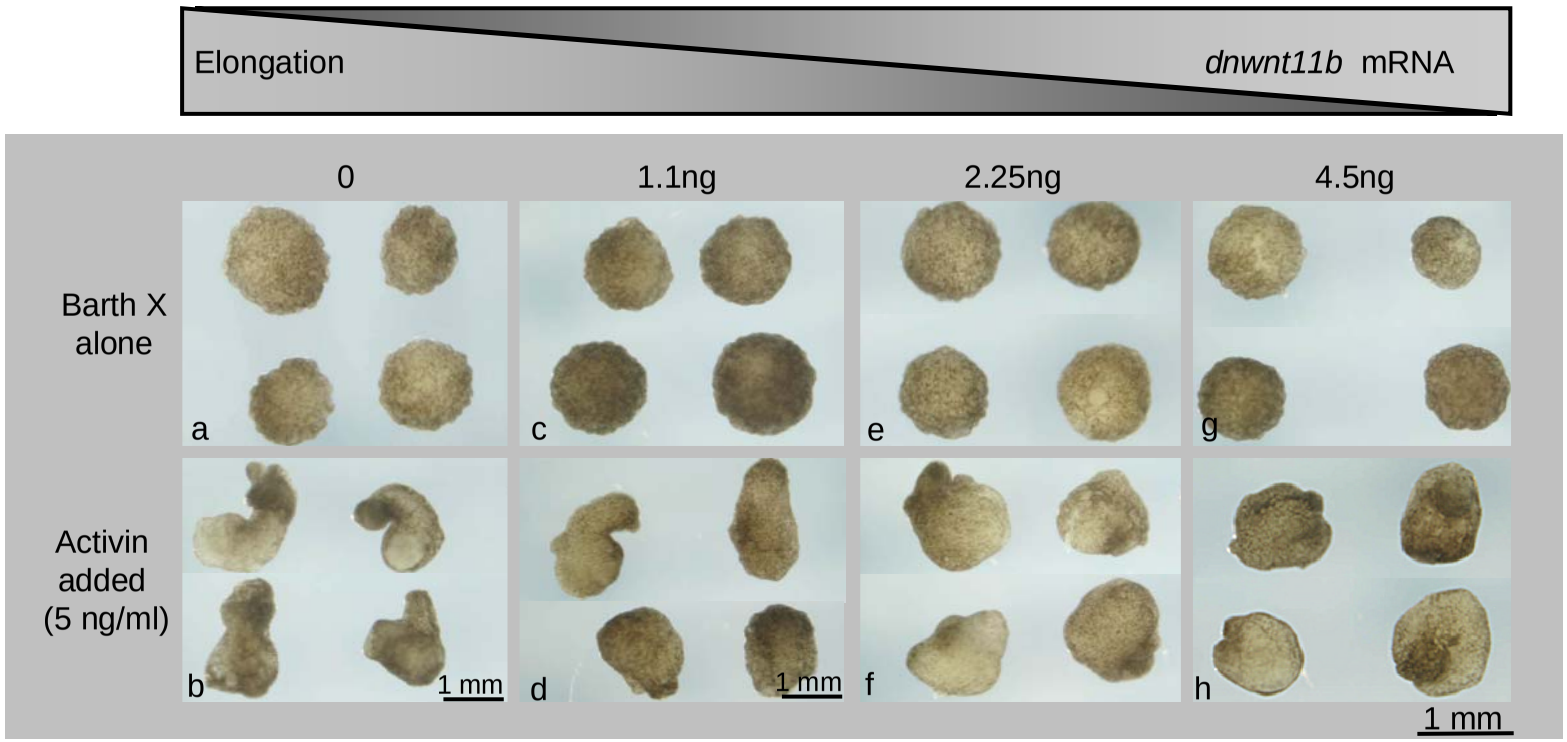

Figure 6.7 *dnwnt11b* can inhibit elongation in animal caps treated with activin. One-cell stage *X. laevis* embryos were injected with 1.1ng to 4.5ng of *dnwnt11b* mRNA. After over-night incubation, animal caps were dissected from normal embryos and from embryos injected with *dnwnt11b* mRNA. Half of the dissected animal caps were cultured for 24 hours in full strength Barth X and half were cultured in the presence of 5ng/ml of activin. Animal caps over-expressing 1.1 to 4.5ng of *dnwnt11b* cultured in Barth X alone look round (c, e and g) and are morphologically identical to the normal animal caps (a). On another hand, normal animal caps cultured under the influence of growth factor activin showed elongation (b). However, when 1.1 to 2.25ng of *dnwnt11b* mRNA was previously injected, the elongation of animal caps is reduced (d, f). Injection of 4.5ng of *dn-wnt11b* results in inhibition of animal caps elongation (h).

6.3.2.2 Morphological phenotypes of *X. laevis* embryos over-expressing *dnwnt11b.*

We first examined the morphological defects caused by the inhibition of *wnt11b* using a dominant-negative *wnt11b* (*dnwnt11b*) in *X. laevis* embryos. 1ng of *dnwnt11b* mRNA was injected into the one-cell stage embryo and embryos were left to develop until late tailbud, stage 28. Figure 6.8 shows the *dnwnt11b* morphological phenotypes. Injection of *GFP* mRNA alone results in normal morphology embryos (Fig 6.8 a). Nevertheless, injection of 1ng of *dnwnt11b* results in abnormal embryo morphology. Embryos generally show a delay in development and the anterior-posterior axis is disturbed, tadpoles are lacking posterior structure (Fig 6.8 b), also, embryos display a short anterior-posterior axis and exhibit abnormal enlarged cement glands (Fig 6.8 c).
To conclude, results confirm the study of Smith et al., (2000) showing that *dnwnt11b* blocks the function of *wnt11b* during *Xenopus* gastrulation by disturbing the normal convergent extension movement. We were next interested in exploring the effects of *wnt11b* inhibition in pronephros development using the *dnwnt11b.*

6.3.2.3 Inhibition of *wnt11* using the *dnwnt11b* affects *X. laevis* pronephros morphogenesis during terminal differentiation.

With the aim of asking whether inhibition of *wnt11* signalling affects pronephros morphogenesis, 1 to 1.5ng of the *dnwnt11b* mRNA was injected into one V2 ventral blastomere of 8-cell stage *X. laevis* embryos. Embryos were left to develop until stage 41 when pronephric tubules have fully differentiated. Then, embryos were subjected to 3G8 and 4A6 whole-mount double antibody staining and scored for pronephric proximal and intermediate/distal tubules morphology respectively. Figure 6.9 shows that *dnwnt11b* affects normal *X. laevis* pronephros development. Figure 6.9, panel A shows a normal *Xenopus* embryo at stage 40 stained in purple with the specific pronephric proximal tubules antibody, 3G8 and in pink with the specific pronephric intermediate/distal tubules antibody, 4A6. Figure 6.9, panel B shows that injection of 1ng of *GFP* mRNA alone results in normal pronephric tubules morphology on both the injected and the uninjected sides (Fig 6.9 a, b) and therefore constitutes the control experiment. However, injection of 1.5ng of *dnwnt11b* results, on the injected side, in drastic reduction of pronephric proximal and

Figure 6.8 Morphology of *X. laevis* embryos resulting from *dnwnt11b* over-expression. Embryos were injected with 1ng of the *dnwnt11b* into one-cell stage *Xenopus* embryos. Embryos were left to develop until stage 28. Injection of *GFP* mRNA alone results in normal embryo morphology (a). However, injection with 1ng of *dnwnt11b* mRNA results in embryos lacking posterior structures (b), and in embryos with a shortened anterior-posterior axis and enlarged cement gland (arrow) (c).

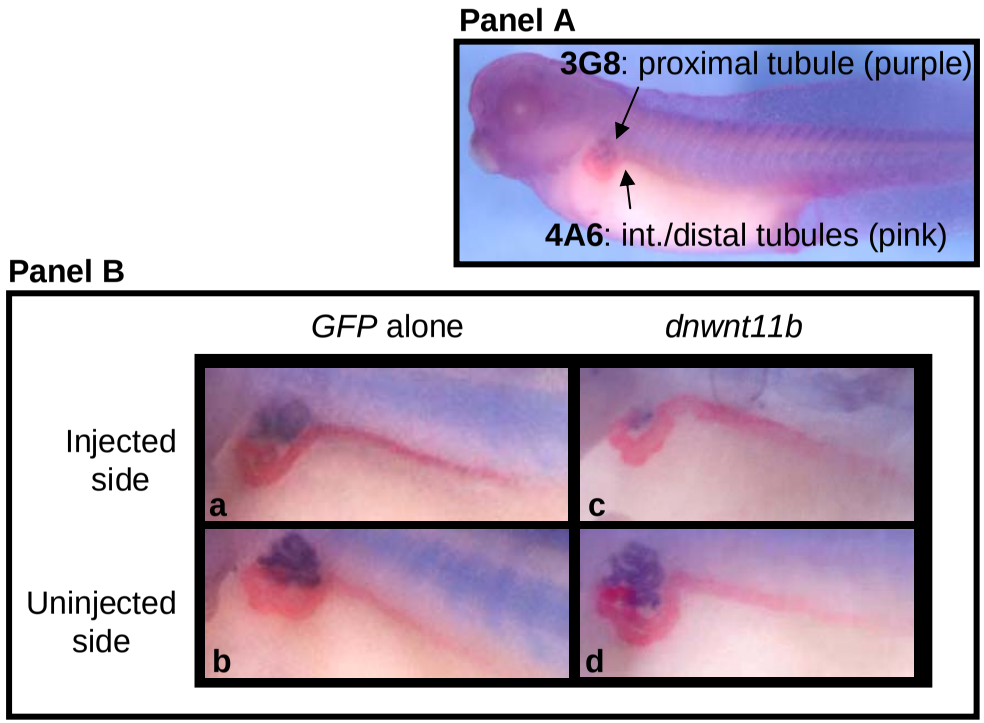

Figure 6.9 Inhibition of *wnt11b* using the *dnwnt11b* affects normal *Xenopus* pronephros formation. Embryos were injected in one V2 blastomere at the 8-cell stage with *GFP* mRNA and with or without 1.5ng of the *dnwnt11b* mRNA. Embryos were left to develop until stage 40 before being assayed to immuno-staining. Panel A shows a normal *GFP Xenopus* embryo at stage 40 stained in purple with the specific pronephric proximal tubules antibody, 3G8 and in pink with the specific pronephric intermediate/distal tubules antibody, 4A6. Panel B shows that injection of *GFP* mRNA alone results in normal tubules morphology on both the injected and uninjected sides (a, b). However, injection of the *dnwnt11b* results in reduction of the pronephric tubule on the injected side (c) and in normal tubule on the uninjected side (d).

Figure 6.10 Numerical and graphical representation of the pronephros phenotype in *X. laevis* embryos over-expressing 1 to 1.5ng of *dnwnt11b* mRNA. Embryos were injected into one V2 ventral blastomere at the 8-cell stage embryo and left to develop until stage 40 before being analysed by antibody staining using the specific proximal tubule antibody 3G8 and the specific intermediate and distal tubule antibody 4A6.

		Proximal tubule morphology				**Intermediate/distal tubules morphology**			
		Injected side			Uninjected side	Injected side			Uninjected side
mRNA injected		Normal	Reduced	Absent	Normal	Normal	Reduced	Absent	Normal
GFP (1ng)	n=15	15	0	0	15	15	0	0	15
	%	**100**	**0**	**0**	**100**	**100**	**0**	**0**	**100**
dnwnt11b (1ng)	n=22	10	11	1	22	8	14	0	22
	%	**45**	**50**	**5**	**100**	**36**	**64**	**0**	**100**
dnwnt11b (1.5ng)	n=34	13	12	9	34	17	12	5	34
	%	**38**	**35**	**26**	**100**	**50**	**35**	**15**	**100**

Table 6.10.1 Number and percentage of embryos showing pronephros phenotype in embryos injected in one V2 ventral blastomere at the 8-cell stage with1 to 1.5ng of *dnwnt11b* mRNA.

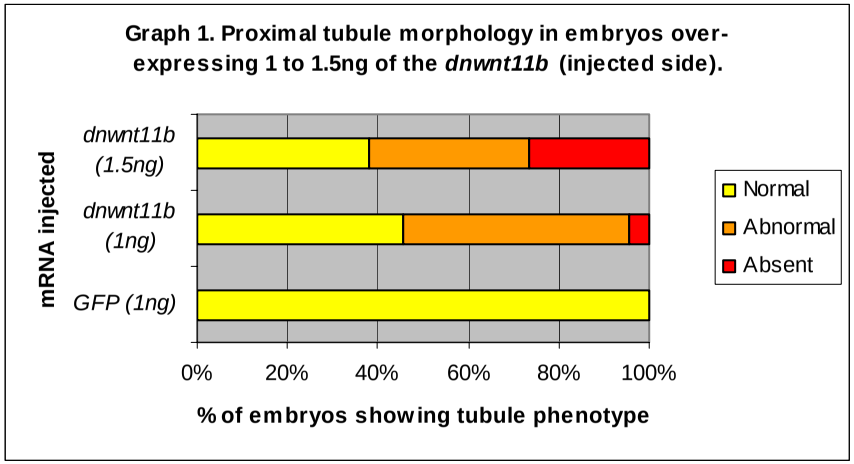

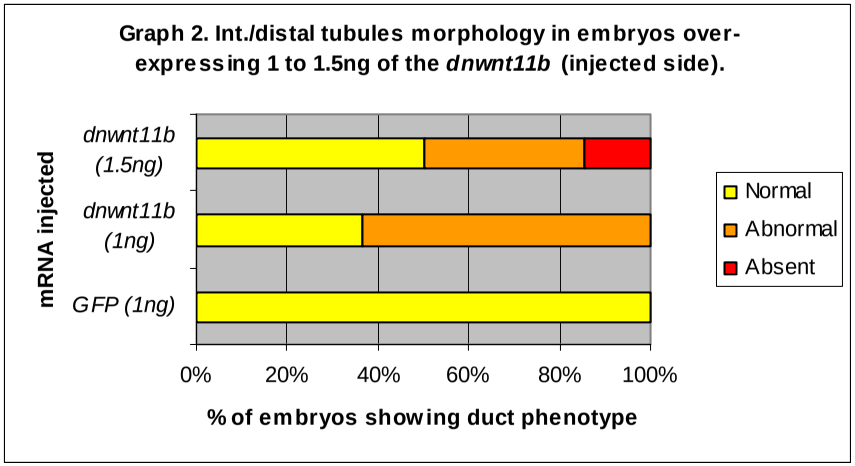

Graph 1 and 2 show the proximal tubule and the intermediate/ distal tubules phenotype in embryos injected in one V2 blastomere of 8-cell stage with 1 to 1.5ng of *dnwnt11b* mRNA.

intermediate/distal tubules structure (Fig 6.9 c), while the pronephros on the uninjected side is not affected (Fig 6.9 d).

Figure 6.10, table 6.10.1, graph 1 and 2 show the numerical and graphical representation of the pronephros phenotype in *X. laevis* embryos injected in V2 ventral blastomere with 1 to 1.5ng of the *dnwnt11b* mRNA. In this experiment, all embryos showed normal morphology and only the ones showing normal tubule morphology on the uninjected side were scored for tubule phenotype on the injected side. Injection of *GPF* mRNA alone results in 100% of embryos forming normal tubules on both the injected and the uninjected sides. 45% and 36% of embryos injected with 1ng of the *dnwnt11b* mRNA in V2 blastomere also formed normal proximal and intermediate/distal tubules respectively. However, approximately half of such embryos showed reduced tubules. A small percentage (5%) of embryos did not form any proximal tubule at all. A large proportion of the embryos injected with 1.5ng of *dnwnt11b* showed normal tubule morphology. However, 26% and 15% of such embryos showed an absence of the pronephric proximal and intermediate/distal tubules respectively. 35% of the embryos over-expressing 1.5ng of the *dnwnt11b* developed reduced tubules.

In conclusion, inhibition of *wnt11b* function by injecting 1 to 1.5ng of the *dnwnt11b* in V2 blastomere mildly affects the pronephros formation. A relatively large proportion of injected embryos formed completely normal pronephric tubules, a similar proportion resulted in reduced pronephric tubules and in extreme case in an absence of tubule formation. This last phenotype is a dose-dependent effect as there were more embryos lacking pronephric tubules structures as the concentration of message injected was increased.

6.3.2.4. Inhibition of *wnt11b* using the *dnwnt11b* have an effect on *X. laevis* pronephros morphogenesis during early differentiation.

In order to confirm the previous result showing that the *dnwnt11b* over-expressed in one V2 blastomere disturbs the normal development of the pronephros, embryos were assayed for whole mount *in situ* hybridization using the pronephric markers *pax8* and *lhx1*. *lhx1*, a Lim homeodomain protein has been shown to act as a *pax8* cofactor. The interaction between *pax8* and *lhx1* constitutes a key early step in the establishment of the pronephric primordium (Carroll and Vize, 1999). Whole-mount

in situ hybridization on normal *Xenopus* embryos has revealed that both *pax8* and *lhx1* are detected from late gastrula (stage 12.5) to early tailbud (stage 28) first in pronephric precursors and later as development occurs, in the differentiated pronephric tubules. This suggests that *lhx1* and *pax8* are the markers of choice to detect the earliest morphological defects caused by modulation of gene expression. Embryos were injected with 1.5ng of the *dnwnt11b* mRNA into one V2 ventral blastomere of 8-cell stage *X. laevis* embryos and allowed to develop until early tadpole stage, stage 26. Pronephric anlagen morphology was analysed using antisense DIG-labelled *lhx1* and *pax8 in situ* probes. Figure 6.11, table 6.11.1 and graphs 1 and 2 show the number and the percentage of embryos injected with 1.5ng of the *dnwnt11b* in one V2 blastomere and scored for the pronephric anlagen morphology on the injected side when the embryo morphology and the pronephric anlagen on the uninjected side were normal. Results show that injection of *GPF* mRNA alone does not disturb the normal formation of the pronephric anlagen. *In situ* hybridization using the pronephric marker *lhx1* show that 29% of the embryos over-expressing the *dnwnt11b* developed normal pronephric anlagen, 38% showed reduced pronephric anlagen and 33% showed enlarged pronephric tissue. Similarly, *in situ* hybridization using the pronephric marker *pax8* showed that 19% of the embryos exhibited normal pronephros morphology, 50% formed reduced pronephric anlagen and 31% showed enlarged pronephric anlagen.

In conclusion, both early pronephric markers, *lhx1* and *pax8* give essentially the same results regarding the *dnwnt11b* pronephric anlagen phenotype. Inhibition of *wnt11b* function seems to moderately affect the normal formation of the pronephric anlagen since only 20% to 30% of embryos over-expressing the *dnwnt11b* targeted in the pronephric region formed completely normal pronephric anlagen shape. The rest of the embryos showed reduced or completely disorganised pronephric anlagen. In no cases did embryos develop without a pronephric anlagen. In order to complete this study, morphology of the third pronephric component, the glomus, was analysed when embryos are injected with the *dnwnt11b* in one V2 blastomere at the 8-cell stage.

Figure 6.11 Numerical and graphical representation of the pronephros phenotype in *X. laevis* embryos over-expressing 1.5ng of *dnwnt11b* mRNA and analysed by *in situ* hybridization. Embryos were injected into one V2 ventral blastomere at the 8-cell stage embryo and left to develop until stage 26 before being analysed by whole mount *in situ* hybridization using the pronephric markers *lhx1* and *pax8*.

			Pronephric anlagen morphology			
			Injected side			Uninjected side
Pronephric marker	mRNA injected		Normal	Reduced	Enlarged	Normal
lhx1	*GFP* (1ng)	n= 25	23	0	2	25
		%	**92**	**0**	**8**	**100**
	dnwnt11b (1.5ng)	n= 21	6	8	7	21
		%	**29**	**38**	**33**	**100**
pax8	*GFP* (1ng)	n= 25	25	0	0	25
		%	**100**	**0**	**0**	**100**
	dnwnt11b (1.5ng)	n= 16	3	8	5	16
		%	**19**	**50**	**31**	**100**

Table 6.11.1 Number and percentage of embryos showing pronephros phenotype in embryos injected in one V2 ventral blastomere at the 8-cell stage with 1.5ng of *dnwnt11b* mRNA and analysed by *in situ* hybridization with the pronephric markers *lhx1* and *pax8*.

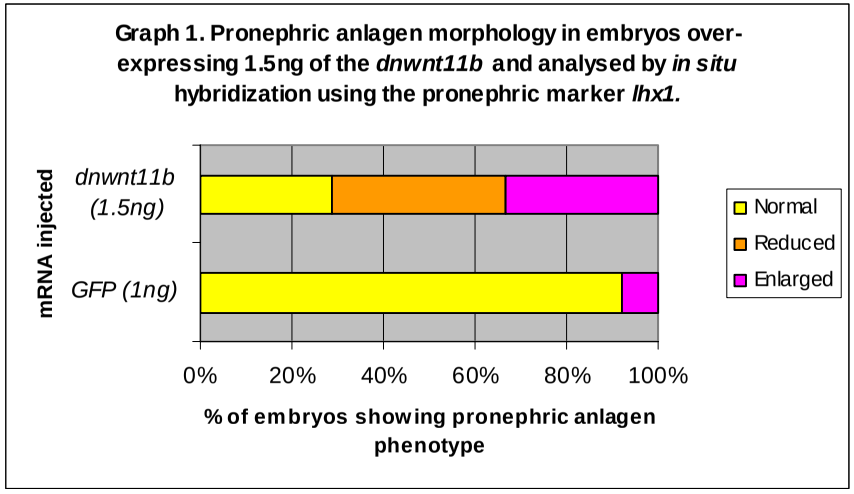

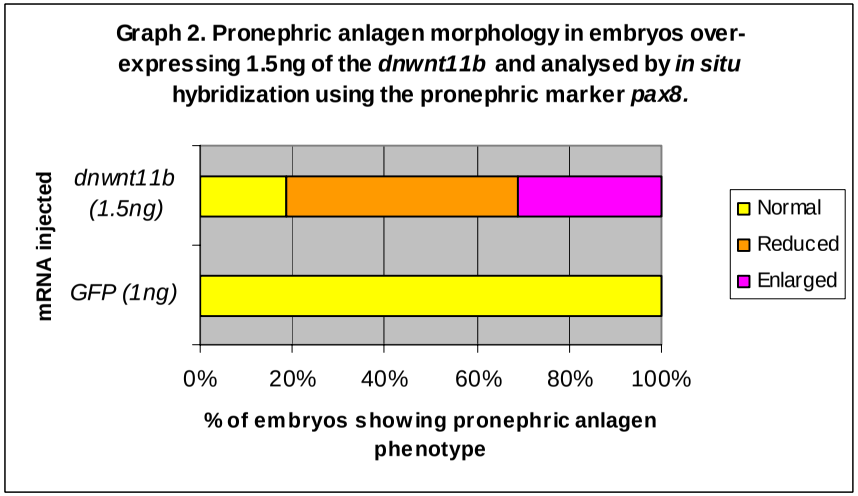

Graphs 1 and 2 show the pronephric anlagen morphology in embryos over-expressing 1.5ng of the *dnwnt11b* and analysed by *in situ* hybridization using the pronephric markers *lhx1* and *pax8* respectively.

6.3.2.5 Inhibition of *wnt11b* using the *dnwnt11b* have an effect on pronephric glomus formation.

Embryos were injected in one V2 ventral blastomere at the 8-cell stage with 1 to 1.5ng of the *dnwnt11b* mRNA. Embryos were left to develop until stage 35 before being assayed for *in situ* hybridization using the specific glomus marker *Wilm's Tumor-1 gene (wt1)*. Figure 6.12 shows that injection of *GFP* mRNA alone results in normal glomus morphology on both the injected and the uninjected sides (Fig 6.12 a and b), and therefore constitute the control experiment. Nevertheless, embryos injected with 1 to 1.5ng of the *dnwnt11b* show reduced glomus on the injected side (Fig 6.12 c, e) and relative to the uninjected side (Fig 6.12 d, f).
Figure 6.13, table 6.13.1 and graph 1 show numerical and graphical representation of the pronephric glomus phenotype in *X. laevis* embryos over-expressing 1ng of the *dnwnt11b* mRNA and analysed by *in situ* hybridization using the glomus marker *wt1*. Embryos injected with 1.5ng of *dnwnt11b* showed abnormal glomus morphology on both the injected and the uninjected sides and therefore were discarded from this analysis. The control experiment shows that 100% of embryos injected with *GFP* mRNA alone show normal glomus morphology in the left and right sides. Injection with 1ng of the *dnwnt11b* results in 50% of embryos exhibiting completely normal glomus morphology and in 50% of embryos having reduced glomus, on the injected side. Glomus on the uninjected side was developing perfectly normally.
In conclusion, over-expression of the *dnwnt11b* also moderately affects glomus formation since half of the embryos developed normal glomus and half developed reduced structure. This result suggests *wnt11b* is involved in the earliest phases of differentiation of the pronephric anlagen giving rise to all three pronephric components.

All together, inhibition of *wnt11b* using the *dnwnt11b* targeted in the pronephric area affects normal formation of the three pronephric components to a moderate extent but also strongly suggests that inhibition of *wnt11b* alone is not sufficient to inhibit the pronephros formation. This raises the issue that the very closely related *wnt11b* gene might be compensating for the defects caused by over-expression of the *dnwnt11*. In order to test this hypothesis antisense morpholinos were designed in the

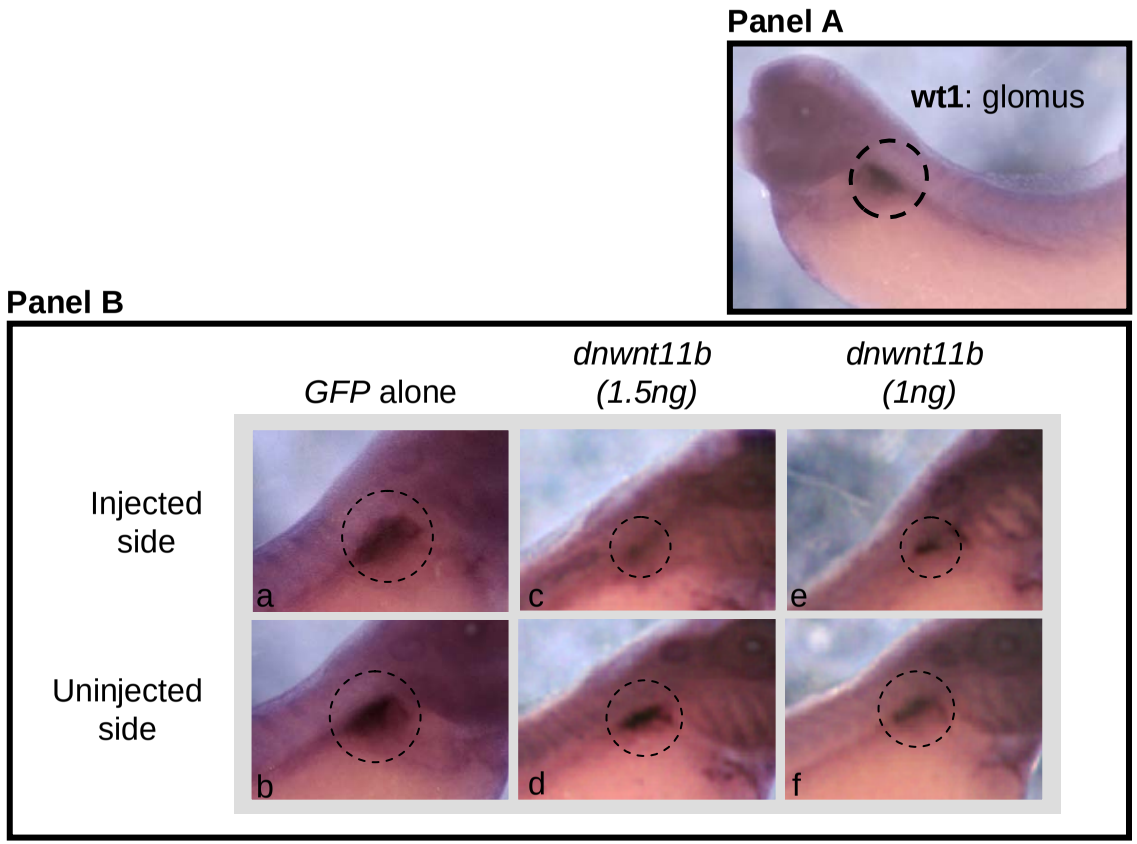

Figure 6.12 Embryos over-expressing the *dnwnt11b* show defects in glomus formation. Embryos were injected in one V2 blastomere at 8-cell stage with *GFP* mRNA and with or without 1 to 1.5ng of the *dnwnt11b* mRNA. Embryos were left to develop until stage 35 before being subjected to whole-mount *in situ* hybridization using the specific glomus markers, *wt1.* Embryos injected with *GFP* mRNA only show normal glomus morphology on both the injected and the uninjected sides (a, b). By contrast, embryos injected with 1 to 1.5ng of the *dnwnt11b* show reduced glomus on the injected side (c, e) and in slightly reduced glomus on the uninjected side (d, f).

Figure 6.13 Numerical and graphical representation of the pronephros glomus phenotype in *X. laevis* embryos over-expressing 1ng of the *dnwnt11b* mRNA and analysed by *in situ* hybridization using the glomus marker *wt1*. Embryos were injected into one V2 ventral blastomere at the 8-cell stage embryo and left to develop until stage 35 before being analysed by whole mount *in situ* hybridization using the pronephric glomus marker *wt1*.

		Glomus morphology		
		Injected side		Uninjected side
mRNA injected		Normal	Reduced	Normal
GFP (1ng)	n=15	15	0	15
	%	**100**	**0**	**100**
dnwnt11b (1ng)	n=20	10	10	20
	%	**50**	**50**	**100**

Table 6.13.1 Number and percentage of embryos showing glomus phenotype in embryos injected in one V2 ventral blastomere at the 8-cell stage with 1ng of *dnwnt11b* mRNA and analysed by *in situ* hybridization with the pronephric markers *wt1.*

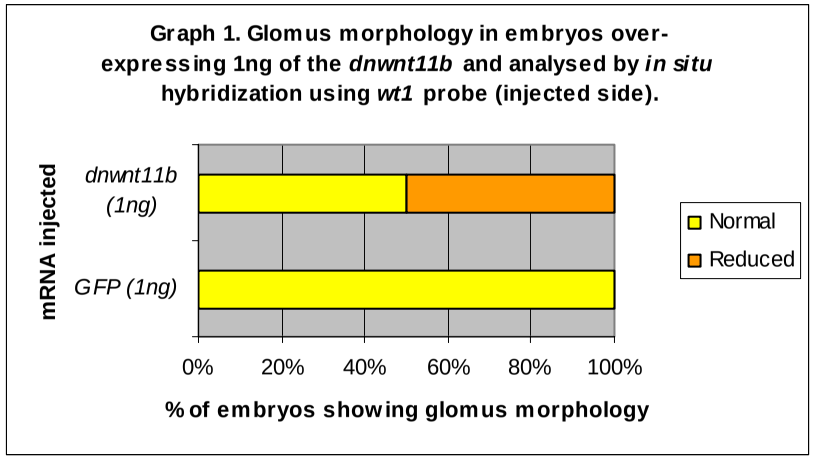

Graphs 1 show the glomus morphology in embryos over-expressing 1ng of the *dnwnt11b* and analysed by *in situ* hybridization using the glomus marker *wt1*.

aim to specifically inhibit the function in the developing pronephros of *wnt11b* and the closely related *wnt11*.

6.3.3 Inhibition of both *wnt11b* and *wnt11* using morpholinos result in a more severely abnormal pronephros phenotype.

6.3.3.1 *wnt11b* and *wnt11* morpholinos targeted in V2 blastomere give rise to abnormal kidney formation.

As it was shown previously, *dnwnt11b* specifically inhibits the function of *wnt11b* during *X. laevis* pronephros formation but might not block the activity of the closely related *wnt11b* gene, *wnt11*. In order to study the function of both *wnt11b* and *wnt11* during pronephros formation, an antisense morpholino approach was carried out. Both *wnt11b* and *wnt11* morpholinos were used in previously studies and their activity in inhibiting their respective gene product within the cell was confirmed. A *wnt11b* morpholino was designed by Pandur et al., 2002 and a *wnt11* morpholino was designed by Garriock et al., 2005. The *Xenopus wnt11b* and *wnt11* antisense morpholinos were designed across the boundary between the 5'UTR and the start of the coding region for the both genes. The two morpholinos overlap the AUG of mRNA from their respective genes and will therefore inhibit the translation of *wnt11b* and *wnt11* proteins (Fig 6.14).
In order to study the effects of inhibition of *wnt11b* and *wnt11* on *X. laevis* pronephros development, 15ng of *wnt11b* and 15ng of *wnt11* antisense morpholinos were injected, first of all, separately and then together. Both morpholinos were co-injected with the lineage tracer *ß-GAL* in one V2 ventral blastomere at the 8-cell stage with the aim of targeting the pronephric region. *ß-GAL* mRNA acts as a lineage tracer to follow those cells which inherited injected material, thus checking for correct targeting. Embryos were left to develop until stage 40 before being subjected to double antibody staining for pronephros phenotype. Figure 6.15, panel A shows a normal *Xenopus* embryos immuno-stained in purple with the specific pronephric proximal tubule antibody, 3G8 and in pink with the specific pronephric intermediate/distal tubule antibody, 4A6. *ß-GAL* stained the targeted cells in red in the somites resulting from mRNA injection into one V2 blastomere at the 8-cell stage embryo. Figure 5.24, panel B shows the pronephros phenotypes obtained in embryos

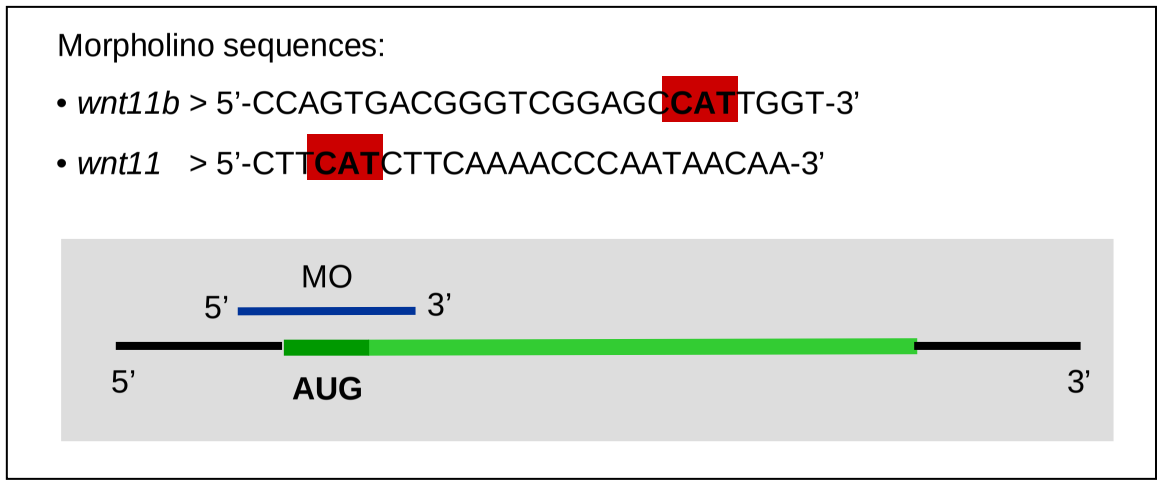

Figure 6.14 Diagram explaining the design of antisense oligonucleotide morpholinos. The *Xenopus wnt11b* and *wnt11* antisense morpholinos were designed across the boundary between the 5'UTR and the start of the coding region for the both genes. The two DNA morpholinos overlap the AUG of mRNA from their respective genes and will therefore inhibit the translation of *wnt11b* and *wnt11* proteins.

Panel A

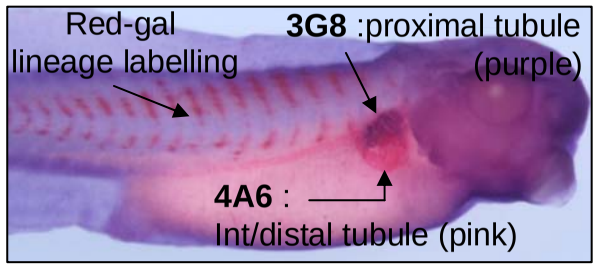

Panel B

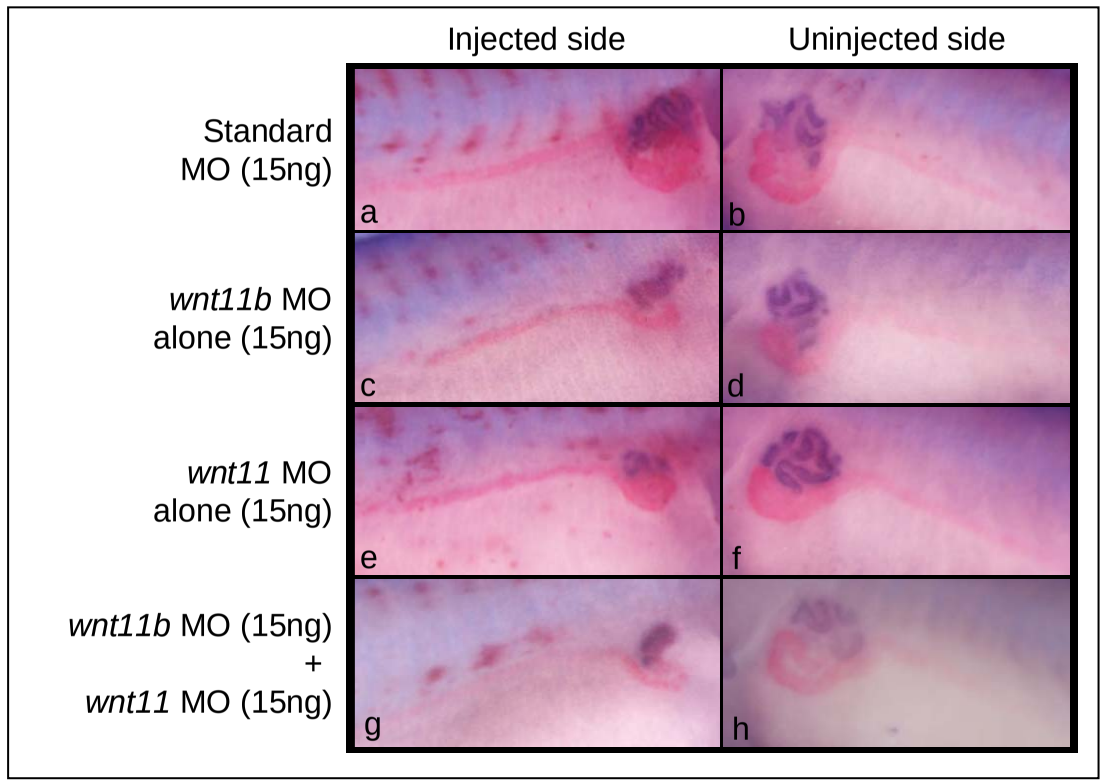

Figure 6.15 Morpholino knock-down of *wnt11b* and *wnt11* act additionally to perturb pronephros formation. Panel A shows a normal *X. laevis* embryos immuno-stained in purple with the specific pronephric proximal tubule antibody, 3G8 and in pink with the specific pronephric intermediate/distal tubule antibody, 4A6. *β-GAL* mRNA acts as a lineage tracer to follow those cells which inherited injected materiel, thus checking for correct targeting. Here, such cells are stained red in the somites resulting from mRNA injection into one V2 blastomere at the 8-cell stage embryo. Panel B shows pronephros phenotypes obtained in embryos co-injected with *β-GAL* and *wnt11b* morpholino and/or *wnt11* morpholino in V2 blastomere at the 8-cell stage embryo. Injection of a control standard morpholino shows normal tubule morphology on both injected and uninjected sides (a and b). Injection of 15ng of *wnt11b* morpholino shows reduced pronephric tubules tissues on the injected side (c) while the pronephric components remain normal on the uninjected side (d). A similar phenotype is observed with injection of 15ng of *wnt11* morpholino (e and f). However, when 15ng of each *wnt11b* and *wnt11* morpholinos were co-injected, reduction of pronephric tubules is greatly accentuated (g) when compared to the uninjected side (h) and in some cases is totally lost (see table 5.23).

Morpholino injected		Proximal tubule morphology: Injected side Normal	Red.	Enl.	Abs.	Proximal tubule morphology: Uninjected side Normal	Intermediate/distal tubules morphology: Injected side Normal	Red.	Enl.	Abs.	Intermediate/distal tubules morphology: Uninjected side Normal
ß-gal alone	n= 69	60	9	0	0	69	69	0	0	0	69
	%	**87**	**13**	**0**	**0**	**100**	**100**	**0**	**0**	**0**	**100**
Standard morpholino	n= 38	37	1	0	0	38	34	4			38
	%	**97**	**3**	**0**	**0**	**100**	**89**	**11**	**0**	**0**	**100**
wnt11b alone (15ng)	n= 36	18	16		2	36	18	16	2		36
	%	**50**	**44**		**6**	**100**	**50**	**44**	**6**		**100**
wnt11 alone (15ng)	n= 72	31	39	0	2	72	29	39	2	2	72
	%	**43**	**54**	**0**	**3**	**100**	**40**	**54**	**3**	**3**	**100**
wnt11b (15ng) + wnt11 (15ng)	n= 110	22	79	1	8	110	21	66		23	110
	%	**20**	**72**	**1**	**7**	**100**	**19**	**60**	**0**	**21**	**100**

Table 6.16.1 Number and percentage of embryos showing pronephros phenotype in embryos injected in one V2 ventral blastomere at the 8-cell stage with15ng of *wnt11b* and *wnt11* antisense morpholinos.

Figure 6.16 Numerical and graphical representation of the pronephros phenotype in *X. laevis* embryos injected with 15ng of *wnt11b* and *wnt11* antisense morpholinos. Embryos were injected into one V2 ventral blastomere at the 8-cell stage embryo and left to develop until stage 40 before being analysed by antibody staining using the specific pronephric tubules antibodies 3G8/4A6.

Key: **Red.**: Reduced. **Enl.**: Enlarged. **Abs.**: Absent.

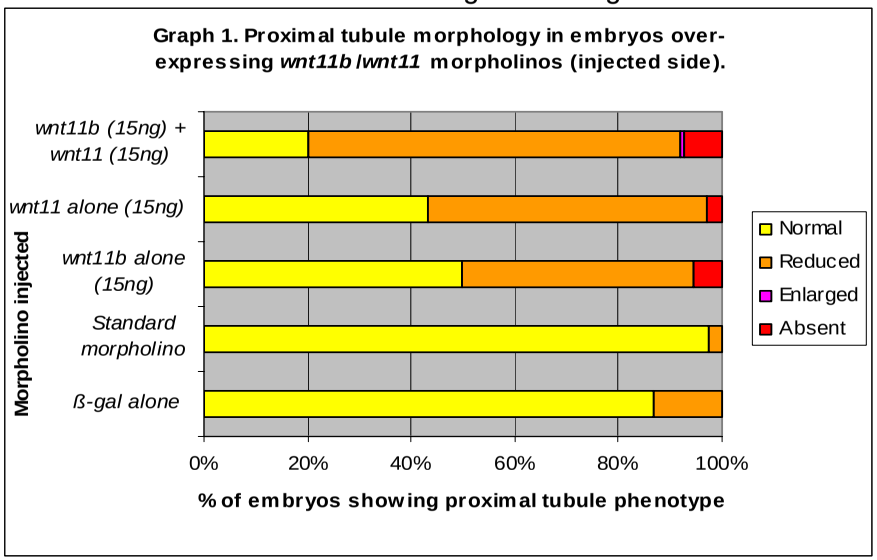

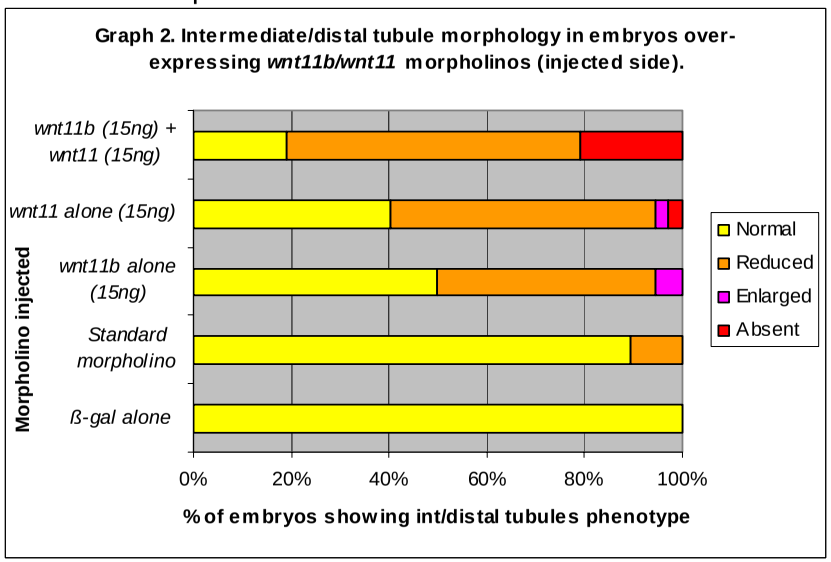

Graph 1 and 2 show the proximal tubule and the intermediate/ distal tubules phenotype in embryos injected in one V2 blastomere of 8-cell stage with 15ng of *wnt11b* and *wnt11* antisense morpholinos.

co-injected with *ß-GAL* and *wnt11b* morpholino and/or *wnt11* morpholino into the V2 blastomere at the 8-cell stage. Injection of a control standard morpholino shows normal tubule morphology on both injected and uninjected sides (Fig 6.15 a and b). Injection of 15ng of *wnt11b* morpholino shows reduced pronephric tubules tissues on the injected side (Fig 6.15 c) while the pronephric components remain normal on the uninjected side (Fig 6.15 d). A similar phenotype is observed with injection of 15ng of *wnt11* morpholino (Fig 6.15 e and f). However, when 15ng of each *wnt11b* and *wnt11* morpholinos were co-injected, reduction of pronephric tubules is greatly accentuated (Fig 6.15 g) when compared to the uninjected side (Fig 6.15 h) and in some cases is totally lost.

Figure 6.16, table 1.16.1 and graphs 1 and 2 show numerical and graphical representation of the pronephros phenotype in *X. laevis* embryos injected with 15ng of *wnt11b* and/or *wnt11* antisense morpholinos. Embryos showing abnormal morphology or abnormal pronephros morphology on the uninjected side were rejected from this study. Most of the embryos injected with the lineage tracer *ß-GAL* alone or *ß-GAL* and the standard control morpholino show normal tubule formation. This result suggests that *ß-GAL* and the standard control morpholino do not affect pronephros formation. Injection of 15ng of the *wnt11b* morpholino shows that half of the embryos developed normal pronephric tubules and the other half developed reduced pronephric tubules structure. Injection of 15ng of the *wnt11* morpholino shows a very similar result. However, co-injection of 15ng of each *wnt11b* and *wnt11* morpholino results in a greater number of embryos showing reduced proximal tubule (72%) and intermediate/distal tubules (60%) and in the most extreme cases, embryos did not form any proximal tubules (7%) and intermediate/distal tubules (21%). Co-injection of *wnt11b* and *wnt11* morpholinos resulted in a higher number of embryos showing this phenotype and also in more severe phenotype than the one observed of each individual morpholino injection (Fig 6.15).

To conclude, results of this experiment indicate that it is very likely that *wnt11b* and *wnt11* can compensate for each other in pronephros formation.

6.4 Discussion.

6.4.1 *wnt11b* and *wnt11,* two closely related genes, have distinct spatial expression patterns in *X. laevis* embryos.

The use of gene specific 3'UTR *wnt11b* and 5'UTR *wnt11* mRNA probes has allowed clarification of the temporal and spatial expression pattern of both *wnt11b* and *wnt11* genes in *X. laevis* embryos. Additionally to the published data showing that *wnt11b* is expressed in the somites and the branchial arches in early tadbud (Ku and Melton, 1993), our result also suggests that *wnt11b* is expressed in the developing pronephros at stage 26. Despite the fact that expression of *wnt11b* in pronephros at stage 26 remains to be confirmed by sectioning, this result is supported by the RT-PCR analysis (chapter 4) showing that *wnt11b* is expressed throughout pronephros formation from stage 12.5 to stage 35. However, *in situ* hybridization has failed to detect *wnt11b* in the pronephros of embryos post stage 26, presumably due to the different sensitivities of the two techniques.

Controversially to the published data showing that *wnt11* is expressed in the brain, the neural tube, the branchial arches, the somites and the heart in early *Xenopus* tadpole (Garriock et al., 2005), our result suggests that *wnt11* is not expressed in the branchial arches and is visible only at the very most dorsal tip of the somites in a very different expression pattern to that of *wnt11b*. In agreement with studies on the mammalian metanephric kidney, reporting that *Wnt11* plays a role in regulating mouse ureteric branching (Yu et al., 2004), RT-PCR analysis (chapter 4) showed that *wnt11* starts to be expressed in the pronephros at stage 25. However, *in situ* hybridization failed to detect *wnt11* in the forming pronephros. Finally, expression of *wnt11* in the nasal placode in early tadpole remains to be confirming by sectioning.

In conclusion, the discordance between the *wnt11* published expression pattern and our data which refines the *in situ* expression pattern, probably arises from the fact that our probe was designed to specifically recognized *wnt11* without detecting *wnt11b* expression domain.

6.4.2 Identification of a possible role for *wnt11b* in pronephros formation.

In mouse embryos *wnt11* has been shown to play a role in regulating the ureteric branching process in association with g*dnf* and *ret* (Yu et al., 2004, Majumdar et al., 2003). In *Xenopus* embryos, studies on *in vitro* Holtfreter cultures suggest that *wnt11* and *wnt11b* share some biological activity and can act as pronephros inducers.

However, *in vivo* studies comparing tubule morphology in embryos over-expressing *wnt11b* and in embryos lacking *wnt11b* expression, showed that both groups of embryos show a similar pronephric phenotype. Pronephric tubules are reduced with intermediate/distal tubules shorted, enlarged and straighter. This observation suggests that *wnt11b* is required for normal pronephros morphogenesis and that perhaps this requirement needs to be finely balanced. Similar effects have also been observed by De Calisto et al. in 2005, who reported that over-expression and inhibition of *wnt11b* results in the same phenotype, an inhibition of neural crest migration. One possible explanation could be that *wnt11b* might be required for normal cell movement within developing tissue and that excess or deficiency of the level of *wnt11b* would result in blocking cell movement and leading to the same phenotypically abnormal pronephros formation.

Co-injection of *wnt11* and *wnt11b* antisense morpholinos in an attempt to inhibit pronephros formation, resulted in a greater reduction of the pronephric tubules, suggesting that more than one type of *wnt* molecules are also involved in pronephros formation. Because canonical *wnt* molecules are also expressed in the early pronephric anlagen (Chapter 4) and that *wnt6* and *wnt8* are capable of inducing pronephros formation in Holtfreter sandwich cultures, the role of the canonical *wnt* pathway during pronephros formation will be investigated in the next chapter.

Chapter 7 The role of the canonical *wnt/ß-catenin* pathway in *Xenopus* pronephros formation.

7.1 Introduction.

This chapter investigates the potential role of canonical *wnt* signalling molecules during early pronephros formation in *Xenopus* embryos. A novel hormone-inducible *wnt* responsive system developed in transgenic *X. laevis* embryos revealed high canonical *wnt* activity at tadpole stage in specific tissues such as the pronephric tubules (Denayer et al., 2006). Members of the canonical *wnt* class, such as *wnt1, wnt2, wnt3, wnt6, wnt7, wnt8,* and *wnt9,* cause the stabilisation of β-catenin in the cell, resulting in the nuclear activation of the transcription factor *tcf* and downstream targeted genes. An initial study focuses on specifically inhibiting the *wnt/ß-catenin* pathway, in the pronephros, by using a dominant-negative *tcf3* (*dntcf3*) construct, which will prevent downstream transcriptional activation following canonical *wnt* signalling. We have shown that canonical *wnt6* is expressed throughout pronephros formation (Chapter 4) and that is capable of inducing pronephros formation in Holtfreter sandwich cultures (Chapter 5). Moreover, Lavery et al., 2008 showed by using a DIG-labelled LNA modified oligonucleotides *in situ* probe that *wnt6* is detected in the pronephric anlagen of *X. laevis* stage 23 embryos and in later stages, stage 28 onwards, in the developing pronephros. Therefore we decided to extend this previous work by confirming the expression of *wnt6* in a wider stage series of *X laevis* and *X tropicalis* embryos before investigating the consequences of *wnt6* over-expression on pronephros formation.

7.2 The over-expression of the *dntcf3* to inhibit all canonical *wnt* signalling.

7.2.1 The *dntcf3* molecular construct and its functional mode of action in the cell.

In order to interfere with the *wnt/ß-catenin* pathway, the *dominant-negative tcf3* (*dntcf3*) that binds DNA but not ß-catenin was generated by Molenaar et al., in 1996. Figure 7.1 panel A illustrates the domain structures of the dntcf3 protein compared to

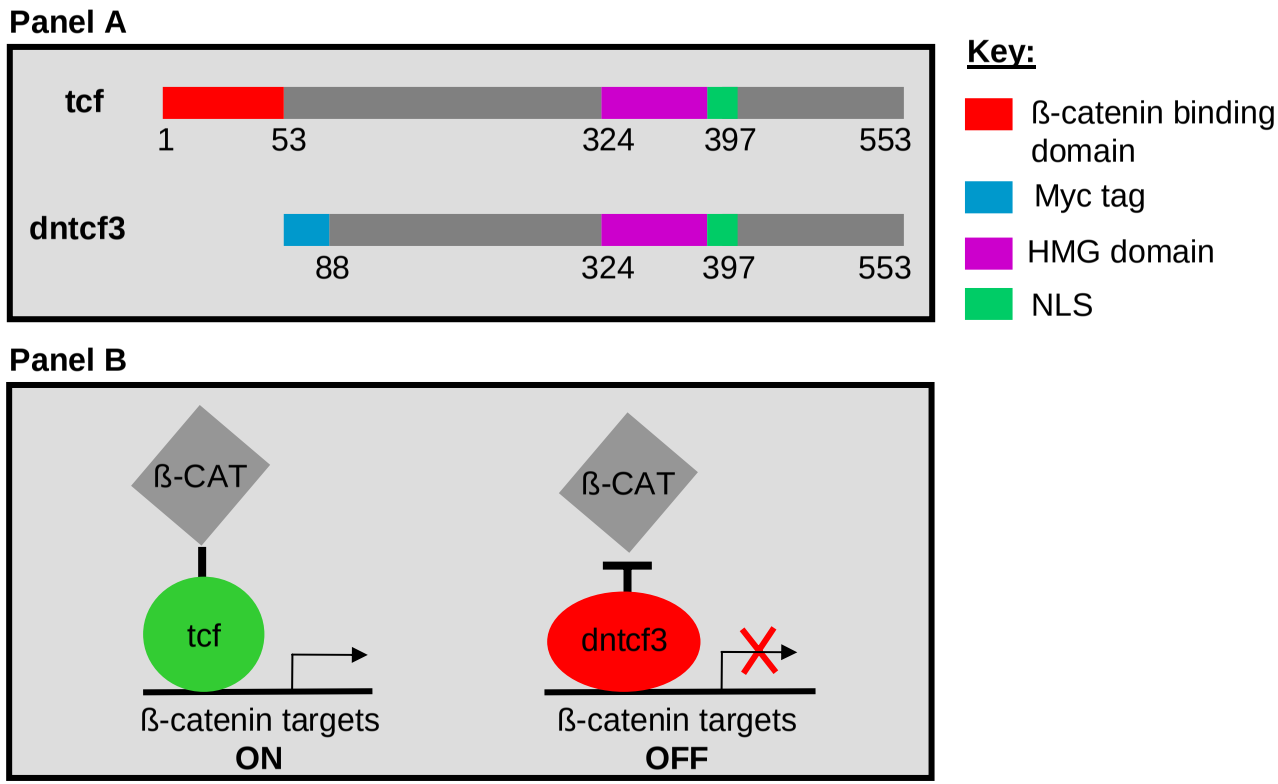

Figure 7.1 The dntcf3 construct used in microinjection and its functional mode of action in the cell. Panel A shows the domain structure of the dominant negative tcf3 (dntcf3) compared to wild-type tcf. dntcf3 lacks the N-terminal ß-catenin binding domain. Panel B shows that ß-catenin forms a complex with tcf that results in nuclear translocation of ß-catenin to activate transcription of specific gene targets. The dntcf3 blocks the nuclear translocation of ß-catenin which result in inhibition of downstream gene targets transcription.

the wild-type tcf. All members of the tcf family share an N-terminal ß-catenin binding domain. ß-catenin binds directly to the N-terminus of tcf/lef factors. Since the dntcf3 protein lacks the N-terminal ß-catenin binding domain, ß-catenin cannot bind to tcf/lef.

The *wnt* signal is received at the cell surface by the frizzled family of receptors and activates the responsive *wnt* molecular cascade in the cytoplasm to result in stabilisation of ß-catenin. Figure 7.1 panel B explains the functional mode in the cell of tcf and its dominant-negative, dntcf3. In the wild-type situation, stabilized ß-catenin accumulated in the cytoplasm translocates to the nucleus and binds to the N-terminal ß-catenin binding domain of the tcf/lef HMG domain family of transcriptional regulators and activates downstream *wnt* gene targets. The dntcf3 is incapable of interacting with ß-catenin and does not result in nuclear translocation of ß-catenin thus prevents the transcription of *wnt* gene targets.

7.2.2 The *dntcf3* translates *in vivo* in *X. laevis* oocytes.

In order to verify that *in vivo* transcribed *dntcf3* mRNA message was correctly translated within *Xenopus* cells, *in vivo* translation of *dntcf3* mRNA in *Xenopus* oocytes was carried out. 25ng of *dntcf3* mRNA message was microinjected into oocytes and incubated in the presence of ^{35}S methionine for 18 hours at 18˚C. Total radiolabelled protein was extracted and run out on a 10% SDS PAGE gel. Figure 7.2 shows an SDS/PAGE protein gel of *dntcf3,* over-expressed in oocytes, compared to normal uninjected oocytes. The *dntcf3* mRNA which is not normally present in normal oocytes, is translated into dntcf3 protein of the correct molecular weight of 62 kDa (black arrow) when over-expressed in oocytes. Control oocytes did not translate any dntcf3 protein. This result suggests that the *in vivo* transcribed *dntcf3* mRNA is correctly translated when over-expressed in *Xenopus* oocytes.

7.2.3 Demonstration of the effectiveness of the dominant-negative construct to inhibit canonical *wnt8* signalling in animal caps explants.

In order to confirm that *dntcf3* mRNA is biologically active and is capable of specifically inhibiting the *wnt/ß-catenin* pathway in *Xenopus* embryos, an animal cap assay was carried out. *nodal3* (previously called *Xnr3*) constitutes a downstream

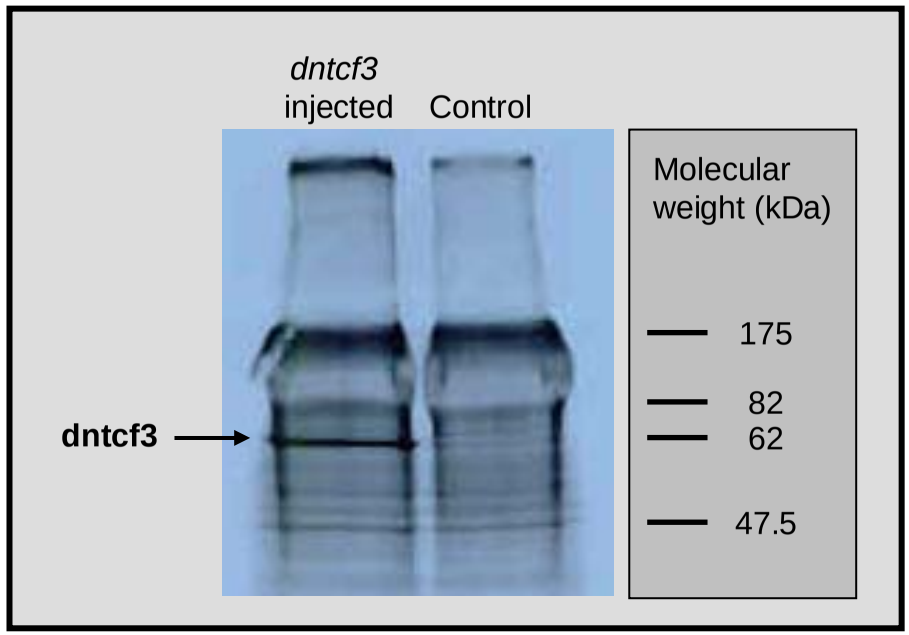

Figure 7.2 *In vivo* translation of *dntcf3* mRNA in *X. laevis* oocytes. Oocytes were injected with 25ng of *dntcf3* mRNA, incubated over-night at 18˚C in the presence of ^{35}S methionine, and then the protein was extracted and separated on a 10% polyacrylamide gel. The injected oocytes clearly show an extra band at 62 kDa representing the translated protein from the injected mRNA (black arrow). Control oocyte did not translate any dntcf3 protein.

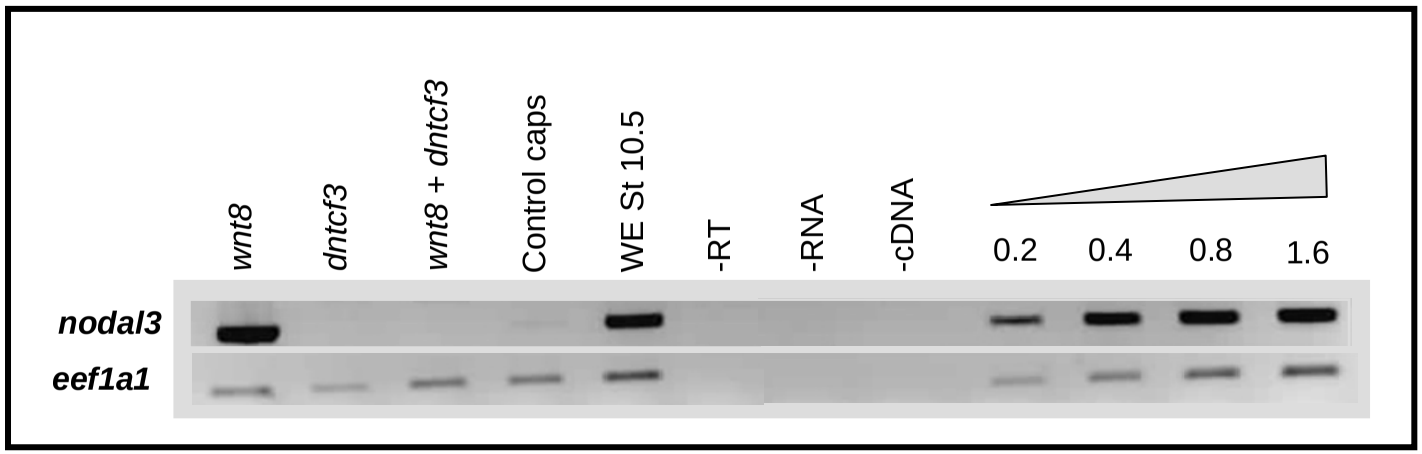

Figure 7.3 *dntcf3* inhibits *wnt/ß-catenin* signalling in animal caps. One-cell stage *X. laevis* embryos were injected with 0.5ng of *wnt8* mRNA or with 1ng of *dntcf3* mRNA or with both mRNAs. After over-night incubation, animal caps were dissected from normal embryos at stage 9 and from embryos over-expressing *wnt8, dntcf3* and *wnt8* with *dntcf3.* Animal caps were cultured until stage 10.5 equivalent. Total RNA was extracted from each sample before being subjected to RT-PCR analysis using one of the wnt/ß-catenin downstream gene targets, *nodal3*. *eef1a1* was used to equalize the cDNA samples. The triangle illustrates sequentially increasing cDNA inputs of whole embryo cDNA. *dntcf3* alone blocks *nodal3* expression. Translation of *wnt8* mRNA actives expression of *nodal3*. However, cotranslation of both *wnt8* and *dntcf3* mRNAs blocks the expression of nodal3. *wnt8* and *nodal3* are not normally expressed in control caps.

target of the canonical *wnt8* and can be used as a biological "read-out" for active *wnt/ß-catenin* signalling (Yang-Snyder et al., 1996). To test the biological activity of the *dntcf3* mRNA, one-cell stage *X. laevis* embryos were injected with 0.5ng of *wnt8* mRNA or with 1ng of *dntcf3* mRNA or with both mRNAs. After over-night incubation, animal caps were dissected and cultured until stage 10.5 equivalent. Total RNA was extracted from each sample before being subjected to RT-PCR analysis using one of the *wnt/ß-catenin* downstream gene targets, *nodal3*. Figure 7.3 shows the result of the RT-PCR analysis testing for the presence or the absence of *nodal3* marker expression in normal or injected animal caps. *eef1a1* expressed strongly at stage 10.5, was used to equalize the cDNA input into the RT-PCR samples. Control animal caps and animal caps over-expressing *wnt8*, *dntcf3* and *wnt8* plus *dntcf3* show nearly the same intensity of *eef1a1* expression, confirming that samples contain approximately the same quantity of cDNA. Whole embryo (WE) stage 10.5, showed strong expression of *nodal3*, providing the experiment positive control and was used for increasing volumes of cDNA input (0.2-1.6 µl) demonstrating that the RT-PCR was carried out in the linear range and could therefore be considered as semi-quantitative. As expected, negative controls, minus reverse-transcriptase (-RT), minus mRNA (-RNA) and minus cDNA (-cDNA) showed no band, confirming the specificity of this assay. *wnt8* and *nodal3* are not normally expressed in normal animal caps. Over-expression of *wnt8* induces expression of *nodal3,* the responsive gene. Over-expression of *dntcf3* alone blocks *nodal3* expression. Co-expression of both *wnt8* and *dntcf3* show no induction of *nodal3*. This result indicates that the *dntcf3* is capable of blocking the induction of expression of one of the *wnt8*-responsive genes, *nodal3*, in *Xenopus* explants, suggesting that the canonical *wnt* signalling pathway was inhibited.

To conclude, this result confirms that *dntcf3* mRNA message is active and blocks *wnt8* expression and its downstream target, *nodal3*, by interfering with the *wnt/ß-catenin* pathway, the signalling pathway by which *wnt8* activates its gene targets.

7.3 Over-expression of *dntcf3* causes severe morphological abnormalities in developing *X. laevis* embryos.

In *Xenopus*, the *wnt/ß-catenin* pathway plays a crucial role in defining the patterning of embryonic axis (Funayama et al., 1995). We examined the morphological

consequences of microinjecting *dntcf3* mRNA into *X. laevis* embryos. Various concentrations of *dntcf3* mRNA were injected into one ventral blastomere at 4-cell stage *X. laevis* embryos, a blastomere that will contribute to the pronephric anlagen amongst other ventrolateral tissues (Nieuwkoop and Faber, 1956 and 1994, Moody, 1987 and Dale and Slack, 1987). Figure 7.4 shows the graded morphological defects of *dntcf3* injected embryos, that could be characterised as a gradual loss of axial structures when the amount of injected mRNA increases. Tadpoles were fixed at stage 42. Embryos injected with *GFP* alone showed completely normal morphology and so provided the control experiment (Fig 7.4 a). This showed that *GFP* does not interfere with early development and also that micromanipulation of embryos by itself does not cause any significant disturbance in development. Injection of 100pg of the *dntcf3* mRNA resulted in embryos with abnormal head structure (Fig 7.4 b). Injection of 200pg of *dntcf3* mRNA resulted in embryos with a bent anterior-posterior axis (Fig 7.4 c). Injection of 400pg of the *dntcf3* mRNA resulted in a short and disturbed anterior-posterior axis, an increase in size of ventral trunk structures and an enlarged head (Fig 7.4 d). Injection of 800pg to 1.6ng of the *dntcf3* mRNA resulted in embryos with a very abnormal morphology, embryos were missing substantial amounts of the anterior-posterior axis (Fig 7.4 e and f).

In conclusion, injection of *dntcf3* mRNA into only one single ventral blastomere at the 4-cell stage embryo causes dramatic defects on both dorso-ventral and anterior-posterior axes formation, in a dose-dependent manner, with embryos showing gradual lost of anterior-posterior structures as the concentration of message was increased.

What would be the consequences of inhibiting the canonical *wnt* signalling, using the *dntcf3,* on kidney development?

7.4 The role of canonical *wnt* signalling in *X. laevis* kidney development.

To investigate the role of the *wnt/ß-catenin* pathway on pronephros development, a targeted loss-of-function experiment was carried out using *dntcf3* mRNA. In this section, we asked whether or not inhibiting canonical *wnt* signalling using the *dntcf3* has an effect on early kidney development and if it does, when this effect first become apparent.

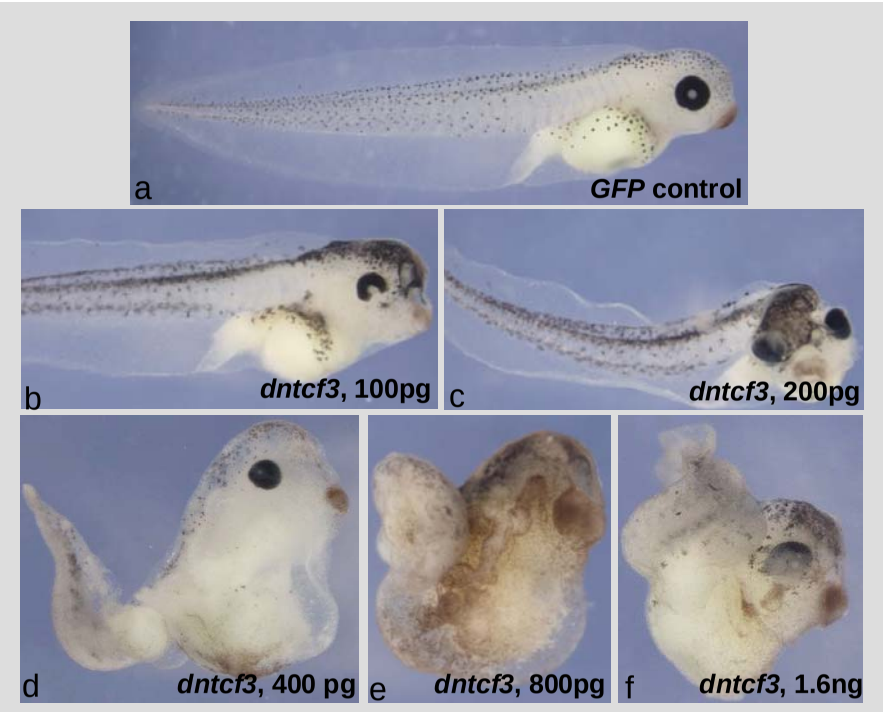

Figure 7.4 Morphological defects caused by over-expression of *dntcf3* in *X. laevis* embryos. 100pg to 1.6ng of *dntcf3* mRNA was injected into the equatorial region of one ventral blastomere of 4-cell stage *Xenopus* embryos. Embryos were left to develop until stage 42. Injection of *GFP* mRNA alone results in normal embryos (a) and was used as a experimental control. Embryos over-expressing gradually increasing concentrations of the *dntc*f3 mRNA, 100pg to 1.6ng, show concentration dependent defects in axis formation (b, c, d, e and f).

7.4.1 Inhibition of canonical *wnt* signalling using the *dntcf3* affects *X. laevis* pronephros terminal differentiation.

Figure 7.5 shows that inhibition of canonical *wnt* signalling, using the *dntcf3* construct, affects *X. laevis* pronephros development in a dose-dependent manner. *X. laevis* embryos were co-injected into one ventral blastomere at the 4-cell stage with *GFP* mRNA and with gradually increasing concentrations of the *dntcf3*, 100pg to 800pg. Embryos were left to develop until stage 41 before being subjected to immuno-staining. Figure 7.5, panel A shows a *GFP* control embryo at stage 41 stained in purple with the specific pronephric proximal tubule antibody, 3G8 and in pink with the specific intermediate/distal tubules antibody, 4A6. Panel B shows that embryos injected with *GFP* alone develop normal pronephric tubules (Fig 7.5 a and b). Injection of 100pg of *dntcf3* mRNA resulted in perfectly normal pronephros morphology on the uninjected side, although on the injected side, the distal tubule is shorted and proximal tubules did not seem to be affected (Fig 7.5 c-d). Injection of 200pg of *dntcf3* mRNA resulted in a reduction of the pronephric tissues on the injected side. Proximal tubules were reduced and intermediate tubule was less coiled and distal tubule looked shortened (Fig 7.5 e-f). Embryos injected with 400pg of *dntcf3* mRNA presented a more severe phenotype. Proximal tubules were absent on the injected side and intermediate/distal tubules were clearly affected showing a reduction in length and no coiled structure. However, kidney components on the uninjected side were still unaffected (Fig 7.5 g-h). Injection of 800pg of *dntcf3* mRNA resulted in absence of proximal tubules and intermediate/distal tubules were reduced to a single spot of immuno-stained material (Fig 7.5 i-j).

In conclusion, embryos injected with increasing concentrations of the *dntcf3* show, on the injected side, progressive regression of development of the pronephric tubules as the concentrations of mRNA increased (c, e, g and i). On the uninjected side, the morphology of the pronephros remains fairly normal for all embryos over-expressing the *dntcf3* (d, f, h and j). Only embryos showing normal pronephric morphology on the uninjected side were chosen to be presented in Figure 7.5.

Figure 7.6 shows the numbers and graphic representations of embryos over-expressing gradual concentration of the *dntcf3* mRNA. As previously described in section 7.3, injection of *dntcf3* affects the normal morphology of embryos and often results in embryos developing a reduced or bent anterior-posterior axis (Fig 7.6, table

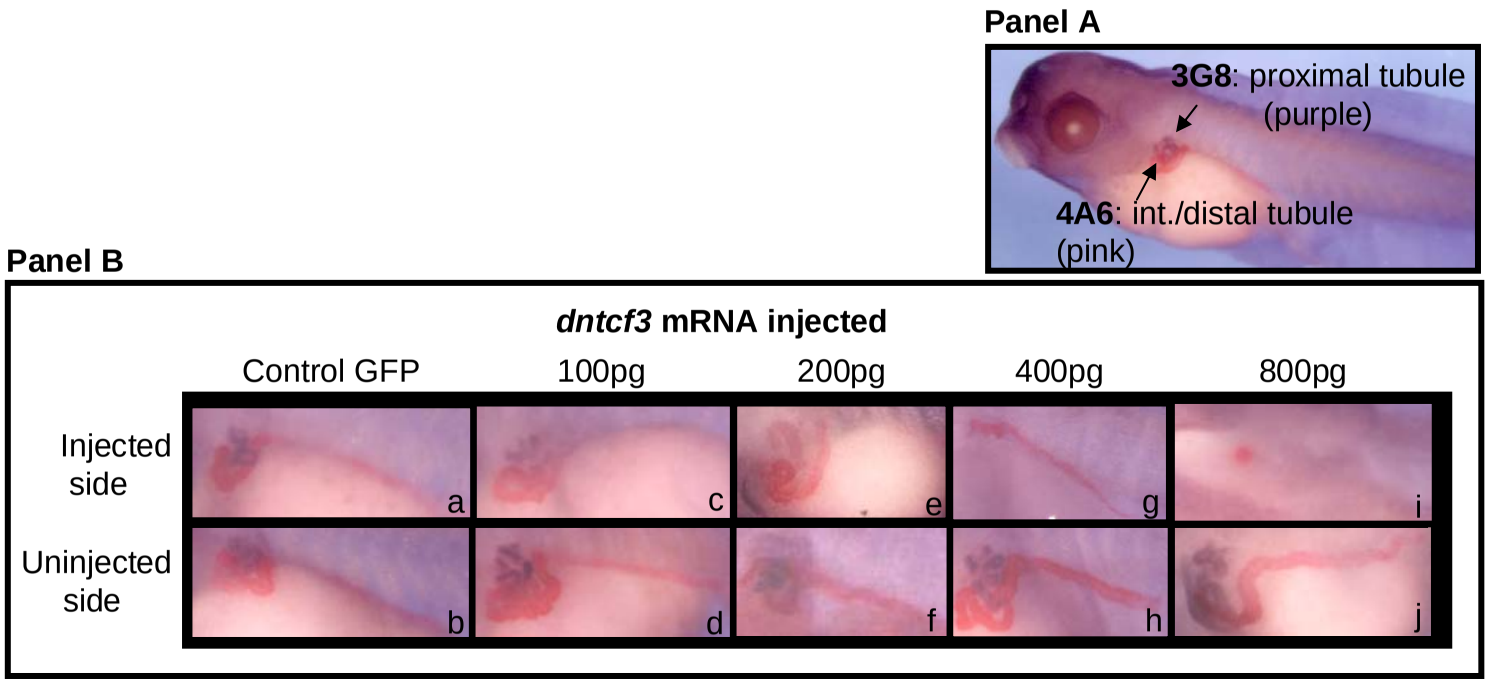

Figure 7.5 Inhibition of canonical *wnt* signalling using the *dntcf3* construct affects the *X. laevis* pronephros development in a dose-dependent manner. *X. laevis* embryos were co-injected into one ventral blastomere at the 4-cell stage with *GFP* mRNA and with gradually increasing concentrations of the *dntcf3*, 100pg to 800ng. Embryos were left to develop until stage 41 before being subjected immuno-staining. Panel A shows a *GFP* control embryo at stage 41 stained in purple with the specific pronephric proximal tubule antibody, 3G8 and in pink with the specific intermediate/distal tubules antibody, 4A6. Panel B shows that embryos injected with *GFP* alone develop normal pronephric tubules (a and b). Embryos injected with increasing concentrations of the *dntcf3* show, on the injected side, progressive reduction of the pronephric tubules as the concentrations increase (c, e, g and i). On the uninjected side, the morphology of the pronephros remains fairly normal for all embryos over-expressing the *dntcf3* (d, f, h and j).

Figure 7.6 Numerical and graphical representation of the pronephros phenotype and embryo morphology in *X. laevis* embryos injected with various concentrations of the *dntcf3*. Embryos were injected into one ventral blastomere at the 4-cell stage embryo and left to develop until stage 40 before being analysed by antibody staining using the specific proximal tubule antibody 3G8 and the specific intermediate and distal tubule antibody 4A6.

		Embryo morphology		
mRNA injected		Normal	Bent	Reduced axis
GFP	n=48	45	3	0
	%	**94**	**6**	**0**
dntcf3 (100pg)	n=24	22		2
	%	**92**	**0**	**8**
dntcf3 (200pg)	n=22	0	0	22
	%	**0**	**0**	**100**
dntcf3 (400pg)	n=46	8	24	14
	%	**17**	**52**	**30**
dntcf3 (800pg)	n=44	3	35	6
	%	**7**	**80**	**14**
dntcf3 (1.6ng)	n=42	2	40	0
	%	**5**	**95**	**0**

Table 7.6.1 Morphology of embryos injected with 100pg to 1.6ng of *dntcf3* in one ventral blastomere at the 4-cell stage and analysed for pronephros phenotype.

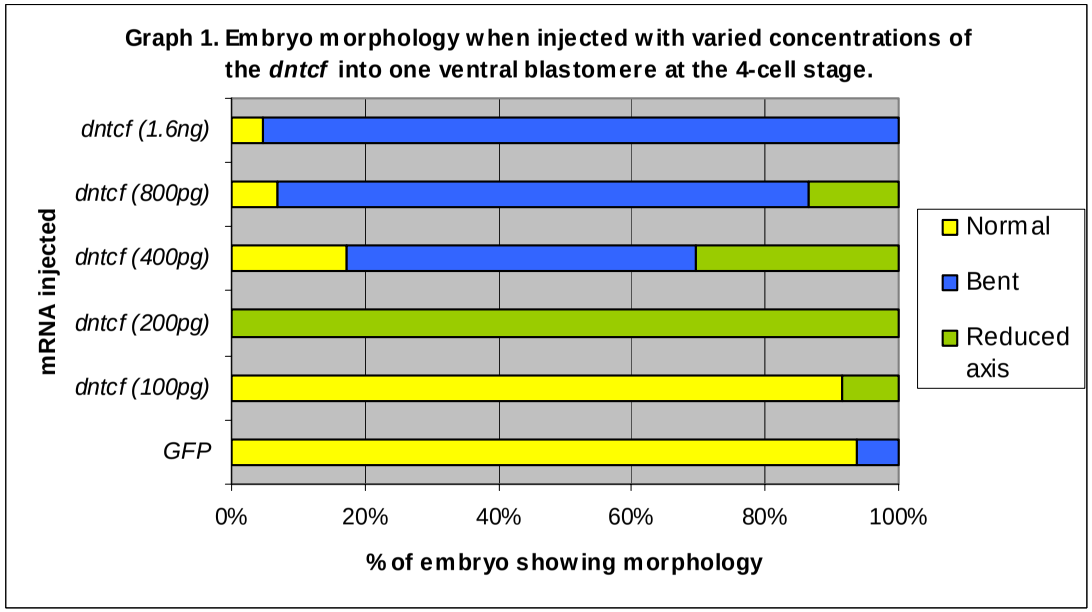

Graph 1 shows the morphology of embryos injected with 100pg to 1.6ng of *dntcf3* in one ventral blastomere at the 4-cell stage and analysed for pronephros phenotype.

mRNA injected		Proximal tubule morphology					Intermediate/distal tubules morphology				
		Injected side			Uninjected side		Injected side			Uninjected side	
		Normal	Reduced	Absent	Normal	Reduced	Normal	Reduced	Absent	Normal	Reduced
GFP	n=48	42	5	1	48	0	45	2	1	48	0
	%	**88**	**10**	**2**	**100**	**0**	**94**	**4**	**2**	**100**	**0**
dntcf3 (100pg)	n=24	6	16	2	17	7	8	14	2	18	6
	%	**25**	**67**	**8**	**71**	**29**	**33**	**58**	**8**	**75**	**25**
dntcf3 (200pg)	n=22	1	11	10	11	11	1	12	9	11	11
	%	**5**	**50**	**45**	**50**	**50**	**5**	**55**	**41**	**50**	**50**
dntcf3 (400pg)	n=46	4	4	38	38	8	5	5	36	41	5
	%	**9**	**9**	**83**	**83**	**17**	**11**	**11**	**78**	**89**	**11**
dntcf3 (800pg)	n=44	0	6	38	15	29	2	4	38	18	26
	%	**0**	**14**	**86**	**34**	**66**	**5**	**9**	**86**	**41**	**59**
dntcf3 (1.6ng)	n=42	0	2	40	4	38	0	3	39	6	36
	%	**0**	**5**	**95**	**10**	**90**	**0**	**7**	**93**	**14**	**86**

Table 7.6.2 Number and percentage of embryos showing on pronephros phenotype when injected into one ventral blastomere at the 4-cell stage with 100pg to 1.6ng of *dntcf3* mRNA.

Graphs 2 and 3 compare the proximal tubule phenotype on injected and uninjected sides respectively and graphs 4 and 5 compare the intermediate/distal tubules phenotype on injected and uninjected sides respectively in embryos injected in one ventral blastomere at the 4-cell stage with 100pg to 1.6ng of *dntcf3* mRNA.

Key: normal reduced absent

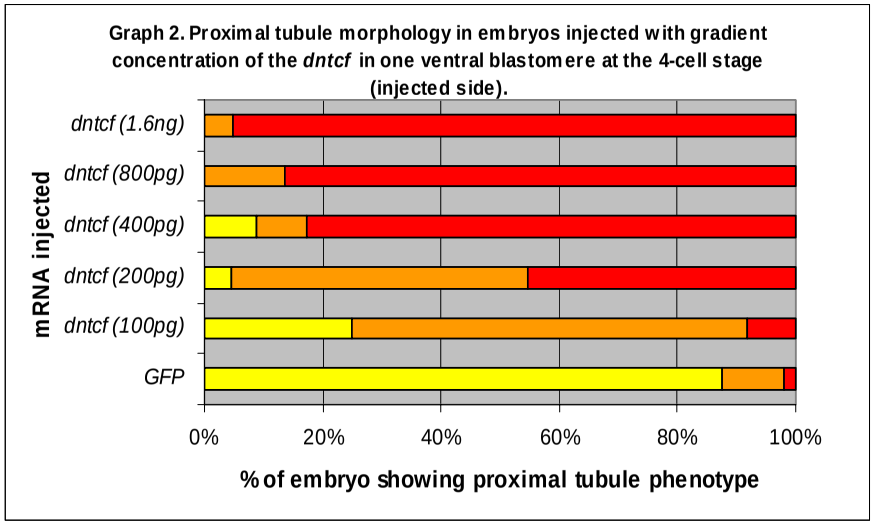

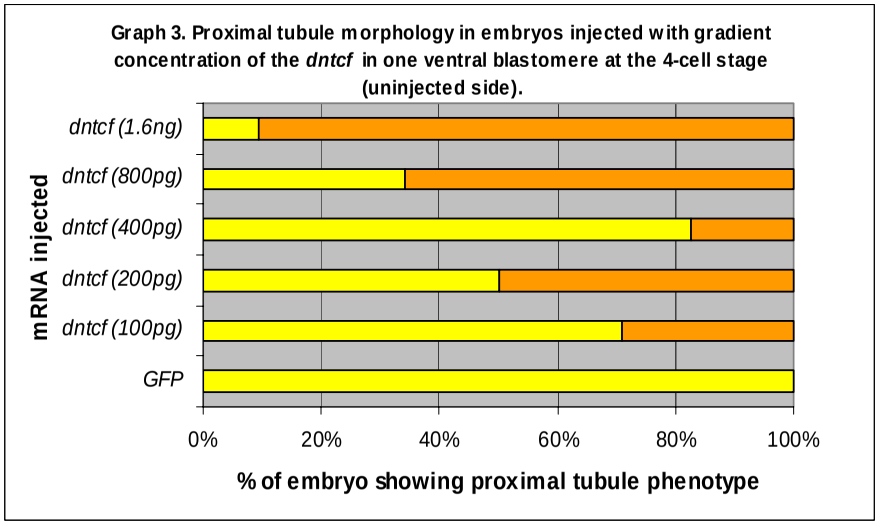

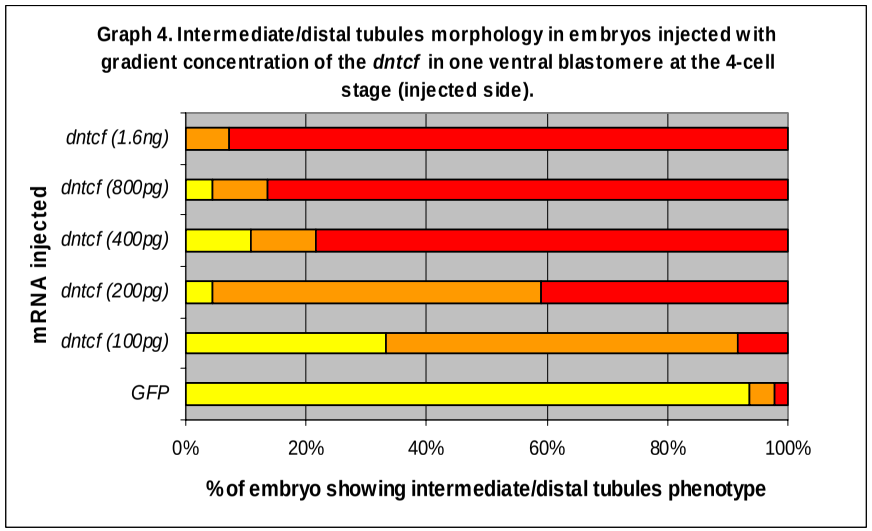

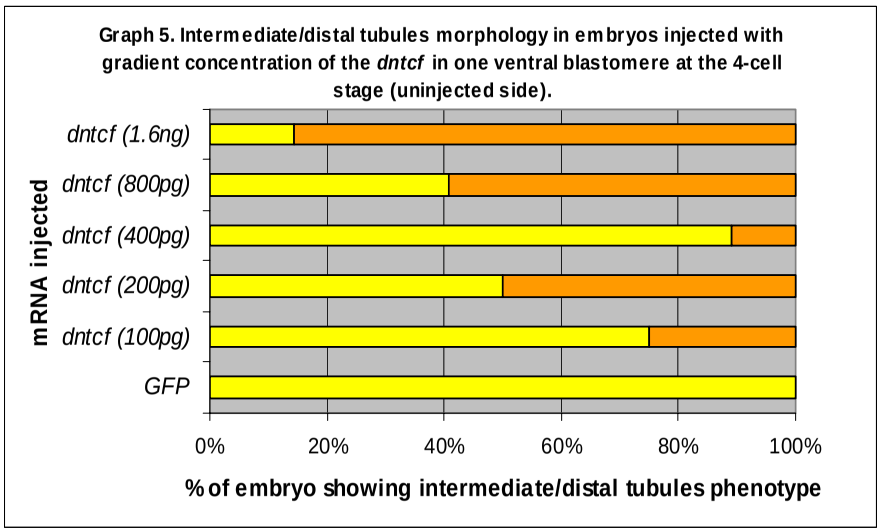

7.6.1 and graph 1). However, a large number of embryos were assayed in this study allowing the rejection of abnormally developing embryos. Figure 7.6, table 7.6.2 and graphs 2 to 5 show the number and percentage of embryos showing a pronephros phenotype when injected in one ventral blastomere at the 4-cell stage with 100pg to 1.6ng of *dntcf3* mRNA. Injection of *GFP* mRNA only, results in most embryos developing normal tubules structures on both the injected and the uninjected sides. However, injection of 100pg of *dntcf3* results in a large proportion of embryos developing reduced proximal tubules (67%) and reduced intermediate/distal tubules embryos (58%), on the injected side, while on the uninjected side, approximately 75% of the embryos showed normal pronephros morphology. Injection of 200pg of *dntcf3* results in half of the embryos developing reduced tubules, on both the injected and uninjected sides, and half of the embryos not developing any pronephric tubules at all. Injection of 400pg to 1.6ng of the *dntcf3* mRNA results in much more severe pronephric phenotypes. Abnormalities in pronephros formation were apparent in a dose-dependent manner. The number of embryos showing absence of pronephros formation increased with gradual increase of mRNA message concentration. On the injected side, 83%, 86% and 95% of embryos injected with 400pg, 800pg and 1.6ng of *dntcf3* show a complete absence of proximal tubules respectively. Similar results were obtained for the formation of intermediate/distal tubules. Pronephros formation was also affected to an extent on the uninjected side, the number of embryos showing reduced pronephric structure increased as the concentration of mRNA increased. 17%, 60% and 90% of embryos injected with 400pg, 800pg and 1.6ng of *dntcf3* showed reduced proximal tubules respectively, and intermediate/distal pronephros showed a similar profile.

All together, observations made on pronephric tubule morphology when *X. laevis* embryos were injected with the *dntcf3* mRNA, demonstrated that *dntcf3* affects kidney development in a dose-dependent manner. Embryos injected with a small concentration of message such as 100pg, showed a slight reduction of pronephric structures. However, embryos that received 200pg of *dntcf3* mRNA started to show severe reduction of tubule formation. When more than 400pg of *dntcf3* message was injected in *Xenopus* embryos, tubules formation was greatly affected, often resulting in total absence of tubule formation on the injected side but also in a dramatic reduction of tubule structures on the uninjected side. The abnormal pronephros phenotype observed on the uninjected side could be explained by the fact that *dntcf3*

disturbs the normal embryonic axis formation, and therefore affects the normal development of the pronephros on the uninjected side. However, there is a notable difference in the degree of severity of pronephros abnormality between the two sides of the embryos.
We next investigated whether or not *dntcf3* also affects glomus formation in *X. laevis* embryos.

7.4.2 Inhibition of the canonical *wnt* signalling using *dntcf3* over-expression disturbs the normal development of the pronephric glomus.

In order to determine whether or not *dntcf3* has an effect on the development of the glomus, embryos over-expressing the *dntcf3* mRNA were assayed by *in situ* hybridization using the specific glomus marker *Wilm's Tumor-1 gene (wt1).* The zinc-finger transcription factor encoded by the *Xenopus Wilms' tumor suppresser gene (wt1)* appears to be required primarily for podocyte development in the vascular component of the pronephros, the glomus (Carroll et al., 1996). *wt1* expression becomes visible by *in situ* hybridization around stage 18 in the *Xenopus* embryo and is restricted to the glomus until late tadpole stages, and is not visible in the pronephric tubules by *in situ* analysis (Carroll and Vize, 1996).
Figure 7.7 shows that inhibition of the canonical wnt signalling using the *dntcf3* disturbs the normal formation of the pronephric glomus. Embryos were co-injected in one ventral blastomere at the 4-cell stage with *GFP* mRNA and with 100 to 400pg of the *dntcf3* mRNA. Embryos were allowed to develop until stage 35 before being subjected to whole-mount *in situ* hybridization using the specific glomus marker, *wt1*. Although staining is weak, injection of *GFP* mRNA alone shows that *wt1* is expressed in a sickle-shaped pattern on both the injected (Fig 7.7 a) and the uninjected sides (Fig 7.7 b), indicating that injection of *GFP* mRNA alone does not affect the normal development of the pronephric glomus. However, injection of 100pg of the *dntcf3* results in a reduction in size of the glomus on the injected side (Fig 7.7 c) and in fairly normal glomus morphology on the uninjected side (Fig 7.7 d). Injection of 200pg of *dntcf3* mRNA also leads to a modification of the glomus shape on the injected side (Fig 7.7 e), while the glomus on the uninjected side retains fairly normal sickle-shape morphology (Fig 7.7 f). The same phenotype was observed when embryos were injected with 400pg of the *dntcf3* mRNA (Fig 7.7 g and h).

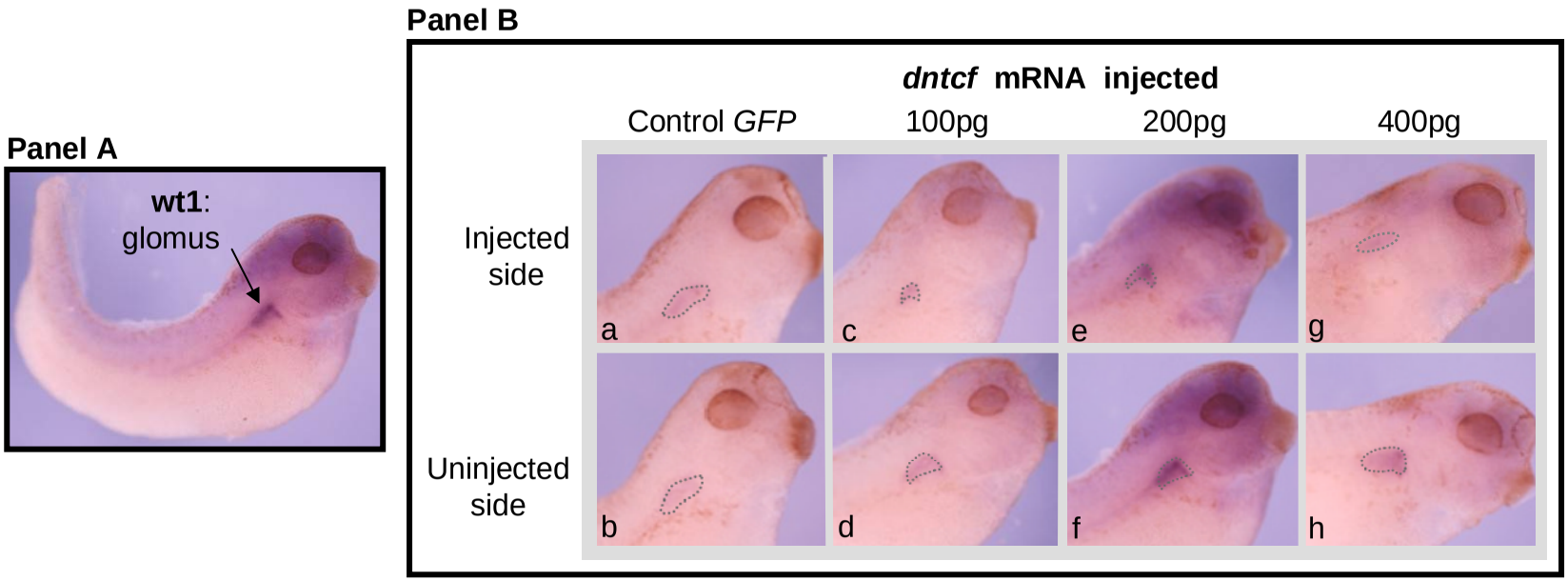

Figure 7.7 Inhibition of the canonical *wnt* signalling using *dntcf* disturbs pronephric glomus formation in *X. laevis* embryos. Embryos were co-injected into one ventral blastomere at the 4-cell stage with *GFP* mRNA and with 100 to 400pg of the *dntcf* mRNA. Embryos were allowed to develop until stage 35 before being subjected to whole-mount *in situ* hybridization using the specific glomus marker, *wt1.* Embryos injected with *GFP* mRNA only show weak staining but normal glomus morphology on both the injected and the uninjected sides (a, b). Injection of 100 to 400pg of the *dntcf* results in reduced glomus forming on the injected side, (c, e and g) and in fairly normal glomus morphology on the uninjected side (d, f and h).

Figure 7.8 Numerical and graphical representation of the glomus morphology in *X. laevis* embryos injected with various concentrations of the *dntcf3*. Embryos were injected into one ventral blastomere at the 4-cell stage embryo and left to develop until stage 35 before being analysed by whole-mount *in situ* hybridization using the specific glomus marker, wt*1*.

		Glomus morphology		
		Injected side		Uninjected side
mRNA injected		Normal	Reduced	Normal
GFP (1ng)	n=35	35	0	35
	%	**100**	**0**	**100**
dntcf3 (100pg)	n=38	27	11	38
	%	**71**	**29**	**100**
dntcf3 (200pg)	n=38	8	30	38
	%	**21**	**79**	**100**
dntcf3 (400pg)	n=44	7	37	44
	%	**16**	**84**	**100**

Table 7.8.1 Number and percentage of embryos showing glomus phenotype when injected in one ventral blastomere at the 4-cell stage with 100pg to 400pg of *dntc3f* mRNA.

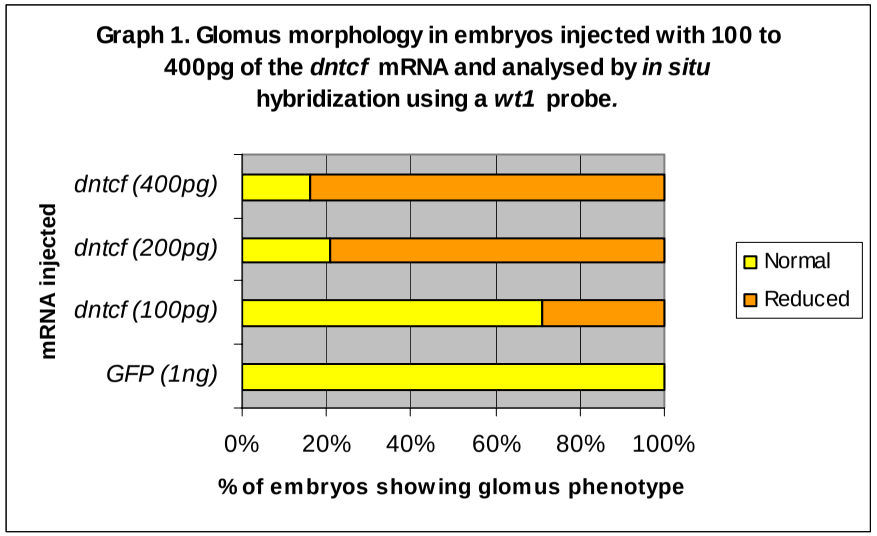

Graph1 shows the percentage of embryos showing glomus phenotype when embryos were injected with gradual increasing concentrations of the *dntcf3*.

In conclusion, injection of *dntcf3* mRNA into one single ventral blastomere at the 4-cell stage of *X. laevis* embryos results in disruption of normal glomus development. Figure 7.8 tabulates the glomus morphological disturbances observed in embryos over-expressing the *dntcf3* mRNA. Control embryos injected with *GFP* mRNA alone developed in 100% of the cases normal glomus morphology on both the injected and the uninjected sides. However, injection of 100pg of the *dntcf3* mildly affected the glomus formation and approximately 30% of the embryos developed a reduced pronephric glomus. Moreover, injection of 200pg to 400pg of the *dntcf3* mRNA resulted in approximately 80% of the embryos developing with reduced glomus.
To conclude, inhibition of the *wnt/ß-catenin* pathway using 100 to 400pg of the *dntcf3* results in embryos developing reduced pronephric glomus, indicating that *wnt/ß-catenin* pathway acting through activation of the *tcf* transcription factor is also required for the normal development of the third pronephric component, the glomus.
To summarise, inhibition of canonical *wnt* signalling affects the normal development of all the pronephric components, the glomus, the proximal, intermediate and distal tubules. Since *wnt6* has been shown to be continuously expressed in the forming pronephros (Chapter 4) and acts as an indirect pronephric inducer in Holtfreter sandwich cultures (Chapter 5), we have chosen to explore in more details the role of one particular canonical *wnt* molecule, *wnt6*, during pronephros development.

7.5 Spatial and temporal expression of *wnt6*, a canonical *wnt*, in *X. laevis* and *X. tropicalis* embryos.

The spatial and temporal *Xenopus* embryonic expression pattern of *wnt6* was elucidated by Lavery et al., (2008), who utilised a DIG-labelled LNA modified oligonucleotides probes, which are more sensitive than the conventional RNA *in situ* probes and can detect micro RNAs. Their result shows that *wnt6* is expressed during early organogenesis in the developing eye, heart and pronephros and is up-regulated in the epidermis overlaying these organs. We decided to confirm and extend this work by analysing the expression of *wnt6* in both *X. laevis* and *X. tropicalis* embryos using the classical *in situ* hybridization method and a *X. laevis* DIG-labelled antisense probe. A *wnt6* DNA clone was generously offered by the Hoppler lab. Figure 7.9 shows the temporal and spatial expression of *wnt6* during *X. laevis* and *X. tropicalis* development. Figure 7.9, panel A shows *in situ* hybridization analysis in

Panel A

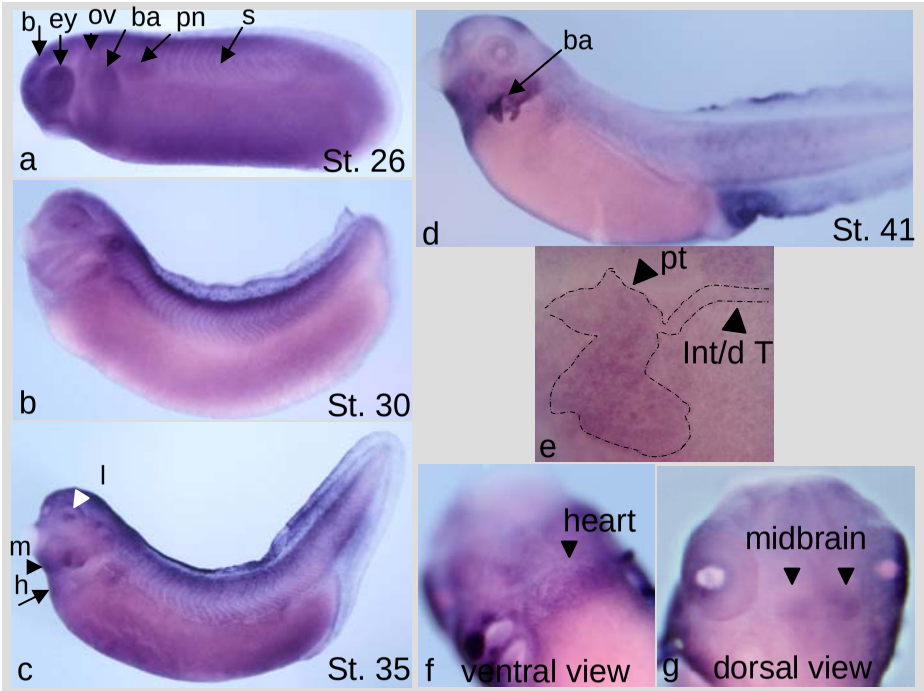

Panel B

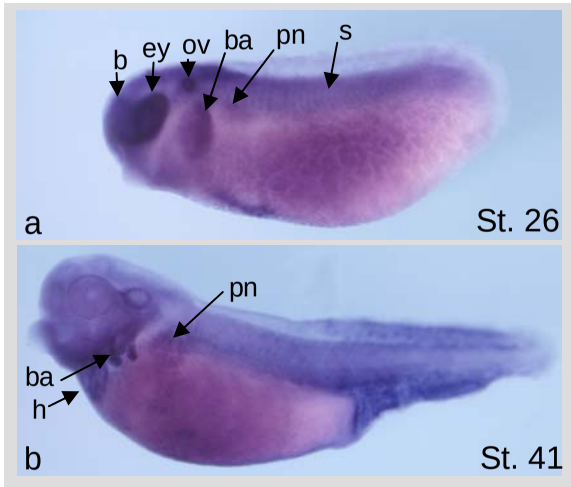

Key

b: brain. **ey**: eye. **ov**: otic vesicule.
pn: pronephros. **s**: somite.
h: heart. **l**: lens. **m**: mouth.
ba: branchial arches.

Figure 7.9 The temporal and spatial expression of *wnt6* during *X. laevis* and *X. tropicalis* development. Panel A shows *in situ* hybridization analysis in whole-mount *X. laevis* embryos using a DIG-labelled antisense probe. From stage 26, *wnt6* is expressed in the epidermis, the brain, the eye, the presumptive branchial arch, the pronephric anlagen, the somites, and weakly in the otic vesicule (a). *wnt6* expression pattern continues at later stage, stage 30 (b). At stage 35, *wnt6* starts to be expressed in the heart (c, arrow), in the mouth (black arrowhead) and its expression in the eye in refined to the lens (c, white arrowhead). By stage 41, *wnt6* expression remains in the epidermis, the pronephros, the heart, the branchial arches, the midbrain but weakens in the somites (d). High magnification of stage 41 embryos shows that *wnt6* is expressed in the pronephric proximal tubules (pt) and the pronephric intermediate/distal tubules (int/d T) after the epidermis was removed (e). A ventral view enhances the view of *wnt6* expression in the heart (f) and anterior dorsal view shows expression of *wnt6* in the midbrain (g). Panel B shows the expression of *wnt6* in *X. tropicalis* embryos at stage 26 and 41 using a *X. laevis* DIG-labelled antisense probe (a, b). *wnt6* expression in *X. tropicalis* embryos shows a similar pattern to that of *X. laevis* embryos.

whole-mount *X. laevis* embryos. From stage 26, *wnt6* is expressed in the epidermis, the brain, the eye, the presumptive branchial arch, the pronephric anlagen, the somites, and weakly in the otic vesicle (Fig 7.9 a). *wnt6* expression continues at later stage, stage 30 (Fig 7.9 b). At stage 35, *wnt6* starts to be expressed in the heart (Fig 7.9 c, arrow) and its expression in the eye is refined to the lens (Fig 7.9 c). By stage 41, *wnt6* expression remains in the epidermis, the pronephros, the heart, the branchial arches, the midbrain but weakens in the somites (Fig 7.9 d). High magnification of stage 41 embryos shows that *wnt6* is expressed in the pronephric proximal tubules (pt) and the pronephric intermediate/distal tubules (int/d T) after the epidermis was removed (Fig 7.9 e). A ventral view enhances the view of *wnt6* expression in the heart (Fig 7.9 f) and an anterior dorsal view shows expression of *wnt6* in the midbrain (Fig 7.9 g). With the aim of verifying that *wnt6* expression pattern was conserved between frog species (Massé et al., 2007), *wnt6* whole-mount *in situ* hybridization was carried out in *X. tropicalis* embryos at stage 26 and 41 using a *X. laevis* DIG-labelled antisense probe. Figure 7.9, panel B shows that expression of *wnt6* in *X. tropicalis* embryos follows exactly the spatial and temporal expression pattern of *wnt6* in *X. laevis* embryos (Fig 7.9, panel b, a- b).

To conclude, *wnt6* is broadly expressed in early *Xenopus* embryos, confirming the result of Lavery et al., 2008. *wnt6* expression persists from stage 26 to stage 35 in the epidermis, the brain, the branchial arches, the pronephros, and the somites. *wnt6* is also detected in the otic vesicle and the eye until stage 35, the stage around which *wnt6* starts to be expressed in the heart. At stage 41, the latest stage tested, *wnt6* is strongly expressed in the epidermis, the pronephros, the heart and the branchial arches.

wnt6 in situ hybridization in *X. laevis* and in *X. tropicalis* embryos has allowed the confirmation of results of Chapter 4, section 4.2.2 showing that *wnt6* is strongly expressed within the developing pronephros. In order to investigate what role *wnt6* plays in pronephros formation, a gain-of-function experiment was carried out in *X. laevis* embryos.

7.6 Over-expression of *wnt6* in the epidermis leads to abnormal pronephros formation.

With the aim of examining the potential role that *wnt6* might play in pronephros formation, mis-expression of *wnt6* in *X. laevis* embryos was carried out. Embryos were injected in the animal pole of one blastomere at the 2-cell stage with 1ng of *wnt6* mRNA. Fluorescent *GFP* lineage tracer was used to follow during development the cells that received the correct targeted mRNA. Thus, allowing the selection of correctly targeted embryos showing fluorescence in the epidermis overlying the pronephros. Embryos were left to develop until stage 40 before being assayed by immunostaining. Figure 7.10 shows that embryos over-expressing *wnt6* in the epidermis develop an abnormal pronephros. Figure 7.10, panel A shows a normal *X. laevis* embryo at stage 40 stained in purple with the specific pronephric proximal tubules antibody, 3G8 and in pink with the specific pronephric intermediate/distal tubules antibody, 4A6. Figure 7.10, panel B shows that injection of *GFP* mRNA alone results in normal pronephros morphology (Fig 7.10 a-b), suggesting that injection of *GFP* mRNA alone does not disturb the normal development of the pronephros. However, injection of 1ng of *wnt6* mRNA results in a complete absence of pronephric tubules on the injected side (Fig 7.10 c). The uninjected side also shows some signs of pronephric defect and the pronephric proximal, intermediate and distal tubules appear reduced (Fig 7.10 d). The abnormal pronephros phenotype observed on the uninjected side is caused by the severe defects that *wnt6* over-expression triggers on embryos general morphology. Figure 7.11, table 7.11.1 and graphs 1 and 2 give numerical and graphical representation of the pronephros phenotype in *X. laevis* embryos over-expressing 1ng of *wnt6* mRNA. Most of the embryos injected with *wnt6* (and even lower concentration as much as 0.25ng) develop abnormally showing abnormal axis formation, an abnormally large head or microhead and form an oedema, indicative of reduced kidney function. The abnormal general embryos morphology does not allow an accurate scoring of the pronephros phenotype. Thus, even if the original set up of the experiment assayed a large number of embryos injected with various concentrations of the *wnt6* message, only the embryos with reasonably normal morphology and fairly normal pronephros phenotype on the uninjected side were taken in consideration in this study. Injection of *GFP* mRNA alone results in 100% of embryos developing normal pronephros on

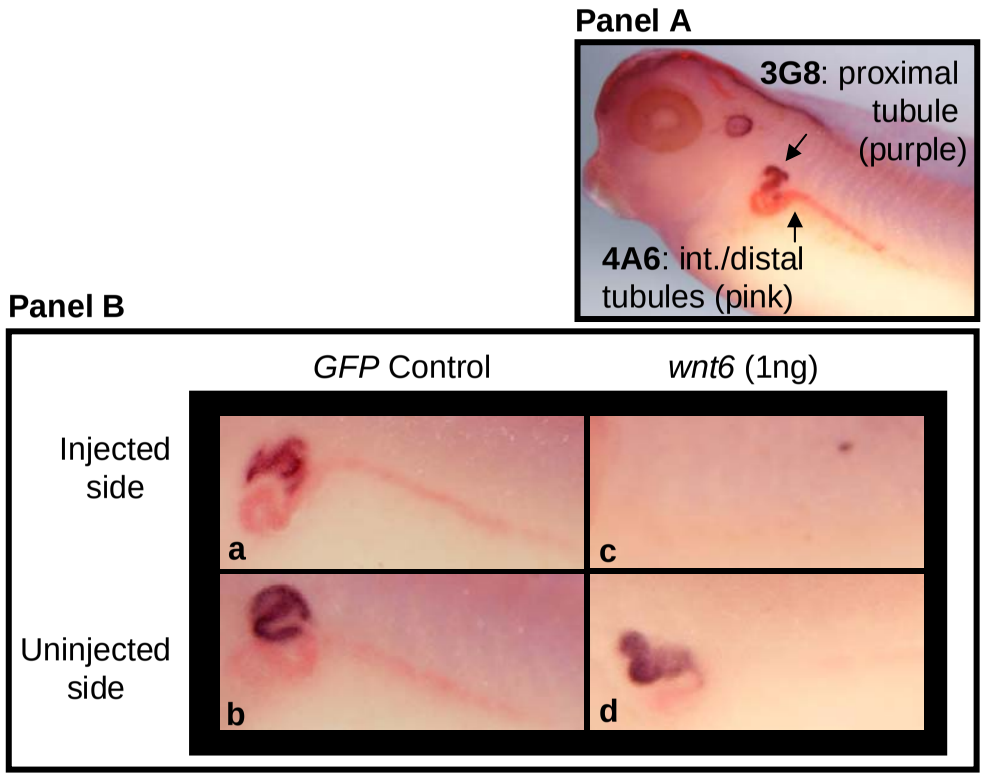

Figure 7.10 Embryos over-expressing *wnt6* in the epidermis develop an abnormal pronephros. Embryos were injected in the animal pole of one blastomere at the 2-cell stage with *GFP* mRNA and with or without 1ng of *wnt6* mRNA. Embryos were left to develop until stage 40 before being assayed by immunostaining. Panel A shows a normal *X. laevis* embryos at stage 40 stained with the specific pronephric proximal tubules antibody, 3G8 (purple) and with the specific pronephric intermediate/distal tubules antibody, 4A6 (pink). Panel B shows that injection of *GFP* mRNA alone does not disturb pronephric development (a-b). However, injection of 1ng of *wnt6* mRNA results in an absence of pronephric tubules on the injected side (c), while the uninjected side also shows signs of pronephric defect (d). This is caused by the gross axial defects triggered by *wnt6* over-expression.

Figure 7.11 Numerical and graphical representation of the pronephros phenotype in *X. laevis* embryos over-expressing 1ng of *wnt6* mRNA in the epidermis. Embryos were injected into the animal pole of one cell at the 2-cell stage and left to develop until stage 40 before being analysed by antibody staining using the specific proximal tubule antibody 3G8 and the specific intermediate and distal tubules antibody 4A6.

		Proximal tubule morphology						**Intermediate/distal tubule morphology**				
		Injected side				Uninjected side		Injected side			Uninjected side	
mRNA injected		Normal	Reduced	Enlarged	Absent	Normal	Reduced	Normal	Reduced	Absent	Normal	Reduced
GFP (1ng)	n=80	80	0	0	0	80	0	80	0	0	80	0
	%	**100**	**0**	**0**	**0**	**100**	**0**	**100**	**0**	**0**	**100**	**0**
wnt6 (1ng)	n=44	8	31	3	2	15	29	4	19	21	12	32
	%	**18**	**70**	**7**	**5**	**34**	**66**	**9**	**43**	**48**	**27**	**73**

Table 7.11.1 Number and percentage of embryos showing pronephros phenotype in embryos injected in the animal pole of one cell at the 2-cell stage with 1ng of *wnt6* mRNA.

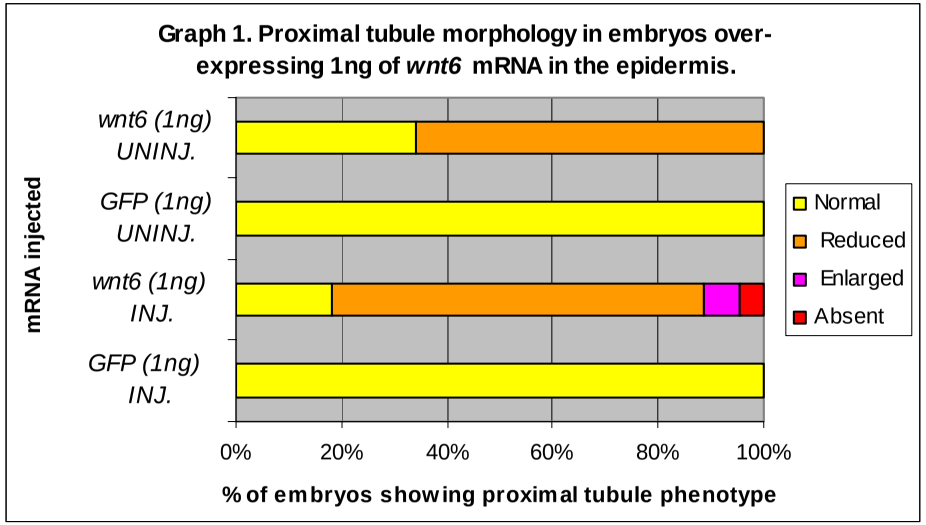

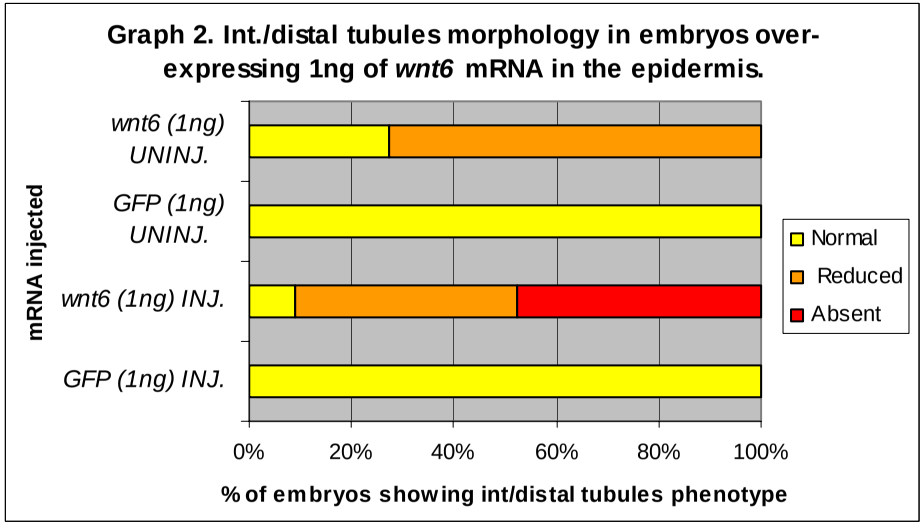

Graphs 1 and 2 show the proximal tubule and the intermediate/ distal tubules phenotype in embryos injected in the animal pole of one cell at the 2-cell stage with 1ng of *wnt6* mRNA.

both the injected and the uninjected sides. However, injection of 1ng of *wnt6* mRNA disturbs the normal development of the pronephros. Approximately 70% of the embryos developed reduced proximal tubules on both the injected and the uninjected sides. On the injected side, about half of the embryos developed reduced intermediate/distal tubules and half of the embryos did not form intermediate/distal tubules, while on the uninjected side approximately 70% of the embryos formed reduced intermediate/distal tubules.

To conclude, results suggest that *wnt6* might have a role in pronephros formation since unbalanced levels of *wnt6* mRNA in the epidermis of one side of the embryos results in much reduced pronephric tubules.

7.7 Discussion.

7.7.1 Inhibition of the canonical *wnt* pathway using the *dntcf3* leads to abnormal embryo morphology and abnormal pronephros formation.

Members of the *wnt/ß-catenin* pathway have been shown to function during mammalian metanephros formation. For example, mouse *wnt7b* is expressed within the epithelia of the ureteric bud and collecting duct (Kispert et al., 1996) and *wnt7b* homozygote mutant mice die prior to the onset of metanephric development due to kidney failure (Parr et al., in 2001).

In order to analyse the effects of interfering with this pathway in *Xenopus* pronephros, *dntcf3* mRNA was over-expressed in one single ventral blastomere at the 4-cell stage embryo. Inhibition of *tcf* transcription factor activity caused severe axis formation defects in a dose-dependent manner. Embryos showed abnormal head structures and were missing substantial amounts of the normal anterior-posterior and dorso-ventral axes. These axes are essentially required for the development of the embryo, consequently a loss of the anterior-posterior and dorso-ventral axes lead to a high mortality rate (data not shown). In order to maximise the normality of the whole embryo, embryos were injected with 100 to 400pg of *dntcf3* mRNA that produced viable embryos. However, many embryos still showed morphological abnormalities.

The use of specific pronephric markers demonstrated that blocking *tcf* activity causes abnormal kidney formation. Firstly, we looked at the terminal differentiation of the *Xenopus* embryos pronephros (stage 41), using the monoclonal antibodies, 3G8 and

4A6. Embryos injected with the *dntcf3* mRNA showed two major phenotypes, an absence of proximal tubule formation and a dramatic reduction of intermediate/distal tubules structure or severe reduction in all tubules depending on the dose of *dntcf3* mRNA previously injected. This result suggests that *tcf* transcription factor activity of the *wnt/ß-catenin* pathway is required for normal formation of the pronephric tubules.

We wanted to establish when the effects of the *dntcf3* mRNA first become apparent in *Xenopus* pronephros development. Published studies of Carroll and Vize in 1999 have established that *lhx1* and co-factor *pax8* are expressed in pronephric precursors and could be used as pronephric markers. Whole-mount *in situ* hybridization using the *lhx1* probe in embryos injected with *dntcf3* and fixed at key stages of embryonic development revealed that *dntcf3* effects on pronephros morphology first appeared in late neurula stages, around stage 20 and gave rise to the phenotype of absence and reduction of the pronephric anlagen. This result was confirmed by using *pax8 in situ* hybridization probe (data not shown). However, we know that specification of proximal tubule happens at stage 12.5 and specification of intermediate/distal tubules at stage 14 (Brennan et al., 1999). We hypothesise that *dntcf3* could act during the early steps of tubules and duct specification. We were actually unable to provide any direct evidence showing that *dntcf3* plays a role in pronephric anlagen specification since the marker genes which indicate that specification has taken place are switched on at this time.

Examination of the third pronephric component, the glomus, in embryos over-expressing the *dntcf3* using the specific glomus marker *wt1* as an *in situ* hybridization probe, revealed that the *tcf* transcription factor activity also plays a role in glomus formation, suggesting that the whole pronephric anlagen was affected. As a matter of fact, injection of *dntcf3* in *Xenopus* embryos resulted in absence or in reduction of glomus structure in a dose-dependent manner. Using the specific glomus marker, *wt1*, Brennan et al., in 1999 have shown that glomus is specified between stages 12 and 12.5. As explained above, we were unable to show that *dntcf3* plays an early role in glomus anlagen specification.

7.7.2 Spatial and temporal expression of *wnt6* in *X. laevis* and *X. tropicalis* embryos.

The spatial and temporal expression pattern of *wnt6* during early development of *X. laevis* embryos has been recently published by Lavery et al., 2008. As Wolda and Moon, 1992, they had difficulties in getting convincing and reliable results using conventional RNA probe *in situ* hybridization and suggested that it might be due to low abundance and secondary structure of the *wnt6* mRNA molecule. Therefore, they developed a novel whole-mount *in situ* hybridization approach using LNA probes, which have an increased affinity for RNA molecules.

Before the work of Lavery et al. was published, we also tried, one more time, to obtain the expression pattern of *wnt6* during *Xenopus* embryogenesis using the traditional DIG-labelled antisense RNA *in situ* probes and present reasonably reliable data. The difficulty we encountered in getting clear *wnt6* expression pattern relied on its expression in multiple organs and in the epidermis that covers the entire embryo. The timing for developing the colour reaction had to be carefully followed, as too short a development time would have resulted in weak staining leading to difficulties in examining accurately *wnt6* expression pattern and too long would have resulted in a very strong expression in the epidermis that would have hidden *wnt6* expression in other organs. However, we were unable to provide any evidence for *wnt6* expression before the embryos reached tailbud stage, (stage 26). This result is consistent with the temporal and quantitative expression analysis of *wnt6* using quantitative PCR showing that *wnt6* expression level peaks around stage 28 (Lavery et al., 2008 and this thesis, Chapter 4, section 4.2.2).

Overall, the published *wnt6* expression pattern and this work show similar results. Nonetheless, the published data show that *wnt6* can be detected in the ectoderm overlaying the developing heart as early as stage 28, whereas, we could not detect *wnt6* expression in the heart before stage 35. Similarly, Lavery et al., showed that *wnt6* is expressed in the pronephric anlagen at stage 23, while our *in situ* probe could detect *wnt6* in the pronephric tubules at stage 28 only. However, we can confirm that *wnt6* expression overcomes spatial refinements during the development of the eye, and is firstly observed broadly in the eye primordial, secondly around stage 35, in the lens, then around stage 41, seems to disappear from the lens itself by migrating to the surrounding of the lens. However, as the published data, sectioning of the head within few stages of development could fully confirm this dynamic expression

pattern of *wnt6* within the developing ocular system. Finally, our *in situ* analysis identifies one new expression domain of *wnt6* expression in the head. Our result shows that, for the first time, *wnt6* was detected in the otic vesicle from stage 28 to stage 35 and was also strongly expressed within the developing brain. A dorsal view of stage 41 embryos shows that *wnt6* is expressed in the midbrain. Sectioning would be required to confirm this last result.

7.7.3 *wnt6* plays a role of in *X. laevis* pronephros formation.

We have shown that over-expression of even as a small quantity as 0.25ng of *wnt6* mRNA in one animal pole of two cell stage *Xenopus* embryos, that will later on in development give rise to the epidermis, has an effect on the normal development of the embryos and on the pronephros formation. Mainly, we observed that such embryos developed reduced proximal tubules and reduced or no intermediate/distal tubules on the injected side. This result suggests that *wnt6* plays a role in pronephros formation and that unbalanced level of *wnt6* signalling from the epidermis generates severe embryonic kidney malformation. A role for *wnt6* in kidney formation was also observed in mouse embryos. *wnt6* was shown to be expressed in the ureter bud and throughout the bud during ingrowth of the epithelium into the nephric mesenchyme and in the branching ureter tip during subsequent development. Cell lines that expressed *wnt6* induce tubulogenesis and express early induction kidney markers (Itäranta et al., 2002). These observations suggest that *wnt6* might have a conserved role in kidney formation in several vertebrate species.

Chapter 8 General Discussion

The aim of this thesis was to identify the *wnt* signalling molecules involved in the formation of the primary kidney form, the pronephros. The *wnt* molecules expressed in early pronephric anlagen and in the anterior somites, the tissues responsible for kidney induction, were analysed in a kidney induction assay using Holtfreter sandwich cultures. Finally, within the developing pronephros *in vivo*, the function of non-canonical *wnt11b* and the canonical *wnt6*, both being capable of inducing the intermediate mesoderm to become kidney in *in vitro* assay, was investigated by gain and loss-of-function experiments.

8.1 *wnt4*, required for nephrostome and glomus formation.

The results of *wnt4* Holtfreter sandwich cultures are very surprising, as there are several lines of evidence which suggest that *wnt4* could be a pronephric inducer. During embryogenesis, *wnt4* was shown to be critically required for pronephros and metanephros tubulogenesis (Saulnier et al., 2002, Stark et al., 1994). In mouse embryos, *Wnt4* was shown to be required for tubule formation, and sufficient to trigger tubulogenesis in isolated metanephric mesenchyme (Kispert et al., 1998). In this work, we have shown that *wnt4* is expressed throughout pronephros formation from stage 15 onwards and is also equally expressed in anterior and posterior somites at stage 17. Thus, when we tested whether or not *wnt4* could form kidney when over-expressed in two animal caps and cultured with unspecified intermediate mesoderm, we were surprised to observe that no pronephric tubules were formed. However, the number of sandwich cultures assayed for tubule formation was small and therefore the experiment should be repeated to confirm this result. Or, it is possible that *wnt4* does not act as a pronephric inducer and carries out other functions during pronephros formation. As it was previously shown, over-expression of 0.25ng of *wnt4* into a single V2 blastomere at the 8-cell stage resulted into fused nephrostomes (Saulnier et al., 2002). Additionally, in our lab, it was recently shown that over-expression of 1ng of *wnt4* into a single V2 blastomere at the 8-cell stage resulted in

ectopic formation of nephrostomal and glomeral tissues and in drastic reduction of proximal/intermediate and distal tubular tissues. These results suggest that *wnt4* is likely to be required for nephrostome and glomus formation rather than proximal/ intermediate and distal pronephric tubule formation (Naylor and Jones, personal communication). This might explain why no pronephric proximal, intermediate or distal tubules were observed in *wnt4* Holtfreter sandwich cultures.

8.2 *wnt8,* indirect pronephric inducer.

In the literature *wnt8* has never been described to have a role during kidney formation. *wnt8* has been shown to play a role in dorsoventral patterning of *Xenopus* embryos, normally functioning to specify a ventral fate to newly induced mesoderm (Christian et al., 1992, Moon and Christian, 1992). In this work, *wnt8* was shown to be expressed in the pronephric anlagen but only from stage 12.5 to 20 and was detected more strongly in the posterior somites than in the anterior somites. These data suggested that *wnt8* would be unlikely to control the early events of pronephros formation. However, *wnt8* Holtfreter sandwich cultures showed very unexpected results and formation of pronephric tubules was observed in a highly significant frequency. The formation of somites in such cultures should be investigated to explain this result but we hypothesize that *wnt8* is capable of indirectly inducing pronephric tubules in Holtfreter cultures. In fact, *wnt8* sandwich cultures showed tail-like structure, possibly containing notochord structure and *wnt8* was previously shown to be able to divert the fate of the prospective notochord cells along a more ventral fate perhaps directing these cells to differentiate as muscle rather than notochord (Moon and Christian, 1992).

8.3 *wnt6,* a somite epithelialisation factor from the ectoderm, acts as an indirect pronephric inducer.

In this work, we have shown that inhibition of the canonical *wnt* signalling pathway affects the normal development of all the pronephric components, the glomus, the proximal, intermediate and distal tubules. We have chosen to investigate the role of one particular canonical *wnt* molecule, *wnt6,* during pronephros formation. RT-PCR analysis revealed that *wnt6* is expressed throughout pronephros formation from stage

15 onwards. However, *wnt6* was not detected in somites in embryos at stage 17, and this result was confirmed by *in situ* hybridization, although less sensitive than RT-PCR analysis, showing that *wnt6* expression in whole embryo could not be detected before stage 23 (Lavery et al., 2008) and in this work before stage 26. More importantly, *wnt6* was shown to be required for the epithelialisation leading to somite formation and subsequent compartmentalisation into the sclerotome and the dermomyotomes (Schmidt et al., 2004, Geetha-Loganathan et al., 2005, Schubert et al., 2002, Rodríguez-Niedenführ et al., 2003). Holtfreter sandwich cultures have allowed us to show that *wnt6* over-expressed in two ectoderm wraps and cultured with unspecified intermediate mesoderm, was capable of inducing somite formation that is likely, in turn, to induce pronephric tubule formation. From these results, we would like to suggest that *wnt6* might act as a somite epithelialisation factor from the ectoderm, that ultimately generates somite formation which can then induces pronephros formation. This hypothesis correlates with the expression of *wnt6* in the ectoderm throughout *Xenopus* embryo development and in the somites later on, from stage 23 onwards and in the migrating hypaxial muscle at stage 40-43 (Lavery et al., 2008).

8.4 *wnt11b*, direct pronephric inducer, regulates morphogenetic movements with *wnt11* during pronephros formation.

In this thesis, we have shown that *wnt11b* is expressed throughout pronephros development and equally in anterior and posterior somites in embryos at stage 17. However, the closely related *wnt11* gene is expressed later in pronephros, from stage 25 onwards and is more expressed in anterior somites than in posterior somites. Interestingly, both genes were capable to directly induce pronephric tubules formation in Holtfreter sandwich cultures without forming muscle. This result suggested that *wnt11* and *wnt11b* share some biological activity and can act as pronephric inducers in *in vitro* Holtfreter sandwich cultures. Ironically, in mouse embryos *wnt11*, which is expressed in the tip of the growing ureter, is not sufficient to trigger tubulogenesis in isolated metanephric mesenchyme (Kispert et al., 1998). Because in *Xenopus* embryos, *wnt11* is not expressed before pronephros differentiation (stage 25), it is possible that *wnt11* does not act as a true pronephric

inducer but has the same biological activity as *wnt11b* and can insure identical function if displaced.

In vivo, inhibition or gain-of-function of *wnt11b* gave similar pronephric phenotype, resulting in deregulation of normal pronephrogenesis with embryos showing, in the injected side, a reduction or an absence of pronephros. This observation suggests that *wnt11b* is required for normal pronephros morphogenesis and that perhaps the level of this requirement needs to be finely balanced. Although, the frequency of abnormal pronephros was moderated when the *dnwnt11b* was injected. This result suggested that inhibition of *wnt11b* alone was not sufficient to inhibit the pronephros formation and that the very closely related *wnt11b* gene might be compensating for the defects caused by inhibition of *wnt11b*. This idea was confirmed by co-injection of 15ng of each *wnt11b* and *wnt11* morpholinos. Embryos showed that reduction of pronephric tubules formation was greatly accentuated when compared to the embryos injected with 15ng of *wnt11* or *wnt11b* morpholino alone. This experiment showed that *wnt11* and *wnt11b* have redundant functions, and it is possible that *wnt11b* and *wnt11* can compensate for each other in pronephros formation.

The question that arises from these studies is why over-expression of *wnt11b* in animal caps cultured with intermediate mesoderm lead to formation of pronephric tubules, while *in vivo,* over-expression of *wnt11b* in one ventral blastomere at the 8-cell stage does not lead to formation of ectopic pronephric tubules? One possible explanation could be that *wnt11b* might be required twice during pronephros formation. The first time, *wnt11b* gives the signal to the intermediate mesoderm to become kidney. As *wnt11b* induces the presumptive renal cells, more inducing signal would not induce more cells. This could be due to the availability of the correct receptor and so the cells reach a “plateau effect” due to saturation of the receptors. Secondly, *wnt11b* would act to regulate the normal morphogenetic movement throughout pronephros formation. Thus, excess or deficiency of the level of *wnt11b* would result in blocking cell movement, leading to a phenotypically disturbed pronephric anlagen, rather than ectopic tissue.

8.5 *wnt5a*, modulator of morphogenetic movements during pronephros development.

WNT5A has been detected in the mesonephros of 38-day human embryos and also in the forming metanephros, in the mesenchyme surrounding the Müllerian duct, the Wolfian duct and the nephric tubule (Danielson et al., 1995). So far, in *Xenopus* embryos, *wnt5a* has never been shown to be involved in pronephros formation and its role during embryogenesis was been attributed to modulation of morphogenetic movements (Moon et al., 1993) through the activating a non-canonical *wnt* pathway (Wallingford et al., 2001, Slusarski et al., 1997). In this work, although *wnt5a* has been shown to be expressed throughout pronephros formation from stage 12.5, *wnt5a* is expressed only in posterior somites and does not induce pronephros formation when over-expressed in animal caps and cultured with intermediate mesoderm. Thus, it is possible that the role of *wnt5a* during pronephros formation is to direct cells movements to enable correct morphology in the aim of forming a functional organ.

8.6. *wnt9a* and *wnt9b,* general organizing molecules of the pronephros.

In the mouse embryo, *Wnt9b* is mainly restricted to the kidney (Qian et al., 2003) and has been shown to be responsible for the induction of the metanephric mesenchyme and the generation of a functional female reproductive tract (Carroll et al., 2005).
In *Xenopus* embryos, RT-PCR analysis in whole embryos, showed that *wnt9a* is strongly expressed continually from stage 13 onwards while *wnt9b* is weakly detectable at stage 13 and becomes strong from stage 19 onwards. In isolated pronephric anlagen, *wnt9a* and *wnt9b* are both expressed throughout pronephros formation. *wnt9a* is expressed in the pronephros anlagen from stage 15 until stage 35 and appears to be up-regulated twice, once at stage 25 and once at stage 35. *wnt9b* is weakly detected in the pronephros at stage 15, but shows significant expression from stage 20 that remains constant until stage 35. *In situ* analysis confirmed the presence of *wnt9a* and *wnt9b* mRNA in the pronephros of both *Xenopus* species tested and although relatively late, were detectable from stage 30-35 onwards. At stage 17, *wnt9a* is not expressed in somites, however its expression in whole embryo at stage 17 should have been detected since we showed previously that *wnt9a* is strongly expressed in whole embryo from stage 13 onwards. This apparent anomaly is possibly due to a poor quality cDNA sample. *wnt9b* showed weak expression in the

anterior somites but is absent in the posterior somites. *wnt9b* is in fact weakly expressed in whole embryo at stage 17, as we have seen before that its zygotic expression peaks only from stage 19.
In adult tissue, *wnt9a* is expressed in almost all tissues but is relatively stronger in the eye and kidney, while *wnt9b* is much more tissue restricted to the eye, kidney, stomach and reproductive organs. All together these results lift up the issue raised by Garriock et al., 2007, in which they point out that the *wnt9b* renal expression pattern looked variable between mouse and *Xenopus* species. We have been able to confirm several times that *wnt9b* is expressed in the embryonic and adult *Xenopus* kidney and this is consistent with studies in mouse in which *Wnt9b* was shown to be strongly expressed in the kidney and the reproductive organs (Qian et al., 2003, Carroll et al., 2005).

Moreover, over-expression of *wnt9b* in one V2 blastomere at the 8-cell stage or into one animal pole at the 2-cell stage of *Xenopus* embryos, resulted in drastic reduction of the pronephric proximal and intermediate/distal tubules. Disorganised intermediate/distal tubules were observed in approximately 30% of the embryos, indicating that *wnt9b* might act as a pronephric organiser. This is again consistent with the studies carried out in mouse embryos, showing that *Wnt9b* is involved in multiple aspects of metanephros formation by acting as a general organisation signal for the elaboration of several distincts components of the mouse urogenital system (Carroll et al., 2005).

However, despite numerous attempts to generate *wnt9b* Holtfreter sandwich cultures with the aim of testing whether or not *wnt9b* over-expressed in two animal caps could induce the intermediate mesoderm to become kidney, none of the cultures survived and regrettably could not be tested for tubule formation. We would speculate that *wnt9b* would induce pronephric tubules formation in Holtfreter sandwich cultures since it is expressed in both the early pronephric anlagen and the anterior somites and is also capable of inducing a secondary axis when over-expressed in one ventral blastomere at 4-cell stage embryos. This suggests that *wnt9b* could induce formation of dorsal structure and therefore induce indirectly pronephros formation as it was observed for the other canonical *wnt* molecules, *wnt6* and *wnt8*.

However, not enough information is available to predict whether or not *wnt9a* would have this ability.

8.7 *wnt7b*, possibly required for pronephros differentiation.

wnt7b was shown to induce neural crest markers in *Xenopus* embryos (Chang and Hemmati-Brivanlou, 1998), tubulogenesis in cell lines (Kispert et al., 1998) but its expression in the embryonic mouse collecting ducts makes it unlikely to be involved in inductive events between the ureter and the mesenchyme (Kispert et al., 1996). In this thesis, we showed that *wnt7b* is expressed only late within the pronephric anlagen (stage 25 onwards), not at all in the somites and does not induce pronephric tubules formation in Holtfreter sandwich cultures. This results suggest that *wnt7b* is unlikely to play a role during the early events that control pronephros formation, but is possibly involved during later event such as pronephros differentiation.

8.8 Conclusion.

To conclude, we would like to suggest a simple model of the interactions of the *wnt* signalling molecules during the early events of the *Xenopus* pronephros formation. The model is based on the knowledge from the literature of the *wnt* signalling molecules during organogenesis in several vertebrate species, on the temporal expression of the *wnt* molecules in the *Xenopus* prospective pronephric anlagen, in the pronephros and in the somites, on the ability of the *wnt* molecules to induce or not pronephric tubules formation in Holtfreter sandwich cultures and on the consequences of inhibiting *wnt* signalling pathways in whole *Xenopus* embryo. The model is shown in figure 8.1. In this model, *wnt4* would be required for the glomus and nephrostomes formation. *wnt6* would acts as an indirect pronephric inducer not from the somites but from the ectoderm. *wnt8* might potentially as well act as an indirect pronephric inducer by dorsalising mesoderm. *wnt11b* could act as a direct pronephric inducer and would have the unique potentiality to directly commit the cells from intermediate mesoderm to form pronephric tubules and would act throughout pronephros development with the complementary function of *wnt11* in regulating cell movements to result in the formation of a functional organ. *wnt5a* would be required as well, all way through pronephros development for normal cell

movements. *wnt7b* would act only later on, around stage 25, the stage of pronephros differentiation. Finally, *wnt9b* would act as a general organizer and its potentiality in inducing pronephric tubule formation is still yet unknown. The number of the *wnt* molecules chosen in this study is not exhaustive, and it is possible that some other *wnt* molecules are involved during pronephros formation. However, this study has clearly given evidences that both canonical and non-canonical *wnt* molecules are required for normal pronephros formation and perhaps the requirement for one molecule from another might be regulated by availability of the frizzled receptors.

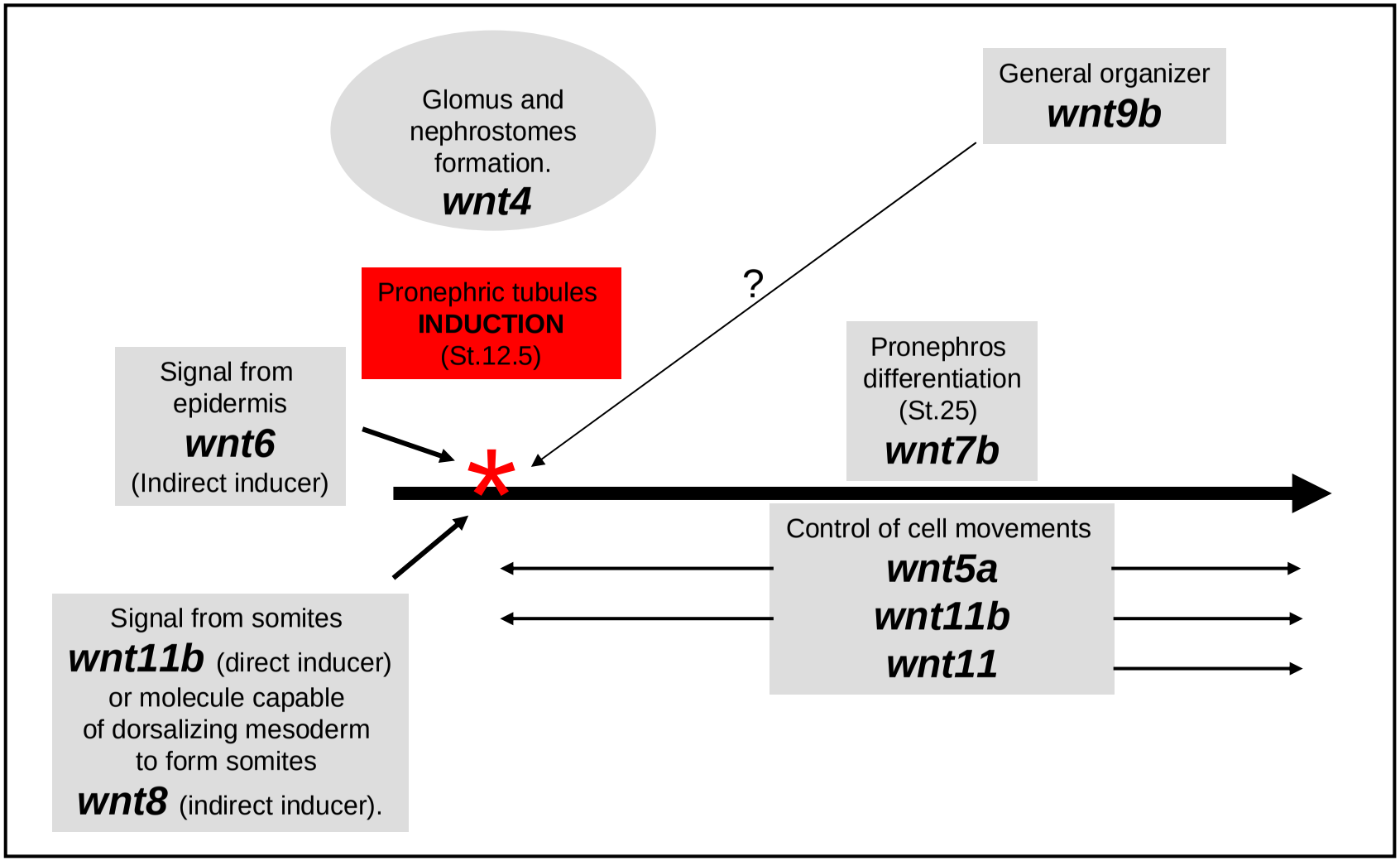
Glomus and
nephrostomes
formation.
wnt4
General organizer
wnt9b
?
Pronephric tubules
INDUCTION
(St.12.5)
Signal from
epidermis
wnt6
(Indirect inducer)
Pronephros
differentiation
(St.25)
wnt7b
*
Control of cell movements
wnt5a
wnt11b
wnt11
Signal from somites
wnt11b (direct inducer)
or molecule capable
of dorsalizing mesoderm
to form somites
wnt8 (indirect inducer).

Figure 8.1 Simple view of the role of the *wnt* signalling molecules during early *Xenopus* pronephros formation. *wnt4* would be required for the glomus and nephrostomes formation. *wnt6* would acts as an indirect pronephric inducer not from the somites but from the ectoderm. *wnt8* might potentially as well act as an indirect pronephric inducer by dorsalising mesoderm. *wnt11b* could act as a direct pronephric inducer and would have the unique potentiality to directly commit the cells from intermediate mesoderm to form pronephric tubules and would act throughout pronephros development with the complementary function of *wnt11* in regulating cell movements to result in the formation of a functional organ. *wnt5a* would be required as well, all way through pronephros development for normal cell movements. *wnt7b* would act only later on, around stage 25, the stage of pronephros differentiation. Finally, *wnt9b* would act as a general organizer and its potentiality in inducing pronephric tubule formation is still yet unknown.

References

Axelrod, J. D., Miller, J. R., Shulman, J. M., Moon, R. T. and Perrimon, N. (1998). Differential recruitment of Dishevelled provides signaling specificity in the planar cell polarity and Wingless signaling pathways. *Genes Dev* **12**, 2610-22.

Bafico, A., Liu, G., Yaniv, A., Gazit, A. and Aaronson, S. A. (2001). Novel mechanism of Wnt signalling inhibition mediated by Dickkopf-1 interaction with LRP6/Arrow. *Nat Cell Biol* **3**, 683-6.

Bang, A. G., Papalopulu, N., Kintner, C. and Goulding, M. D. (1997). Expression of Pax-3 is initiated in the early neural plate by posteriorizing signals produced by the organizer and by posterior non-axial mesoderm. *Development* **124**, 2075-85.

Barnett, M. W., Old, R. W. and Jones, E. A. (1998). Neural induction and patterning by fibroblast growth factor, notochord and somite tissue in Xenopus. *Dev Growth Differ* **40**, 47-57.

Barrett, K., Leptin, M. and Settleman, J. (1997). The Rho GTPase and a putative RhoGEF mediate a signaling pathway for the cell shape changes in Drosophila gastrulation. *Cell* **91**, 905-15.

Bassez, T., Paris, J., Omilli, F., Dorel, C. and Osborne, H. B. (1990). Post-transcriptional regulation of ornithine decarboxylase in Xenopus laevis oocytes. *Development* **110**, 955-62.

Bejsovec, A. (2000). Wnt signaling: an embarrassment of receptors. *Curr Biol* **10**, R919-22.

Bellefroid, E. J., Kobbe, A., Gruss, P., Pieler, T., Gurdon, J. B. and Papalopulu, N. (1998). Xiro3 encodes a Xenopus homolog of the Drosophila Iroquois genes and functions in neural specification. *Embo J* **17**, 191-203.

Boutros, M., Paricio, N., Strutt, D. I. and Mlodzik, M. (1998). Dishevelled activates JNK and discriminates between JNK pathways in planar polarity and wingless signaling. *Cell* **94**, 109-18.

Bradley, R. S. and Brown, A. M. (1990). The proto-oncogene int-1 encodes a secreted protein associated with the extracellular matrix. *Embo J* **9**, 1569-75.

Brändli, A. W. (1999). Towards a molecular anatomy of the Xenopus pronephric kidney. *Int J Dev Biol* **43**, 381-95.

Brennan, H. C., Nijjar, S. and Jones, E. A. (1998). The specification of the pronephric tubules and duct in Xenopus laevis. *Mech Dev* **75**, 127-37.

Brennan, H. C., Nijjar, S. and Jones, E. A. (1999). The specification and growth factor inducibility of the pronephric glomus in Xenopus laevis. *Development* **126**, 5847-56.

Brophy, P. D., Ostrom, L., Lang, K. M. and Dressler, G. R. (2001). Regulation of ureteric bud outgrowth by Pax2-dependent activation of the glial derived neurotrophic factor gene. *Development* **128**, 4747-56.

Burns, R.K. (1955). Urogenital system: analysis of development B. J. Willier, P. Weiss and V. Hamburger, eds, 462-491. Saunders, Philadelphia.

Cadigan, K. M. and Liu, Y. I (2006). Wnt signalling: complexity at the surface. *J. Cell Sci.* **119**, 395-402

Carroll, T. J., Park, J. S., Hayashi, S., Majumdar, A. and McMahon, A. P. (2005). Wnt9b plays a central role in the regulation of mesenchymal to epithelial transitions underlying organogenesis of the mammalian urogenital system. *Dev Cell* **9**, 283-92.

Carroll, T. J. and Vize, P. D. (1996). Wilms' tumor suppressor gene is involved in the development of disparate kidney forms: evidence from expression in the Xenopus pronephros. *Dev Dyn* **206**, 131-8.

Carroll, T. J. and Vize, P. D. (1999). Synergism between Pax-8 and lim-1 in embryonic kidney development. *Dev Biol* **214**, 46-59.

Carron, C., Bourdelas, A., Li, H. Y., Boucaut, J. C. and Shi, D. L. (2005). Antagonistic interaction between IGF and Wnt/JNK signaling in convergent extension in Xenopus embryo. *Mech Dev* **122**, 1234-47.

Chang, C. and Hemmati-Brivanlou, A. (1998). Neural crest induction by Xwnt7B in Xenopus. *Dev Biol* **194**, 129-34.

Chi, L., Zhang, S., Lin, Y., Prunskaite-Hyyrylainen, R., Vuolteenaho, R., Itaranta, P. and Vainio, S. (2004). Sprouty proteins regulate ureteric branching by coordinating reciprocal epithelial Wnt11, mesenchymal Gdnf and stromal Fgf7 signalling during kidney development. *Development* **131**, 3345-56.

Chow, R. L. and Lang, R. A. (2001). Early eye development in vertebrates. *Annu Rev Cell Dev Biol* **17**, 255-96.

Christian, J. L., Olson, D. J. and Moon, R. T. (1992). Xwnt-8 modifies the character of mesoderm induced by bFGF in isolated Xenopus ectoderm. *Embo J* **11**, 33-41.

Christiansen, J. H., Dennis, C. L., Wicking, C. A., Monkley, S. J., Wilkinson, D. G. and Wainwright, B. J. (1995). Murine Wnt-11 and Wnt-12 have temporally and spatially restricted expression patterns during embryonic development. *Mech Dev* **51**, 341-50.

Conlon, F. L., Fairclough, L., Price, B. M., Casey, E. S. and Smith, J. C. (2001). Determinants of T box protein specificity. *Development* **128**, 3749-58.

Cui, S., Schwartz, L. and Quaggin, S. E. (2003). Pod1 is required in stromal cells for glomerulogenesis. *Dev Dyn* **226**, 512-22.

Dale, L. and Slack, J. M. (1987a). Fate map for the 32-cell stage of Xenopus laevis. *Development* **99**, 527-51.

Dale, L. and Slack, J. M. (1987b). Regional specification within the mesoderm of early embryos of Xenopus laevis. *Development* **100**, 279-95.

Danielson, K. G., Pillarisetti, J., Cohen, I. R., Sholehvar, B., Huebner, K., Ng, L. J., Nicholls, J. M., Cheah, K. S. and Iozzo, R. V. (1995). Characterization of the complete genomic structure of the human WNT-5A gene, functional analysis of its promoter, chromosomal mapping, and expression in early human embryogenesis. *J Biol Chem* **270**, 31225-34.

Dantzler, W. H. and Silbernagl, S. (1988). Amino acid transport by juxtamedullary nephrons: distal reabsorption and recycling. *Am J Physiol* **255**, F397-407.

De Calisto, J., Araya, C., Marchant, L., Riaz, C. F. and Mayor, R. (2005). Essential role of non-canonical Wnt signalling in neural crest migration. *Development* **132**, 2587-97.

Denayer, T., Van Roy, F. and Vleminckx, K. (2006) In vivo tracing of canonical Wnt signaling in Xenopus tadpoles by means of an inducible transgenic reporter tool. *FEBS Letters* **580**, 393-398.

Doolittle, R. F. (1981). Similar amino acid sequences: chance or common ancestry? *Science* **214**, 149-59.

Drummond, I. A., Majumdar, A., Hentschel, H., Elger, M., Solnica-Krezel, L., Schier, A. F., Neuhauss, S. C., Stemple, D. L., Zwartkruis, F., Rangini, Z. et al. (1998). Early development of the zebrafish pronephros and analysis of mutations affecting pronephric function. *Development* **125**, 4655-67.

Du, S. J., Purcell, S. M., Christian, J. L., McGrew, L. L. and Moon, R. T. (1995). Identification of distinct classes and functional domains of Wnts through expression of wild-type and chimeric proteins in Xenopus embryos. *Mol Cell Biol* **15**, 2625-34.

Dudley, A. T., Lyons, K. M. and Robertson, E. J. (1995). A requirement for bone morphogenetic protein-7 during development of the mammalian kidney and eye. *Genes Dev* **9**, 2795-807.

Dunty, W. C., Jr., Biris, K. K., Chalamalasetty, R. B., Taketo, M. M., Lewandoski, M. and Yamaguchi, T. P. (2008). Wnt3a/beta-catenin signaling controls posterior body development by coordinating mesoderm formation and segmentation. *Development* **135**, 85-94.

Eid, S. R., Terrettaz, A., Nagata, K. and Brandli, A. W. (2002). Embryonic expression of Xenopus SGLT-1L, a novel member of the solute carrier family 5 (SLC5), is confined to tubules of the pronephric kidney. *Int J Dev Biol* **46**, 177-84.

Funayama, N., Fagotto, F., McCrea, P. and Gumbiner, B. M. (1995). Embryonic axis induction by the armadillo repeat domain of beta-catenin: evidence for intracellular signaling. *J Cell Biol* **128**, 959-68.

Galceran, J., Sustmann, C., Hsu, S. C., Folberth, S. and Grosschedl, R. (2004). LEF1-mediated regulation of Delta-like1 links Wnt and Notch signaling in somitogenesis. *Genes Dev* **18**, 2718-23.

García-Castro, M. I., Marcelle, C. and Bronner-Fraser, M. (2002). Ectodermal Wnt function as a neural crest inducer. *Science* **297**, 848-51.

Garriock, R. J., D'Agostino, S. L., Pilcher, K. C. and Krieg, P. A. (2005). Wnt11-R, a protein closely related to mammalian Wnt11, is required for heart morphogenesis in Xenopus. *Dev Biol* **279**, 179-92.

Garriock, R. J. and Krieg, P. A. (2007). Wnt11-R signaling regulates a calcium sensitive EMT event essential for dorsal fin development of Xenopus. *Dev Biol* **304**, 127-40.

Garriock, R. J., Warkman, A. S., Meadows, S. M., D'Agostino, S. and Krieg, P. A. (2007). Census of vertebrate Wnt genes: isolation and developmental expression of Xenopus Wnt2, Wnt3, Wnt9a, Wnt9b, Wnt10a, and Wnt16. *Dev Dyn* **236**, 1249-58.

Gavin, B. J., McMahon, J. A. and McMahon, A. P. (1990). Expression of multiple novel Wnt-1/int-1-related genes during fetal and adult mouse development. *Genes Dev* **4**, 2319-32.

Geetha-Loganathan, P., Nimmagadda, S., Huang, R., Scaal, M. and Christ, B. (2006). Role of Wnt-6 in limb myogenesis. *Anat Embryol (Berl)* **211**, 183-8.

Gérard, P. and Corbier, R. (1934). Esquise d'une histopathologie comparée du rein des vertebrates. *Biol. Rev. Camb. Phil. Soc* **9**, 110-131.

Harland, R. M. (1991). In situ hybridization: an improved whole-mount method for Xenopus embryos. *Methods Cell Biol* **36**, 685-95.

Harlow, E. and Lane, D. (1988). Antibodies: A laboratory manuel: Cold Spring Harbour Laboratory Press, Cold Spring Harbour, New York.

Hausen, P. and Riebesel, M. (1991). The early development of Xenopus laevis. Springer-Verlag.

Heasman, J., Kofron, M. and Wylie, C. (2000). Beta-catenin signalling activity dissected in the early Xenopus embyos: a novel antisense approach. *Dev Biol.* **222**, 124-34.

Heller, N. and Brändli, A. W. (1997). Xenopus Pax-2 displays multiple splice forms during embryogenesis and pronephric kidney development. *Mech Dev* **69**, 83-104.

Heller, N. and Brändli, A. W. (1999). Xenopus Pax-2/5/8 orthologues: novel insights into Pax gene evolution and identification of Pax-8 as the earliest marker for otic and pronephric cell lineages. *Dev Genet* **24**, 208-19.

Hemmati-Brivanlou, A., Frank, D., Bolce, M. E., Brown, B. D., Sive, H. L. and Harland, R. M. (1990). Localization of specific mRNAs in Xenopus embryos by whole-mount in situ hybridization. *Development* **110**, 325-30.

Hemmati-Brivanlou, A., Kelly, O. G. and Melton, D. A. (1994). Follistatin, an antagonist of activin, is expressed in the Spemann organizer and displays direct neuralizing activity. *Cell* **77**, 283-95.

Hirsch, N. and Harris, W. A. (1997). Xenopus Pax-6 and retinal development. *J Neurobiol* **32**, 45-61.

Holewa, B., Zapp, D., Drewes, T., Senkel, S. and Ryffel, G. U. (1997). HNF4beta, a new gene of the HNF4 family with distinct activation and expression profiles in oogenesis and embryogenesis of Xenopus laevis. *Mol Cell Biol* **17**, 687-94.

Hollemann, T., Schuh, R., Pieler, T. and Stick, R. (1996). Xenopus Xsal-1, a vertebrate homolog of the region specific homeotic gene spalt of Drosophila. *Mech Dev* **55**, 19-32.

Hoppler, S., Brown, J. D. and Moon, R. T. (1996). Expression of a dominant-negative Wnt blocks induction of MyoD in Xenopus embryos. *Genes Dev* **10**, 2805-17.

Hoppler, S. and Moon, R. T. (1998). BMP-2/-4 and Wnt-8 cooperatively pattern the Xenopus mesoderm. *Mech Dev* **71**, 119-29.

Horster, M. (2000). Embryonic epithelial membrane transporters. *Am J Physiol Renal Physiol* **279**, F982-96.

Houweling, A. C., Dildrop, R., Peters, T., Mummenhoff, J., Moorman, A. F., Ruther, U. and Christoffels, V. M. (2001). Gene and cluster-specific expression of the Iroquois family members during mouse development. *Mech Dev* **107**, 169-74.

Hsieh, J. C., Kodjabachian, L., Rebbert, M. L., Rattner, A., Smallwood, P. M., Samos, C. H., Nusse, R., Dawid, I. B. and Nathans, J. (1999). A new secreted protein that binds to Wnt proteins and inhibits their activities. *Nature* **398**, 431-6.

Hsu, D. R., Economides, A. N., Wang, X., Eimon, P. M. and Harland, R. M. (1998). The Xenopus dorsalizing factor Gremlin identifies a novel family of secreted proteins that antagonize BMP activities. *Mol Cell* **1**, 673-83.

Huelsken, J. Behrens, J. (2002). The wnt signalling pathway. *Journal of Cell Sciences* **115**, 3977-3978.

Itäranta, P., Lin, Y., Perasaari, J., Roel, G., Destree, O. and Vainio, S. (2002). Wnt-6 is expressed in the ureter bud and induces kidney tubule development in vitro. *Genesis* **32**, 259-68.

Jessen, J. R. and Solnica-Krezel, L. (2005). Axis formation-beta-catenin catches a Wnt. *Cell* **120**, 736-7.

Kispert, A., Koschorz, B. and Herrmann, B. G. (1995). The T protein encoded by Brachyury is a tissue-specific transcription factor. *Embo J* **14**, 4763-72.

Kispert, A., Vainio, S. and McMahon, A. P. (1998). Wnt-4 is a mesenchymal signal for epithelial transformation of metanephric mesenchyme in the developing kidney. *Development* **125**, 4225-34.

Kispert, A., Vainio, S., Shen, L., Rowitch, D. H. and McMahon, A. P. (1996). Proteoglycans are required for maintenance of Wnt-11 expression in the ureter tips. *Development* **122**, 3627-37.

Kofron, M., Birsoy, B., Houston, D., Tao, Q., Wylie, C. and Heasman, J. (2007). Wnt11/beta-catenin signaling in both oocytes and early embryos acts through LRP6-mediated regulation of axin. *Development* **134**, 503-13.

Kohn, A. D. and Moon, R. T. (2005). Wnt and calcium signaling: beta-catenin-independent pathways. *Cell Calcium* **38**, 439-46.

Koseki, C., Herzlinger, D. and al-Awqati, Q. (1992). Apoptosis in metanephric development. *J Cell Biol* **119**, 1327-33.

Kreidberg, J. A., Sariola, H., Loring, J. M., Maeda, M., Pelletier, J., Housman, D. and Jaenisch, R. (1993). WT-1 is required for early kidney development. *Cell* **74**, 679-91.

Ku, M. and Melton, D. A. (1993). Xwnt-11: a maternally expressed Xenopus wnt gene. *Development* **119**, 1161-73.

Kühl, M., Sheldahl, L. C., Park, M., Miller, J. R. and Moon, R. T. (2000). The Wnt/Ca2+ pathway: a new vertebrate Wnt signaling pathway takes shape. *Trends Genet* **16**, 279-83.

Lavery, D. L., Davenport, I. R., Turnbull, Y. D., Wheeler, G. N. and Hoppler, S. (2008). Wnt6 expression in epidermis and epithelial tissues during Xenopus organogenesis. *Dev Dyn* **237**, 768-79.

Lawrence, W. D., Whitaker, D., Sugimura, H., Cunha, G. R., Dickersin, G. R. and Robboy, S. J. (1992). An ultrastructural study of the developing urogenital tract in early human fetuses. *Am J Obstet Gynecol* **167**, 185-93.

Li, H. Y., Bourdelas, A., Carron, C., Gomez, C., Boucaut, J. C. and Shi, D. L. (2006). FGF8, Wnt8 and Myf5 are target genes of Tbx6 during anteroposterior specification in Xenopus embryo. *Dev Biol* **290**, 470-81.

Lin, Y., Liu, A., Zhang, S., Ruusunen, T., Kreidberg, J. A., Peltoketo, H., Drummond, I. and Vainio, S. (2001). Induction of ureter branching as a response to Wnt-2b signaling during early kidney organogenesis. *Dev Dyn* **222**, 26-39.

Liu, C., Kato, Y., Zhang, Z., Do, V. M., Yankner, B. A. and He, X. (1999). beta-Trcp couples beta-catenin phosphorylation-degradation and regulates Xenopus axis formation. *Proc Natl Acad Sci U S A* **96**, 6273-8.

Lyons, J. P., Mueller, U. W., Ji, H., Everett, C., Fang, X., Hsieh, J. C., Barth, A. M. and McCrea, P. D. (2004). Wnt-4 activates the canonical beta-catenin-mediated Wnt pathway and binds Frizzled-6 CRD: functional implications of Wnt/beta-catenin activity in kidney epithelial cells. *Exp Cell Res* **298**, 369-87.

Majumdar, A., Lun, K., Brand, M. and Drummond, I. A. (2000). Zebrafish no isthmus reveals a role for pax2.1 in tubule differentiation and patterning events in the pronephric primordia. *Development* **127**, 2089-98.

Majumdar, A., Vainio, S., Kispert, A., McMahon, J. and McMahon, A. P. (2003). Wnt11 and Ret/Gdnf pathways cooperate in regulating ureteric branching during metanephric kidney development. *Development* **130**, 3175-85.

Marlow, F., Topczewski, J., Sepich, D. and Solnica-Krezel, L. (2002). Zebrafish Rho kinase 2 acts downstream of Wnt11 to mediate cell polarity and effective convergence and extension movements. *Curr Biol* **12**, 876-84.

Mauch, T. J., Yang, G., Wright, M., Smith, D. and Schoenwolf, G. C. (2000). Signals from trunk paraxial mesoderm induce pronephros formation in chick intermediate mesoderm. *Dev Biol* **220**, 62-75.

Maulet, Y., Lambert, R. C., Mykita, S., Mouton, J., Partisani, M., Bailly, Y., Bombarde, G. and Feltz, A. (1999). Expression and targeting to the plasma membrane of xClC-K, a chloride channel specifically expressed in distinct tubule segments of Xenopus laevis kidney. *Biochem J* **340 (Pt 3)**, 737-43.

Massé, K., Collins, R. J., Bhamra, S., Seville, R. A. and Jones, E. A. (2007). Anxa4 genes are expressed in distinct organ systems in Xenopus laevis and tropicalis but are functionally conserved. *Organogenesis* **3:2,** 83-92.

Maye, P., Zheng, J., Li, L. and Wu, D. (2004). Multiple mechanisms for Wnt11-mediated repression of the canonical Wnt signaling pathway. *J Biol Chem* **279**, 24659-65.

Mayor, R., Morgan, R. and Sargent, M. G. (1995). Induction of the prospective neural crest of Xenopus. *Development* **121**, 767-77.

McLaren, A. (2000). Germ and somatic cell lineages in the developing gonad. *Mol Cell Endocrinol* **163**, 3-9.

McLaughlin, K. A., Rones, M. S. and Mercola, M. (2000). Notch regulates cell fate in the developing pronephros. *Dev Biol* **227**, 567-80.

McMahon, A. P. and Moon, R. T. (1989). Ectopic expression of the proto-oncogene int-1 in Xenopus embryos leads to duplication of the embryonic axis. *Cell* **58**, 1075-84.

Medvinsky, A. and Dzierzak, E. (1996). Definitive hematopoiesis is autonomously initiated by the AGM region. *Cell* **86**, 897-906.

Mei, W., Yang, J., Tao, Q., Geng, X., Rupp, R. A. and Ding, X. (2001). An interferon regulatory factor-like binding element restricts Xmyf-5 expression in the posterior somites during Xenopus myogenesis. *FEBS Lett* **505**, 47-52.

Mitchell, T., Jones, E. A., Weeks, D. L. and Sheets, M. D. (2007). Chordin affects pronephros development in Xenopus embryos by anteriorizing presomitic mesoderm. *Dev Dyn* **236**, 251-61.

Miyazaki, Y., Oshima, K., Fogo, A., Hogan, B. L. and Ichikawa, I. (2000). Bone morphogenetic protein 4 regulates the budding site and elongation of the mouse ureter. *J Clin Invest* **105**, 863-73.

Miyazaki, Y., Oshima, K., Fogo, A. and Ichikawa, I. (2003). Evidence that bone morphogenetic protein 4 has multiple biological functions during kidney and urinary tract development. *Kidney Int* **63**, 835-44.

Molenaar, M., van de Wetering, M., Oosterwegel, M., Peterson-Maduro, J., Godsave, S., Korinek, V., Roose, J., Destree, O. and Clevers, H. (1996). XTcf-3 transcription factor mediates beta-catenin-induced axis formation in Xenopus embryos. *Cell* **86**, 391-9.

Moody, S. A. (1987a). Fates of the blastomeres of the 16-cell stage Xenopus embryo. *Dev Biol* **119**, 560-78.

Moody, S. A. (1987b). Fates of the blastomeres of the 32-cell-stage Xenopus embryo. *Dev Biol* **122**, 300-19.

Moon, R. T., Brown, J. D., Yang-Snyder, J. A. and Miller, J. R. (1997). Structurally related receptors and antagonists compete for secreted Wnt ligands. *Cell* **88**, 725-8.

Moon, R. T., Campbell, R. M., Christian, J. L., McGrew, L. L., Shih, J. and Fraser, S. (1993). Xwnt-5A: a maternal Wnt that affects morphogenetic movements after overexpression in embryos of Xenopus laevis. *Development* **119**, 97-111.

Moon, R. T. and Christian, J. L. (1992). Competence modifiers synergize with growth factors during mesoderm induction and patterning in Xenopus. *Cell* **71**, 709-12.

Moore, K. L. (1977). The urogenital system in the developing human: clinically oriented embryology (K. L. Moore, eds), 220-259. Sauners, Philadelphia.

Moriya, N. Uchiyama, H. and Asashima, M. (1993). Induction of pronephric tubules by activin and retinoic acid in presumptive ectoderm of Xenopus laevis. *Dev. Growth Diff.* **35**, 123-128.

Munro, A. F. (1953). The ammonia and urea excretion of different species of amphibia during their development and metamorphosis. *Biochem. J.* **54**, 29-36.

Nadeau, J. H. and Sankoff, D. (1998a). Counting on comparative maps. *Trends Genet* **14**, 495-501.

Nadeau, J. H. and Sankoff, D. (1998b). The lengths of undiscovered conserved segments in comparative maps. *Mamm Genome* **9**, 491-5.

Nagata, K., Hori, N., Sato, K., Ohta, K., Tanaka, H. and Hiji, Y. (1999). Cloning and functional expression of an SGLT-1-like protein from the Xenopus laevis intestine. *Am J Physiol* **276**, G1251-9.

Nakamura, H., Tashiro, K., Nakamura, T. and Shiokawa, K. (1995). Molecular cloning of Xenopus HGF cDNA and its expression studies in Xenopus early embryogenesis. *Mech Dev* **49**, 123-31.

Nascone, N. and Mercola, M. (1995). An inductive role for the endoderm in Xenopus cardiogenesis. *Development* **121**, 515-23.

Nelson, W. J. and Nusse, R. (2004). Convergence of Wnt, beta-catenin, and cadherin pathways. *Science* **303**, 1483-7.

Nieuwkoop, P. D. and Faber, J. (1994). Normal table of Xenopus laevis (Daudin) 4th edition. Garland Publishing, Inc. New York.

Noselli, S. and Agnes, F. (1999). Roles of the JNK signaling pathway in Drosophila morphogenesis. *Curr Opin Genet Dev* **9**, 466-72.

Nusse, R. (2001). Developmental biology. Making head or tail of Dickkopf. *Nature* **411**, 255-6.

Ogino, H., McConnell, W. B. and Grainger, R. M. (2006). Highly efficient transgenesis in Xenopus tropicalis using I-SceI meganuclease. *Mech Dev* **123**, 103-13.

Ohkawara, B., Yamamoto, T. S., Tada, M. and Ueno, N. (2003). Role of glypican 4 in the regulation of convergent extension movements during gastrulation in Xenopus laevis. *Development* **130**, 2129-38.

Osafune, K., Nishinakamura, R., Komazaki, S. and Asashima, M. (2002). In vitro induction of the pronephric duct in Xenopus explants. *Dev Growth Differ* **44**, 161-7.

Pandur, P. and Kuhl, M. (2001). An arrow for wingless to take-off. *Bioessays* **23**, 207-10.

Pandur, P., Lasche, M., Eisenberg, L. M. and Kuhl, M. (2002). Wnt-11 activation of a non-canonical Wnt signalling pathway is required for cardiogenesis. *Nature* **418**, 636-41.

Parr, B. A., Cornish, V. A., Cybulsky, M. I. and McMahon, A. P. (2001). Wnt7b regulates placental development in mice. *Dev Biol* **237**, 324-32.

Parr, B. A., Shea, M. J., Vassileva, G. and McMahon, A. P. (1993). Mouse Wnt genes exhibit discrete domains of expression in the early embryonic CNS and limb buds. *Development* **119**, 247-61.

Patterson, L. T., Pembaur, M. and Potter, S. S. (2001). Hoxa11 and Hoxd11 regulate branching morphogenesis of the ureteric bud in the developing kidney. *Development* **128**, 2153-61.

Piccolo, S., Agius, E., Leyns, L., Bhattacharyya, S., Grunz, H., Bouwmeester, T. and De Robertis, E. M. (1999). The head inducer Cerberus is a multifunctional antagonist of Nodal, BMP and Wnt signals. *Nature* **397**, 707-10.

Piscione, T. D., Phan, T. and Rosenblum, N. D. (2001). BMP7 controls collecting tubule cell proliferation and apoptosis via Smad1-dependent and -independent pathways. *Am J Physiol Renal Physiol* **280**, F19-33.

Polakis, P. (2000). Wnt signaling and cancer. *Genes Dev* **14**, 1837-51.

Qian, J., Jiang, Z., Li, M., Heaphy, P., Liu, Y. H. and Shackleford, G. M. (2003). Mouse Wnt9b transforming activity, tissue-specific expression, and evolution. *Genomics* **81**, 34-46.

Raciti, D., **Reggiani, L**., **Geffers, L**., **Jiang, Q**., **Bacchion, F**., **Subrizi, A. E**., **Clements, D**., **Tindal, C**., **Davidson, D. R**., **Kaissling, B**., **Brändli, A.W** (2008). Organization of the pronephric kidney revealed by large-scale gene expression mapping. *Genome Biol.* **9** (5):R84.

Reggiani, L., Raciti, D., Airik, R., Kispert, A. and Brandli, A. W. (2007). The prepattern transcription factor Irx3 directs nephron segment identity. *Genes Dev* **21**, 2358-70.

Reichsman, F., Smith, L. and Cumberledge, S. (1996). Glycosaminoglycans can modulate extracellular localization of the wingless protein and promote signal transduction. *J Cell Biol* **135**, 819-27.

Rodríguez-Niedenführ, M., Dathe, V., Jacob, H. J., Prols, F. and Christ, B. (2003). Spatial and temporal pattern of Wnt-6 expression during chick development. *Anat Embryol (Berl)* **206**, 447-51.

Ryffel, G. U. (2001). Mutations in the human genes encoding the transcription factors of the hepatocyte nuclear factor (HNF)1 and HNF4 families: functional and pathological consequences. *J Mol Endocrinol* **27**, 11-29.

Sainio, K., Hellstedt, P., Kreidberg, J. A., Saxen, L. and Sariola, H. (1997a). Differential regulation of two sets of mesonephric tubules by WT-1. *Development* **124**, 1293-9.

Sainio, K., Suvanto, P., Davies, J., Wartiovaara, J., Wartiovaara, K., Saarma, M., Arumae, U., Meng, X., Lindahl, M., Pachnis, V. et al. (1997b). Glial-cell-line-derived neurotrophic factor is required for bud initiation from ureteric epithelium. *Development* **124**, 4077-87.

Sambrook, J., Fritsch, E. F. and Maniatis, T. (1989). molecular cloning: a laboratory manuel.

Saulnier, D. M., Ghanbari, H. and Brandli, A. W. (2002). Essential function of Wnt-4 for tubulogenesis in the Xenopus pronephric kidney. *Dev Biol* **248**, 13-28.

Schmidt, C., Stoeckelhuber, M., McKinnell, I., Putz, R., Christ, B. and Patel, K. (2004). Wnt 6 regulates the epithelialisation process of the segmental plate mesoderm leading to somite formation. *Dev Biol* **271**, 198-209.

Saxén, L. (1987) Organogenesis of the kidney. Cambridge Univ. Press, Cambridge.

Schroeder, K. E., Condic, M. L., Eisenberg, L. M. and Yost, H. J. (1999). Spatially regulated translation in embryos: asymmetric expression of maternal Wnt-11 along the dorsal-ventral axis in Xenopus. *Dev Biol* **214**, 288-97.

Schubert, F. R., Mootoosamy, R. C., Walters, E. H., Graham, A., Tumiotto, L., Munsterberg, A. E., Lumsden, A. and Dietrich, S. (2002). Wnt6 marks sites of epithelial transformations in the chick embryo. *Mech Dev* **114**, 143-8.

Semënov, M. V., Tamai, K., Brott, B. K., Kuhl, M., Sokol, S. and He, X. (2001). Head inducer Dickkopf-1 is a ligand for Wnt coreceptor LRP6. *Curr Biol* **11**, 951-61.

Seufert, D. W., Brennan, H. C., DeGuire, J., Jones, E. A. and Vize, P. D. (1999). Developmental basis of pronephric defects in Xenopus body plan phenotypes. *Dev Biol* **215**, 233-42.

Sheldahl, L. C., Park, M., Malbon, C. C. and Moon, R. T. (1999). Protein kinase C is differentially stimulated by Wnt and Frizzled homologs in a G-protein-dependent manner. *Curr Biol* **9**, 695-8.

Shimizu, H., Julius, M. A., Giarre, M., Zheng, Z., Brown, A. M. and Kitajewski, J. (1997). Transformation by Wnt family proteins correlates with regulation of beta-catenin. *Cell Growth Differ* **8**, 1349-58.

Simrick, S., Masse, K. and Jones, E. A. (2005). Developmental expression of Pod 1 in Xenopus laevis. *Int J Dev Biol* **49**, 59-63.

Slack, J. M. W. (1993). Embryonic induction. *Mech. Dev.* **41**, 91-107.

Slusarski, D. C., Yang-Snyder, J., Busa, W. B. and Moon, R. T. (1997). Modulation of embryonic intracellular Ca2+ signaling by Wnt-5A. *Dev Biol* **182**, 114-20.

Smith, C. and Mackay, S. (1991). Morphological development and fate of the mouse mesonephros. *J Anat* **174**, 171-84.

Smith, J. C., Conlon, F. L., Saka, Y. and Tada, M. (2000). Xwnt11 and the regulation of gastrulation in Xenopus. *Philos Trans R Soc Lond B Biol Sci* **355**, 923-30.

Spemann, H. (1938). Embryonic development and induction. New Haven, Yale University Press.

Stark, K., Vainio, S., Vassileva, G. and McMahon, A. P. (1994). Epithelial transformation of metanephric mesenchyme in the developing kidney regulated by Wnt-4. *Nature* **372**, 679-83.

Tada, M. and Smith, J. C. (2000). Xwnt11 is a target of Xenopus Brachyury: regulation of gastrulation movements via Dishevelled, but not through the canonical Wnt pathway. *Development* **127**, 2227-38.

Taelman, V., Van Campenhout, C., Solter, M., Pieler, T. and Bellefroid, E. J. (2006). The Notch-effector HRT1 gene plays a role in glomerular development and patterning of the Xenopus pronephros anlagen. *Development* **133**, 2961-71.

Tahinci, E., Thorne, C. A., Franklin, J. L., Salic, A., Christian, K. M., Lee, L. A., Coffey, R. J. and Lee, E. (2007). Lrp6 is required for convergent extension during Xenopus gastrulation. *Development* **134**, 4095-106.

Taira, M., Otani, H., Jamrich, M. and Dawid, I. B. (1994). Expression of the LIM class homeobox gene Xlim-1 in pronephros and CNS cell lineages of Xenopus embryos is affected by retinoic acid and exogastrulation. *Development* **120**, 1525-36.

Takahashi, H. and Ikeda, T. (1996). Transcripts for two members of the transforming growth factor-beta superfamily BMP-3 and BMP-7 are expressed in developing rat embryos. *Dev Dyn* **207**, 439-49.

Takeuchi, M., Nakabayashi, J., Sakaguchi, T., Yamamoto, T. S., Takahashi, H., Takeda, H. and Ueno, N. (2003). The prickle-related gene in vertebrates is essential for gastrulation cell movements. *Curr Biol* **13**, 674-9.

Tao, Q., Yokota, C., Puck, H., Kofron, M., Birsoy, B., Yan, D., Asashima, M., Wylie, C. C., Lin, X. and Heasman, J. (2005). Maternal wnt11 activates the canonical wnt signaling pathway required for axis formation in Xenopus embryos. *Cell* **120**, 857-71.

Thomas, H., Jaschkowitz, K., Bulman, M., Frayling, T. M., Mitchell, S. M., Roosen, S., Lingott-Frieg, A., Tack, C. J., Ellard, S., Ryffel, G. U. et al. (2001). A distant upstream promoter of the HNF-4alpha gene connects the transcription factors involved in maturity-onset diabetes of the young. *Hum Mol Genet* **10**, 2089-97.

Tiedemann, K. and Egerer, G. (1984). Vascularization and glomerular ultrastructure in the pig mesonephros. *Cell Tissue Res* **238**, 165-75.

Torres, M., Gomez-Pardo, E., Dressler, G. R. and Gruss, P. (1995). Pax-2 controls multiple steps of urogenital development. *Development* **121**, 4057-65.

Ultsch, G. R., Bradford, D. F. and Freda, J. (1999). Physiology: Coping with the environment. In "*Tadpoles: The Biology of Anuran Larvae"* (R. W. McDiarmid and R. Altig, eds.). University of Chicago Press, Chicago.

Urban, A. E., Zhou, X., Ungos, J. M., Raible, D. W., Altmann, C. R. and Vize, P. D. (2006). FGF is essential for both condensation and mesenchymal-epithelial transition stages of pronephric kidney tubule development. *Dev Biol* **297**, 103-17.

Uusitalo, M., Heikkila, M. and Vainio, S. (1999). Molecular genetic studies of Wnt signaling in the mouse. *Exp Cell Res* **253**, 336-48.

Vainio, S. and Lin, Y. (2002). Coordinating early kidney development: lessons from gene targeting. *Nat Rev Genet* **3**, 533-43.

Vize, P. D., Jones, E. A. and Pfister, R. (1995). Development of the Xenopus pronephric system. *Dev Biol* **171**, 531-40.

Vize, P. D., Seufert, D. W., Carroll, T. J. and Wallingford, J. B. (1997). Model systems for the study of kidney development: use of the pronephros in the analysis of organ induction and patterning. *Dev Biol* **188**, 189-204.

Vize, P. D., Carroll, T. J. and Wallingford, J. B. (2003). Induction, development and physiology of the pronephric tubules. The Kidney, Academic Press.

Waddington, C. H. (1938). The morphogenetic fucntion of vestigial organ in the chick. *J. Exp. Biol.* **15**, 371-376.

Waldner, C., Sakamaki, K., Ueno, N., Turan, G. and Ryffel, G. U. (2006). Transgenic Xenopus laevis strain expressing cre recombinase in muscle cells. *Dev Dyn* **235**, 2220-8.

Wallingford, J. B., Vogeli, K. M. and Harland, R. M. (2001). Regulation of convergent extension in Xenopus by Wnt5a and Frizzled-8 is independent of the canonical Wnt pathway. *Int J Dev Biol* **45**, 225-7.

Wheeler, G. N., Hamilton, F. S. and Hoppler, S. (2000). Inducible gene expression in transgenic Xenopus embryos. *Curr Biol* **10**, 849-52.

White, J. A. and Heasman, J. (2008). Maternal control of pattern formation in Xenopus laevis. *J Exp Zoolog B Mol Dev Evol* **310**, 73-84.

Wiggan, O. and Hamel, P. A. (2002). Pax3 regulates morphogenetic cell behavior in vitro coincident with activation of a PCP/non-canonical Wnt-signaling cascade. *J Cell Sci* **115**, 531-41.

Wild, W., Pogge von Strandmann, E., Nastos, A., Senkel, S., Lingott-Frieg, A., Bulman, M., Bingham, C., Ellard, S., Hattersley, A. T. and Ryffel, G. U. (2000). The mutated human gene encoding hepatocyte nuclear factor 1beta inhibits kidney formation in developing Xenopus embryos. *Proc Natl Acad Sci U S A* **97**, 4695-700.

Winning, R. S. and Sargent, T. D. (1994). Pagliaccio, a member of the Eph family of receptor tyrosine kinase genes, has localized expression in a subset of neural crest and neural tissues in Xenopus laevis embryos. *Mech Dev* **46**, 219-29.

Wolda, S. L. and Moon, R. T. (1992). Cloning and developmental expression in Xenopus laevis of seven additional members of the Wnt family. *Oncogene* **7**, 1941-7.

Wrobel, K. H. and Süß, F. (1999). On the origin and prenatal development of the bovine adrenal gland. *Anat Embryol (Berl)* **199**, 301-18.

Wu, G., Bohn, S. and Ryffel, G. U. (2004). The HNF1beta transcription factor has several domains involved in nephrogenesis and partially rescues Pax8/lim1-induced kidney malformations. *Eur J Biochem* **271**, 3715-28.

Yamada, T. (1950). Dorsalization of the ventral marginal zone of the triturus gastrula. I. Ammonia-treatment of the medioventral marginal zone. *Biol Bull* **98**, 98-121.

Yamagata, K., Furuta, H., Oda, N., Kaisaki, P. J., Menzel, S., Cox, N. J., Fajans, S. S., Signorini, S., Stoffel, M. and Bell, G. I. (1996). Mutations in the hepatocyte nuclear factor-4alpha gene in maturity-onset diabetes of the young (MODY1). *Nature* **384**, 458-60.

Yamaguchi, T. P., Bradley, A., McMahon, A. P. and Jones, S. (1999). A Wnt5a pathway underlies outgrowth of multiple structures in the vertebrate embryo. *Development* **126**, 1211-23.

Yang-Snyder, J., Miller, J. R., Brown, J. D., Lai, C. J. and Moon, R. T. (1996). A frizzled homolog functions in a vertebrate Wnt signaling pathway. *Curr Biol* **6**, 1302-6.

Yang, Q., Tian, Y., Wada, J., Kashihara, N., Wallner, E., Peterson, D. and Kanwar, Y. S. (2000). Expression characteristics and relevance of sodium glucose cotransporter-1 in mammalian renal tubulogenesis. *Am J Physiol Renal Physiol* **279**, F765-77.

Yoshida, M., Suda, Y., Matsuo, I., Miyamoto, N., Takeda, N., Kuratani, S. and Aizawa, S. (1997). Emx1 and Emx2 functions in development of dorsal telencephalon. *Development* **124**, 101-11.

Yu, J., McMahon, A. P. and Valerius, M. T. (2004). Recent genetic studies of mouse kidney development. *Curr Opin Genet Dev* **14**, 550-7.

Zhou, X. and Vize, P. D. (2004). Proximo-distal specialization of epithelial transport processes within the Xenopus pronephric kidney tubules. *Dev Biol* **271**, 322-38.